Robust Stabilization and Disturbance Rejection for Autonomous Helicopter

A. Danapalasingam, Kumeresan

Publication date:
2010

Document Version
Accepted author manuscript, peer reviewed version

Kumeresan A. Danapalasingam

Robust Stabilization and Disturbance Rejection for Autonomous Helicopter

Robust Stabilization and Disturbance Rejection for Autonomous Helicopter
Ph.D. thesis

ISBN: 987-87-92328-40-3
October 2010

Contents

Preface and Acknowledgements

This thesis is submitted as a collection of papers in the partial fulfilment of the requirements for a Doctor of Philosophy at the Section of Automation and Control, Department of Electronic Systems, Aalborg University, Denmark. The work has been carried out in the period from February 2007 to September 2010 under the supervision of Associate Professor Anders la Cour-Harbo and Assistant Professor Morten Bisgaard.

This Ph.D. study is supported by Ministry of Higher Education Malaysia (MOHE) and Universiti Teknologi Malaysia (UTM).

First and foremost I would like to express my deepest gratitude to John-Josef Leth for his support, guidance and encouragement that have made this thesis a fruitful one. His sincere assistance and dedication have certainly helped me in completing the critical stage of this Ph.D. study. I am thankful to my supervisors, Anders la Cour-Harbo and Morten Bisgaard whose effort in all these years led to the completion of this project. I am also very much indebted to Professor Rafal Wisniewski whose kind heart and seemingly abundant knowledge in mathematics saved me whenever I felt like drowning in the turbulence of this research.

I would like to take this opportunity to acknowledge all the employees at the Section of Automation and Control who have contributed either directly or indirectly in making this journey as gratifying as possible. Special thanks go to the lovely secretaries of the section, Karen Drescher and Jette Damkjær for their warmth, hospitality and kindness that I will treasure forever in my memory.

To my family and friends who have been my pillars of support during my ups and downs in the course of my stay in Denmark, I say thank you very much. Finally, I would like to thank MOHE and UTM for the given opportunity and financial support that made this Ph.D. study possible.

Abstract

The applicability of autonomous helicopters in execution of various tasks including some of the critical ones such as wind turbine inspection, deep-sea search and rescue and natural disaster monitoring demands a high performance controller. In wind turbine inspection for instance, a helicopter would be required to fly autonomously from a suitable location to the rotating structure. In cases where an inspection routine involves prolonged and detailed measurements, it is expected that the helicopter is able to fly as close as possible to the wind turbine with minimum deviations. And since the undesirable influence from wind disturbances and rotor wake interactions between the helicopter and the structure are unavoidable, wind turbine inspection using an autonomous helicopter presents itself as a challenging control problem.

To meet general requirements of practical applications utilizing autonomous helicopters, it is highly desirable to be equipped with a controller that is capable of carrying out designated objectives from an arbitrary initial helicopter state in the presence of wind disturbances. Often, exact values of helicopter physical parameters and aerodynamic coefficients are not known. Thus, a control design should be able to cope with model and parameter uncertainties. However, the design of such a controller is challenging due to the highly nonlinear and coupled helicopter model. The difficulty to obtain measurements of the wind disturbance for stabilizing control input generation further aggravates the control design problem.

In this research, for a general nonlinear control system with a persistent disturbance as one of its external inputs whose measurements are available, it is shown that the existence of a smooth uniform control Lyapunov function implies the existence of a stabilizing state feedback with feedforward control which is insensitive to small measurement errors and small external disturbance for fast sampling. Conversely, it is shown that there exists a smooth uniform control Lyapunov function if there is such a stabilizer. By introducing the notion of disturbance effect, a feedforward control scheme that can be augmented to an existing state feedback control is proposed to guarantee asymptotic stability. However, in the helicopter case due to the difficulty in obtaining accurate wind disturbance measurements, an estimate of the wind disturbance is introduced to be adapted using state measurements for stabilization of position and translational velocity. By assuming that the wind disturbance is a sum of a fixed number of sinusoids with unknown amplitudes, frequencies and phases, a nonlinear controller is designed based on nonlinear adaptive output regulation and robust stabilization of a chain of integrators by a saturated feedback. Even though the control design is based on a simplified model, simulations of the controller implementation in a model of higher complexity show a satisfactory performance in the stabilization of helicopter motion in the presence of model and parameter uncertainties.

Synopsis

At anvende autonome helikoptere i forbindelse med opgaver som inspektion af vindmller, sredning, overvgning og lignende stiller store krav til stabiliten og prcisionen af flyvningen. For eksempel, ved vindmlleinspektion er det ndvendigt for helikopteren at starte fra et egnet startpunkt og flyve autonomt til de roterende blade. I tilflde, hvor en inspektion indebrer langvarige og detaljerede mlinger, forventes det, at helikopteren er i stand til at flyve s tt som muligt p vindmllen. Eftersom helikopteren uundgligt vil blive pvirket af turbulens fra vindmllen, er inspektion af denne ved hjlp af en autonom helikopter et udfordrende reguleringsproblem.

For at opfylde sdanne krav i applikationer for autonome helikoptere, er det ndvendigt med en regulering, der er i stand til at udfre missioner og stabilisere helikopteren fra en vilkrlig starttilstand under vindforstyrrelser. Helikopterens fysiske parametre og aerodynamiske koefficienter er ofte ikke prcist kendte og et reguleringsdesign m derfor vre i stand til at hndtere model- og parameterusikkerheder. Et design af en sdan regulator er dog udfordrende p grund af den meget ikke-linere og koblede helikoptermodel. Vanskelighederne ved at mle vindforstyrrelserne til brug i stabilisering gr reguleringsproblemet svrere.

Det er i denne afhandling vist at eksistensen af en glat uniform control Lyapunov funktion for et generelt ikke-linert system med en uafbrudt forstyrrelse som et output, forudstter eksistensen af en stabiliserende feedback tilstandsregulering med feedforward regulering, der er uflsom over for sm mlefejl og eksterne forstyrrelser ved hurtig sampling. Det er ogs vist, at der eksisterer en glat uniform control Lyapunov funktion, hvis en sdan stabiliserende regulering eksisterer. En feedforward regulering, der kan supplere en eksisterende feedback tilstandsregulator, kan garantere asymptotisk stabilitet ved at introducere begrebet forstyrrelseseffekt. Da det i forbindelse med en helikopter er vanskeligt direkte at mle vindforstyrrelserne er en adaptiv estimator til bestemmelse af vindforstyrrelserne ud fra tilstandsmlinger blevet introduceret. En ikke-liner regulator, baseret p ikke-liner adaptiv output regulering og robust stabilisering af en kde af integratorer ved satureret feedback, kan designes ved at antage at vindforstyrrelserne er en sum af et fast antal sinus-funktioner med ukendt amplitude, frekvens og fase. Selv om reguleringsdesigned er baseret p en simplificeret model, vister simuleringer af regulatoren med en model af hjere kompleksitet tilfredsstillende performance under stabilisering af helikopteren med model- og parameterusikkerheder.

1 | Introduction

An autonomous helicopter is an airborn vehicle capable of flying without a human pilot. Equipped with onboard sensors and a computing capability, an autonomous helicopter can be a reliable mechanical assistant to humans in a variety of applications including reconnaissance, agriculture, firefighting and land mine detection. While a human pilot can successfully fly a helicopter in a wide range of maneuvers, the execution of even the simplest unmanned helicopter flight is widely regarded as a challenging control problem. The challenge stems from the fact that a helicopter is a nonlinear, high dimensional, coupled and underactuated control system. The presence of wind disturbances, measurement errors, and model and parameter uncertainties poses further complications in the control design. The main theme of this thesis is helicopter stabilization in the presence of a wind disturbance. In this chapter, motivation behind the need for a concept of disturbance effect and feedforward control for a general nonlinear control system, and disturbance estimation in helicopter stabilization is presented. An overview of recent developments in related research fields is also given. To begin with, some practical applications of autonomous helicopters are proposed.

1.1 Autonomous Helicopter in Practical Applications

In many specialized tasks, while humans are highly reliable in performing desired activities, a better alternative that would result in a higher precision, cost saving, increased efficiency and better safety is often considered. Due to its small size, agility, manuevverability and unique hovering capability, potrayal of autonomous helicopters as a good candidate in real life implementations is inevitable.

An example of application of autonomous helicopters to assist human beings is wind turbine inspection. Periodic inspections of wind turbines are crucial to ensure consistent integrity and to avoid inconvenient shutdowns due to system failures. To curb complications in a wind turbine before serious problems involving increased down time and profit loss could ensue, preventive maintenance inspections are essential. Visual inspections and other non-destructive tests including ultrasonic inspection, eddy current inspection and alternating current field measurement to detect cracks, corrosion, weld flaws and other defects are conventionally conducted by using rope access techniques. Rope access is a method that allows workers to inspect and perform maintanence services on wind turbines using ropes. As the involvement of humans in such a risky environment naturally raises safety and cost issues, wind turbine inspection using autonomous helicopters can be an advantageous procedure. A group of autonomous helicopters can be dispatched in

a wind farm for simultaneous inspection of the wind turbines. The coordinated approach will not only be time efficient, but could also enable a reduced cost and increased persistent quality inspection method. However, one should realize that the windy and turbulent conditions in wind farms are the greatest hurdle in accomplishing effective wind turbine inspections using autonomous helicopters.

Another potential real life application in which autonomous helicopters can be utilized is air-sea rescue. In search and rescue operations of survivors of an aircraft crash and distressed ship crew members and passengers for instance, autonomous helicopters can be an excellent aid to search and locate victims in a prescribed area. Generally, full scale manned helicopters play a major function in search and rescue operations. While they can handle harsh weather conditions and are able to transport survivors in need of medical care to emergency facilities, the loud noise disrupts communication between rescuers and survivors. Another drawback is the deteriorating effect of strong helicopter downdraft on cold and possibly hypothermic survivors during rescue operations. The high expenditures involved in the purchase of helicopters, and in search and rescue operations including salaries of onboard and standy crew members could further demotivate the application of full scale helicopters. On the other hand, using a number of autonomous helicopters in coordination, a wider search area can be covered for a faster search process. Once a crash site or survivors have been identified, crucial information can be sent to a ground station or rescue boats for further actions. While waiting for the rescue boats to arrive, one or more autonomous helicopters can remain hovering close to the survivors to provide emergency supplies and to boost the spirits of the victims. Note that the search and rescue operations using autonomous helicopters could be considerably affected without controllers that could cope with harsh weather conditions at sea.

Even though the involvement of autonomous helicopters in the above mentioned applications is an appealing approach, great challenges and implementation issues that immediately arise have to be addressed before it could be put into practice. For an example, in both wind turbine inspection and air-sea rescue, the ability of an autonomous helicopter to perform instructions accurately despite the windy condition is obligatory. It is expected that an autonomous helicopter is capable of starting an operation by flying autonomously from a given ground base to a required destination on a computed path while avoiding obstacles. Since the design of a controller to enable an autonomous flight often requires the knowledge of helicopter physical parameters, aerodynamic coefficients, wind disturbance, etc., robustness against uncertainties in the values of these quantities is important.

1.2 Motivation

In general, helicopter control is made possible by using a state feedback that generates control inputs using state measurements (see e.g., [ACN10], [Xu10] and [BlCHB10]). If wind disturbance measurements are available in addition to the state measurements, the design of a state feedback with feedforward can be proven advantageous since more information about the system to be controlled is now available. However in helicopter control, a useful disturbance measurement is often hard to obtain. In such a case, disturbance estimation can be a method to quantify the effects of the external influence for a controller synthesis.

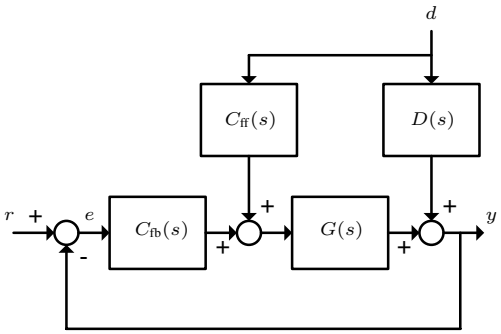

Figure 1.1: Feedback with feedforward control

Disturbance Effects

In a single-input-single-output (SISO) linear control system, while a feedback controller responds to a disturbance once the controlled variable is affected, a feedforward controller anticipates the effect of the disturbance and compensates in advance [Lov07]. Consider a SISO linear system G affected by a disturbance d with dynamics D as depicted in Fig. 1.1. If d can be measured and D is known, a feedforward controller C_{ff} can be designed to cancel the disturbance effect Dd on output y. While the effect that a disturbance has on the output of a SISO linear control system can be understood in a direct manner, disturbance effects in nonlinear control systems is not readily quantifiable. For a general nonlinear control system, before a feedforward controller can be designed for disturbance rejection, it would be useful to establish a notion of disturbance effect in a general nonlinear control system.

Feedforward Control

Instead of only using state measurements as in state feedback control, state feedback with feedforward control includes both state and disturbance measurements in the design of the control law. Now that the controller is provided with full information on external inputs affecting the system, a more efficient control action can be taken. For instance, in disturbance decoupling problem for nonlinear control systems affine in both control and disturbance, with a control consisting of both feedback and feedforward terms, the output can be decoupled from the disturbance under weaker conditions as compared to using only a state feedback [Isi95, Section 4.6]. In output regulation problem for general nonlinear control systems, asymptotic decay of an error variable is possible with an error feedback. However, the condition for the existence of such an error feedback is stricter than a condition for the existence of a control solution for the problem of output regulation where full information is available [Isi95, Section 8.4]. While the control methods developed in [Isi95] to solve the disturbance decoupling problem and output regulation problem eliminates the effects of external disturbances, the feasibility of such control laws in real world applications is vague. This is because in the design of the controllers, a perfect knowledge of the plant, and accurate state and disturbance measurements are assumed when in fact such a luxury almost only exists in theory. In reality, the performance of a controller is often subject to degradation due to the presence of measurement

errors and other uncertainties. To address the aforementioned implementation issues and to benefit from state feedback with feedforward control, a controller that is robust with respect to state measurement errors, disturbance measurement errors and model mismatch is needed. Therefore, it is important to set up a condition for the existence of a state feedback with feedforward for general nonlinear control systems, that is less sensitive to state and disturbance measurement errors, and model uncertainties. The establishment of such an existence condition will aid the design of a robust state feedback with feedforward controller for the stabilization of a plant to be controlled.

Disturbance Estimation

While the availability of the information on wind disturbances is highly preferred in helicopter control, the reality is that such measurements are difficult to obtain. The challenge primarily emerges due to main rotor downwash that would corrupt wind sensor readings. In addition to the installation problem, the need for a sensor of a suitable size and accuracy which is directly proportional to the cost, further dampens the effort to obtain reliable data for control purposes. Other factors related to wind disturbance measurements that influence a control performance include range, response time, precision, sensitivity and dead band of a wind sensor. In order to still deliver information on the exogenous input to the controller for helicopter stabilization, a disturbance estimate can be a promising option. The disturbance estimate can be generated by an internal model tuned by means of an appropriate adaptation law driven by state measurements. This then can be used for the synthesis of a robust controller which is less sensitive to parameter uncertainties for helicopter stabilization in the presence of a wind disturbance. However, given the involvement of state measurements in the disturbance estimation, once again the accuracy of measurements has to be taken into account. Morever, the reliability of a wind disturbance model assumed in the estimation in representing actual external wind disturbances plays an important role to ensure a high quality helicopter control.

1.3 State of the Art and Background

In line with the main theme of this thesis that is helicopter stabilization with wind disturbance rejection, the motivation for a concept of disturbance effect and feedforward control for general nonlinear control systems, and disturbance estimation in helicopter stabilization is laid out in Section 1.2. With regards to the aforementioned components of control theory, some preliminaries and related developments in state feedback with feedforward control of nonlinear systems, nonlinear adaptive output regulation and helicopter control are presented in this section. Concerning the control that depends on both state of the system and external disturbance input, well established nonlinear control theories on disturbance decoupling and full information output regulation are reviewed here. Lastly, a concise study of various helicopter control techniques are given. The literature review on helicopter control covers previous works done in trajectory tracking, robust stabilization and disturbance attenuation.

State Feedback with Feedforward Control of Nonlinear Systems

Provided that the state and external disturbance input of a nonlinear system are available for measurements, a state feedback with feedforward control consists of a feedback on the state of the system and a feedforward on the disturbance. While occasionally it is possible to measure disturbances in nonlinear control applications, one should not expect such an advantage in general control settings. Even though desired control actions are feasible by only using state or error measurements in control input generation, the inclusion of disturbance measurements certainly simplies the design of control laws. Next, two state feedback with feedforward control methods are reviewed.

Disturbance Decoupling

In this part, a control method to produce an output free from the influence of disturbances affecting the state of a nonlinear system is reviewed. Firstly, the category of nonlinear control systems considered in the disturbance decoupling problem is stated. Secondly, the form of the control law that depends on state and disturbance measurements is introduced to solve the disturbance decoupling problem.

Consider a single-input-single-output nonlinear system affine in control and disturbance of the form

$$\begin{aligned} \dot{x} &= f(x) + g(x)u + p(x)w, \\ y &= h(x), \end{aligned} \tag{1.1}$$

where $f(x)$, $g(x)$, $p(x)$ and $h(x)$ are smooth functions with state x belonging to an open set $U \subset \mathbb{R}$, control input $u \in \mathbb{R}$ and disturbance $w \in \mathbb{R}$.

If measurements of the disturbance w is available, then the disturbance decoupling problem is that of finding a static state feedback with feedforward control

$$u = \alpha(x) + \beta(x)v + \gamma(x)w \tag{1.2}$$

such that the output y of system (1.1) is decoupled from the disturbance w. As shown in [Isi95, Section 4.6], there exists a necessary and sufficient condition to solve the disturbance decoupling problem with such a control (1.2) defined locally. It turns out that if one opts to use a feedback control of the form

$$u = \alpha(x) + \beta(x)v,$$

a stricter condition has to be satisfied to have the output y of system (1.1) completely independent of the disturbance w [Isi95, Proposition 4.6.1].

Full Information Output Regulation

In the disturbance decoupling problem as decribed above, using the state feedback with feedforward control (1.2) the output of the nonlinear system (1.1) is completely decoupled from the disturbance w. Subsequently, one can further design the control v in (1.2) to achieve an additional control performance such as asymptotic stability [Isi95]. Another problem in nonlinear control theory is the design of a control law such that the output of a nonlinear system tracks a reference output in a given family. A similar control problem

involves having the output of a nonlinear system asymptotically rejecting a disturbance belonging to a certain class. In both cases, it is required that the tracking error, i.e. the difference between the reference output and the actual output, reduces to zero for every reference output and every undesired disturbance from certain classes of functions. The full information output regulation that addresses the abovementioned control problem is decribed next.

Consider now a nonlinear system of the form

$$\begin{aligned} \dot{x} &= f(x, w, u), \\ e &= h(x, w), \end{aligned} \tag{1.3}$$

where $f(x, w, u)$ and $h(x, w)$ are smooth functions with $f(0, 0, 0) = 0$ and $h(0, 0) = 0$. The state x is defined in a neighborhood U of the origin in $\mathbb{R}^n$ with control input $u \in \mathbb{R}^m$ and error $e \in \mathbb{R}^m$. The disturbance $w \in \mathbb{R}^r$ is assumed to be generated by a homogeneous exosystem of the form

$$\dot{w} = s(w), \tag{1.4}$$

with initial condition $w(0)$ belonging to a neighbourhood W of the origin of $\mathbb{R}^r$.

Then the full information output regulation problem for system (1.3) given a neutrally stable exosystem (1.4), is that of finding a state feedback with feedforward control $\alpha(x, w)$ such that

1. the equilibrium $x = 0$ of

$$\dot{x} = f\big(x, 0, \alpha(x, 0)\big) \tag{1.5}$$

   is asymptotically stable in the first approximation,

2. there exists a neighborhood $V \subset U \times W$ of $(0, 0)$ such that, for each initial condition $(x(0), w(0)) \in V$, the solution of

$$\begin{aligned} \dot{x} &= f\big(x, w, \alpha(x, w)\big), \\ \dot{w} &= s(w) \end{aligned} \tag{1.6}$$

   satisfies

$$\lim_{t \to \infty} h\big(x(t), w(t)\big) = 0.$$

From [Isi95, Theorem 8.3.2], the necessary and sufficient conditions to solve the full information output regulation problem are

1. the Jacobian matrix of (1.5) at $x = 0$,

$$J = A + BK,$$

   where

$$A = \left[\frac{\partial f}{\partial x}\right]_{(0,0,0)} \quad B = \left[\frac{\partial f}{\partial u}\right]_{(0,0,0)} \quad K = \left[\frac{\partial \alpha}{\partial x}\right]_{(0,0)}$$

   has all eigenvalues with negative real part;

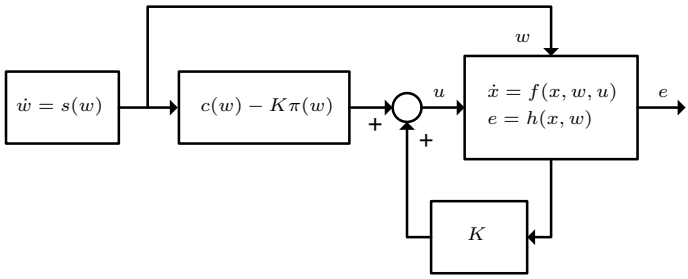

Figure 1.2: State feedback with feedforward control law

2. there exist mappings $x = \pi(w)$, $u = c(w)$, with $\pi(0) = 0$, $c(0) = 0$, both defined in a neighborhood $W^\circ \subset W$ of the origin, satisfying

$$\begin{aligned} \frac{\partial \pi}{\partial w} s(w) &= f\big(\pi(w), w, c(w)\big), \\ 0 &= h\big(\pi(w), w\big) \end{aligned} \tag{1.7}$$

for all $w \in W^\circ$.

In the proof of sufficiency part of [Isi95, Theorem 8.3.2], it is shown that if there exist solutions $\pi(w)$, $c(w)$ such that (1.7) holds, a state feedback with feedforward given by

$$\alpha(x, w) = c(w) + K\big(x - \pi(w)\big) \tag{1.8}$$

solves the full information output regulation problem, where K is any matrix such that the pair of matrices (A, B) is stabilizable. The closed loop system described by (1.6) with the control (1.8) is depicted in Fig. 1.2.

The two control solutions presented above are now briefly discussed. The state feedback with feedforward control approaches that generate control inputs using state and disturbance measurements eliminate the effects of nonzero disturbances that upsets a controlled plant. The effectiveness of the controllers in rejecting external disturbances is demonstrated mathematically in [Isi95] with the assumption that exact knowledge of a plant to be controlled and accurate measurements of state and disturbance are available. Unfortunately in a real world control application such as autonomous helicopter control, uncertainties pertaining the mathematical model, system parameters and measurements are unavoidable. Therefore, a control solution that addresses the stated drawbacks is compulsory.

Nonlinear Adaptive Output Regulation

Even though it is highly favourable to have both the state x and disturbance w measurements for a controller synthesis, such a luxury is not always realistic. A more common situation in control applications is where these measurements are not readily available. Occasionally, only the components of the error e are available for measurements. To provide a controller with the information on disturbances acting upon a system, an estimation of the disturbance can be proven to be advantageous. An internal model incorporating a

prespecified disturbance model to be adapted using error measurements can be setup to produce the disturbance estimation. Addressing nonlinear control systems with external disturbances that belong to a prescribed class and parameter uncertainties, the semiglobal robust output regulation problem from [SI00] is studied concisely here.

To solve the semiglobal robust output regulation problem, an error feedback controller is taken as modeled by equations of the form

$$\begin{aligned} \dot{\xi} &= \eta(\xi, e), \\ u &= \theta(\xi), \end{aligned} \tag{1.9}$$

with state $\xi \in \mathbb{R}^m$ and smooth $\eta(\xi, e)$, $\theta(\xi)$ where $\eta(0,0) = 0$, $\theta(0) = 0$. Since the disturbance w to be rejected is not known, the controller (1.9) must include an internal model to reconstruct the required external information.

Consider a single-input-single-output finite-dimensional nonlinear system described by

$$\begin{aligned} \dot{x} &= f(x, w, u, \mu), \\ y &= h(x, w, \mu), \\ e &= y - q(w, \mu), \end{aligned} \tag{1.10}$$

with state $x \in \mathbb{R}^n$, control input $u \in \mathbb{R}$, disturbance $w \in \mathbb{R}^d$ and error $e \in \mathbb{R}$. The system depends on a vector of unknown parameters μ from a known compact set $\mathcal{P} \subset \mathbb{R}^p$. The functions $f(x, w, u, \mu)$, $h(x, w, \mu)$ and $q(w, \mu)$ are assumed to be smooth with $f(0,0,0,\mu) = 0$, $h(0,0,\mu) = 0$ and $q(0,\mu) = 0$ for every μ. The disturbance w is generated by a neutrally stable linear time-invariant exosystem of the form

$$\dot{w} = S(\sigma) w$$

that depends on a vector of unknown parameters σ belonging to a known compact set $\Sigma \subset \mathbb{R}^\nu$.

The semiglobal robust output regulation problem for system (1.10) can then be formalized as the following: given arbitrary fixed compact sets $K_x \subset \mathbb{R}^n$ and $K_w \subset \mathbb{R}^d$, find a controller of the form (1.9) and a compact set $K_\xi \subset \mathbb{R}^m$, such that

1. the equilibrium $(x, \xi) = (0, 0)$ of the unforced closed loop system

$$\begin{aligned} \dot{x} &= f\big(x, \theta(\xi), 0, \mu\big), \\ \dot{\xi} &= \eta\big(\xi, h(x, 0, \mu)\big) \end{aligned}$$

   is asymptotically stable for every $\mu \in \mathcal{P}$, with domain of attraction containing the set $K_x \times K_\xi$;

2. the trajectory $\big(x(t), \xi(t)\big)$ of the closed loop system

$$\begin{aligned} \dot{w} &= S(\sigma) w, \\ \dot{x} &= f\big(x, \theta(\xi), w, \mu\big), \\ \dot{\xi} &= \eta\big(\xi, h(x, w, \mu) - q(w, \mu)\big), \end{aligned}$$

with initial conditions $\big(x(0), \xi(0), w(0)\big) \in K_x \times K_\xi \times K_w$ exists for all $t \geq 0$, is bounded and satisfies

$$\lim_{t \to \infty} e(t) = 0$$

for every $\mu \in \mathcal{P}$ and every $\sigma \in \Sigma$.

Provided that system (1.10) can be represented in a suitable form (see [SI00, Eq. (10)]), if there exist globally defined mappings $x = \pi_\sigma(w, \mu)$ and $u = c_\sigma(w, \mu)$, with $\pi_\sigma(0, \mu) = 0$ and $c_\sigma(0, \mu) = 0$, where $c_\sigma(w, \mu)$ is a polynomial in the components of w with coefficients dependent on μ and σ, of a degree not exceeding a fixed number independent of μ and σ, then it is shown in [SI00] that the problem of semiglobal robust output regulation for the class of systems under consideration is solvable. By constructing an adaptive canonical internal model that asymptotically estimates the disturbance w and the nonlinearities of the plant, a controller of the form (1.9) can be tuned to achieve asymptotic regulation in the presence of possibly large parameter uncertainties.

Helicopter Control

Despite being a demanding control problem, various attempts have been made to enable autonomous helicopter flights with successful results. Human pilots can undoubtedly perform a spectrum of manned and unmanned helicopter maneuvers guided by their innate biological intelligence. Given the stated advantage, apprenticeship learning algorithms are presented in [ACN10] that involve teaching controllers to execute a wide range of autonomous aerobatic maneuvers as supervised by a human expert. The authors have implemented the apprenticeship learning algorithms for learning a trajectory-based task specification from demonstrations and for modeling the dynamics of the helicopter. A controller is then designed by combining the apprenticeship learning algorithms with a receding horizon variation of linear quadratic control methods for nonlinear systems. By combining the concepts of dynamic inversion and sliding manifold, a nonlinear controller that is robust with respect to functional and parametric uncertainties is developed in [Xu10] for a full helicopter flight envelop. By dividing the control problem into a three-timescale structure, a nonlinear robust controller is designed for each timescale by explicitly considering parametric uncertainties and unmodeled dynamics. In the control design method, the flapping motion is regarded as the fastest mode and the settling time in faster modes is guaranteed to be less than the fixed step size of the slower modes. Acknowledging the unique capability of a helicopter to carry loads hanging in wires, estimation and control of a helicopter slung load system is considered in [BlCHB10]. The length of the suspension system and the system states are estimated by using an adaptive slung load estimator given vision-based sensor data. To enable a helicopter with slung load to perfom maneuvers without inducing residual oscillations, a feedforward control system based on input shaping is developed. Together with a feedback control system that actively dampens oscillations of the slung load, a significant load swing reduction is demonstrated as compared to using only a baseline controller. With the development of a combined inner-outer loop adaptive control architecture, autonomous helicopter flight control to track position, velocity, attitude and angular rate reference commands is solved in [JK02]. The helicopter control loop is separated into an innerloop that controls the attitude and an outerloop that controls the trajectory of the helicopter. By linearizing the attitude and translational dynamics separately using the dynamic inversion method,

linear compensators are designed to control the forces and moments acting on the helicopter. To handle parametric uncertainties in the linearized helicopter model, an artificial neural network is used as an adaptive element. With the use of Pseudo-Control-Hedging, unwanted adaptations to plant input characteristics such as actuator dynamics and to innerloop dynamics are successfully prevented. Isidori et al. addressed a challenging problem in [IMS01] regarding the control of vertical motion of a helicopter while stabilizing the lateral and longitudinal positions and maintaining a constant attitude. Considering an application involving landing operations of an autonomous helicopter on a ship deck, the unknown motion of the ship deck is taken as the sum of a fixed number of sinusoidal signals. By assuming that state measurements are available, a semiglobal robust stabilization scheme is developed based on nonlinear adaptive regulation and robust stabilization of systems in feedforward form by means of saturated controls. It is shown by simulations that the proposed controller performs well in the presence of parametric uncertainties and unmodeled dynamics. While a helicopter vertical trajectory tracking problem is considered in [IMS01], Bejar et al. expand the control solution to include horizontal motion control. In spite of the nonlinearity of helicopter dynamics and strong coupling between forces and torques in a helicopter, vertical and horizontal trajectory control problem is dealt with successfully in [BIMN05]. Given references with specific bounds on the higher order time derivatives, a nonlinear controller is constructed that asymptotically tracks the desired trajectories in the presence of physical and aerodynamical parameter uncertainties. In the derivation of the control law, engine dynamics of the main rotor is included. Simulation results justify the reliability of the proposed control scheme in the face of uncertainties concerning helicopter parameters and actuator model.

In all of the above reviewed research works, the controller designs for an autonomous helicopter do not include wind disturbances either in the control synthesis or controller performance testing. In outdoor flights, the influence of wind disturbances on a helicopter is inevitable and measures to counter its effects have to be taken. In another multi-loop helicopter control design, a control structure combining robust H-infinity and PI control in the presence of model uncertainty, gust disturbance and multi-mode flight requirements is developed in [WMWD09]. By taking a state space representation of the helicopter mathematical model including parameter uncertainties and gust disturbance, a H-infinity controller is designed in the innerloop for robust stability and gust attenuation. To address tracking performance according to flight requirements, PI control is implemented in the outerloop. Stabilization of a simple nonlinear helicopter model in the face of vertical wind gusts is studied in [MLA09]. To achieve disturbance compensation in the 3 degrees of freedom model helicopter mounted on an experimental platform, robust control approaches including robust nonlinear feedback control, active disturbance rejection control based on a nonlinear extended state observer and backstepping control are simulated for comparison purposes. While each of the control techniques possesses its own advantage over the others, simulation results verify the effectiveness of the controllers in handling disturbances and modeling uncertainties. In [GSC$^+$09], a high bandwidth inner loop controller is developed for an autonomous helicopter to provide attitude and velocity stabilization in the presence of wind disturbances based on the L_1 adaptive control theory. The L_1 adaptive controller is designed using a linear time-varying helicopter model with the control objective to track desired bounded reference trajectory and orientation. By simulating the designed controller in a full nonlinear helicopter model with wind disturbances generated using the Von Karman wind model and wind gusts, the superiority of

the L_1 controller over a linear state feedback controller is verified.

To land autonomous helicopters on ships at sea poses an immediate challenge due to ship motion caused by waves and the presence of hostile turbulence. Even though helicopter landing control problem is successfully resolved in [IMS01], the effect of wind disturbances is not taken into account. As analyzed above, although the performance of the controllers developed in [WMWD09, MLA09, GSC+09] is tested for robustness against wind disturbances, the disturbance information is not included explicitly in the control design. To address the problem of controlling heave motion of an autonomous helicopter in the presence of horizontal wind gusts, Yang et al. derived a heave motion model of an autonomous helicopter to capture the main influence of thrust variations in hover [YPG09]. A gust estimator is developed to obtain information on wind gust levels in the presence of sensor errors including accelerometer vibration, accelerometer drift and measurement error of vertical velocity. The estimation of the wind gusts is then fed to a feedback-feedforward proportional derivative controller to compensate for the effects from the horizontal gusts in the stabilization of helicopter heave motion.

1.4 Outline of the Thesis

In the next chapter, research methodology is presented describing undertaken approaches to find solutions for the problems in hand. After a summary of contributions of the Ph.D. project is given in Chapter 3, this thesis in concluded in Chapter 4.

The following papers are part of the thesis.

1. **Paper A [DCHB09b]**
   In this paper, a simple feedforward control scheme for wind disturbance rejection in an autonomous helicopter is introduced. The feedforward control inputs that are generated by trimming the helicopter model subjected to wind disturbance is added to a feedback controller for helicopter stabilization in the presence of wind disturbance.

2. **Paper B [DCHB09a]**
   Assuming that a disturbance affecting a nonlinear plant could be measured, the concept of disturbance effect is defined here. This is then used in the development of a feedforward control scheme independent of an existing feedback controller for disturbance rejection in nonlinear control systems.

3. **Paper C [DCHCB10]**
   In this work, a necessary and sufficient condition for the existence of a stabilizing state feedback with feedforward control that is robust with respect to state and disturbance measurement errors, and external disturbances for a nonlinear control system is developed.

4. **Paper D [DLCHB10]**
   Taking a sum of a fixed number of sinusoidal signals of unknown amplitudes, frequencies and phases as the wind disturbance, a feedback controller incorporating an adaptive internal model is constructed for helicopter stabilization that is insensitive to parameter uncertainties.

5. **Paper E [BCHD10]**
   By inverting a simplified helicopter model provided wind disturbance measurements, feedforward main rotor collective and cyclic pitch angles are generated here. The model based nonlinear feedforward control design for vertical and horizontal wind disturbance rejection is tested in actual flights in a laboratory with controllable wind sources.

6. **Paper F [DLCHB]**
   This journal paper is a extended version of Paper D that includes derivations of equations and proofs of theorems presented in the conference paper.

Based on the definition of disturbance effect and feedforward control strategy for disturbance rejection in nonlinear control systems developed in Paper B, the feedforward control scheme using trim inputs for helicopter stabilization with wind disturbance elimination is proposed in Paper A. Using a higher complexity approach to produce feedforward control inputs given wind disturbance measurements, wind disturbance rejection is demonstrated in Paper E with reference to the same background obtained from Paper B. The control scheme introduced in Paper B and adapted in Paper A and E is a model based approach with the assumption that accurate state and disturbance measurements are available. To address a more realistic scenario, a state feedback with feedforward control that is less sensitive to measurement errors and additive model uncertainties is studied in Paper C. Realizing the challenge in autonomous helicopter control to obtain precise wind disturbance measurements for control input generation, three dimensional wind disturbance estimation is developed in Paper D for robust helicopter stabilization. Although the developed control law is highly mathematical, only a fraction of the steps taken in the control development is presented in Paper D due to the limited number of pages of the conference paper. In Paper F, details of controller constructed in Paper D is elaborated and more simulation results are included.

2 | Methodology

In Section 1.2 of the previous chapter, challenging aspects of the helicopter control design for stabilization with wind disturbance elimination are identified. Given the motivation along with the nature of practical helicopter control, some of the relevant tools that are utilized to solve the problem in hand are listed here. Among others, in [DCHB09a] Lyapunov stability analysis is used to quantify the effects that external disturbances have in nonlinear control systems for the development of a feedforward control strategy for disturbance rejection. With reference to the contribution in [DCHB09a], feedforward control inputs generated by trimming a helicopter model subject to wind disturbances are used for helicopter stabilization. In the derivation of the necessary and sufficient condition for the existence of a robustly stabilizing state feedback with feedforward, the concepts of π-trajectory and differential inclusions play an important role in [DCHCB10]. In [DLCHB10, DLCHB], input-to-state stability of an autonomous helicopter system perturbed by wind disturbances with parameter uncertainties is analyzed. In general, even though a controller developed is mathematically sound, simulations and actual implementations need to be carried out for the verification of proposed control methods. While only a brief introduction on the research methods is given in this chapter, detailed steps and approaches can be referred to in the papers attached as cited below.

2.1 Trim

Trimming a helicopter model involves computing a control input such that the rate of change of a helicopter state is zero and the resultant applied forces and moments is zero [Pad07]. Consider for instance, that a helicopter is in hover in the presence of a wind disturbance with a certain velocity in the negative x direction (see Fig. 5.3). Note that the control needed to sustain such a flight condition is equivalent to a control required to enable the helicopter to fly in the positive x direction with the same velocity (as the wind disturbance in the case). Therefore, if measurements of a wind disturbance are available, control inputs to counter the effects of the wind disturbance can be computed by including the wind velocity measurements in the trim equations [DCHB09b]. Depending on the complexity of a helicopter mathematical model used in the control approach proposed in [DCHB09b], real time implementations can be an issue. Note that the control scheme using trim values assumes a perfect knowledge of the plant to be controlled with precise state and disturbance measurements. Thus, any model mismatch or measurement inaccuracies will possibly affect the performance of the controller.

2.2 Lyapunov Stability

As explained in the previous chapter, in a SISO linear control system, the effect that a disturbance has on output y is known provided that the measurements of disturbance d are available and dynamics D of the disturbance are known (see Fig. 1.1). The importance of the knowledge of disturbance effect in linear control systems is easily noticed as the design of a feedforward controller C_{ff} explicity involves the cancellation of the disturbance effect on the output. In a nonlinear control system (see for e.g. (6.1)) however, since disturbance w is just one of the arguments of nonlinear function f, an effort to design a feedforward controller for a complete disturbance rejection could be dampened due to the lack of information on how an output is actually affected by the disturbance. In view of the Lyapunov stability criterion, if there exists a control-Lyapunov pair as described by [DCHB09a, Definition 2] for nonlinear systems considered therein with zero disturbance input, asymptotic controllability is not guaranteed in the presence of nonzero disturbance w. Keeping that in mind, a concept of disturbance effect for nonlinear systems is defined. As stated in [DCHB09a, Definition 3], the disturbance effect is taken as the difference between state derivative of a control system with a nonzero disturbance and state derivative of an asymptotically controllable disturbance free nonlinear system with feedback control. With the establishment of the disturbance effect notion for nonlinear systems, a feedforward control scheme is proposed to nullify the disturbance effect to retain asymptotic controllability.

2.3 π-trajectory

In real world control applications, due to finite sampling frequencies of sensors used in state and disturbance measurements, constant control inputs over each sampling period is applied to continuous plants. Furthermore, stabilizing control laws are in general discontinuous for general nonlinear control systems [LS99]. Thus it is natural to ponder how to define the solutions of differential equations governing the nonlinear control systems with discontinuous right-hand sides. In other words, a clear definition of the state trajectories under piecewise constant control inputs is needed before stability conditions can be established. By adopting the notion of π-trajectory introduced in [CLSS99], the existence of a robustly stabilizing state feedback with feedforward is studied in [DCHCB10].

2.4 Differential Inclusions

The main theorem in [DCHCB10] establishes a necessary and sufficient condition for the existence of a robustly stabilizing state feedback with feedforward for a general nonlinear control system. In the proof of [DCHCB10, Theorem 1], even though the necessary part is done in a direct way with minimum difficulty, the sufficiency part of the proof requires a more elaborate approach involving the converse Lyapunov function theorem for a strongly asymptotically stable differential inclusion as stated in [DCHCB10, Theorem 2]. If there exists a stabilizing state feedback with feedforward m that is robust with respect to state and disturbance measurement errors and external disturbances for control system (7.1), then it is shown that differential inclusion

$$\dot{x} \in G(x)$$

with multivalued function

$$G(x) := \bigcap_{\varepsilon>0} \overline{\text{co}} \bigcup_{d\in\mathbb{D}} f\big(x, m(x+\varepsilon B, d+\varepsilon B), d\big)$$

is strongly asymptotically stable, where f is a continuous function and d is a persistent disturbance ranging in a compact set $\mathbb{D}$. In the equation above, B is a closed unit ball and $\overline{\text{co}}\, S$ is the closure of the convex hull of a set S. From [DCHCB10, Theorem 2], this implies the existence of a smooth strong Lyapunov function for differential inclusion (7.12) and (7.13). It can be easily observed that the function is a smooth uniform control Lyapunov function for control system (7.1).

2.5 Input-to-State Stability

In general, control systems are subject to the influence of undesired external inputs. The stability of a plant to be controlled in the presence of disturbances can be studied using the Input-to-State Stability (ISS) paradigm.

Consider a nonlinear system

$$\dot{x} = f(x, u), \tag{2.1}$$

with state $x \in \mathbb{R}^n$, input $u \in \mathbb{R}^m$ where $f(x, u)$ is locally Lipschitz on $\mathbb{R}^n \times \mathbb{R}^m$ and $f(0, 0) = 0$. The input function $u : [0, \infty) \to \mathbb{R}^m$ is taken to be any piecewise continuous bounded function with the supremum norm

$$\|u(\cdot)\|_\infty = \sup_{t\geq 0} \|u(t)\|.$$

The property of system (2.1) of having a globally asymptotically stable equilibrium point $x = 0$ in the absence of the forcing input and of exerting bounded trajectories given the bounded input u is characterized by the notion of ISS.

In [DLCHB10, DLCHB], the horizontal dynamics stabilization problem is tackled by showing that different subsystems considered therein can be made input-to-state stable separately with appropriate selections of design parameters. For one of the two subsystems, this is done by proving the existence of an ISS-Lyapunov function which is a necessary and sufficient condition for a system to be input-to-state stable [IMS03, Theorem B.2.1]. It is shown that the state trajectories of each subsystem are bounded by linear gains on the bounds of respective inputs and that the feedback interconnection of the input-to-state stable subsystems satisfies the small gain theorem.

2.6 Simulation

To verify the effectiveness of proposed control methods, simulations of controlled plants are carried out in this thesis. In [DCHB09b], the feedforward control scheme is simulated using a mathematical model of the Aalborg University Bergen Industrial Twin Radio controlled (RC) helicopter. The nonlinear helicopter model has 30 states and includes second order actuator dynamics, blade element theory for main and tail rotor forces and torques, flapping dynamics for main rotor and stabilizer bar, and momentum theory for

the inflow model. Using wind velocity measurements obtained from a WindSonic II wind sensor, trim feedforward control inputs are computed and used in the simulations to demonstrate the feasibility of the proposed approach. Due to the advanced control design in [DLCHB10, DLCHB], a simpler mathematical model of a helicopter is considered. In this model, the overall control input is provided by the main rotor thrust, tail rotor thrust, longitudinal flapping angle and lateral flapping angle. While the control design is carried out based on a simplified resultant external force model, the performance of the controller in a model of higher complexity is investigated by means of simulations.

2.7 Flight Tests

The model based nonlinear feedforward controller developed in [BCHD10] is tested in actual flights of the Aalborg University Corona Rapid Prototyping Platform. The autonomous helicopter is capable of performing full autonomous flights and due to its small size, all control computations are done on ground and transmitted through a standard RC system. The helicopter state and wind disturbance measurements are provided by a Vicon motion tracking system and a R.M. Young 81000 3D ultrasonic anemometer respectively. To enable a controlled experimental setup, the flight tests are carried out in a laboratory equipped with three Big Bear II fans with a diameter of $0.6\,m$. In order to demonstrate the feasibility of the proposed feedforward control technique for measured wind disturbance compensation, two different flight tests are carried out consisting hovering in front of the fans which are then turned on and flying the helicopter through wind stream of running fans.

3 | Summary of Contributions

Attached to this thesis, are published and submitted papers in chronological order to indicate the progressive steps taken towards achieving helicopter stabilization in the presence of wind disturbances. Each paper reports separate contributions of this Ph.D. project detailing specific targeted problems, solutions and verifications of proposed designs. In this chapter, main contributions of this thesis are highlighted with regards to the identified research problems.

3.1 Disturbance Effects

The first contribution of this Ph.D. work is published in [DCHB09a] where the definition of disturbance effects in a nonlinear control system influenced by an external disturbance is given. As pointed out in Section 1.2 with reference to Fig. 1.1, the effect that a disturbance d has on the output y of a single-input-single-output (SISO) linear control system is quantifiable if measurements of the disturbance are available and the disturbance dynamics D are known. With appropriate conditions concerning a SISO linear control system, this information is useful to derive a feedforward controller to produce a disturbance free output (see Section 6.2). In a general nonlinear control system however (see e.g. (6.1)), since disturbance w is one the external inputs of system f, the influence of the disturbance on system state is not readily understood. If one desires to employ feedforward control for disturbance rejection, a clear definition of disturbance effect is crucial so that its elimination can be verified to ensure a disturbance free system response. In [DCHB09a], guided by the outcome obtained from disturbance feedforward control of a SISO linear control system with a known disturbance effect, the notion of disturbance effect $\mathcal{D}$ in a nonlinear control system affected by an external disturbance w is introduced using Lyapunov stability analysis. The disturbance effect $\mathcal{D}$ is defined as the difference between state derivative of a control system f with nonzero disturbance w and state derivative of an asymptotically controllable disturbance free nonlinear system with feedback control u_{fb} (see (6.5)).

3.2 Feedforward Control Strategy for Disturbance Rejection

With the establishment of the disturbance effects notion, the next contribution concerning a feedforward control scheme for disturbance rejection is reported in [DCHB09a]. Given a SISO linear control system as depicted in Fig. 1.1, provided that the disturbance d and its dynamics D are known, feedforward control is an efficient technique of controlling the

undesirable disturbance effect Dd on system output y by compensating before the effects take place. As elaborated in Section 6.2, with the inclusion of the feedforward controller C_{ff}, system output y appears to be only controlled by a feedback C_{fb} with complete elimination of the external disturbance d. Keeping that in mind, and given the definition of disturbance effect $\mathcal{D}$ when disturbance w is included in an asymptotically controllable disturbance free nonlinear system with feedback u_{fb} (see (6.5)), a feedforward control u_{ff} is taken as the control signal that can be added to the feedback u_{fb} such that $\mathcal{D} = 0$ as in (6.6). It is shown that the addition of feedforward control u_{ff} in a nonlinear control system (6.1) affected by external disturbance w would result in a system appearing to behave as if only feedback control u_{fb} is present with zero disturbance input. Thus, the feedforward control retains the asymptotic controllability of the feedback control system without disturbance as shown in (6.7).

3.3 Robustly Stabilizing State Feedback with Feedforward

Even though the feedforward controller proposed in [DCHB09a] is effective in disturbance rejection, the existence of such a control solution is not guaranteed. By developing a condition for the existence of a stabilizing state feedback with feedforward for nonlinear control systems, a significant contribution is made in this thesis as published in [DCHCB10]. Consider general nonlinear control systems of the type

$$\dot{x} = f(x, u, d), \quad x \in \mathbb{R}^n, u \in \mathbb{U}, d \in \mathbb{D}, \tag{3.1}$$

where $\mathbb{U} \subset \mathbb{R}^c$ is a compact set, persistent disturbance $d = d(\cdot)$ is a measurable function taking values in some compact set $\mathbb{D} \subset \mathbb{R}^w$ and $f : \mathbb{R}^n \times \mathbb{U} \times \mathbb{D} \to \mathbb{R}^n$ is a continuous function.

In [LS99], it is shown that the existence of a smooth uniform control Lyapunov function V for system (3.1) satisfying the following infinitesimal decrease condition

$$\min_{u \in \mathbb{U}} \max_{d \in \mathbb{D}} \langle \nabla V(x), f(x, u, d) \rangle \leq -W(x) \quad \forall x \in \mathbb{X}, x \neq 0, \tag{3.2}$$

where $W : \mathbb{R}^n \to \mathbb{R}_{\geq 0}$ is a continuous function and $\mathbb{X} \subset \mathbb{R}^n$ is a bounded set, implies the existence of a robustly stabilizing state feedback. Futhermore, it is also proven that if there exists a robustly stabilizing state feedback then there exists a smooth uniform control Lyapunov function. Robustness in this context means that given any pair $0 < r < R$, the state feedback drives all states in the ball of radius R into the ball of radius r after some time T for fast enough sampling and small enough measurement errors and external disturbances.

In this Ph.D. work, guided by the approach taken in [LS99], for control applications where measurements of a persistent disturbance d are available, a necessary and sufficient condition for the existence of a stabilizing state feedback with feedforward which is insensitive to measurement errors and external disturbances is developed.

Concerning the sufficiency part, if there exists a smooth uniform control Lyapunov function V for system (7.1) satisfying the infinitesimal decrease condition (see (7.3))

$$\min_{u \in \mathbb{U}} \langle \nabla V(x), f(x, u, d) \rangle \leq -W(x) \quad \forall x \in \mathbb{X}, x \neq 0, \forall d \in \mathbb{D}, \tag{3.3}$$

then there always exists a (discontinuous in general) state feedback with feedforward $m : \mathbb{R}^n \times \mathbb{R}^w \to \mathbb{U}$ which satisfies

$$\big\langle \nabla V(x), f\big(x, m(x,d), d\big)\big\rangle \leq -W(x), \quad \forall x \in \mathbb{X}, x \neq 0, \forall d \in \mathbb{D}. \tag{3.4}$$

Note that the infinitesimal decrease condition (3.3) adopted in this thesis is different than (3.2) considered in [LS99]. To prove that the state feedback with feedforward m satisfying (3.4) is robustly stabilizing, [DCHCB10, Lemma 2] is developed. The lemma shows that given fast enough sampling and small enough measurement errors and external disturbances, every π-trajectory of (7.6) does not blow-up and that the time derivative of V remains negative in each sampling interval.

The establishment of the necessary condition involves a more elaborate formulation. A necessary and sufficient condition is developed for the existence of a robustly stabilizing state feedback with feedforward m concerning the stability property of differential inclusion (7.12) with multivalued right-hand side (7.13). This result is formulated in [DCHCB10, Proposition 2] whose proof requires a relationship between solutions of perturbed system (7.6) and solutions of differential inclusion (7.12) and (7.13) as devised in [DCHCB10, Lemma 1]. Subsequently, using the converse Lyapunov function theorem from [CLS98] for differential inclusions with upper semicontinuous right-hand side, the existence of a smooth uniform control Lyapunov function V for system (7.1) is verified.

3.4 Wind Disturbance Estimation and Helicopter Stabilization

Acknowledging the challenge involved in obtaining reliable wind disturbance measurements for helicopter control, a state feedback controller equipped with an adaptive internal model for three dimensional wind disturbance estimation is developed in [DLCHB10, DLCHB] and is considered as the main contribution of this thesis. In [IMS03], a specific helicopter control application is addressed where an autonomous helicopter is required to land on the deck of a ship which is subject to oscillations due to sea waves. To solve the control problem, an adaptive internal-model-based controller is designed for enable the helicopter to track a vertical reference trajectory given as the sum of a fixed number of sinusoidal functions of time, of unknown frequency, amplitude and phase, that has to be estimated using tracking errors. Despite large uncertainties in parameters characterizing the motion of the landing deck and large model uncertainties, the control solution which is based on nonlinear adaptive output regulation and robust stabilization of systems in feedforward form by means of saturated controls, solves the trajectory tracking problem for any arbitrary large set of initial conditions.

Motivated by the satisfactory performance reported in [IMS03], a more challenging problem is tackled in this thesis involving helicopter stabilization in the presence of wind disturbances in all three axes. While one of the objectives of the adaptive internal model included in the vertical dynamics in [IMS03] is to estimate the vertical motion of a ship deck, adaptive internal models are used in [DLCHB10, DLCHB] to estimate wind disturbances affecting translational motions of the helicopter in all axes. Realizing the importance of information on the wind disturbance in stabilizing control input generation and addressing a realistic scenario where accurate onboard disturbance measurements are not available, the estimation is considered as an integral part of the control design. To develop an adaptive internal-model-based controller, the wind disturbances are taken to be the sum

of a fixed number of sinusoids whose frequencies, amplitudes and phases are unknown constants. This assumption is crucial so that the wind disturbance can be viewed as an output of an linear autonomous exosystem to facilitate the synthesis of a robust nonlinear controller of the following form

$$\begin{aligned} \dot{\boldsymbol{\xi}} &= \phi(\boldsymbol{\xi}, p^i, \dot{p}^i), \\ \mathbf{u} &= \theta(\boldsymbol{\xi}, p^i, \dot{p}^i, q, \omega^b), \end{aligned} \tag{3.5}$$

incorporating the linear internal model ϕ, where p^i and ω^b denote the position (expessed in an inertial coordinate frame) of the center of mass and angular velocity (expessed in a body-fixed coordinate frame) of the helicopter respectively, q is the vector part of unit quarternions and $\boldsymbol{\xi}$ is the state of the feedback controller. The vector $\mathbf{u} = [T_M \ a \ b \ T_T]^\top$ is taken as the control input, where T_M, T_T, a and b are main rotor thrust, tail rotor thrust, longitudinal main rotor tip path plane tilt angle and lateral main rotor tip path plane tilt angle respectively.

The problem of helicopter stabilization with wind disturbance elimination is solved by first designing a control law to generate the main rotor thrust T_M for vertical dynamics stabilization. Since the objective of the control law is to compensate for the gravity force gM and the vertical wind disturbance d_z (see (10.7)), an internal model is required to estimate the unknowns. It is shown in [DLCHB10, DLCHB] that the control law (10.15), (10.18) and (10.19) renders the vertical dynamics stable provided that q is sufficiently small, which can be ensured by tuning the control law (10.23) and (10.25) for control input $\mathbf{v} = [a \ b \ T_T]^\top$ (see [DLCHB, Proposition 5]). Next, the stability of longitudinal and lateral dynamics is proven by showing that the feedback interconnection of input-to-state stable subsystems (10.30) and (10.36) satisfies the small gain theorem as formalized in [DLCHB, Proposition 6]. As part of the proof of [DLCHB, Proposition 6], [DLCHB, Lemma 3] establishes the existence of a selection of tuning parameters of control law $\mathbf{v}$ (that matches the requirements of [DLCHB, Proposition 5]) which assures that subsystem (10.36) is input-to-state stable.

4 | Conclusion

With numerous application possibilities of autonomous helicopters, an immediate challenge arises involving the ability to cope with wind disturbances. While state feedback controllers without any information on the external effects would suffice in some instances, control input generation which relies on knowledge on the wind disturbances is certainly desired for higher quality flights. This is because, given the wind disturbance measurements a complete information on external inputs affecting the controlled plant is now available which is crucial for an effective helicopter control.

4.1 Objectives of the Project

Given the primary objective of this thesis that is to achieve helicopter stabilization in the face of wind disturbances, helicopter control that requires the influence of wind disturbances in control input generation is studied. In other words, stabilization of an autonomous helicopter using control inputs as a function of the measurements or estimation of wind disturbances is the main goal here. In nonlinear control systems where measurements of external disturbances are available, state feedback with feedforward control methods such as full information output regulation and disturbance decoupling can ensure stabilization despite the influence of the disturbance. Under suitable conditions, these control schemes that require system state and disturbance measurements guarantee disturbance free outputs. In helicopter stabilization where wind disturbances could be measured, in addition to disturbance attenuation, it is also of interest to understand the effects that the wind disturbances have on the helicopter system. With the quantification of the disturbance effects, a feedforward control added to an existing feedback can be the one that nullifies the disturbance effects. Acknowledging the challenges in reality to obtain accurate mathematical description of a helicopter and state and disturbance measurements, the development of a state feedback with feedforward that is insensitive to measurement errors and model uncertainties is set as one the goals of this research. An immediate concern in the design of a state feedback with feedforward for helicopter control is regarding the availability of wind disturbance measurements. Crucial issues pertaining sensor mounting location, accuracy, cost, time delay, etc. hamper the development of such a control scheme. Given the problem of having reliable wind disturbance measurements and realizing the importance of the information on wind disturbances in stabilizing control input generation, three dimensional wind disturbance estimation presents itself as an important objective of this thesis.

4.2 Contributions of the Project

In this thesis, a preliminary idea based on disturbance feedforward control in SISO linear control systems led to the establishment of the definition of disturbance effects in nonlinear control systems influenced by external disturbances. The effects of a disturbance in a nonlinear control system are described through comparison with the same control system that is asymptotically controllable with a feedback control in the absence of the disturbance. As a consequence of the first contribution on this thesis, a feedforward control strategy for disturbance rejection in nonlinear control systems that can be added to an existing feedback to cancel the disturbance effects is proposed. The formulation of the disturbance effects and the related feedforward control scheme for nonlinear control systems form the foundation of the development of feedforward control approaches for autonomous helicopters using trim inputs and inverted helicopter model. The feasibility of the proposed control methods for wind disturbance cancellation is demonstrated through simulations and flight tests. Since the performance of the control approach depends entirely on the availability of an exact mathematical model of a system to be controlled and precise disturbance measurements, application issues involving model and measurement uncertainties need to be addressed. This led to the establishment of a necessary and sufficient condition for the existence of a robust state feedback with feedforward control for the stabilization of nonlinear control systems. Given the fact that in general such a control is discontinuous, the notion of π-trajectory is used to define the solution of a nonlinear control system under a possibly discontinuous state feedback with feedforward control, in the presence of disturbances, state and disturbance measurement errors, and additive model uncertainties. The result presented in this thesis concerning the state feedback with feedforward control that is insensitive to measurement errors and external disturbances is derived employing among others, the converse Lyapunov function theorem for strongly asymptotically stable differential inclusions with upper semicontinuous right-hand side. Even though the specified contribution in nonlinear control deals with uncertainties that is inevitable in practical implementations, in helicopter control even wind disturbance measurements of modest quality can be a luxury given the influence of main rotor downwash. Therefore, three dimensional wind disturbance estimation for autonomous helicopter stabilization is developed and considered as the main contribution of this thesis. Equipped with an adaptive internal model for wind disturbance estimation and to handle parameter uncertainties, a controller is designed based on nonlinear adaptive output regulation and robust stabilization of systems in feedforward form by saturated feedback controls. The developed control law solves the problem of helicopter stabilization with wind disturbance elimination whose performance is verified through simulations.

In practical autonomous helicopter control, some complications due to the presence of model and parameter uncertainties, measurement errors and unmodelled dynamics will naturally arise. If a persistently acting wind disturbance can be measured, a robustly stabilizing state feedback with feedforward is expected to render the helicopter asymptotically stable provided that the measurement errors and model uncertainties are small enough and that the sampling is fast enough. However, since it is cumbersome to measure the wind disturbance on an autonomous helicopter, an estimate of the wind disturbance using an adaptive internal model can be a good substitute. While the nonlinear controller with an internal model can handle parameter uncertainties, there is no surety that it is insensitive to measurement errors. Returning to the wind turbine inspection application, owing

to the contribution of this thesis, a helicopter can now be dispatched from any permitted location around a wind turbine to execute designated routines. This is because the internal model based nonlinear controller guarantees helicopter stabilization in the face of wind disturbances from any initial conditions ranging in an arbitrarily large compact set. Equipped with the explicit capability to handle parameter uncertainties, the proposed helicopter control technique is an enabling technology in wind turbine inspection and a spectrum of other unmanned real world applications.

4.3 Future Work

In the course of this Ph.D. project, several contributions related to nonlinear control and helicopter stabilization are achieved. Even though significant results are obtained satisfying the objectives of this thesis, there is still room for more works. In particular, to test the feasibilty of the proposed adaptive internal model based controller developed in [DLCHB10, DLCHB], an actual helicopter flight implementation will certainly be the action to be taken next. Recall that in this thesis, the control input is provided by main rotor thrust, tail rotor thrust, longitudinal main rotor tip path plane tilt angle and lateral main rotor tip path plane tilt angle. While significant simplification is obtained in the control design due to the absence of nonlinearities of servo and rotor flapping dynamics, the use of such an actuator model does not represent the real world helicopter control problem. Hence, before the proposed control could be applied on an actual helicopter, servo and rotor flapping dynamics have to be included in the control synthesis.

When the helicopter equipped with the improved controller is ready for actual flights, a subsequent future work could involve a suitable practical application. In wind turbine inspection using autonomous helicopters for instance, while the stabilization of a helicopter with wind disturbance elimination plays a major role in effective test and check routines, it is still inadequate to perform a fully autonomous inspection. To carry out desired tasks with minimum intervention from human operators, a helicopter has to be equipped with more autonomous capabilities such as autonomous lift-off and landing, path planning, trajectory tracking, obstacle avoidance, etc.

In general, autonomous helicopters are small in size. Consequently, with limited ability to generate force to drive its dynamic motion, the level of wind disturbances that could be withstood is limited. In critical applications where only a small error margin is allowed, it would be beneficial to identify the constraint in wind disturbances that could be handled for helicopter stabilization. This would be another important course of research since by knowing the intrinsic limitation of an autonomous helicopter in wind disturbance rejection, efficiency and safety in practical implementations will be certainly improved.

References

[ACN10] Pieter Abbeel, Adam Coates, and Andrew Y. Ng. Autonomous Helicopter Aerobatics through Apprenticeship Learning. *The International Journal of Robotics Research*, 29(8), 2010.

[BCHD10] M. Bisgaard, A. Cour-Harbo, and K. A. Danapalasingam. Nonlinear feedforward control for wind disturbance rejection on autonomous helicopter. In *2010 IEEE/RSJ International Conference on Intelligent Robots and Systems*, October 2010.

[BIMN05] M. Bejar, A. Isidori, L. Marconi, and R. Naldi. Robust vertical/lateral/longitudinal control of an helicopter with constant yaw-attitude. In *Decision and Control, 2005 and 2005 European Control Conference. CDC-ECC '05. 44th IEEE Conference on*, pages 6192 – 6197, 12-15 2005.

[BlCHB10] Morten Bisgaard, Anders la Cour-Harbo, and Jan Dimon Bendtsen. Adaptive control system for autonomous helicopter slung load operations. *Control Engineering Practice*, 18(7):800 – 811, 2010. Special Issue on Aerial Robotics.

[CLS98] F. H. Clarke, Yu. S. Ledyaev, and R. J. Stern. Asymptotic stability and smooth Lyapunov functions. *J. Differential Equations*, 149(1):69–114, 1998.

[CLSS99] F. H. Clarke, Yu. S. Ledyaev, E.D. Sontag, and A. I. Subbotin. Asymptotic controllability implies feedback stabilization. *IEEE Trans. Autom. Control*, 42:1394–1407, 1999.

[DCHB09a] K. A. Danapalasingam, A. Cour-Harbo, and M. Bisgaard. Disturbance effects in nonlinear control systems and feedforward control strategy. In *The 7th IEEE International Conference on Control and Automation*, December 2009.

[DCHB09b] K. A. Danapalasingam, A. Cour-Harbo, and M. Bisgaard. Feedforward control of an autonomous helicopter using trim inputs. In *AIAA Infotech@Aerospace Conference and AIAA Unmanned...Unlimited Conference*, April 2009.

[DCHCB10] K. A. Danapalasingam, A. Cour-Harbo, G. Chowdhary, and M. Bisgaard. A robust stabilization using state feedback with feedforward. In *2010 American Control Conference*, June 2010.

[DLCHB] K. A. Danapalasingam, J. Leth, A. Cour-Harbo, and M. Bisgaard. Robust helicopter stabilization with wind disturbance elimination. *Submitted to International Journal of Robust and Nonlinear Control*.

[DLCHB10] K. A. Danapalasingam, J. Leth, A. Cour-Harbo, and M. Bisgaard. Robust helicopter stabilization in the face of wind disturbance. In *49th IEEE Conference on Decision and Control*, December 2010.

[GSC+09] B.J. Guerreiro, C. Silvestre, R. Cunha, C. Cao, and N. Hovakimyan. L1 adaptive control for autonomous rotorcraft. pages 3250 –3255, jun. 2009.

[IMS01] A. Isidori, L. Marconi, and A. Serrani. Robust nonlinear motion control of a helicopter. volume 5, pages 4586–4591 vol.5, 2001.

[IMS03] Alberto Isidori, Lorenzo Marconi, and Andrea Serrani. *Robust autonomous guidance: An internal model approach*. Advances in Industrial Control. Springer-Verlag New York, Inc., Secaucus, NJ, USA, 2003.

[Isi95] Alberto Isidori. *Nonlinear control systems*. Communications and Control Engineering Series. Springer-Verlag, Berlin, third edition, 1995.

[JK02] E.N. Johnson and S.K. Kannan. Adaptive flight control for an autonomous unmanned helicopter. In *Proceedings of the AIAA Guidance, Navigation, and Control Conference*, pages 2002–4439, 2002.

[Lov07] Jonathan Love. *Process Automation Handbook: A Guide to Theory and Practice*. Springer, London, 2007.

[LS99] Yuri S. Ledyaev and Eduardo D. Sontag. A Lyapunov characterization of robust stabilization. *Nonlinear Anal.*, 37(7, Ser. A: Theory Methods):813–840, 1999.

[MLA09] Adnan Martini, Franois Lonard, and Gabriel Abba. Dynamic modelling and stability analysis of model-scale helicopters under wind gust. *Journal of Intelligent and Robotic Systems*, 54:647–686, 2009.

[Pad07] G. Padfield. *Helicopter Flight Dynamics, Second Edition: The Theory and Application of Flying Qualities and Simulation Modeling*. Blackwell Science Ltd, 2nd edition, 2007.

[SI00] A. Serrani and A. Isidori. Semiglobal nonlinear output regulation with adaptive internal model. In *Decision and Control, 2000. Proceedings of the 39th IEEE Conference on*, volume 2, pages 1649 –1654 vol.2, 2000.

[WMWD09] Hong-qiang Wang, Ashfaq Mian, Dao-bo Wang, and Hai-bin Duan. Robust multi-mode flight control design for an unmanned helicopter based on multi-loop structure. *International Journal of Control, Automation and Systems*, 7:723–730, 2009.

[Xu10] Yunjun Xu. Multi-timescale nonlinear robust control for a miniature helicopter. *Aerospace and Electronic Systems, IEEE Transactions on*, 46(2):656 –671, april 2010.

[YPG09] X. Yang, H. Pota, and M. Garratt. Design of a gust-attenuation controller for landing operations of unmanned autonomous helicopters. In *18th IEEE International Conference on Control Applications*, pages 1300 – 1305, July 2009.

Paper A

Feedforward Control of an Autonomous Helicopter using Trim Inputs

Kumeresan A. Danapalasingam, Anders la Cour-Harbo and Morten Bisgaard

This paper was published in:
Proceedings of the AIAA Unmanned...Unlimited 2009 Conference and Exhibit
06–09 April 2009, Seattle, Washington, United States of America

Abstract

In this paper, a feedforward control strategy augmented to an existing feedback controller is demonstrated for an autonomous helicopter. The sole purpose of the feedforward controller is to assist the feedback loop in rejecting wind disturbances based on wind velocity measurements made onboard the helicopter. The feedforward control actions are obtained through trimming of the helicopter model subjected to a simulated wind, while a linear quadratic regulator (LQR) is implemented as the feedback controller. Based on simulations performed using mathematical model of the Bergen Industrial Twin autonomous helicopter with various wind velocity measurements, the feasibility of this approach for wind disturbance rejection is verified.

Nomenclature

d	external disturbance
r	reference input
y	plant output
C_{ff}	feedforward controller
C_{fb}	feedback controller
P	linear plant
D	external disturbance dynamics
f	helicopter nonlinear equation of motion
u	control input vector
x	state vector
$\dot{x}$	state derivative vector
n	state space dimension
m	control input space dimension
x_e	equilibrium state vector
u_e	trim control input vector
x	position in x-axis
y	position in y-axis
z	position in z-axis
v_x	body translational velocity in x-axis
v_y	body translational velocity in y-axis
v_z	body translational velocity in z-axis
d_x	wind velocity in x-axis
d_y	wind velocity in y-axis
d_z	wind velocity in z-axis
ξ_b	trim condition based on body velocity
ξ_d	trim condition based on wind disturbance velocity
ξ_0	trim condition for hover
$\mathbf{V_b}$	helicopter body velocity vector $[v_x\ v_y\ v_z]$
$\mathbf{V_d}$	wind disturbance velocity vector $[d_x\ d_y\ d_z]$
V_b	length of $\mathbf{V_b}$
γ_w	sideslip angle
γ_{fp}	flight plane angle
$\dot{\psi}_{\text{trim}}$	yaw rotation rate
T	trim function

u_{fb}	feedback control input
u_{ff}	feedforward control input
Δu_{fb}	change in feedback control input
Imp	performance measure
x_{fb}	output state vector with feedback control only
$x_{\text{fb+ff}}$	output state vector with feedback and feedforward control

5.1 Introduction

Autonomous helicopters are small-scale helicopters, mostly equipped with on-board intelligence capable of performing various tasks to assist human beings in their daily lives. Due to the physical scaling effects and specific design features found in helicopters of that size, unmanned autonomous helicopters are agile and highly maneuverable making them the best candidates for many applications [1]. Such applications include surveillance, search and rescue, law enforcement, aerial mapping, cinematography, inspection, etc. In agricultural applications for instance, autonomous helicopters can be used to detect pest infestations, pesticide and fertilizer distribution, seed application, etc. In carrying out designated tasks as accurately as possible, the design of high performance controllers that could reject known and unknown disturbances and at the same time guarantee stability to produce desired flight quality is crucial. To date, numerous controller designs for autonomous helicopters have been accomplished with excellent results and a brief review will be given here.

In Ref. [2] and [3], a hierarchical flight control system for unmanned aerial vehicles is designed where the lower level of stabilization and tracking problem is solved by using both multi-loop PID controller and nonlinear MPC separately for comparison purposes. At each sample time, a nonlinear MPC computes a finite control sequence, which minimizes a cost function, typically a weighted quadratic sum of states and input over a finite horizon. Kim et al. used a discretized internal model obtained from a partially nonlinear continuous-time model (with nonlinear force terms and full nonlinear kinematic equations). In another work, Kim et al. investigated the feasibility of a nonlinear model predictive tracking control by formulating a nonlinear MPC algorithm for planning paths under input and state constraints and tracking the generated position and heading trajectories, and implement an on-line optimization controller using gradient-descent method. It was shown in Ref. [4] that the nonlinear MPC outperforms the conventional multi-loop PD controller in the tracking performance when the nonlinear kinematics and coupling dominate the vehicle dynamics even in the presence of model uncertainty.

In Ref. [5], an interesting problem is solved by Shim et al. with the implementation of MPC in unmanned aerial vehicle autonomous exploration in unknown urban environment. Here, information about the surroundings is gathered, and obstacles in the flight path are avoided by building local obstacle maps and solving for conflict-free trajectory using MPC framework. An MPC algorithm with a cost function that penalizes the proximity to the nearest obstacle plans recurrently the flight path in real-time. It is reported that the proposed approach successfully guided the vehicle safely through the urban canyon.

Wan et al. [6] described a method for helicopter control through the use of the FlightLab simulator coupled with nonlinear control techniques. FlightLab is a commercial software product developed by Advanced Rotorcraft Technologies. One of the outstanding features of the FlightLab is its ability to accurately model the main rotor and the

interaction between it and other components, such as the tail rotor (through the use of empirical formulas), external wind (e.g., through an external wind server), ground effects (including both in- and out-of-ground effects with an image method, a free wake model, and horse-shoe ground vortex model), etc. It also includes the modeling of dynamic stall, transonic flow, aero elastic response, vortex wake, blade element aerodynamics, and can also provide finite element structure analysis. In the approach which referred to as model predictive neural control (MPNC), a feedback controller as a combination of a state-dependent Riccati equation (SDRE) controller and an optimal neural controller is utilized. The SDRE controller provides a robust stabilizing control, while the weights of the neural networks are optimized to minimize the overall receding horizon MPC cost. FlightLab has the built-in capability of incorporating some forms of winds (e.g., sinusoidal gusts, stochastic atmospheric turbulent wind, etc.) into the calculation of total air loads on the rotors as well as fuselage. In Ref. [6], the existing atmospheric turbulent wind component (ATMTUR) is replaced with the one developed to allow inputs from an external wind server.

It is common to separate the autonomous helicopter flight control problem into an innerloop that controls attitude and an outerloop that controls the trajectory of the helicopter [7]. A neural network based direct adaptive control was applied in Ref. [7] to control a helicopter where the reference commands include position, velocity, attitude and angular rate. E. N. Johnson and S. K. Kannan used the neural network to minimize the effects of parametric uncertainty due to approximate inversion and pseudo control hedging to modify the innerloop reference model dynamics. With the control approach along with correct placement of the combined poles of the linearized system, it was reported that the inner/outer loop interaction problems was mitigated and outer loop bandwidth increased, improving tracking performance further.

In this paper, the capability of a combination of feedback and feedforward controllers to remove the effects of wind disturbance on an autonomous helicopter will be demonstrated. As opposed to feedback controllers where unknown disturbances with unknown effects are handled to obtain desired output response, feedforward controllers eliminate disturbances more effectively by responding to measured disturbances with known dynamics before the system is affected [8]. Here, the authors generate the feedforward control inputs from a trimmed helicopter model given wind disturbance measurements. A trimmed helicopter model is defined as a mathematical model where the rate of change of the helicopter's state vector is zero and the resultant of the applied forces and moments is zero [9]. By providing wind velocity measurements to the trim equations, feedforward control inputs needed to reject the disturbances are calculated.

In the remainder of this paper, main concepts of feedforward control of an autonomous helicopter using trim control inputs is explained after which a brief introduction on the helicopter model used and simulation results are given. In Section 5.2, the idea of feedforward control using trim inputs is detailed. The hardware which the simulation is based on and simulation results are given in Section 5.3. In Section 5.4 and 5.5, discussion and conclusion are provided respectively.

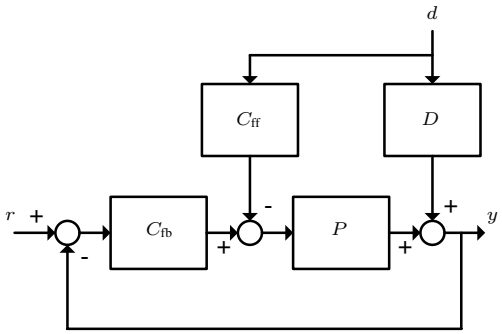

Figure 5.1: Feedforward control

5.2 Concept

Feedforward controllers eliminate disturbances by taking action to measured disturbances with known dynamics before the system is affected [8]. In the helicopter case, a feedforward controller could be designed if wind disturbance dynamic model that affects the end response is available and additive control signals to reject or to minimize this disturbance could be computed. Due to the complexity in obtaining these models, a new approach is presented in this paper where helicopter trim control inputs are considered as alternative solutions for wind disturbance rejection. In this section, the aforementioned concept of feedforward control using trim inputs is clarified in stages after which a conceptual example is presented.

Feedforward Controllers

Generally there are two main concepts in automatic control strategy, namely the feedback (closed-loop) control and feedforward (open-loop) control. Relatively, feedback control is more commonly used and is the underlying concept in most automatic control theories that exist today [8]. A feedback controller C_{fb} as shown in Fig. 5.1, provides corrective control actions if the output y of the linear plant P deviates from reference input r for any reason. On the other hand, the main idea of the classical feedforward controller C_{ff} is to counteract the disturbance d with dynamics D before it affects y [10]. In concept, feedforward control yields much faster correction than feedback control since theoretically, the effects of d is eliminated as soon as it enters the control system [8].

For a helicopter control system however, wind disturbance dynamics is not augmented to the output state vectors as shown in Fig. 5.1, but propagated through the model. This means that in the helicopter model used in this paper, the authors do not have the luxury of having a disturbance model as D which is decoupled from the plant since the effects of external wind is included by adding the wind velocity vector to body velocity vector [11].

Trim

The general nonlinear equations of motion of an autonomous helicopter are given by

$$\dot{x} = f(x, u), \tag{5.1}$$

where $x \in \mathbb{R}^n$ is the n element state vector and $u \in \mathbb{R}^m$ is the m element control input vector.

Trimming involves computing the trim solution which is given by the zero of Eq. (5.1), where the controls u_e required to hold a defined state x_e in equilibrium are calculated. Referring to Eq. (5.2), a trim flight condition is defined as one in which the time derivative of the aircraft's state vector is zero and the resultant of the applied forces and moments is zero [9].

$$f(x_e, u_e) = 0. \tag{5.2}$$

This is formulated as a minimization problem which enables us to solve the nonlinear set of equations with a numerical approach. However, with both the state vector of n elements and the input vector of m elements as the unknowns and only n system equations, the problem is not square. For the helicopter, we have an input vector of four elements and therefore for the system to be solvable, another four equations must be added to the system. This is done by introducing four equations that represent the actual trim condition. A trim condition $\xi_b \in \mathbb{R}^4$ is given as

$$\xi_b = \begin{bmatrix} V_b \\ \gamma_w \\ \gamma_{\text{fp}} \\ \dot{\psi}_{\text{trim}} \end{bmatrix}, \tag{5.3}$$

where V_b is the length of the body velocity vector $\mathbf{V_b}$, γ_w is the sideslip angle, γ_{fp} is the flight plane angle and $\dot{\psi}_{\text{trim}}$ is the yaw rotation rate [11]. For the rest of this paper, trim function T in Eq. (5.4) is defined as a function that provides the trim control input values given the trim condition ξ_b.

$$T : \xi_b \mapsto u_e, \tag{5.4}$$

where $u_e \in \mathbb{R}^4$. Readers should note that solving Eq. (5.2) also gives x_e but it is the u_e that of interest here.

Trim Feedforward Control Values

In trimming, control inputs required to hold the output state vector at certain values are computed. If wind velocity measurements that would disturb the autonomous flight are available, these disturbance values could be included in Eq. (5.1) as constituents of v_x, v_y and v_z. It is assumed that the effects of wind disturbance could be included in the simulation model by adding the wind velocity components to helicopter body velocities. The general idea to eliminate the wind disturbance is to have the helicopter fly in the opposite direction of the wind velocity. For an example, if the helicopter encounters a wind disturbance in the negative direction of the helicopter motion, the most logical way to counter this disturbance is by flying opposing the direction of the disturbance with the same speed as the wind. Therefore, as a feedforward control measure, trim solution or control input values based on wind velocity measurement could then be calculated and added to feedback control signals to eliminate the influence of the disturbance.

The basic idea is to counter the wind disturbance by adding a feedforward control signal u_{ff} to the signal u_{fb} from the feedback controller before it enters the plant. This is

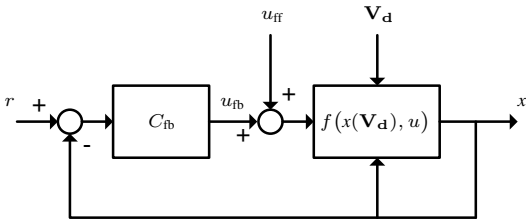

Figure 5.2: A simple representation of feedforward control for helicopter

shown in Fig 5.2. Since $T(\xi_d)$ is the control input needed to keep the helicopter in the equilibrium state related to the wind disturbance trim condition, $T(\xi_b)$ provided by the feedback controller from the given body velocity must be subtracted. This is illustrated in Fig. 5.2, where the plant is disturbed by a wind velocity $\mathbf{V_d}$ as depicted in Fig. 5.3. Thus, effective values of feedforward control inputs would be given by

$$u_{\text{ff}} = T(\xi_d) - T(\xi_b), \tag{5.5}$$

where ξ_d is the trim condition based on disturbance velocity vector $\mathbf{V_d} = [d_x \ d_y \ d_z]$ and ξ_b is the trim condition based on current body velocity $\mathbf{V_b}$. For better understanding of the trim condition based on $\mathbf{V_d}$, Fig. 5.4 illustrates the flight condition that results from the application of $T(\xi_d)$. Now, assume a hover flight condition and that the wind disturbance is coming from the front of the helicopter. These assumptions do not cause loss of generality since the feedforward control concept is independent of wind direction, and trim values can be computed for any equilibrium flight condition. Consequently, we now assume $\mathbf{V_d} = [d_x \ 0 \ 0]$. With the assumption that the feedback controller always brings the helicopter back to hover in the face of disturbances, corrective feedforward control inputs

$$u_{\text{ff}} = T(\xi_d) - T(\xi_0) \tag{5.6}$$

is added to feedback control signals where ξ_d is trim condition based on $\mathbf{V_d} = [d_x \ 0 \ 0]$ and ξ_0 is trim condition based on $\mathbf{V_b} = [0 \ 0 \ 0]$. Referring to Fig. 5.5, conceptually, the effects of wind disturbance could be eliminated by providing only $T(\xi_d)$ control signals to the helicopter but this would eliminate the feedback loop and make the system vulnerable to even the slightest perturbations. In a hover flight, it is valid to assume that the feedback controller generates the trim control inputs for hover $T(\xi_0)$ plus some perturbations Δu_{fb} (Fig. 5.6). By only considering the steady-state output value of the feedback controller ($T(\xi_0)$) in the absence of disturbance and to still include the feedback loop, u_{ff} as given by Eq. (5.6) is acceptable as the feedforward control signal. This setup is used in the following section for simulation.

Artificial Neural Network (ANN)

In the field of artificial intelligence, artificial neural networks have been applied successfully to pattern recognition, speech recognition, machine learning, control problems and various other engineering and nonengineering issues [12],[13],[14],[15].

As stated earlier, to enable a feedforward control action in the simulation, trim control inputs have to be calculated using wind velocity as desired equilibrium states and added

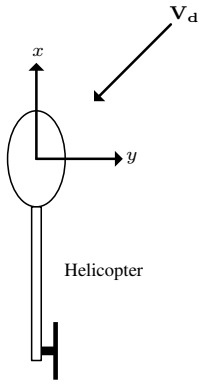

Figure 5.3: Wind disturbance direction

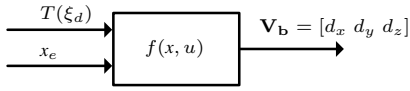

Figure 5.4: Trimmed flight. *When the plant is given trim control input* u_e *and the related trim state* x_e*, the resultant body velocity* $\mathbf{V_b}$ *is as provided in* ξ_d*.*

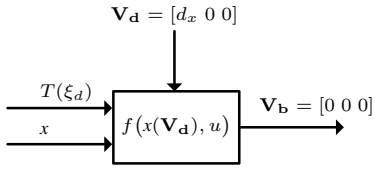

Figure 5.5: Trim flight in the face of disturbance

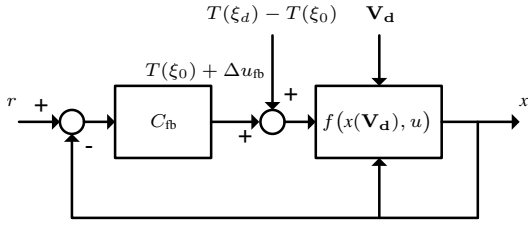

Figure 5.6: Feedforward control in the face of wind disturbance

to feedback control inputs. To calculate these control inputs in real time is computationally expensive and time consuming and therefore not suitable for simulation or practical applications. One way to solve this problem is by using a lookup table that could be referred to access pre-calculated trim control inputs. This method however requires all possible values of wind disturbance velocity to be known prior and that could lead to a large table. A more practical and advantageous way to implement feedforward control using trim control inputs is to utilize ANN. Using ANN, only a fraction of data is required for training for a complete coverage of data retrieval. In this work, a two layer ANN with 10 hidden neurons is trained by using the Levenberg-Marquardt backpropagation training algorithm with the wind disturbance velocity as input to the network and trim control inputs as targets.

5.3 Results

In this simulation experiment, the mathematical model of the Aalborg University Bergen Industrial Twin radio controlled (RC) helicopter with a 52cc, 8HP engine is used. As shown in Fig. 5.7, the model helicopter is fully equipped for autonomous flight with a 1.8GHz onboard computer, a Novatel GPS, a HMR2300 magnetometer, a Falcon GX IMU, and a WindSonic wind sensor.

The helicopter model has 30 states and includes second order actuator dynamics, blade element theory for main and tail rotor forces and torques, flapping dynamics for main rotor and stabilizer bar, and momentum theory for the inflow model. The mathematical model has been validated against flight data to within an acceptable accuracy. The actual helicopter model is not shown in this paper, for details see Ref. [11]. The control system contains a state estimator, a path planner and a controller. Currently the AAU Bergen Twin features a linear state feedback controller that is capable of hover and slow ($< 10\ m/s$) trajectory flight.

In a control problem generally, a measure of disturbances or its effects are needed. In this paper specifically, where the feedforward control problem is dealt with, wind velocity measurement is compulsory for feedforward control signals generation. Due to its light weight and reasonably small size, the WindSonic II wind sensor (Fig. 5.8) by Gill Instruments Ltd. is chosen for this work. The sensor measures wind speed and direction using ultrasonic technology and provides outputs at 4Hz. To obtain a realistic wind profile, the wind sensor is placed on the roof of a university building for a few days.

To demonstrate the feasibility of the proposed feedforward control method for a hover flight, autonomous helicopter simulation in the presence of wind disturbance in the negative x direction of the helicopter body fixed frame is performed for 200 seconds. From the wind data collected at 4Hz over a few days, a wind speed sample size of 200 seconds is used in the simulations as wind velocity in x-axis. Since the wind is sampled at 4Hz, while the simulation runs at 200Hz, a second-order interpolation of the wind data is used as a disturbance to the helicopter. In this section, the results of the simulation will be compared for a significant window of 30 seconds where the wind velocity values are the highest. The time series of the interpolated wind velocity is shown in Fig. 5.9.

Because the feedback and feedforward controllers run at 50Hz, a zero order hold interpolated values of the wind velocity is used to train the ANN. Using 50% of the data available that consists of wind velocity values and its respective trim control inputs, the

Figure 5.7: Aalborg University Bergen Industrial Twin model helicopter

Figure 5.8: WindSonic II

ANN is trained after which tested using other samples and its accuracy is verified. Table 5.1 lists the average of error percentage of the feedforward control inputs comparing ANN outputs and calculated trim control inputs.

In order to quantify the improvement given by the incorporation of feedforward control as compared to the usage of feedback control only, a performance measure as the following is used,

$$Imp = \frac{rms(x_{\text{fb}}) - rms(x_{\text{fb+ff}})}{rms(x_{\text{fb}})} \times 100, \tag{5.7}$$

where $rms(x)$ is the *root-mean-square* value of the time-series of state x. Here, since the desired flight condition is hover where the desired positions and velocities of the helicopter are zeros, *rms* values of the states that provide a measure of average distance from the origin is considered a suitable performance measure.

The figures below show the comparison of the helicopter position and velocity between feedback with feedforward control and feedback only control setups. For a better understanding of the helicopter performance both time series and frequency plots are included. Table 5.2 lists the improvement percentages (Eq. (5.7)) of the helicopter performance using feedback with feedforward control as compared to feedback control only. Table 5.3 lists the peak to peak values of helicopter positions and velocities along with its respective percentages of change comparing feedback control and feedback with feedforward control.

5.4 Discussion

In this simulation work, only wind disturbance in the x-axis is considered. It is assumed that the wind measurement is made onboard the helicopter and any delay that could result

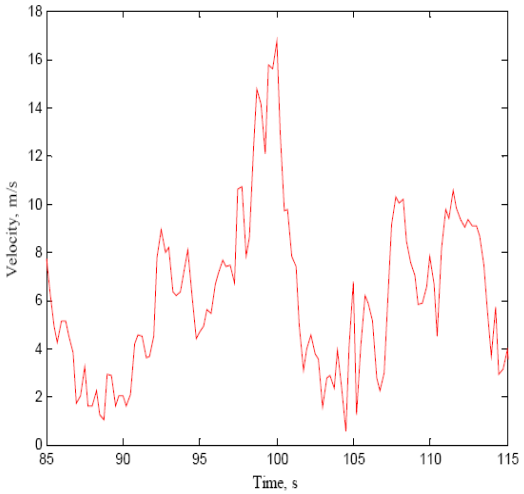

Figure 5.9: Wind velocity. *Interpolated wind velocity as a disturbance applied in the x-axis*

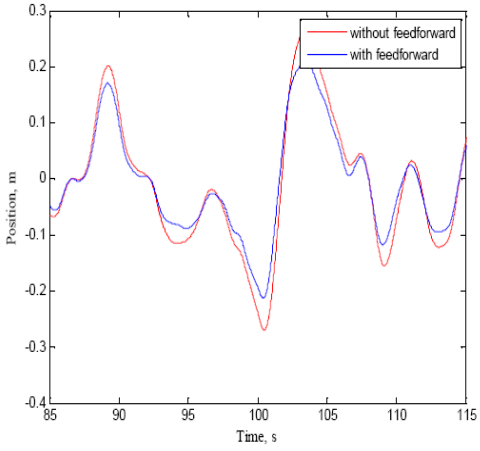

Figure 5.10: Position in x-axis, x. *Imp*$= 17\%$

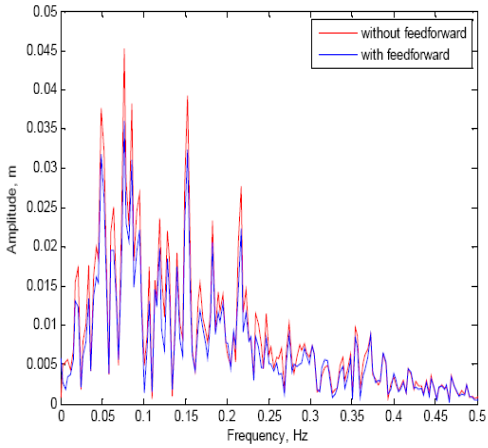

Figure 5.11: Single-Sided Amplitude Spectrum of x

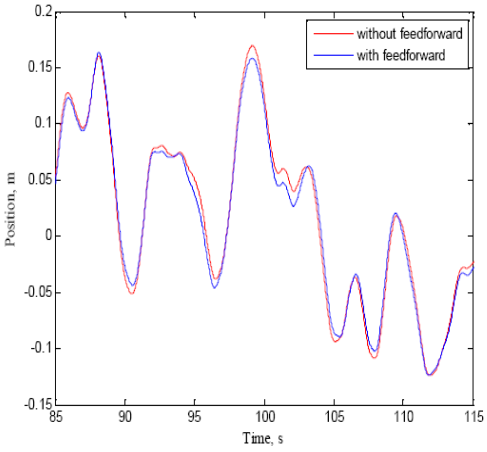

Figure 5.12: Position in y-axis, y. *Imp*$= 1\%$

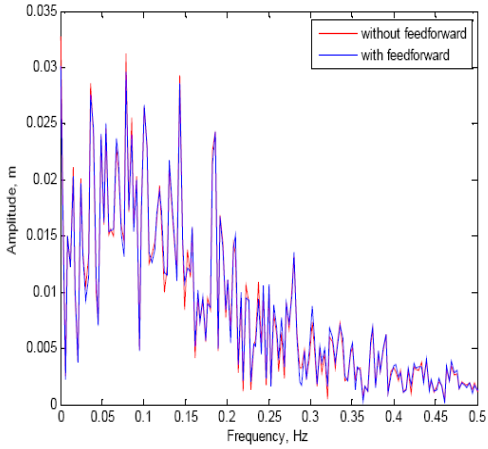

Figure 5.13: Single-Sided Amplitude Spectrum of y

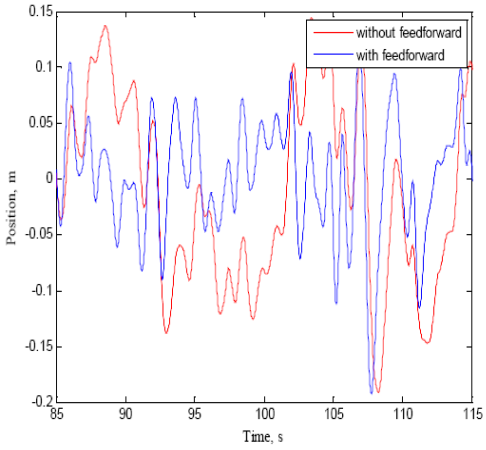

Figure 5.14: Position in z-axis, z. *Imp*$= 32\%$

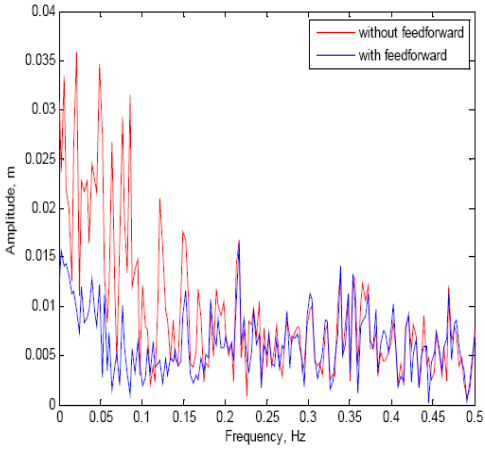

Figure 5.15: Single-Sided Amplitude Spectrum of z

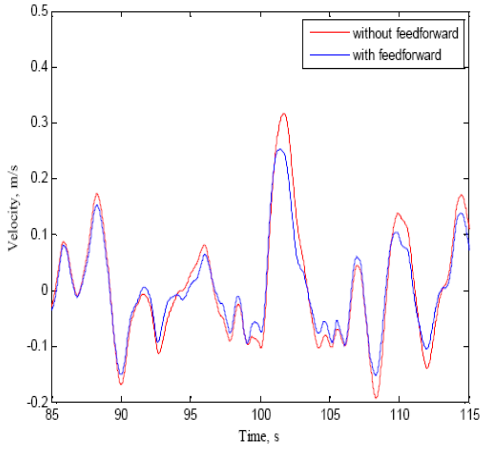

Figure 5.16: Translational Velocity in x-axis, v_x. *Imp*$= 15\%$

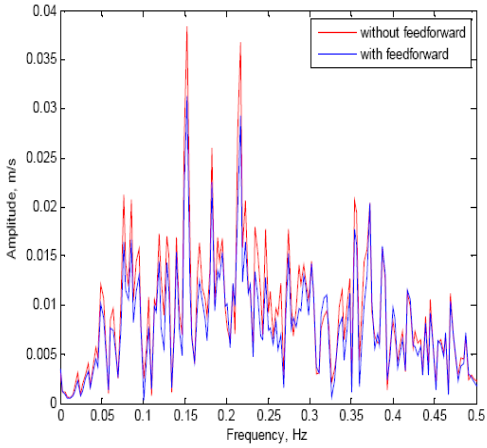

Figure 5.17: Single-Sided Amplitude Spectrum of v_x

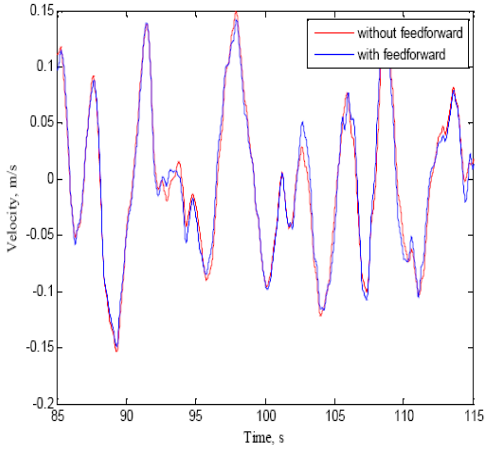

Figure 5.18: Translational Velocity in y-axis, v_y. *Imp*$= -3\%$

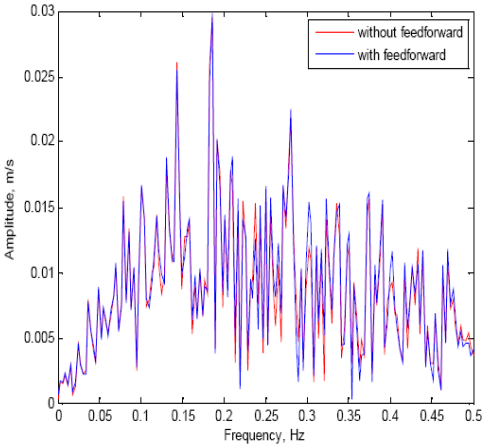

Figure 5.19: Single-Sided Amplitude Spectrum of v_y

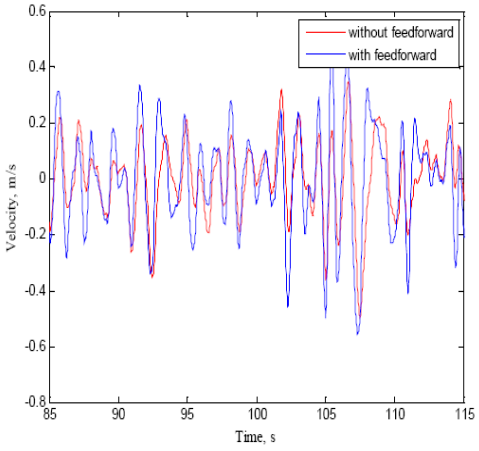

Figure 5.20: Translational Velocity in z-axis, v_z. *Imp*$= -25\%$

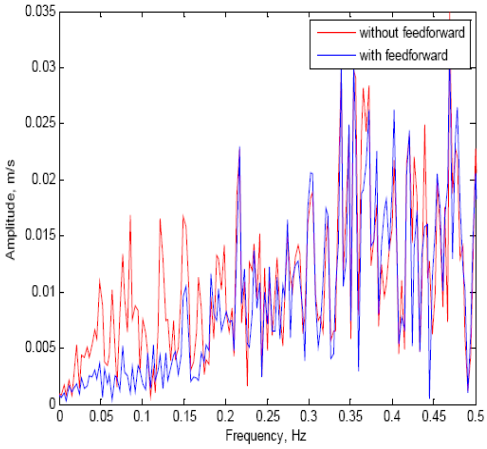

Figure 5.21: Single-Sided Amplitude Spectrum of v_z

from servo dynamics, wind sensor measurement, etc. is neglected.

From Table 5.1, it could be verified that the ANN is trained well to generate the feedforward control inputs according to measured wind velocity. Even though only 50% of the data is used for training, based on the error produced, it could be concluded that the ANN generalized accurately and could be used as a feedforward controller with full confidence.

In addition to the time series plots of positions and velocities of the helicopter, amplitude spectrum plots were also given to demonstrate the performance in frequency domain. Referring to Figures 5.10-5.15, it could be seen that for position control, improvements are made in all axis by adding the feedforward controller with the highest improvement of 32% in the z-axis. Since the wind disturbance affects the helicopter in the negative x direction, x and z positions are affected the most and thus it is acceptable that the effects in y axis is the smallest with only 1% of improvement. From Figures 5.10-5.13, it could be observed that with the addition of the feedforward controller, the frequency components of the original x and z-axis output responses are retained but with reduced amplitudes. However, this pattern is not present in the z position in Fig. 5.14 where a different response is obtained. This could be explained by analyzing Fig. 5.15 that with feedforward control, lower reduction in amplitude is obtained for low frequencies as compared to high frequency amplitude reduction.

For the translational velocity control, feedforward control does not seem to be helpful in the y and z direction (Figures 5.18-5.21) even though an improvement of 15% is made in the x velocity. As in the position response, from Figures 5.16 and 5.17 for x velocity, it could be seen that with feedforward control, the same response as with feedback control only is obtained but with reduced magnitude. With feedforward control, the worst deterioration in velocity is obtained in the z-axis with -25% of improvement. Even with a poorer velocity control, the improvement achieved in position control with feedforward shows that in hover, the helicopter is more capable of maintaining its position which could be advantageous in many applications.

Table 5.1: Mean-squared-error of the feedforward control inputs generated by ANN.

Control Inputs	Error, %
θ_{col}	0.0087
θ_{lat}	0.0030
θ_{lon}	0.0010
θ_{tr}	0.0082

Table 5.2: List of improvement percentages.

State	Axis	*Imp*, %
Position	x	17
	y	1
	z	32
Translational velocity	x	15
	y	-3
	z	-25

Table 5.3: Peak to peak values of positions and velocities.

State	Axis	Feedback only	With feedforward	$\%\Delta$
Position, m	x	0.5367	0.4217	21
	y	0.5977	0.6102	-2
	z	0.4536	0.3651	20
Translational velocity, m/s	x	0.5505	0.4518	18
	y	0.5728	0.5852	-2
	z	1.0530	1.4724	-40

Analyzing the peak to peak values listed in Table 5.3, almost the same conclusion could be made as done quantitatively using Eq. (5.7). As before, with the aid of the feedforward controller a significant improvement is made in x and z-axis for position and x-axis for velocity. When a helicopter is required to fly as close as possible to a building or structure, this quantity shows that the feedforward control allows a closer flight as compared to using the feedback controller only.

It is important to note that in this work, system delay is neglected and it is assumed that ideal wind disturbance measurement is made onboard. In practical helicopter applications however, system delay that arise from servo mechanical linkage, sensor readings, etc. is often inevitable. Another important issue is obtaining reliable onboard wind disturbance measurement. The performance of the proposed feedforward controller is expected to deteriorate in actual flight tests.

5.5 Conclusion

From the simulation results, it is clear that the inclusion of the feedforward controller improves the performance of the helicopter. Based on the discussion above, it could be

deduced that in order to control the position of the helicopter, it is unavoidable that the velocity control to be expensed to a certain degree. This is not regarded as a weakness since in an application such as flying a helicopter in hover close to a building, the velocity variation is less crucial than the position variation. In this work, only wind disturbance in x-axis is handled and the authors acknowledge the simplicity involved in formulating the feedforward control law. The authors are also aware of the difficulty in obtaining accurate onboard wind disturbance measurements in real life. However, due to the promising results obtained, it is considered as an acceptable control approach for simulation purposes and would be a good start off point for a more practical work. As a future work, the mathematical approach of the proposed method will be explored for multi directional wind disturbances. It is also expected that this method to be applied on a model helicopter for actual autonomous flights in the near future.

References

[1] V. Gavrilets, B. Mettler, and E. Feron, "Dynamic model for a miniature aerobatic helicopter," Massachusetts Institute of Technology, MIT-LIDS report #LIDS-P-2579, 2003.

[2] H. Kim and D. Shim, "A flight control system for aerial robots: algorithms and experiments," *Control Engineering Practice*, vol. 11, no. 12, pp. 1389 – 1400, 2003, award winning applications-2002 IFAC World Congress. [Online]. Available: http://www.sciencedirect.com/science/article/B6V2H-48PV8YC-4/2/928287d2c91e0da0c2d54415dec97ebf

[3] H. Kim, D. Shim, and S. Sastry, "Flying robots: Sensing, control and decision making," University of California at Berkeley," Submitted to 2002 IEEE International Conference on Robotics and Automation, 2002.

[4] ——, "Nonlinear model predictive tracking control for rotorcraft-based unmanned aerial vehicles," in *American Control Conference, 2002. Proceedings of the 2002*, vol. 5, 2002, pp. 3576 – 3581 vol.5.

[5] D. Shim, H. Chung, H. Kim, and S. Sastry, "Autonomous exploration in unknown urban environments for unmanned aerial vehicles," in *in Proc. AIAA GN&C Conference*, 2005.

[6] E. Wan, A. Bogdanov, R. Kieburtz, A. Baptista, M. Carlsson, Y. Zhang, and M. Zulauf, "Model predictive neural control for aggressive helicopter maneuvers," in *Software Enabled Control: Information Technologies for Dynamical Systems, chapter 10*. IEEE Press, John Wiley & Sons, 2003, pp. 175–200.

[7] E. Johnson and S. Kannan, "Adaptive flight control for an autonomous unmanned helicopter," in *Proceedings of the AIAA Guidance, Navigation, and Control Conference*, 2002, pp. 2002–4439.

[8] B. Liptak, *Instrument Engineers' Handbook, 4th Edition, Vol. 2: Process Control and Optimization*, 4th ed. ISA/CRC Press, 2005.

[9] G. Padfield, *Helicopter Flight Dynamics, Second Edition: The Theory and Application of Flying Qualities and Simulation Modeling*, 2nd ed. Blackwell Science Ltd, 2007.

[10] J. van de Vegte, *Feedback control systems (3rd ed.)*. Upper Saddle River, NJ, USA: Prentice-Hall, Inc., 1994.

[11] M. Bisgaard, "Modeling, estimation, and control of helicopter slung load system," Aalborg University," Ph.D. Thesis, 2007.

[12] M. Negnevitsky, *Artificial Intelligence: A Guide to Intelligent Systems*. Boston, MA, USA: Addison-Wesley Longman Publishing Co., Inc., 2001.

[13] B. Chowdary, "Back-propagation artificial neural network approach for machining centre selection," *Journal of Manufacturing Technology Management*, vol. 18, no. 3, pp. 315 – 332, 2007.

[14] D. E. Rumelhart, G. E. Hinton, and R. J. Williams, "Learning internal representations by error propagation," pp. 318–362, 1986.

[15] S. Ng, S. Leung, and A. Luk, "A generalized back-propagation algorithm for faster convergence," in *Neural Networks, 1996., IEEE International Conference on*, vol. 1, June 1996.

Paper B

Disturbance Effects in Nonlinear Control Systems and Feedforward Control Strategy

Kumeresan A. Danapalasingam, Anders la Cour-Harbo and Morten Bisgaard

This paper was published in:
In Proceedings of the 7th IEEE International Conference on Control & Automation
09-11 December 2009, Christchurch, New Zealand

Abstract

This work concerns the development of a feedforward control strategy for measurable disturbance rejection in general nonlinear systems with feedback control. In other words, a separate design of disturbance feedforward controller is carried out to be augmented to an existing nonlinear feedback control system. With reference to a well known disturbance feedforward control of linear systems, feedforward control problem for general nonlinear control systems is formulated. The notion of disturbance effect is introduced with the aid of Lyapunov stability analysis of an asymptotically stable disturbance free nonlinear system with feedback control. With the establishment of the disturbance effect description, a feedforward control scheme that guarantees asymptotic stability in the presence of external disturbance is proposed and verified using the inverted pendulum system as an illustrative example.

6.1 Introduction

In a feedback control system with external disturbance, corrective action to eliminate the disturbance effects is only taken after the process has been affected. If the disturbance is measurable, feedforward control can be an effective open-loop control technique to prevent undesirable response due to the ability to take corrective actions before the disturbance affects the system. Feedforward control has been widely used in industry [1] and this efficient approach for disturbance rejection has motivated extensive research in the combination of feedback and feedforward control methods [2, 3, 4, 5, 6, 7].

Some significant results in feedforward control involving nonlinear systems will be reviewed here. In [8], discrete-time feedforward/feedback controllers are developed for general nonlinear processes with stable zero dynamics and its connections with model predictive approaches are established. It is claimed that the derived controllers could reduce if not eliminate completely the effect of measurable disturbances and produce a prespecified linear response with respect to a reference input. The design of the controllers is synthesized in a coupled manner where separate objectives of the feedforward and feedback controllers are realized by means of one unified control law. In a recent work, an adaptive neural network feedforward compensator for external disturbances affecting a specific class of closed-loop system is introduced [9]. A nonlinear disturbance model is estimated to counteract the disturbance affecting a linear discrete closed-loop system. In this scheme, the disturbance model output is required to match the compensation signal for an effective rejection of the disturbance. Another feedforward control scheme using artificial neural networks is reported in [10] describing a nonlinear adaptive feedforward controller for compensation of external load disturbances in the idle speed control of an automotive engine. The feedforward only approach is based on Radial Basis Function network approximation of certain input-output mappings describing the system. The mapping involves optimal control input and a system variable that minimizes a quadratic performance index as the control objective. In another related work, the problem of adaptive feedforward compensation for input-to-state (and locally exponentially) convergent nonlinear systems is investigated [11]. The proposed scheme achieved disturbance rejection of a harmonic disturbance at the input of the nonlinear system class.

In this paper, preliminary results concerning feedforward control for external disturbance rejection in general nonlinear feedback control systems is presented. Given an

asymptotically controllable disturbance free nonlinear system with feedback control, a decoupled design of feedforward control is accomplished for disturbance elimination and hence to guarantee asymptotic controllability in the face of disturbance. Before a strategy could be developed involving measuring the disturbance and generating appropriate feedforward control signals, the effects of the disturbance on the system has to be well understood. For better understanding of the concept and to be aware of the objective of a feedforward control, the notion of disturbance effect in a nonlinear system affected by an external disturbance is introduced using Lyapunov stability analysis. A feedforward control strategy therefore can be one that nullifies the disturbance effect completely. It is shown that the proposed feedforward controller (to assist the feedback controller) that measures current disturbance and generates a corrective control signal warrants a decreasing control-Lyapunov function to achieve asymptotic controllability.

The paper is organized as follows: Section 6.2 introduces preliminary background on nonlinear dynamical systems and classical approach of disturbance feedforward control for linear systems with additive disturbance, after which the problem statement of disturbance feedforward control of nonlinear systems is described. In Section 6.3, properties of Lyapunov stability is given and some definitions are introduced. A disturbance feedforward control scheme to assist a feedback controller for nonlinear systems is proposed in Section 6.4. Finally, a simulation example is given in Section 6.5 followed by conclusion in Section 6.7.

6.2 Preliminaries and Problem Statement

Before the concept of disturbance effect and disturbance feedforward control for nonlinear systems could be formulated, the classical approach of feedforward control of linear systems with additive disturbance has to be reviewed. This is essential to gain insights for deriving an equivalent technique for effective external disturbance rejection in nonlinear control systems.

Nonlinear Dynamical Systems

We deal with a nonlinear finite-dimensional control system of the following form:

$$\dot{x}(t) = f\big(x(t), u(t), w(t)\big), \tag{6.1}$$

where states $x(t) \in \mathbb{R}^n$ (the integer n is the dimension of the system), controls inputs are measurable locally essentially bounded maps

$$u : [0, +\infty) \to \mathbb{U} \subseteq \mathbb{R}^m$$

into the control-value set and external disturbance $w(t) \in \mathbb{R}^d$. It is assumed that f is locally Lipschitz on (x, u, w) and $f(0, 0, 0) = 0$. The maximal solution $x(\cdot)$ of (6.1) corresponding to a given initial state $x(t_0) = x_0$, control u and disturbance w, is defined on some maximal interval $[t_0, t_{\max}(x_0, u, w))$ and is denoted by $x(t; x_0, u, w)$.

The notion of state plays a central role in the definition of a dynamical system. State variables describe processes in the interior of the system and for system (6.1), two basic conditions are required [12]:

- The present state, the chosen control function and disturbance together determine the future states of the system. More precisely, given the state x_0 of the system at some time $t_0 \in T = [0, \infty)$, a control $u(\cdot)$ and disturbance $w(\cdot)$, the evolution of the system's state $x(t)$ is uniquely determined for all t in the time interval $[t_0, t_{\max}(x_0, u, w))$.
- Given x_0 at some $t_0 \in T$, the state $x(t)$ at any later time $t \in [t_0, t_{\max}(x_0, u, w))$, only depends on the input values $u(s)$ and disturbance $w(s)$ for $s \in [t_0, t)$. Thus, at time t, the present state $x(t)$ is not influenced by the present and future values u(s) and w(s), $s \geq t$ of the control and disturbance respectively. Moreover, knowledge of the state $x(t_1)$ at some time $t_1 \in [t_0, t_{\max}(x_0, u, w))$ supersedes the information about all previous state, input and disturbance values.

Feedforward Control of Linear Systems

If external disturbances are measurable, feedforward control is a useful method of canceling the disturbance effects on system output. By feedforward control, it is meant the control of undesirable effects of measurable disturbance by approximately compensating before they materialize [13]. Fig. 6.1 illustrates the concept of disturbance feedforward control for a *single-input-single-output* (SISO) linear system on which the disturbance effect is predictable (additive and known dynamics). Given a linear plant G with additive disturbance dynamics D and feedback controller C_{fb}, a disturbance feedforward controller C_{ff} can be described by

$$C_{\text{ff}} = -DG^{-1}$$

assuming G^{-1} is stable and proper [14]. Substituting in the output equation

$$y = G(C_{\text{fb}}e + C_{\text{ff}}d) + Dd,$$

a disturbance free output is produced

$$\begin{aligned} y &= G(C_{\text{fb}}e - DG^{-1}d) + Dd \\ &= GC_{\text{fb}}e - GDG^{-1}d + Dd \\ &= GC_{\text{fb}}e - Dd + Dd = GC_{\text{fb}}e, \end{aligned}$$

where d is external disturbance and e is error or difference between setpoint r and output y.

Problem Statement

For a linear control system with additive disturbance as described above, it could be clearly seen that the disturbance effect is given by Dd. Provided that the magnitude of the feedforward control input $-DG^{-1}$ is within an admissible range, the analysis above shows that the inclusion of feedforward control completely eliminates the disturbance. This is evident since the feedforward control cancels out the disturbance effect such that the disturbance term d does not appear in the output equation. With feedforward control, the system appears to be only controlled by a feedback with zero external disturbances.

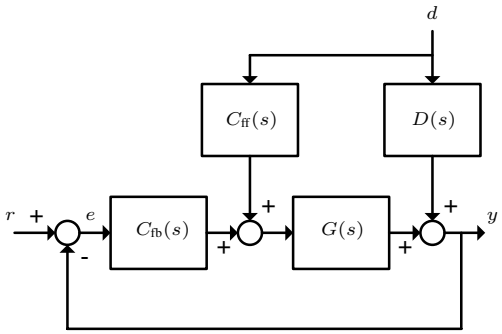

Figure 6.1: Concept of feedforward control for a linear system with known additive disturbances.

One promising approach to derive a feedforward controller for a nonlinear system with external disturbance (6.1) is to expect the same outcome as obtained in the linear case above. It is desirable to have the nonlinear system behave as if there is no disturbance acting upon it with feedforward control. In addition, the nonlinear system should now appear to be controlled by only a feedback, i.e.

$$f(x, u_{\text{fb}} + u_{\text{ff}}, w) = f(x, u_{\text{fb}}, 0), \tag{6.2}$$

where locally bounded functions $u_{\text{fb}} : \mathbb{R}^n \to \mathbb{U}$ and $u_{\text{ff}} : \mathbb{R}^n \times \mathbb{R}^d \to \mathbb{U}$ are called *feedback* and *feedforward* respectively.

6.3 Lyapunov Stability Analysis

Even though it is made clear in (6.2) the desired system behavior with feedforward control, it is not obvious what is being compensated for. In feedforward control for disturbance rejection, a clear definition of disturbance effect is compulsory so that its elimination can be verified to produce a disturbance free system response. In this section, the notion of disturbance effect will be defined with the aid of Lyapunov stability analysis of system (6.1). Some related definitions and theorem are given as follows [15], [16].

Definition 1. System (6.1) is *asymptotically controllable* if:

1. (*attractiveness*) for each $x_0 \in \mathbb{R}^n$ there exists some control u such that the trajectory $x(t) = x(t; x_0, u, w)$ is defined for all $t \geq 0$ and $x(t) \to 0$ as $t \to +\infty$;

2. (*Lyapunov stability*) for each $\varepsilon > 0$ there exists $\delta > 0$ such that for each $x_0 \in \mathbb{R}^n$ with $|x_0| < \delta$ there is a control u as in 1 such that $|x(t)| < \varepsilon$ for all $t \geq 0$;

3. (*bounded controls*) there are a neighbourhood $\mathbb{X}_0$ of 0 in $\mathbb{R}^n$ and a compact subset $\mathbb{U}_0$ of $\mathbb{U}$ such that, if the initial state x_0 in 2 satisfies also $x_0 \in \mathbb{X}_0$, then the control in 2 can be chosen with $u(t) \in \mathbb{U}_0$ for almost all t.

Definition 2. A *control-Lyapunov pair* for (6.1) consists of two continuous functions $V, W : \mathbb{R}^n \to \mathbb{R}_{\geq 0}$ such that the following properties hold.

1. (*positive definiteness*) $V(x) > 0$ and $W(x) > 0$ for all $x \neq 0$, and $V(0) = W(0) = 0$;

2. (*properness*) the set $\{x|V(x) \leq \beta\}$ is bounded for each β;

3. (*infinitesimal decrease*) for each bounded subsets $\mathbb{X} \subseteq \mathbb{R}^n$ and $\mathbb{D} \subseteq \mathbb{R}^d$, there is some compact subset $\mathbb{U}_0 \subseteq \mathbb{U}$ such that for smooth V,

$$\min_{u \in \mathbb{U}_0} \langle \nabla V(x), f(x, u, w) \rangle \leq -W(x) \tag{6.3}$$

for every $x \in \mathbb{X}$ and $w \in \mathbb{D}$ where $\langle x, y \rangle$ denote the inner product of vector x and y.

If V is part of a control-Lyapunov pair (V, W), it is a *control-Lyapunov function (clf)*.

Theorem 1 in [15] states that system (6.1) is asymptotically controllable if and only if it admits a clf. Now, consider system (6.1) with zero disturbance input

$$\dot{x} = f(x, u, 0). \tag{6.4}$$

If there exists a feedback u_{fb} as the control input such that the clf V for system (6.4) decreases along the state trajectory, then system (6.4) is asymptotically controllable. Important to note that the decrement of V is not guaranteed by u_{fb} for nonzero w, i.e. in the presence of disturbance, u_{fb} designed for (6.4) may not assure asymptotic controllability. Hence, the disturbance effect is defined as follows.

Definition 3. Given an asymptotically controllable system (6.4), *disturbance effect* $\mathcal{D}$ is defined by

$$\mathcal{D} = f(x, u, w) - f(x, u_{\text{fb}}, 0). \tag{6.5}$$

It is claimed that given an asymptotically controllable disturbance free system, asymptotic controllability is not guaranteed in the face of disturbance. And since it is system (6.1) that of interest here, feedforward controller is to be designed to ensure asymptotic controllability.

6.4 Disturbance Feedforward Control

In (6.2), nonlinear counterpart of disturbance feedforward control concept is adopted from one of linear control systems. As in the linear case, we assumed that the addition of feedforward control in a nonlinear system affected by external disturbance would result in a system appearing to behave as if only feedback control is present with the exclusion of disturbance input. In (6.5), disturbance effect when disturbance is included in an asymptotically controllable disturbance free system is defined.

For system (6.1) with existing feedback control designed to guarantee asymptotic controllability when no disturbance is present, a feedforward control action u_{ff} would be one that cancels out the disturbance effect $\mathcal{D}$, i.e.

$$f(x, u_{\text{fb}} + u_{\text{ff}}, w) - f(x, u_{\text{fb}}, 0) = 0, \tag{6.6}$$

where now $u := u_{\text{fb}} + u_{\text{ff}}$ in (6.5). Rearranging,

$$f(x, u_{\text{fb}} + u_{\text{ff}}, w) = f(x, u_{\text{fb}}, 0)$$

and a similar disturbance feedforward control approach as agreed in (6.2) is obtained. Substituting in (6.3) yields

$$\begin{aligned} \langle \nabla V(x), f(x, u_{\text{fb}} + u_{\text{ff}}, w) \rangle &= \langle \nabla V(x), f(x, u_{\text{fb}}, 0) \rangle \\ &\leq -W(x) \end{aligned} \tag{6.7}$$

Observe that with both feedback and feedforward, asymptotic controllability of system (6.4) is inherited in system (6.1) and thus we provide the following proposition.

Proposition 1. *Given a feedback u_{fb} such that system* (6.4) *is asymptotically controllable, if there exists a feedforward u_{ff} that satisfies* (6.6) *then system* (6.1) *is asymptotically controllable.*

In summary, a feedforward control strategy for disturbance rejection is proposed for system (6.1) to assist an existing feedback controller of an asymptotically controllable system (6.4). If there exists a solution u_{ff} that nullifies the disturbance effect $\mathcal{D}$ as in (6.6), it could be deduced that the feedforward control does reject external disturbance. It is also shown in (6.7) that the inclusion of the feedforward control retains the asymptotic controllability of the feedback control system without disturbance. In the next section, the proposed technique is simulated for an inverted pendulum system.

6.5 Simulation Results

The inverted pendulum is an unstable nonlinear system that consists of a pendulum pivoted on a cart that can move in a horizontal direction. The states of the system are given by the cart position Y, cart velocity $\dot{y}$, pendulum angle θ and pendulum angular velocity $\dot{\theta}$ while the control input is cart applied force F. The control objective is to balance the pendulum in upright position (0 radian) by applying appropriate external force F on the cart. With reference to Fig. 6.2, taking moments about the center of gravity and applying a horizontal Newton's law for the cart yield the following dynamic equations

$$\begin{aligned} I\ddot{\theta} &= mgL\sin\theta - mL^2\ddot{\theta} - mL\ddot{y}\cos\theta + DL \\ M\ddot{y} &= F - m(\ddot{y} + L\ddot{\theta}\cos\theta - L\dot{\theta}^2\sin\theta) - k\dot{y} - D\cos\theta, \end{aligned}$$

where m is the mass of the pendulum, M is the mass of the cart, L is the distance from the center of gravity to the pivot, I is the moment of inertia of the pendulum with respect to the center of gravity, k is a friction coefficient, g is the acceleration due to gravity and D is the external disturbance force applied on the pendulum. For detailed derivation of the equation of motion without disturbance, refer [16]. Obtaining closed-form expression of the equations above and solving for u_{ff} from (6.6) gives the feedforward

$$u_{\text{ff}}(\theta, D) = \frac{D(m\cos^2\theta + M + m)}{m\cos\theta} \tag{6.8}$$

for $\theta \neq \pm\pi/2$ radian.

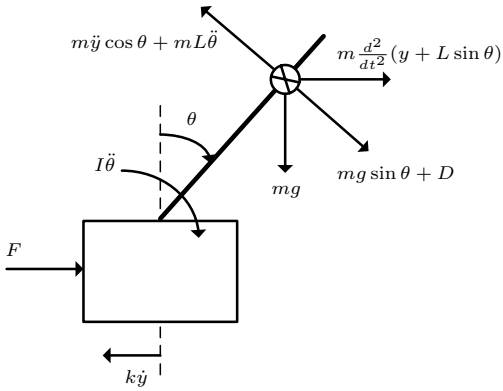

Figure 6.2: Inverted Pendulum.

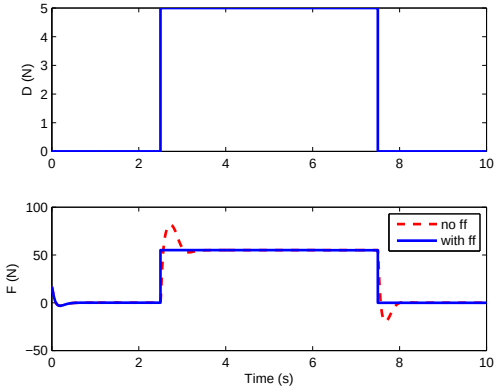

Figure 6.3: Rectangular disturbance and total control input.

Initially, a PID controller is designed for stabilization in upright position based on a linearized model with zero disturbance D and zero friction k. The feedforward (6.8) is then augmented to the PID for stabilization for nonzero disturbances. In the simulation, output responses with and without feedforward control for rectangular and sinusoidal disturbance rejection are demonstrated. Figures 6.3-6.8 show the disturbances applied, control inputs, pendulum angle and cart velocity responses comparing feedback only and feedback with feedforward controls.

6.6 Discussions

The simulation results clearly show the efficiency of the proposed disturbance feedforward control. The PID controller designed based on linearized model of the inverted pendulum at 0 radian is expected to produce an asymptotically controllable system without external disturbance around the equilibrium point. Therefore, this system is identified as a good candidate for the implementation of the proposed feedforward controller for

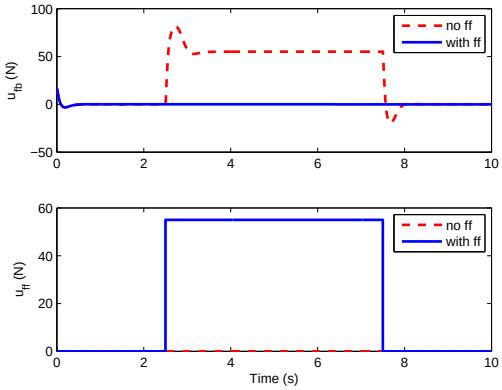

Figure 6.4: Feedback and feedforward control input.

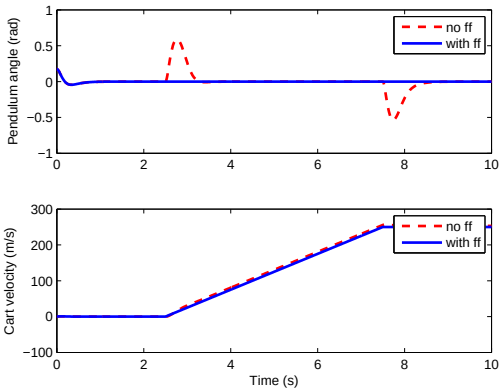

Figure 6.5: Pendulum angle and cart velocity.

disturbance rejection. In the simulation, the system is initialized slightly $(10°)$ off the equilibrium point to test the reliability of both controllers. In Fig. 6.5, the feedback controller seems to be able to asymptotically control the system even in the presence of the rectangular disturbance. However, when a sinusoidal disturbance is presented, feedback control appears to be inadequate as shown in Fig. 6.8. In both cases, the inclusion of feedforward control to assist the feedback controller is proven to be much more effective than using feedback only in realizing asymptotic controllability in the face of disturbance.

It is interesting to observe that with the addition of the feedforward controller, the disturbance is eliminated completely. The inverted pendulum is a control system affine in both input and disturbance, i.e.

$$\ddot{\theta} = f(\theta, \dot{\theta}, \dot{y}) + g(\theta)F + h(\theta)D,$$

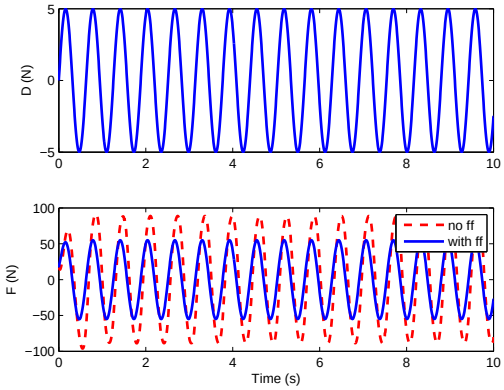

Figure 6.6: Sinusoidal disturbance and total control input.

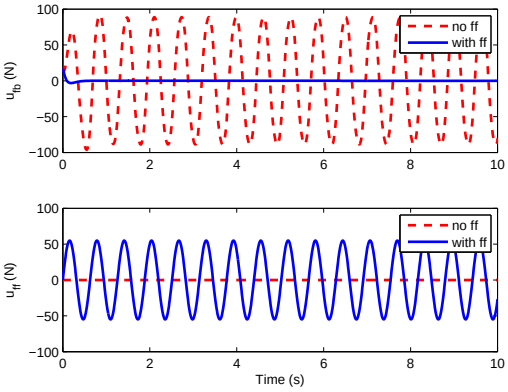

Figure 6.7: Feedback and feedforward control input.

where

$$
\begin{aligned}
f(\theta,\dot{\theta},\dot{y}) &:= \frac{1}{\Delta(\theta)} m^2 g L \sin\theta + mgML\sin\theta \\
&\quad -m^2L^2\dot{\theta}^2\sin\theta\cos\theta + mkL\dot{y}\cos\theta, \\
g(\theta) &:= -\frac{1}{\Delta(\theta)} mL\cos\theta, \\
h(\theta) &:= \frac{1}{\Delta(\theta)} mL\cos^2\theta + ML + mL, \\
\Delta(\theta) &:= (I+mL^2)(m+M) - m^2L^2\cos^2\theta, \\
F &:= u_{\mathrm{fb}}(\theta) + u_{\mathrm{ff}}(\theta, D).
\end{aligned}
$$

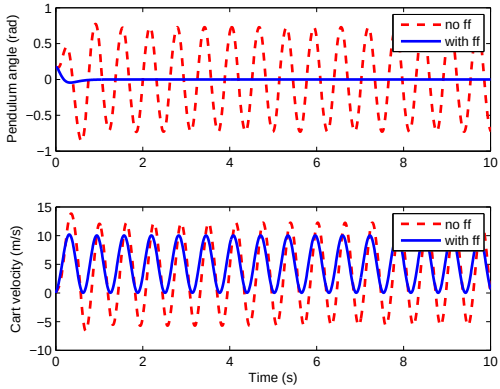

Figure 6.8: Pendulum angle and cart velocity.

Substituting (6.8), the angular dynamics reduce to

$$\ddot{\theta} = f(\theta, \dot{\theta}, \dot{y}) + g(\theta) u_{\text{fb}}$$

resulting the cancellation of the disturbance dynamics $h(\theta)D$, thus explaining the disturbance free responses. The fact that the disturbance can be eliminated in a nonlinear system affine in both control and disturbance by applying the proposed feedforward control is obvious. It is encouraging to note that the concept developed for disturbance rejection in general nonlinear systems works in a direct manner for a specific class of nonlinear systems, thus validating Proposition 1.

The proposed feedforward control scheme for disturbance elimination is advantageous in the sense that the knowledge of a clf is not needed. Given an asymptotically controllable disturbance free system with feedback, it could be assumed that a clf exists. And provided a feedforward control solution u_{ff} such that (6.6) is satisfied, disturbance effect could be cancelled out from the system response. However one should be aware of the large values of u_{ff} that might not be admissible and the difficulty in obtaining disturbance measurements. In the simulation above, no constraint is imposed on the control inputs and availability of the disturbance measurements is assumed, but it is acknowledged that a proper consideration is needed in real life implementation. Also, as this is a model based approach, accuracy of the model compared to the actual plant to be controlled is crucial.

6.7 Conclusion

The contribution of this paper is the proposal of disturbance feedforward control for general nonlinear systems. Using knowledge from linear control systems and Lyapunov stability theorem, we identified a feedforward control scheme for external disturbance elimination. Given an asymptotically controllable disturbance free nonlinear system, the proposed feedforward control could be combined with an existing feedback controller for improved control in the presence of disturbances. Based on the simulation results, the feasibility of the feedforward control technique is confirmed. As future works, control input

constraint is to be included in the formulation and a robust feedforward control method will be investigated to include model uncertainties, inaccurate sensor measurements, etc. In addition, the existence of such a feedforward control solution and methods to obtain them will be studied.

References

[1] F. Shinskey, *Process control systems: Application, design and tuning*. New York: McGraw-Hill, 1988.

[2] J.-P. Calvet and Y. Arkun, "Feedforward and feedback linearization of nonlinear systems with disturbances," *Internat. J. Control*, vol. 48, no. 4, pp. 1551–1559, 1988. [Online]. Available: http://dx.doi.org/10.1080/00207178808906268

[3] ——, "Feedforward and feedback linearization of nonlinear systems with disturbances and its implementation using internal model control," *Ind. Eng. Chem. Res.*, vol. 27, p. 1882, 1988.

[4] P. Daoutidis and C. Kravaris, "Synthesis of feedforward/state feedback controllers for nonlinear processes," *AIChE J.*, vol. 35, no. 10, pp. 1602–1616, 1989.

[5] P. Daoutidis, M. Soroush, and C. Kravaris, "Feedforward/feedback control of multivariable nonlinear processes," *AIChE J.*, vol. 36, no. 10, pp. 1471–1484, 1990.

[6] C. E. Garcia and M. Morari, "Internal model control. 2. design procedure for multivariable systems," *Ind. Eng. Chem. Process Des. Dev.*, vol. 24, no. 2, pp. 472–484, 1985.

[7] Z. Palmor and D. Powers, "Feedforward properties of dead-time compensation controllers," in *American Control Conference*, 1981.

[8] M. Soroush and C. Kravaris, "Synthesis of discrete-time nonlinear feedforward/feedback controllers," *AIChE J.*, vol. 40, no. 3, pp. 473–495, 1994.

[9] G. Herrmann, F. L. Lewis, S. S. Ge, and J. Zhang, "Discrete adaptive neural network disturbance feedforward compensation for non-linear disturbances in servo-control applications," *Internat. J. Control*, vol. 82, no. 4, pp. 721–740, 2009. [Online]. Available: http://dx.doi.org/10.1080/00207170802227191

[10] D. Gorinevsky and L. Feldkamp, "Rbf network feedforward compensation of load disturbance in idle speed control," *Control Systems Magazine, IEEE*, vol. 16, no. 6, pp. 18 –27, dec 1996.

[11] S. Messineo and A. Serrani, "Adaptive feedforward disturbance rejection in nonlinear systems," in *Decision and Control, 2008. CDC 2008. 47th IEEE Conference on*, 9-11 2008, pp. 2575 –2580.

[12] D. Hinrichsen and A. J. Pritchard, *Mathematical Systems Theory I: Modelling, State Space Analysis, Stability and Robustness*, ser. Texts in Applied Mathematics. Springer, 2005, vol. 48.

[13] K. Ogata, *Modern Control Engineering*, fourth edition ed. Prentice-Hall, 2001.

[14] G. C. Goodwin, S. F. Graebe, and M. E. Salgado, *Control System Design*. Upper Saddle River, NJ: Prentice Hall, 2001.

[15] F. H. Clarke, Y. S. Ledyaev, E. D. Sontag, and A. I. Subbotin, "Asymptotic controllability implies feedback stabilization," *IEEE Trans. Automat. Control*, vol. 42, no. 10, pp. 1394–1407, 1997. [Online]. Available: http://dx.doi.org/10.1109/9.633828

[16] H. K. Khalil, *Nonlinear Systems*, 3rd ed. New York: Macmillan, 2001.

Paper C

A Robust Stabilization using State Feedback with Feedforward

Kumeresan A. Danapalasingam, Anders la Cour-Harbo, Girish Chowdhary and Morten Bisgaard

This paper was published in:
In Proceedings of the 2010 American Control Conference
30 June-2 July 2010, Baltimore, Maryland, USA

The layout has been revised

Abstract

In a general nonlinear control system a stabilizing control strategy is often possible if complete information on external inputs affecting the system is available. Assuming that measurements of persistent disturbances are available it is shown that the existence of a smooth uniform control Lyapunov function implies the existence of a stabilizing state feedback with feedforward control which is robust with respect to measurement errors and external disturbances. Conversely, using differential inclusions parameterized as nonlinear systems with state and disturbance measurement errors, it is shown that there exists a smooth uniform control Lyapunov function if there is a robustly stabilizing state feedback with feedforward. This paper demonstrates that if there exists a smooth control Lyapunov function for a general nonlinear system with persistent disturbances for which one has previously designed a feedback controller, a feedforward always exists to be augmented for stability.

7.1 Introduction

In nonlinear systems, the design of stabilizing feedback controllers guarantees stability when no persistent disturbance is present. Even though in some cases a feedback would suffice [1], in general a state feedback with feedforward is inevitable for stability when nonzero disturbances affect the system. It could be advantageous however, if one only has to design a feedforward that can be simply augmented to an existing feedback for required stability in the presence of persistent disturbances. Some previous works on feedforward control will be reviewed here.

In [2] discrete-time feedback/feedforward controllers are developed for general nonlinear processes with stable zero dynamics. The design of the controllers is synthesized in a coupled manner where separate objectives of the feedforward and feedback controllers are realized by means of one unified control law. A feedforward only approach using artificial neural networks is reported in [3] describing a nonlinear adaptive feedforward controller for compensation of external load disturbances in the idle speed control of an automotive engine. In another work, [4] employed a feedforward control to handle measurable additive disturbances with linear dynamics affecting a nonlinear plant. In this paper, we study the existence of a separate robust feedforward whose control inputs can be added to those of an existing feedback to ensure stability of general nonlinear systems with persistent disturbances as one of its external inputs.

In this work, by adding a feedforward term and restricting the persistent disturbance to be a Lipschitz function, [1] is extended using similar approach therein to accommodate our purposes. While only a feedback is considered in the main reference [1], here we employ a feedback with feedforward control and a stricter smooth uniform control Lyapunov function for robust stability. This paper is organized as follows: Section 7.2 contains the problem statement and some definitions. The main theorem of this paper, Theorem 1 as well as the converse Lyapunov theorem from [5], Theorem 2 are also stated here. In addition, nonlinear systems with state and disturbance measurement errors parameterized by differential inclusions are shown to be upper semicontinuous here. This is then used in Section 7.3 to establish a relation between a robustly stabilizing state feedback with feedforward m and asymptotic stability of the aforementioned differential inclusion. Subsequently, the proof of the main theorem is completed in Section 7.4 after which a simulation example is given in Section 7.5. The paper is concluded in Section 7.6.

7.2 Preliminaries

This work concerns the development of a feedforward control strategy for general nonlinear control systems of the type

$$\dot{x} = f(x, u, d), \quad x \in \mathbb{R}^n, u \in \mathbb{U}, d \in \mathbb{D}, \tag{7.1}$$

where $\mathbb{U}$ is a compact subset of $\mathbb{R}^c$, persistent disturbance $d = d(\cdot)$ is a measurable Lipschitz function taking values in some compact set $\mathbb{D} \subset \mathbb{R}^w$ containing 0 and $f : \mathbb{R}^n \times \mathbb{U} \times \mathbb{D} \to \mathbb{R}^n$ is a continuous function. Given an existing stabilizing feedback $k : \mathbb{R}^n \to \mathbb{U}$ designed for (7.1) with $d = 0$, the feedforward stabilization problem is that of finding a feedforward control $l : \mathbb{R}^n \times \mathbb{D} \to \mathbb{U}$ with $l(x, 0) = 0$ such that the origin in $\mathbb{R}^n$ is asymptotically stable with respect to the trajectories of the closed-loop system

$$\dot{x} = f\big(x, k(x) + l(x, d), d\big). \tag{7.2}$$

The remainder of this section provides a series of essential definitions and theorems.

A function $V : \mathbb{R}^n \to \mathbb{R}_{\geq 0}$ is said to be *positive* (definite) if $V(0) = 0$ and $V(x) > 0$ for all $x \neq 0$, and *proper* if the sublevel set $\{x : V(x) \leq a\}$ is compact for all $a > 0$.

Definition 4. A smooth function $V : \mathbb{R}^n \to \mathbb{R}_{\geq 0}$ is defined as a *smooth uniform control Lyapunov function* for system (7.1) if V is positive, proper and satisfies the following *infinitesimal decrease* condition: There exists a continuous positive function $W : \mathbb{R}^n \to \mathbb{R}_{\geq 0}$ such that, for any bounded set $\mathbb{X} \subset \mathbb{R}^n$,

$$\min_{u \in \mathbb{U}} \langle \nabla V(x), f(x, u, d) \rangle \leq -W(x), \quad \forall x \in \mathbb{X}, x \neq 0, \tag{7.3}$$

where $\langle \cdot, \cdot \rangle$ denotes the inner product in $\mathbb{R}^n$ (cf. (14) in [1]).

It follows from the infinitesimal decrease condition (7.3) that there always exists a state feedback with feedforward $m : \mathbb{R}^n \times \mathbb{D} \to \mathbb{U}$ which satisfies

$$\langle \nabla V(x), f\big(x, m(x, d), d\big) \rangle \leq -W(x), \quad \forall x \in \mathbb{X}, x \neq 0. \tag{7.4}$$

Here, we define the state feedback with feedforward as

$$m(x, d) := k(x) + l(x, d). \tag{7.5}$$

Such a control m will be in general discontinuous [6, 7]. It will be shown that a feedback k and a feedforward l satisfying (7.5) and (7.4) will drive the state of the system (7.2) to the origin in $\mathbb{R}^n$ and this stabilizing state feedback with feedforward m is robust with respect to state measurement errors $e_x(\cdot)$, disturbance measurement errors $e_d(\cdot)$ and external disturbances $w(\cdot)$ in the perturbed system

$$\dot{x} = f\Big(x, m\big(x + e_x(t), d(t) + e_d(t)\big), d(t)\Big) + w(t). \tag{7.6}$$

As described in Definition 5, robustness in this context refers to the insensitivity of m in handling measurement errors and additive external disturbances to drive all states to an arbitrary neighborhood of the origin for fast enough sampling and small enough measurement errors and external disturbances.

Next, the state trajectory of a system with a discontinuous control is defined similarly to [6]. Let $\pi = \{t_i\}_{i\geq 0}$ be any partition of $[0, +\infty]$ with

$$0 = t_0 < t_1 < \dots$$

and $\lim_{i\to\infty} t_i = +\infty$. The π-trajectory of the perturbed system (7.6) starting from x_0, under the action of a possibly discontinuous state feedback with feedforward m and in the presence of disturbance $d(\cdot)$, state measurement errors $e_x(\cdot)$, disturbance measurement errors $e_d(\cdot)$ and external disturbances $w(\cdot)$, is defined recursively on the intervals $[t_i, t_{i+1}]$, $i = 0, 1, \dots$, as the solution of the differential equation

$$\dot{x}(t) = f\big(x(t), u_i, d(t)\big) + w(t), \quad \text{a.a. } t \in [t_i, t_{i+1}], \tag{7.7}$$

where $u_i = m\big(x(t_i) + e_x(t_i), d(t_i) + e_d(t_i)\big)$, $x(0) = x_0$. To be noted, $x(\cdot)$ may fail to exist on one of the intervals $[t_i, t_{i+1}]$ when there exists a $T < +\infty$ such that the $x(\cdot)$ only exists on $[0, T)$ and $\lim_{t\uparrow T}|x(t)| = +\infty$, where $|\cdot|$ denotes the Euclidean norm. Such an $x(\cdot)$ is called a *blown-up* trajectory.

Definition 5. The state feedback with feedforward m is *robustly s-stabilizing* (sampling stabilizing) if for any $0 < r < R$ there exists positive $T = T(r, R)$, $\delta = \delta(r, R)$, $\eta = \eta(r, R)$ and $M(R)$ such that for any state measurement error $e_x(\cdot)$, disturbance measurement error $e_d(\cdot)$ (arbitrary bounded functions $e_x : [0, +\infty) \to \mathbb{R}^n$ and $e_d : [0, +\infty) \to \mathbb{D}$) and external disturbance $w(\cdot)$ (measurable essentially bounded function $w : [0, +\infty) \to \mathbb{R}^n$) for which

$$|e_x(t)| \leq \eta, |e_d(t)| \leq \eta, \ \forall t \geq 0, \quad \|w(\cdot)\|_\infty \leq \eta, \tag{7.8}$$

and any partition π with diam $:= \sup_{i\geq 0}(t_{i+1} - t_i) \leq \delta$, every π-trajectory with $|x(0)| \leq R$ does not blow-up and satisfies the following relations:

1. Uniform attractivity

$$|x(t)| \leq r, \quad \forall t \geq T \tag{7.9}$$

2. Bounded overshoot

$$|x(t)| \leq M(R), \quad \forall t \geq 0 \tag{7.10}$$

3. Lyapunov stability

$$\lim_{R\downarrow 0} M(R) = 0. \tag{7.11}$$

The following is the main theorem of this paper.

Theorem 1. *The control system* (7.1) *admits a smooth uniform control Lyapunov function if and only if there exists a robustly s-stabilizing state feedback with feedforward* m.

In the proof of the sufficiency part of Theorem 1, it is shown that if there exists a stabilizing state feedback with feedforward m that is robust with respect to state and disturbance measurement errors and external disturbances for the control system (7.1), then the differential inclusion

$$\dot{x} \in G(x) \tag{7.12}$$

with multivalued function

$$G(x) := \bigcap_{\varepsilon>0} \overline{\text{co}} \bigcup_{d\in\mathbb{D}} f\big(x, m(x+\varepsilon B, d+\varepsilon B), d\big) \tag{7.13}$$

is strongly asymptotically stable, where B is a closed unit ball and $\overline{\text{co}}\, S$ the closure of the convex hull of a set S. As we shall see at the end of this section, the multifunction (7.13) satisfies Hypothesis (H) which is given as follows:

(H1) *The multifunction G is upper semicontinuous, i.e. for any $x \in \mathbb{R}^n$ and any $\varepsilon > 0$ there is a $\delta > 0$ such that,*

$$G(x') \subset G(x) + \varepsilon B, \quad \forall x' \in x + \delta B.$$

(H2) *$G(x)$ is a compact convex subset of $\mathbb{R}^n$ for each $x \in \mathbb{R}^n$.*

Definition 6. The differential inclusion (7.12) is strongly asymptotically stable if it has no blown-up solutions and

1. (Attractivity) for any solution $x(\cdot)$

$$\lim_{t\to\infty} x(t) = 0. \tag{7.14}$$

2. (Strong Lyapunov stability) for any $\varepsilon > 0$, there exists $\delta > 0$ such that every solution of (7.12) with $x(0) \le \delta$ satisfies

$$|x(t)| < \varepsilon, \quad \forall t \ge 0. \tag{7.15}$$

Strong asymptotic stability of differential inclusion (7.12) implies that there are no solutions $x(\cdot)$ of (7.12) exhibiting finite time blow-up and for any positive $r < R$ there exist $T = T(r, R)$ and $M(R)$ such that any solution with $|x(0)| \le R$ satisfies (7.9) and (7.10) and (7.11) holds [5, Prop. 2.2].

Definition 7. The smooth function $V : \mathbb{R}^n \to \mathbb{R}_{\ge 0}$ is said to be a smooth strong Lyapunov function for the differential inclusion (7.12) if it is positive, proper and satisfies the following infinitesimal decrease condition:

$$\max_{z\in G(x)} \langle \nabla V(x), z\rangle \le -W(x), \tag{7.16}$$

where W is a positive continuous function.

The following theorem is proved in [5].

Theorem 2. *Under Hypothesis (H), the multifunction G is strongly asymptotically stable if and only if there exists a smooth strong Lyapunov function for G.*

We end this section by showing that the multifunction (7.13) satisfies Hypothesis (H). Define the set-valued maps $g_\varepsilon, h_\varepsilon : \mathbb{R}^n \to 2^{\mathbb{R}^n}$ by

$$\begin{aligned} g_\varepsilon(x) &:= \bigcup_{d\in\mathbb{D}} f\Big(x, m\big(x+\varepsilon B, d+\varepsilon B\big), d\Big), \\ h_\varepsilon(x) &:= \overline{\mathrm{co}}\, g_\varepsilon(x) \end{aligned}$$

and let $K_{x,\varepsilon} = \{(u,d) \in \mathbb{U}\times\mathbb{D} | f(x,u,d) \in g_\varepsilon(x)\}$. Hence,

$$G(x) := \bigcap_{\varepsilon>0} h_\varepsilon(x) = \bigcap_{\varepsilon>0} \overline{\mathrm{co}}\, g_\varepsilon(x) = \bigcap_{\varepsilon>0} \overline{\mathrm{co}}\, f(\{x\}\times K_{x,\varepsilon}).$$

Let us first note that $f(\{x\}\times\mathbb{U}\times\mathbb{D})$ is compact, since $\mathbb{D}$ and $\mathbb{U}$ are compact and f is continuous. Moreover, $g_\varepsilon(x) := f(\{x\}\times K_{x,\epsilon}) \subset f(\{x\}\times\mathbb{U}\times\mathbb{D})$. Hence, $g_\varepsilon(x)$ is bounded for all x and all $\varepsilon > 0$.

Secondly, by the above we conclude that $h_\varepsilon(x)$ is compact. Hence by the Cantor intersection theorem, $G(x) := \bigcap_{\varepsilon>0} h_\varepsilon(x)$ is closed (and thus compact) and nonempty. This proves Hypothesis (H2) since $G(x)$ is obviously convex.

Finally let us show that G is upper semicontinuous at an arbitrary but fixed $x \in \mathbb{R}^n$. We prove this in terms of sequences, see e.g. [8, p. 4]. Let $x_k \to x$ in $\mathbb{R}^n$ and $A \subset \mathbb{R}^n$ be closed such that $G(x_k)\cap A \neq \emptyset$ for all $k \in \mathbb{N}$. Hence, we need to show that $G(x)\cap A \neq \emptyset$. Now let $y_k \in G(x_k)\cap A$ and for each $\varepsilon > 0$, let $N = N(\varepsilon) \in \mathbb{N}$ be such that $x_k \in x + \frac{\varepsilon}{2}B$ for all $k \geq N$. Then, $y_k \in h_\varepsilon(x) \cap A$ for all $k \geq N$ since $G(x_k) \subset h_{\varepsilon/2}(x_k)$ and $h_{\varepsilon/2}(x_k) \subset h_\varepsilon(x)$ whenever $k \geq N$. Since $h_\varepsilon(x) \cap A$ is compact, $y_{k_j} \to y$ in $h_\varepsilon(x) \cap A$ for some subsequence $\{y_{k_j}\}$ of $\{y_k\}$. In particular, $y \in h_\varepsilon(x) \cap A$ for all $\varepsilon > 0$, hence $y \in G(x) \cap A$ proving that G is upper semicontinuous at x.

7.3 Supplementary Results

According to Theorem 1, the existence of a robustly s-stabilizing state feedback with feedforward m is necessary for system (7.1) to admit a smooth uniform control Lyapunov function. Indeed if (7.3) is satisfied, a possibly discontinuous m always exists. In the next section, it will be shown that the m that satisfies (7.4) is robustly s-stabilizing. The sufficiency part of the theorem is more delicate as the connection between the solutions of (7.6) and solutions of the differential inclusion (7.12) with multivalued right-hand side (7.13) has to be known. The link between solutions of the differential inclusion (7.12) and the limits of π_j-trajectories $x_j(\cdot)$ of the perturbed system

$$\dot{x}_j = f\Big(x_j, m\big(x_j + e_{xj}(t), d(t) + e_{dj}(t)\big), d(t)\Big) + w_j(t), \tag{7.17}$$

with state measurement error $e_{xj}(\cdot)$, disturbance measurement error $e_{dj}(\cdot)$ and external disturbance $w_j(\cdot)$ satisfying

$$|e_{xj}(t)| \leq \eta_j, |e_{dj}(t)| \leq \eta_j,\ t \in [0,T], \quad |w_j(t)| \leq \eta_j,\ \text{a.a. } t \in [0,T] \tag{7.18}$$

is formulated in the next lemma.

Lemma 1. *The absolutely continuous function $x : [0,T] \to \mathbb{R}^n$ is a solution of the differential inclusion* (7.12) *if and only if there exists a sequence of π_j-trajectories $x_j(\cdot)$ of the perturbed system* (7.17) *with $x_j(0) = x(0)$, diam$(\pi_j) \downarrow 0$, $\eta_j \downarrow 0$, that converges uniformly to $x(\cdot)$ on $[0,T]$.*

Proof. We let $x_j(\cdot)$ be a sequence of π-trajectory of (7.17). Define $\delta_j := \text{diam}(\pi_j)$ and

$$\mu := \sup\{|f\big(x, m(x', d'), d\big)| : |x| \leq R, x' \in x + B, d \in \mathbb{D}, d' \in d + B\}.$$

Thus for sufficiently large j, all $x_j(\cdot)$ are Lipschitz of rank μ on $[0,T]$. Moreover, due to the uniform convergence of $x_j(\cdot)$ to $x(\cdot)$, $x(\cdot)$ too is Lipschitz on $[0,T]$ with the same constant μ. With ν as the Lipschitz constant of $d(\cdot)$ on $[0,T]$, from the definition of π-trajectory and (7.18), $x_j(\cdot)$ is a solution of

$$\dot{x}_j(t) \in \overline{\text{co}}\, f\Big(x_j(t), m\big(x_j(t) + (\eta_j + \mu\delta_j)B, d(t) + (\eta_j + \nu\delta_j)B\big), d(t)\Big) + \eta_j B,$$

since

$$\begin{aligned} x_j(t_i) &\in x_j(t) + \mu\delta_j B, \\ d(t_i) &\in d(t) + \nu\delta_j B, \\ x'_j(t_i) &\in x_j(t_i) + \eta_j B, \\ d'(t_i) &\in d(t_i) + \eta_j B, \quad \forall t \in [t_i, t_{i+1}], i = 0, 1, \ldots, \end{aligned}$$

for j large enough, with measured state $x'_j(t_i)$ and measured disturbance $d'(t_i)$. Note that due to the continuity of f, for any $\varepsilon > 0$ there exists a $\delta > 0$ such that

$$\begin{aligned} & \overline{\text{co}}\, f\Big(x', m\big(x' + (\eta_j + \mu\delta_j)B, d(t) + (\eta_j + \nu\delta_j)B\big), d(t)\Big) + \eta_j B \\ \subset\ & \overline{\text{co}}\, f\Big(x(t), m\big(x(t) + (\eta_j + \mu\delta_j)B, d(t) + (\eta_j + \nu\delta_j)B\big), d(t)\Big) + (\varepsilon + \eta_j)B, \\ & \forall x' \in x(t) + \delta B. \end{aligned}$$

And since $x_j(\cdot)$ converges uniformly to $x(\cdot)$ on $[0,T]$, for any $\delta > 0$ there exists an $N > 0$ such that $x_j(\cdot) \in x(\cdot) + \delta B$, for all $j \geq N$. Therefore for sufficiently large j, $x_j(\cdot)$ is a solution of

$$\begin{aligned} \dot{x}_j(t) &\in \overline{\text{co}}\, f\Big(x(t), m\big(x(t) + (\eta_j + \mu\delta_j)B, d(t) + (\eta_j + \nu\delta_j)B\big), d(t)\Big) + (\varepsilon + \eta_j)B \\ &\subset \overline{\text{co}}\, f\Big(x(t), m\big(x(t) + \hat{\varepsilon}B, d(t) + \hat{\varepsilon}B\big), d(t)\Big) + \hat{\varepsilon}B \end{aligned}$$

on $[0,T]$, where $\hat{\varepsilon} := \max\{\eta_j + \mu\delta_j, \eta_j + \nu\delta_j, \varepsilon + \eta_j\}$. Next, formulating the previous differential inclusion as an integral inclusion (see e.g [9]), we obtain

$$x_j(t+h) \in x_j(t) + \int_t^{t+h} \overline{\text{co}}\, f\Big(x(s), m\big(x(s) + \hat{\varepsilon}B, d(s) + \hat{\varepsilon}B\big), d(s)\Big) ds + \hat{\varepsilon}B,$$

for arbitrary $t \in [0,T)$ and any $h > 0$ such that $t + h < T$, where the Aumann integral (see [10, Th. 3.13]) is given by

$$\begin{aligned} & \int_t^{t+h} \overline{\text{co}}\, f\Big(x(s), m\big(x(s)+\hat{\varepsilon}B, d(s)+\hat{\varepsilon}B\big), d(s)\Big) ds \\ = & \int_t^{t+h} f\Big(x(s), m\big(x(s)+\hat{\varepsilon}B, d(s)+\hat{\varepsilon}B\big), d(s)\Big) ds \\ := & \left\{ \int_t^{t+h} f\Big(x(s), u, d(s)\Big) ds : u \in m\big(x(s)+\hat{\varepsilon}B, d(s)+\hat{\varepsilon}B\big) \right\}. \end{aligned}$$

Rearranging,

$$\frac{x(t+h)-x(t)}{h} \in \frac{1}{h}\int_t^{t+h} \overline{\text{co}}\, f\Big(x(t), m\big(x(t)+2\hat{\varepsilon}B, d(t)+2\hat{\varepsilon}B\big), d(t)\Big) ds + 2\hat{\varepsilon}B,$$

as $j \to \infty$ and for all h small enough. Using [1, Eq. (37)] and letting $h \downarrow 0$, $x(\cdot)$ is a solution of the differential inclusion

$$\dot{x}(t) \in \overline{\text{co}}\, f\Big(x(t), m\big(x(t)+2\hat{\varepsilon}B, d(t)+2\hat{\varepsilon}B\big), d(t)\Big) + 2\hat{\varepsilon}B.$$

Since the first term in the right hand side of the above inclusion is closed, $\hat{\varepsilon}$ is arbitrary and $d(t) \in \mathbb{D}$, $x(t)$ satisfies

$$\begin{aligned} \dot{x}(t) \quad & \in \quad \bigcap_{2\hat{\varepsilon}>0} \overline{\text{co}}\, f\Big(x(t), m\big(x(t)+2\hat{\varepsilon}B, d(t)+2\hat{\varepsilon}B\big), d(t)\Big) \\ & \subset \quad \bigcap_{\varepsilon>0} \overline{\text{co}} \bigcup_{d(t)\in\mathbb{D}} f\Big(x(t), m\big(x(t)+\varepsilon B, d(t)+\varepsilon B\big), d(t)\Big), \end{aligned}$$

where $\varepsilon := 2\hat{\varepsilon}$, thus satisfying the differential inclusion (7.12) and concluding the sufficiency part of the lemma.

Now, let $x(\cdot)$ be a solution of the differential inclusion (7.12). Then for any $\varepsilon > 0$,

$$\dot{x}(t) \in \overline{\text{co}} \bigcup_{d(t)\in\mathbb{D}} f\Big(x(t), m\big(x(t)+\varepsilon B, d(t)+\varepsilon B\big), d(t)\Big). \tag{7.19}$$

Define $F(x) := \bigcup_{d(t)\in\mathbb{D}} f\Big(x, m\big(x+\varepsilon B, d(t)+\varepsilon B\big), d(t)\Big)$ and by [1, Lem. 2.5] we obtain g satisfying

$$\begin{aligned} g(t,x) \quad & \in \quad \bigcup_{d(t)\in\mathbb{D}} f\Big(x+2\varepsilon B, m\big(x+3\varepsilon B, d(t)+\varepsilon B\big), d(t)\Big) \\ & \subset \quad \bigcup_{d(t)\in\mathbb{D}} f\Big(x+2\varepsilon B, m\big(x+3\varepsilon B, d(t)+\varepsilon B\big), d(t)+\varepsilon B\Big), \ \forall x \in x(t)+\varepsilon B \end{aligned}$$

such that for any partition π of $[0,T]$ with small enough diameter, $x'(\cdot)$ is the π-trajectory of discontinuous $g(t,x)$ with $x'(0) = x(0)$ and

$$|x(t) - x'(t)| \le \varepsilon, \quad \forall t \in [0,T], \tag{7.20}$$

where $x(\cdot)$ is the solution of the relaxed differential inclusion (7.19). From the definition of π-trajectory and g, there exist vectors $e_x(t_i) \in 3\varepsilon B$ and $e_d(t_i) \in \varepsilon B$ such that

$$\begin{aligned}\dot{x}'(t) \quad \in \quad & \bigcup_{d(t)\in\mathbb{D}} f\Big(x'(t_i) + 2\varepsilon B, m\big(x'(t_i) + e_x(t_i), d(t_i) + e_d(t_i)\big), d(t_i) + \varepsilon B\Big), \\ & t \in [t_i, t_{i+1}],\end{aligned}$$

for any $t_i \in \pi$. From (7.20), we can have both $x(\cdot)$ and any solution $x'(\cdot)$ of the inclusion above lie in the same open ball of a certain radius provided that ε is small enough, e.g. $\varepsilon < 1$. Consequently, it can be assumed that $x(\cdot)$ and $x'(\cdot)$ are Lipschitz of the same rank μ on $[0, T]$. Letting $\mathrm{diam}(\pi) \leq \min\{\varepsilon/\mu, \varepsilon/\nu\}$, there exists an $\eta(\varepsilon) > 0$ such that $x'(\cdot)$ satisfies

$$\begin{aligned}\dot{x}'(t) \quad \in \quad & \bigcup_{d(t)\in\mathbb{D}} f\Big(x'(t), m\big(x'(t_i) + e_x(t_i), d(t_i) + e_d(t_i)\big), d(t)\Big) + \eta(\varepsilon)B, \\ & \text{a.a. } t \in [t_i, t_{i+1}].\end{aligned}$$

Next, for each η_j from a chosen sequence of $\eta_j \downarrow 0$, an $\varepsilon > 0$ and a π-trajectory $x'(\cdot)$ are constructed such that

$$3\varepsilon < \eta_j, \quad \eta(\varepsilon) < \eta_j.$$

Defining the $x'(\cdot)$ as $x_j(\cdot)$,

$$\begin{aligned}\dot{x}_j(t) \quad \in \quad & \bigcup_{d(t)\in\mathbb{D}} f\Big(x_j(t), m\big(x_j(t_i) + e_{xj}(t_i), d(t_i) + e_{dj}(t_i)\big), d(t)\Big) + \eta_j B, \\ & \text{a.a. } t \in [t_i, t_{i+1}]\end{aligned}$$

and $|x(\cdot) - x_j(\cdot)| \leq \eta_j$ from (7.20). From the measurable selection theorem [10, 11], this implies that there exist a disturbance $d(\cdot)$ with values in $\mathbb{D}$ and an external disturbance $w_j(\cdot)$ such that the π_j-trajectory $x_j(\cdot)$ is a solution of

$$\begin{aligned}\dot{x}_j(t) \quad = \quad & f\Big(x_j(t), m\big(x_j(t_i) + e_{xj}(t_i), d(t_i) + e_{dj}(t_i)\big), d(t)\Big) + w_j(t), \\ & \text{a.a. } t \in [t_i, t_{i+1}],\end{aligned}$$

for some partition π_j, state measurement error $e_{xj}(\cdot)$, disturbance measurement error $e_{dj}(\cdot)$ and external disturbance $w_j(\cdot)$ satisfying (7.18) with $x_j(\cdot)$ converging uniformly to $x(\cdot)$. □

The need for Lemma 1 in the proof of Theorem 1 will be appreciated in the next proposition.

Proposition 2. *The state feedback with feedforward m is robustly s-stabilizing if and only if the differential inclusion* (7.12) *is strongly asymptotically stable.*

Proof. Pick arbitrary positive $r < R$ and $r' < r$ such that $M(r') < r$. Suppose that m is robustly s-stabilizing, then there exist $M(R)$, $T = T(r', R)$, $\delta = \delta(r', R)$ and $\eta = \eta(r', R)$ as in Definition 5. Consider sequences $\eta_j \downarrow 0$ and $\delta_j \downarrow 0$. Then for all

j sufficiently large such that $\eta_j \leq \eta$ and $\delta_j \leq \eta$, π-trajectories $x_j(\cdot)$ of the perturbed system (7.17) satisfying (7.18) with $|x_j(0)| \leq R$ satisfy (7.9) and (7.10). Note that by Lemma 1, the sequence $x_j(\cdot)$ converges uniformly to a solution $x(\cdot)$ of the differential inclusion (7.12) on some interval $[0, T']$ with $x_j(0) = x(0)$. Therefore,

1. since $x_j(\cdot)$ for all j large enough satisfy (7.10), $x(\cdot)$ exists on the entire $[0, +\infty)$ and bounded by $M(R)$.
2. $|x(T)| \leq r'$ as all $x_j(\cdot)$ for j sufficiently large satisfy (7.9), with $|x_j(T)| \leq r' < r$. Initializing the differential inclusion (7.12) at T, because $|x(T)| \leq r'$, then $|x(t)| \leq M(r') < r$, $\forall t \geq T$ satisfying (7.9).

Thus, the differential inclusion (7.12) is strongly asymptotically stable. For the proof of the sufficiency part of the proposition, replace feedback k with m in [1, pp. 831-832]. □

7.4 Completion of the proof

The following lemma which is used to show that a feedback k is robustly s-stabilizing in [1] will be adapted here for the same reason regarding a state feedback with feedforward m satisfying (7.4).

Lemma 2. *There exist continuous functions $\tilde{\delta} : \mathbb{R}^n \backslash \{0\} \to \mathbb{R}_{>0}$ and $\tilde{\eta} : \mathbb{R}^n \backslash \{0\} \to \mathbb{R}_{>0}$ such that for any partition π satisfying*

$$t_{i+1} - t_i \leq \tilde{\delta}\big(x(t_i)\big), \quad i = 0, 1, \ldots$$

and any disturbance $d(\cdot)$, as well any measurement errors and external disturbances satisfying

$$|e(t_i)| \leq \tilde{\eta}\big(x(t_i)\big), |w(t)| \leq \tilde{\eta}\big(x(t_i)\big), \quad \textit{a.a. } t \in [t_i, t_{i+1}], i = 0, 1, \ldots,$$

every π-trajectory $x(\cdot)$ of (7.6) *does not blow-up and satisfies*

$$\frac{dV\big(x(t)\big)}{dt} \leq -\frac{1}{2} W\big(x(t)\big) \quad \textit{a.a. } t \in [t_i, t_{i+1}], i = 0, 1, \ldots$$

Proof. Taking the same approach as in [1, pp. 834-836], only this time letting a π-trajectory $x(\cdot)$ to be the solution of (7.7) for some partition π, disturbance $d(\cdot)$, state measurement error $e_x(\cdot)$ and disturbance measurement error $e_d(\cdot)$, suppose that for some $\delta > 0$ and $\eta > 0$,

$$t_{i+1} - t_i \leq \delta, |e(t_i)| \leq \eta, |w(t)| \leq \eta, \quad \text{a.a. } t \in [t_i, t_{i+1}].$$

Since for a.a. $t \in [t_i, t_{i+1}]$,

$$\begin{aligned}
\frac{dV\big(x(t)\big)}{dt} &= \langle \nabla V\big(x(t)\big), f\big(x(t), m(x', d'), d(t)\big) + w(t) \rangle \\
&= \langle \nabla V(x'), f\big(x', m(x', d'), d'\big) \rangle + \langle \nabla V\big(x(t)\big) - \nabla V(x'), \\
&\quad f\big(x', m(x', d'), d'\big) \rangle + \langle \nabla V\big(x(t)\big), f\big(x(t), m(x', d'), d(t)\big) - \\
&\quad f\big(x', m(x', d'), d'\big) \rangle + \langle \nabla V\big(x(t)\big), w(t) \rangle,
\end{aligned}$$

where $x' := x(t_i) + e_x(t_i)$ and $d' := d(t_i) + e_d(t_i)$, the following inequality is obtained.

$$\begin{aligned}\frac{dV\big(x(t)\big)}{dt} \quad \leq \quad & -W(x') + |\nabla V(x(t)) - \nabla V(x')||f\big(x', m(x', d'), d'\big)| + |\nabla V\big(x(t)\big)| \\ & |f\big(x(t), m(x', d'), d(t)\big) - f\big(x', m(x', d'), d'\big)| + |\nabla V\big(x(t)\big)|\eta \quad (7.21)\end{aligned}$$

Because m is bounded on bounded sets, there exists a continuous function $\rho : \mathbb{R}_{\geq 0} \times \mathbb{R}_{\geq 0} \to \mathbb{R}_{>0}$ such that

$$m(x, d) \in \mathbb{U}_{\rho(|x|,|d|)},$$

where $\mathbb{U}_\rho := \{u \in \mathbb{U} : |u - \bar{0}| \leq \rho\}$ for a chosen point $\bar{0} \in \mathbb{U}$. Next the following functions are defined for f, ∇V and W mentioned above,

$$\begin{aligned}
m_f(x, d) &:= \max\{|f(x_1, u, d_1)| + 1 : |x_1 - x| \leq 1, u \in \mathbb{U}_{\rho(|x|+1,|d|+1)}, \\
&\quad d_1 \in \mathbb{D} + B\}, \\
m_{\nabla V}\big(x(t)\big) &:= \max\{\nabla V\big(x(t)\big)\}, \\
\omega_f(x, d; \gamma) &:= \max\{|f(x_1, u, d_1) - f(x_2, u, d_2)| : |x_1 - x_2| \leq \gamma, |x_i - x| \leq 1, \\
&\quad i = 1, 2, u \in \mathbb{U}_{\rho(|x|+1,|d|+1)}, d_1, d_2 \in \mathbb{D} + B\}, \\
\omega_{\nabla V}(x, \gamma) &:= \max\{|\nabla V(x_1) - \nabla V(x_1)| : |x_1 - x_2| \leq \gamma, |x_i - x| \leq 1, i = 1, 2\}, \\
\omega_W(x, \gamma) &:= \max\{|W(x_1) - W(x_1)| : |x_1 - x_2| \leq \gamma, |x_i - x| \leq 1, i = 1, 2\}.
\end{aligned}$$

Defining $x := x(t_i)$ and letting $\eta \leq 1$, $\delta \leq 1/m_f(x, d)$, we have $|x(t) - x| \leq 1$ on $[t_i, t_{i+1}]$. Continuing from (7.21),

$$\frac{dV\big(x(t)\big)}{dt} \leq -\frac{1}{2}W\big(x(t)\big) + \Omega\big(x(t), x, d; \delta, \eta\big) - \frac{1}{2}W(x),$$

where

$$\begin{aligned}\Omega\big(x(t), x, d; \delta, \eta\big) \quad := \quad & m_f(x, d)\omega_{\nabla V}\big(x; m_f(x, d)\delta + \eta\big) \\ & + m_{\nabla V}\big(x(t)\big)\omega_f\big(x, d; m_f(x, d)\delta + \eta\big) + m_{\nabla V}\big(x(t)\big)\eta + \omega_W(x; \eta) + \\ & \frac{1}{2}\omega_W\big(x, m_f(x, d)\delta\big).\end{aligned}$$

By substituting $\Omega(x; \delta, \eta)$ with $\Omega\big(x(t), x, d; \delta, \eta\big)$, choosing $\delta = \eta/m_f(x, d)$ and following the rest of the steps taken in [1, p. 836], the proof of the lemma is completed. □

Now to prove that an m that satisfies (7.4) is a robustly s-stabilizing state feedback with feedforward, redefine m' in [1, pp. 834] as

$$\begin{aligned}m' \quad := \quad & \max\{|f\big(x, m(x', d'), d\big)| + \eta : |x' - x| \leq 2r + \eta, |x| \leq r, d \in \mathbb{D}, \\ & d' \in \mathbb{D} + \eta B\},\end{aligned}$$

where r, R and $\eta := \eta(r, R)$ are as described therein. Equivalently, it can be shown that m is a robustly s-stabilizing state feedback with feedforward.

To summarize the proof of the main theorem, if there exists a smooth uniform control Lyapunov function for system (7.1), then by (7.4) there is always a state feedback with

feedforward m. Using Lemma 2 and the subsequent proof above, we know that such an m is robustly s-stabilizing. Conversely, if there exists a robustly s-stabilizing state feedback with feedforward m, then by Proposition 1 the differential inclusion (7.12) is strongly asymptotically stable. Since it satisfies Hypothesis (H), Theorem 2 warrants the existence of a smooth strong Lyapunov function V that satisfies the infinitesimal decrease condition (7.16). Since

$$f\big(x, m(x,d), d\big) \in \bigcap_{\varepsilon>0} \overline{\text{co}} \bigcup_{d\in\mathbb{D}} f\big(x, m(x+\varepsilon B, d+\varepsilon B), d\big)$$

for any $d \in \mathbb{D}$, from (7.16),

$$\langle \nabla V(x), f\big(x, m(x,d), d\big)\rangle \leq -W(x), \quad \forall d \in \mathbb{D}.$$

Hence, V is a smooth uniform control Lyapunov function for the control system (7.1).

Now we shall return to the earlier problem of finding a robustly s-stabilizing feedforward l for system (7.1) that is equipped with a robustly s-stabilizing feedback k designed to make the system

$$\dot{x} = f(x, u, 0)$$

asymptotically stable. Obviously, the implementation of the feedback k in system (7.1) only guarantees asymptotic stability if there exists a smooth uniform control Lyapunov function satisfying the infinitesimal decrease condition [1]

$$\max_{d\in\mathbb{D}} \langle \nabla V(x), f\big(x, k(x), d\big)\rangle \leq -W(x), \quad \forall x \neq 0, 0 \in \mathbb{D}$$

making the need for a feedforward l redundant. However, if there only exists a smooth uniform control Lyapunov function with a stricter infinitesimal decrease condition (7.3) as considered in this paper, one would then need a controller with a complete knowledge of the system to provide asymptotic stability, i.e. one that has both the state x and disturbance d as its arguments. The existence of a smooth uniform control Lyapunov function implies that there always exists a state feedback with feedforward m as defined by (7.5). Since the state feedback k is given, one only needs to find a feedforward l that satisfies (7.5) and (7.4), and Theorem 1 guarantees that such a combination of a feedback k and a feedforward l is robustly s-stabilizing.

7.5 Simulation Results

We will now show the existence of a robustly s-stabilizing state feedback with feedforward for the control of wing rock motion of an aircraft [12]. From Theorem 1, we know that this is an implication of the existence of a smooth uniform control Lyapunov function for the system in question. The following are the equations governing a wing rock motion with disturbance and neglecting actuator dynamics, see e.g. [13].

$$\begin{aligned} \dot{x}_1 &= x_2 \\ \dot{x}_2 &= u + \Delta(x_1, x_2) + d, \end{aligned} \tag{7.22}$$

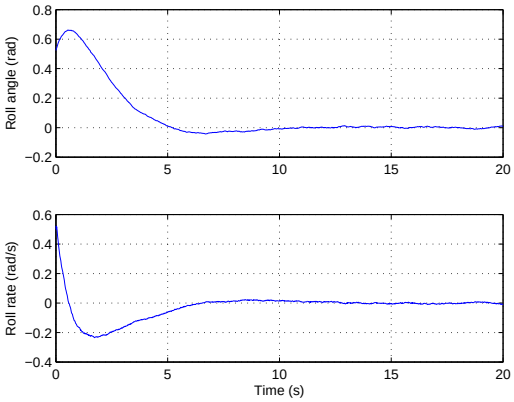

Figure 7.1: Roll angle and roll rate using state feedback only with $d = 0$.

where $x_1 \in \mathbb{R}$ and $x_2 \in \mathbb{R}$ represents the roll angle ϕ and roll rate p respectively, $u \in \mathbb{R}$ is the control input, $d \in \mathbb{R}$ is the persistent disturbance and $\Delta(x_1, x_2) := b_0 + b_1 x_1 + b_2 x_2 + b_3|x_1|x_2 + b_4|x_2|x_2 + b_5 x_1^3$ with $b_0 = 0, b_1 = -0.01859521, b_2 = -0.015162375, b_3 = -0.6245153, b_4 = 0.00954708$ and $b_5 = 0.02145291$. Note that we have assumed $u \in \mathbb{R}$ for simplicity so that given $u := -x_1 - \Delta(x_1, x_2) - d - x_1^2$, the function $V(x_1, x_2) := \frac{1}{2}x_1^2 + \frac{1}{2}x_2^2$ satisfies

$$\min_{u \in \mathbb{R}} \langle \nabla V(x_1, x_2), f(x_1, x_2, u, d) \rangle = \min_{u \in \mathbb{R}} [x_1 x_2 + x_2 u + x_2 \Delta(x_1, x_2) + x_2 d] = -x_1^2$$

and is therefore a smooth uniform control Lyapunov function for (7.22). Using the model reference adaptive controller from [14] as a feedback $k(x)$ and a feedforward $l(d) := -d$, we will demonstrate that they form a robustly s-stabilizing state feedback with feedforward $m(x, d) := k(x) + l(d)$ as assured by Theorem 1. In the simulation we assume that all states and persistent disturbance $d(t) = sin(t)$ can be measured. Additionally we set the state measurement errors, disturbance measurement errors and external disturbances to be uniformly distributed random numbers, i.e., $e_x(\cdot), e_d(\cdot), w(\cdot) \in [-0.1, 0.1]$ and employ a uniform partition π of $[0, 20]$ with $t_{i+1} - t_i = 0.02, i = 1, 2, \ldots$.

The objective of the control is to suppress the wing rock motion ($\phi = p = 0$). In Figure 7.1, in the absence of disturbance, it could be seen that the state feedback is robustly s-stabilizing in the face of state measurement errors $e_x(\cdot)$ and external disturbances $w(\cdot)$. This capability is diminished however, when disturbance is fed to the system as shown in Figure 7.2. The validity of Theorem 1 is proven in Figure 7.3 when the combination of the existing state feedback $k(x)$ and the feedforward $l(d)$ stabilizes the motion and is robust with respect to state measurement errors $e_x(\cdot)$, disturbance measurement errors $e_d(\cdot)$ and external disturbances $w(\cdot)$. Thus, in this example we have shown that if there exists a smooth uniform control Lyapunov function and a previously designed robustly s-stabilizing feedback in the absence of disturbance, one could find a feedforward so that the state feedback with feedforward is robustly s-stabilizing for nonzero disturbances.

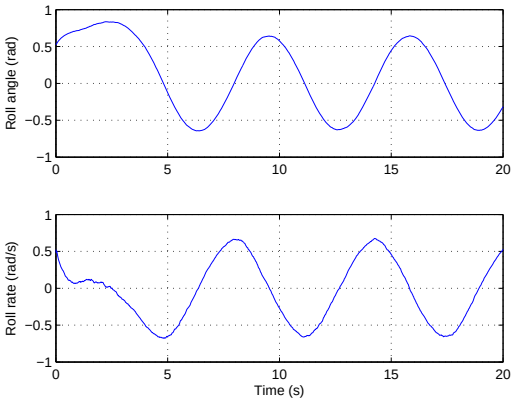

Figure 7.2: Roll angle and roll rate using state feedback only when $d \neq 0$.

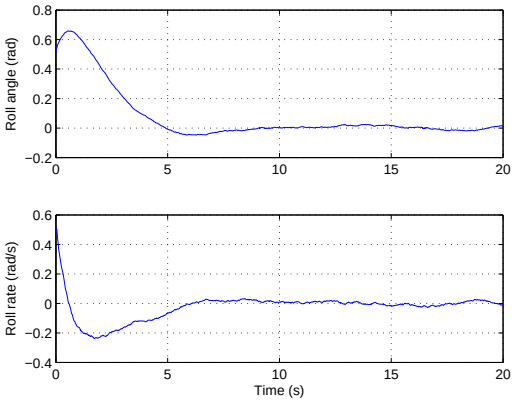

Figure 7.3: Roll angle and roll rate using state feedback with feedforward when $d \neq 0$.

7.6 Conclusion

In this theoretical work, we have proven that given a smooth uniform control Lyapunov function, there always exists a robustly s-stabilizing state feedback with feedforward m which could be implemented as a combination of a feedback k and a feedforward l, that is robust with respect to state and disturbance measurement errors and external disturbances. To prove that the reverse is also true, general nonlinear control systems with state and disturbance measurement errors are represented by parameterized differential inclusions. If there exists a robustly s-stabilizing state feedback with feedforward m, it is shown that the differential inclusion is strongly asymptotically stable. Since strong asymptotic stability implies the attraction of all of the solutions to an arbitrary neighborhood of the origin, a smooth control Lyapunov function is proven to exist. With the establishment of the present theoretical foundation, the authors expect to produce a practical implementation

of the feedforward control for disturbance rejection as a future work.

Acknowledgment

The authors would like to express their uttermost gratitude to John-Josef Leth and Rafal Wisniewski for their guidance and valuable contributions.

References

[1] Y. S. Ledyaev and E. D. Sontag, "A Lyapunov characterization of robust stabilization," *Nonlinear Anal.*, vol. 37, no. 7, Ser. A: Theory Methods, pp. 813–840, 1999.

[2] M. Soroush and C. Kravaris, "Synthesis of discrete-time nonlinear feedforward/feedback controllers," *AIChE Journal*, vol. 40, no. 3, pp. 473–495, 1994.

[3] D. Gorinevsky and L. A. Feldkamp, "RBF network feedforward compensation of load disturbance in idlespeed control," in *Control Systems Magazine, IEEE*, December 1996.

[4] M. J. Grimble, "Non-linear generalized minimum variance feedback, feedforward and tracking control," *Automatica*, vol. 41, no. 6, pp. 957–969, 2005.

[5] F. H. Clarke, Y. S. Ledyaev, and R. J. Stern, "Asymptotic stability and smooth Lyapunov functions," *J. Differential Equations*, vol. 149, no. 1, pp. 69–114, 1998.

[6] F. H. Clarke, Y. S. Ledyaev, E. D. Sontag, and A. I. Subbotin, "Asymptotic controllability implies feedback stabilization," *IEEE Trans. Automat. Control*, vol. 42, no. 10, pp. 1394–1407, 1997.

[7] Y. S. Ledyaev, "Robustness of discontinuous feedback in control under disturbance," in *IEEE Conference on Decision and Control*, Nevada, USA, December 2002.

[8] K. Deimling, *Multivalued differential equations*, ser. de Gruyter Series in Nonlinear Analysis and Applications. Berlin: Walter de Gruyter & Co., 1992, vol. 1.

[9] P. S. Macansantos, "An existence theorem for differential inclusions using the Kurzweil integral," *Science Diliman*, vol. 10, no. 10, pp. 31–38, 1998.

[10] F. H. Clarke, *Optimization and nonsmooth analysis*, 2nd ed., ser. Classics in Applied Mathematics. Philadelphia, PA: Society for Industrial and Applied Mathematics (SIAM), 1990, vol. 5.

[11] G. V. Smirnov, *Introduction to the theory of differential inclusions*, ser. Graduate Studies in Mathematics. Providence, RI: American Mathematical Society, 2002, vol. 41.

[12] M. S. Monahemi and M. Krstic, "Control of wing rock motion using adaptive feedback linearization," *Guidance, Control and Dynamics*, vol. 19, no. 4, pp. 905–912, 1996.

[13] K. Y. Volyanskyy, A. J. Calise, and B.-J. Yang, "A novel Q-modification term for adaptive control," in *American Control Conference*, June 2006.

[14] G. Chowdhary and E. Johnson, "A least squared based modification term for adaptive control," Georgia Institute of Technology, Tech. Rep., 2009.

Corrections

1. Page 14, line 8
   $l : \mathbb{R}^n \times \mathbb{R}^w \to \mathbb{U}$

2. Page 14, (2.3)
   $\min_{u\in\mathbb{U}}\langle \nabla V(x), f(x,u,d)\rangle \le -W(x),\ \forall x \in \mathbb{X}, x \ne 0, \forall d \in \mathbb{D}$

3. Page 14, line 21
   $m : \mathbb{R}^n \times \mathbb{R}^w \to \mathbb{U}$

4. Page 14, (2.4)
   $\langle \nabla V(x), f\big(x, m(x,d), d\big)\rangle \le -W(x),\ \forall x \in \mathbb{X}, x \ne 0, \forall d \in \mathbb{D}$

5. Page 15, line 17
   $e_d : [0, +\infty) \to \mathbb{R}^w$

6. Page 18, line 5-7
   We let $x_j(\cdot)$ be a sequence of π-trajectory of (7.17) on $[0, T]$ contained in a ball of some fixed radius R'. Define $\delta_j := \text{diam}(\pi_j)$ and

   $$\mu := \sup\{|f\big(x, m(x', d'), d\big)| + 1 : |x| \le R', |x'| \le R' + 1, d \in \mathbb{D}, d' \in \mathbb{D} + B\}.$$

7. Page 21, line 21
   $|e_x(t_i)| \le \tilde{\eta}\big(x(t_i)\big), |e_d(t_i)| \le \tilde{\eta}\big(x(t_i)\big), |w(t)| \le \tilde{\eta}\big(x(t_i)\big), ...$

8. Page 21, line 25-28
   ... state measurement error $e_x(\cdot)$, disturbance measurement error $e_d(\cdot)$ and external disturbance $w(\cdot)$, suppose that for some $\delta > 0$ and $\eta > 0$,

   $$t_{i+1} - t_i \le \delta, |e_x(t_i)| \le \eta, |e_d(t_i)| \le \eta, |w(t)| \le \eta, \text{ a.a. } t \in [t_i, t_{i+1}], i = 0, 1, ...$$

9. Page 22, line 9-23

$$\begin{aligned}
m_f(x,d) &:= \max\{|f(x_1,u,d_1)| + 1 : |x_1 - x| \le 1, u \in \mathbb{U}_{\rho(|x|+1,|d|+1)}, \\
&\quad |d_1 - d| \le 1\}, \\
m_{\nabla V}(x) &:= \max\{\nabla V(x_1) : |x_1 - x| \le 1\}, \\
\omega_f(x,d;\gamma) &:= \max\{|f(x_1,u,d_1) - f(x_2,u,d_2)| : |x_1 - x_2| \le \gamma, \\
&\quad |x_i - x| \le 1, i = 1,2, u \in \mathbb{U}_{\rho(|x|+1,|d|+1)}, |d_1 - d_2| \le \gamma, \\
&\quad |d_i - d| \le 1, i = 1,2\}, \\
\omega_{\nabla V}(x;\gamma) &:= \max\{|\nabla V(x_1) - \nabla V(x_2)| : |x_1 - x_2| \le \gamma, |x_i - x| \le 1, \\
&\quad i = 1,2\}, \\
\omega_W(x;\gamma) &:= \max\{|W(x_1) - W(x)| : |x_1 - x| \le \gamma\},
\end{aligned}$$

   for $\gamma > 0$. Defining $x := x(t_i)$, $d := d(t_i)$ and letting $\delta \le \min\{1/m_f(x,d), 1/\nu\}$, we have $|x(t) - x| \le 1$ and $|d(t) - d| \le 1$ on $[t_i, t_{i+1}]$. Next let $\eta \le 1$ and from (7.21),

$$\frac{dV\big(x(t)\big)}{dt} \le -\frac{1}{2}W\big(x(t)\big) + \Omega(x,d;\delta,\eta) - \frac{1}{2}W(x),$$

where

$$\begin{aligned}\Omega(x,d;\delta,\eta) &:= m_f(x,d)\omega_{\nabla V}\big(x; m_f(x,d)\delta+\eta\big)\\ &\quad +m_{\nabla V}(x)\omega_f\big(x,d; m_f(x,d)\delta+\eta\big)+m_{\nabla V}(x)\eta+\omega_W(x;\eta)\\ &\quad +\frac{1}{2}\omega_W\big(x, m_f(x,d)\delta\big).\end{aligned}$$

By substituting $\Omega(x;\delta,\eta)$ with $\Omega(x,d;\delta,\eta)$, ...

10. Page 22, line 27-29

$$\begin{aligned}m' &:= \max\{|f\big(x,m(x',d'),d\big)|+\tilde{\eta}(x) : |x|\le r, |x'-x|\le\tilde{\eta}(x), d\in\mathbb{D},\\ &\quad |d'-d|\le\tilde{\eta}(x)\},\end{aligned}$$

for any positive r and $\tilde{\eta}$ as described in Lemma 2.

11. Page 23, line 18
$\max_{d\in\mathbb{D}}\langle\nabla V(x), f\big(x,k(x),d\big)\rangle \le -W(x),\ \forall x\in\mathbb{X}, x\neq 0$

Paper D

Robust Helicopter Stabilization in the Face of Wind Disturbance

Kumeresan A. Danapalasingam, John-Josef Leth, Anders la Cour-Harbo and Morten Bisgaard

This paper was published in:
In Proceedings of the 49th IEEE Conference on Decision and Control
15-17 December 2010, Atlanta, Georgia, USA

Abstract

When a helicopter is required to hover with minimum deviations from a desired position without measurements of a persistent wind disturbance, a robustly stabilizing control action is vital. In this paper, the stabilization of the position and translational velocity of a nonlinear helicopter model affected by a wind disturbance is addressed. The wind disturbance is assumed to be a sum of a fixed number of sinusoids with unknown amplitudes, frequencies and phases. An estimate of the disturbance is introduced to be adapted using state measurements for control purposes. A nonlinear controller is then designed based on nonlinear adaptive output regulation and robust stabilization of a chain of integrators by a saturated feedback. Simulation results show the effectiveness of the control design in the stabilization of helicopter motion and the built-in robustness of the controller in handling parameter and model uncertainties.

8.1 Introduction

Autonomous helicopters are highly agile and have six degrees of freedom maneuverability making them a favourite candidate for a wide range of practical applications including agriculture, cinematography, inspection, surveillance, search and rescue, reconnaissance, etc. For certain tasks the ability of a helicopter to follow a given state reference is crucial for a successful outcome; for instance when hovering over a ship for rescue operations or when flying close to power lines or wind turbines for inspections. In windy conditions this becomes a significant challenge for any pilot and hence an autopilot capable of accounting effectively for the wind disturbance is a realistic alternative. In this work, the authors present a control design for longitudinal, lateral, and vertical helicopter stabilization in the presence of a wind disturbance, with intrinsic robustness property in handling parameter and model uncertainties.

Firstly, some previous works are reviewed. In [1], a feedback-feedforward proportional differential (PD) controller is developed for heave motion control. With the assistance of a gust estimator, the controller is reported to be able to handle the influence from horizontal gusts. The effects of rotary gusts in forward and downward velocity of a helicopter is addressed in [2]. It is shown that via a state feedback law, the rotary gust rejection problem is always solvable. In a work by Wang et al., a multi-mode linear control stategy is designed for unmanned helicopters in the presence of model uncertainties, atmospheric disturbances and handling qualities requirements [3].

In the present work, assuming that all the state variables (position, attitude and derivatives hereof) are available for measurements, a control strategy combining nonlinear adaptive output regulation and robust stabilization of a chain of integrators by a saturated feedback is carried out (see for instance, [4], [5] and [6]). Guided by a control solution for vertical trajectory tracking presented in [6] and [7], the design technique presented therein is extended here for helicopter stabilization in the presence of horizontal and vertical wind disturbance. This is done by means of a robust longitudinal, lateral and vertical stabilizer capable of compensating for parameter and model uncertainties.

In Section 8.2, a mathematical model governing a model helicopter and a problem statement are given. This is followed by Section 8.3 which covers the vertical, longitudinal and lateral stabilization. After the presentation of simulation results in Section 8.4, conclusion and future works are discussed in Section 8.5.

8.2 Preliminaries

In this section, a mathematical model of a helicopter is described after which a problem statement is given.

Helicopter Model

The motion of the center of mass of a helicopter is expressed in an inertial coordinate frame $\mathcal{F}_i$ as

$$M\ddot{p}^i = \mathrm{R}f^b,$$

where M is the mass and $p^i = [x\ y\ z]^\top \in \mathbb{R}^3$ is the position of the center of mass of the helicopter with respect to the origin of $\mathcal{F}_i$. The rotation matrix $\mathrm{R} := \mathrm{R}(q)$ is parametrized in terms of unit quaternions $\mathbf{q} = (q_0, q) \in S_4$ where q_0 and $q = [q_1\ q_2\ q_3]^\top$ denote the scalar and the vector parts of the quaternion respectively (see [6, Appendix A.2]). With the overall control inputs given by main rotor thrust T_M, tail rotor thrust T_T, longitudinal main rotor tip path plane tilt angle a and lateral main rotor tip path plane tilt angle b, a simplified resultant external force f^b in a body-fixed coordinate frame $\mathcal{F}_b$ is taken as

$$f^b = \begin{bmatrix} 0 \\ 0 \\ -T_M \end{bmatrix} + \mathrm{R}^\top \begin{bmatrix} 0 \\ 0 \\ Mg \end{bmatrix} + \mathrm{R}^\top \begin{bmatrix} d_x \\ d_y \\ d_z \end{bmatrix}, \tag{8.1}$$

where d_x, d_y and d_z are wind disturbances that affect the helicopter motion in x, y and z axis respectively. Subsequently the following equations of translational motion can be derived,

$$\ddot{x} = \frac{-(2q_1q_3 + 2q_0q_2)T_M}{M} + \frac{d_x}{M}, \tag{8.2}$$

$$\ddot{y} = \frac{-(2q_2q_3 - 2q_0q_1)T_M}{M} + \frac{d_y}{M}, \tag{8.3}$$

$$\ddot{z} = \frac{-(1 - 2q_1^2 - 2q_2^2)T_M}{M} + g + \frac{d_z}{M}. \tag{8.4}$$

Now for the angular dynamics,

$$J\dot{\omega}^b = -S(\omega^b)J\omega^b + \tau^b, \quad \dot{\mathbf{q}} = \frac{1}{2}\begin{bmatrix} -q^\top \\ q_0 I + S(q) \end{bmatrix}\omega^b,$$

where $S(\cdot)$ is a skew symmetric matrix, $\omega^b \in \mathbb{R}^3$ represents the angular velocity in F_b and J is the inertia matrix. The external torques τ^b expressed in $\mathcal{F}_b$ are given by the following equation,

$$\tau^b = \begin{bmatrix} \tau_{f_1} \\ \tau_{f_2} \\ \tau_{f_3} \end{bmatrix} + \begin{bmatrix} R_M \\ M_M + M_T \\ N_M \end{bmatrix}, \tag{8.5}$$

where $\tau_{f_1}, \tau_{f_2}, \tau_{f_3}$ are moments generated by the main and tail rotors and R_M, M_M, N_M, M_T are moments of the aerodynamic forces [8]. With some approximations a compact torque equation is obtained,

$$\tau^b = A(T_M)\mathbf{v} + B(T_M), \quad \mathbf{v} := [a\ b\ T_T]^\top, \tag{8.6}$$

where $A(T_M)$ and $B(T_M)$ are a matrix and a vector whose entries are functions of T_M with dependence on the helicopter parameters.

One of the objectives of the controller to be designed is to handle parameter uncertainties. Taking μ as a vector of all uncertain parameters with a nominal value μ_0, the additive uncertainty is given by $\mu_\Delta = (\mu - \mu_0) \in \mathcal{P}$, where $\mathcal{P}$ is a given compact set. Correspondingly, $M = M_0 + M_\Delta$, $J = J_0 + J_\Delta$, $A(T_M) = A_0(T_M) + A_\Delta(T_M)$ and $B(T_M) = B_0(T_M) + B_\Delta(T_M)$.

Problem Statement

The objective of the controller is to stabilize a helicopter affected by a disturbance $\mathbf{d} = [d_x \; d_y \; d_z]^\top$ in the presence of parameter and model uncertainties. The disturbance that affects the acceleration of the helicopter can be written as a linear combination of N (possibly ∞) sinusoidal functions of time modeled in the following form,

$$d_j = \sum_{i=1}^{N} A_{ji} \cos(\Omega_i t + \varphi_{ji}),$$

with unknown amplitudes A_{ji}, phases φ_{ji} and frequencies Ω_i, for $j = x, y, z$. In our setup however, it is assumed that $\mathbf{d}$ can be approximated with a small N. It can be shown that the disturbance is generated by the following linear time-invariant exosystem,

$$\begin{aligned} \dot{w}_j &= \mathrm{S}(\varrho) w_j, \\ d_j &= R\mathrm{S}^2(\varrho) w_j, \quad j = x, y, z, \end{aligned} \tag{8.7}$$

where $w_j \in \mathbb{R}^{2N}$, $\varrho = [\Omega_1 \; \Omega_2 \; \ldots \; \Omega_N]^\top$, $\mathrm{S}(\varrho) = \mathrm{diag}\big(H(\Omega_1), \ldots, H(\Omega_N)\big)$ with

$$H(\Omega_i) = \begin{bmatrix} 0 & \Omega_i \\ -\Omega_i & 0 \end{bmatrix}, \quad i = 1, \ldots, N,$$

and $R = [1 \; 0 \; 1 \; 0 \; \ldots \; 1 \; 0]$ a $1 \times 2N$ matrix (see [6, pp. 89-90]). We remark that the initial condition $w_j(0)$ of the exosystem represents the amplitudes A_{ji} and phases φ_{ji} of the disturbance. In the next section, it will be clear how the representation of the disturbance in such a form can be advantageous in the development of an internal model for stabilizing control input generation.

8.3 Controller Design

In this section, a controller for helicopter stabilization with wind disturbance elimination is designed in two stages. In the first part of this section, a control law is constructed to achieve vertical (motion in z direction) stabilization. Next in second part of this section, it is shown that the stabilizing $\mathbf{v}$ can be tuned separately (without jeopardizing the vertical stabilization) to render the horizontal (x and y direction) motion stable.

Stabilization of Vertical Dynamics

With reference to the vertical dynamics (8.4) given above, to counter the nominal effect of the gravity, the following preliminary control law is chosen,

$$T_M = \frac{gM_0 + u}{1 - \text{sat}_c(2q_1^2 + 2q_2^2)}, \tag{8.8}$$

where $\text{sat}_c(s) := \text{sign}(s)\min\{|s|, c\}$ with $0 < c < 1$ is a saturation function introduced to avoid singularities and u is an input to be designed. This yields

$$\ddot{z} \;=\; -\frac{\psi_c^z(q)u}{M} + g\big(1 - \frac{M_0}{M}\psi_c^z(q)\big) + \frac{d_z}{M},$$

where

$$\psi_c^z(q) = \frac{1 - 2q_1^2 - 2q_2^2}{1 - \text{sat}_c(2q_1^2 + 2q_2^2)}.$$

If q is small enough such that $\psi_c^z(q) = 1$, then a feedforward u needed for vertical stabilization is

$$c_u(w_z, \mu, \varrho) = gM_\Delta + d_z, \tag{8.9}$$

provided that the initial conditions are set to zero. Since the steady-state control $c_u(w_z, \mu, \varrho)$ depends on unknown $M_\Delta \in \mu$ and d_z which is in turn influenced by unknown ϱ and the unmeasurable state w_z, it cannot be produced directly. However, it can be asymptotically generated by the use of an internal model. As a first step in designing a controller with an internal model, the desired control (8.9) is rewritten as an output of a linear system (recall that d_z is given by (8.7))

$$\begin{aligned} \frac{\partial \tau_z}{\partial w_z}\mathrm{S}(\varrho)w_z &= \Phi(\varrho)\tau_z(w_z, \mu), \\ c_u(w_z, \mu, \varrho) &= \Gamma(\varrho)\tau_z(w_z, \mu), \end{aligned}$$

where

$$\tau_z(w_z, \mu) = \begin{bmatrix} gM_\Delta \\ w_z \end{bmatrix}, \Phi(\varrho) = \begin{bmatrix} 0 & 0 \\ 0 & \mathrm{S}(\varrho) \end{bmatrix}, \Gamma(\varrho) = [1\ \Gamma_2(\varrho)],$$
$$\text{and} \quad \Gamma_2(\varrho) = \begin{bmatrix} -\Omega_1^2 & 0 & -\Omega_2^2 & 0 & \dots & -\Omega_N^2 & 0 \end{bmatrix}.$$

It is shown in [6, Lemma 3.3.1] that, by constructing a $(2N+1) \times (2N+1)$ Hurwitz matrix F and a $(2N+1) \times 1$ vector G such that the pair (F, G) is controllable, there exists a $(2N+1) \times (2N+1)$ nonsingular matrix T_ϱ such that $\Phi(\varrho) = T_\varrho^{-1}(F + G\Psi_\varrho)T_\varrho$ and $\Gamma(\varrho) = \Psi_\varrho T_\varrho$ where $\Psi_\varrho = [1\ \Psi_{2,\varrho}]$ is a $1 \times (2N+1)$ vector. Hence,

$$\begin{aligned} \frac{\partial \bar{\tau}_z}{\partial w_z}\mathrm{S}(\varrho)w_z &= (F + G\Psi_\varrho)\bar{\tau}_z(w_z, \mu, \varrho), \\ c_u(w_z, \mu, \varrho) &= \Psi_\varrho \bar{\tau}_z(w_z, \mu, \varrho), \end{aligned}$$

where $\bar{\tau}_z(w_z, \mu, \varrho) = T_\varrho \tau_z(w_z, \mu)$. Consequently for any initial condition of exosystem (8.7) $w_z(0)$, the control $c_u(w_z, \mu, \varrho)$ can be viewed as an output of the linear system

$$\begin{aligned} \dot{\xi}_z &= (F + G\Psi_\varrho)\xi_z, \\ c_u(w_z, \mu, \varrho) &= \Psi_\varrho \xi_z \end{aligned} \tag{8.10}$$

if it is initialized as $\xi_z(0) = \bar{\tau}(w_z(0), \mu, \varrho)$, where

$$\xi_z = \begin{bmatrix} \xi_{z1} \\ \xi_{z2} \end{bmatrix} \in \mathbb{R} \times \mathbb{R}^{2N}.$$

Note that even if Ψ_ϱ and $\bar{\tau}(w_z(0), \mu, \varrho)$ are known and hence enabling the generation of the control $c_u(w_z, \mu, \varrho)$ by (8.10), vertical stabilization can only be achieved if the initial conditions of (8.4) are set correctly (i.e. $z = \dot{z} = 0$). To deal with the unknowns in (8.10) and to obtain vertical stabilization given nonzero initial conditions, choose u in (8.8) as an output of the system

$$\begin{aligned} \dot{\xi}_z &= (F + G\hat{\Psi})\xi_z + g_{\text{stz}}, \\ u &= \hat{\Psi}\xi_z + u_{\text{st}}, \end{aligned} \tag{8.11}$$

where $u_{\text{st}} = k_2(\dot{z} + k_1 z)$ and $g_{\text{stz}} = Gu_{\text{st}} + FGM_0\dot{z}$ for $k_1, k_2 > 0$. The vector $\hat{\Psi} = [1\ \hat{\Psi}_2]$ with a $1 \times 2N$ row vector $\hat{\Psi}_2$ is an estimate of Ψ_ϱ and is to be tuned by the adaptation law

$$\dot{\hat{\Psi}}_2 = \gamma \xi_{z2}^\top (\dot{z} + k_1 z) - \text{tas}_d(\hat{\Psi}_2), \tag{8.12}$$

where $\gamma > 0$ is a design parameter and $\text{tas}_d(\hat{\psi}_i) := \hat{\psi}_i - \text{sat}_d(\hat{\psi}_i)$ is a *dead zone* function in which $\hat{\psi}_i$ is the ith component of $\hat{\Psi}_2$ and $d > \max_{i=1}^{2N} \left\{ |(\Psi_{2,\varrho})_i| \right\}$. Note that the term $\text{tas}_d(\hat{\psi}_i)$ is zero as long as $|\hat{\psi}_i| \leq d$ and has a stabilizing effect on $\hat{\psi}_i$ if the fixed bound is exceeded. As demonstrated next, the inclusion of the stabilizing terms g_{stz} and u_{st} in (8.11) enables the convergence of ξ_z to the desired function $\bar{\tau}_z(w_z, \mu, \varrho)$ and renders $(z, \dot{z})$ globally asymptotically and locally exponentially stable under appropriate conditions.

To prove that the control defined by (8.8) and (8.11) stabilizes (8.4), let

$$\eta = \begin{bmatrix} \eta_1 \\ \eta_2 \end{bmatrix} = \begin{bmatrix} \eta_1 \\ \tilde{\Psi}_2^\top \end{bmatrix}, \tag{8.13}$$

$$\eta_1 = \begin{bmatrix} \chi \\ z \\ \zeta \end{bmatrix}, \tag{8.14}$$

where

$$\begin{aligned} \chi &:= \xi_z - \bar{\tau}_z(w_z, \mu, \varrho) + GM\dot{z}, \\ \tilde{\Psi}_2 &:= \hat{\Psi}_2 - \Psi_{2,\varrho}, \\ \zeta &:= \dot{z} + k_1 z. \end{aligned}$$

The time derivative of η can be derived as,

$$\begin{aligned}\dot{\eta}_1 &= \Big(A + A_1\big(\psi_c^z(q)-1\big)\Big)\eta_1 \\ &\quad - \Big(\frac{1}{M}b + B\big(\psi_c^z(q)-1\big)\Big)\xi_{z2}^\top\eta_2 - B\rho, \\ \dot{\eta}_2 &= \gamma\xi_{z2}b_0^\top\eta_1 - \mathrm{tas}_d(\eta_2 + \Psi_{2,\varrho}^\top),\end{aligned} \tag{8.15}$$

where $\rho = \big(\psi_c^z(q)-1\big)\big(gM_0 + \Psi_\varrho\bar{\tau}_z(w,\mu,\varrho)\big)$,

$$\begin{aligned}A &= \begin{bmatrix} F & k_1FGM_\triangle & -FGM_\Delta \\ 0 & -k_1 & 1 \\ -\frac{1}{M}\Psi_\varrho & -k_1(\Psi_\varrho G + k_1) & (\Psi_\varrho G + k_1 - \frac{1}{M}k_2)\end{bmatrix}, \\ A_1 &= \begin{bmatrix} -G\Psi_\varrho & -G\Psi_\varrho GMk_1 & G\Psi_\varrho GM - Gk_2 \\ 0 & 0 & 0 \\ -\frac{1}{M}\Psi_\varrho & -k_1\Psi_\varrho G & (\Psi_\varrho G - \frac{1}{M}k_2)\end{bmatrix}, \\ b_0 &= \begin{bmatrix}0\\0\\1\end{bmatrix} \text{ and } B = \begin{bmatrix}G\\0\\\frac{1}{M}\end{bmatrix}.\end{aligned}$$

Using the same arguments as in [6, Proposition 3.3.2], it can be shown that there exists $k_2^* > 0$ such that if $k_2 > k_2^*$, then A is a Hurwitz matrix (see [9, Appendix A] for the proof). Subsequently when q is small enough such that $\psi_c^z(q) = 1$, [6, Proposition 5.4.1] guarantees that if the initial state $w_z(0)$ of the exosystem belongs to the compact set $\mathcal{W}$ defined therein, then system (8.15) is globally asymptotically and locally exponentially stable. Hence, η is bounded and $\lim_{t\to\infty}\eta(t) = 0$. Note that even though system equation (8.15) is different than that of in [6, Eq. (5.26)] due to the addition of a disturbance and therefore a different vertical control, the two propositions still apply.

It is only natural now to ensure that the condition $\psi_c^z(q) = 1$ can be achieved in finite time. Setting

$$\mathbf{v} = A_0(T_M)^{-1}\big(\tilde{\mathbf{v}} - B_0(T_M)\big) \tag{8.16}$$

with the assumption that $A_0(T_M(t))$ is nonsingular for all $t \geq 0$ and substituting in (8.6), yields the torque equation

$$\tau^b(\tilde{\mathbf{v}}) = L(T_M)\tilde{\mathbf{v}} + \Delta(T_M), \tag{8.17}$$

where $\tilde{\mathbf{v}}$ is an additional control input to be determined,

$$\begin{aligned}L(T_M) &= I + A_\Delta(T_M)A_0^{-1}(T_M) \text{ and} \\ \Delta(T_M) &= B_\Delta(T_M) - A_\Delta(T_M)A_0^{-1}(T_M)B_0(T_M).\end{aligned}$$

Dropping the superscript b in ω^b, choose

$$\tilde{\mathbf{v}} = K_P\big(\eta_1 - K_D(\omega - \omega_d)\big), \tag{8.18}$$

where $K_P, K_D > 0$ are design parameters,

$$\eta_1 := q_r - q \quad \text{and} \tag{8.19}$$

$$q_r = q^* + q_d. \tag{8.20}$$

To follow the notations in [6] closely, η_1 is redefined in (8.19) to represent a different quantity than (8.14). While the expressions for the reference angular velocity ω_d and reference quaternion q_r are given in the next subsection (see (8.28), (8.22), (8.24)), it is important to mention here that $\|q^*(t)\| \leq \sqrt{3}\lambda_3$ and it is assumed that $\|q_d(t)\| \leq K_d m_{q_d}$, $\|\omega_d(t)\| \leq K_d m_{\omega_d}$, $\|\dot{\omega}_d(t)\| \leq m_{\dot{\omega}_d}$ for all $t \geq 0$, where $K_d > 0$, $\lambda_3 > 0$ are design parameters and $m_{q_d}, m_{\omega_d}, m_{\dot{\omega}_d}$ are fixed positive numbers. Next, for the problem in hand the following proposition is stated.

Proposition 3. *Suppose there exists $l_1^* > 0$ such that*

$$0 < 2l_1^* \leq L(T_M) + L^\top(T_M)$$

and let l_2^*, $\delta^* > 0$ satisfy

$$\|L(T_M)\| \leq l_2^*, \quad \|\Delta(T_M)\| \leq \delta^*.$$

Choose $0 < \varepsilon < 1$ arbitrarily and fix compact sets $\mathcal{Q}$, Ω of initial conditions for $q(t)$ and $\omega(t)$ respectively, with $\mathcal{Q}$ contained in the set

$$\{q \in \mathbb{R}^3 : \|q\| < \sqrt{1-\varepsilon^2}\}.$$

Then for any $T^* > 0$, there exist $K_P^*(K_D) > 0$, $K_D^* > 0$, $K_d^*(K_D) > 0$ and $\lambda_3^*(K_D) > 0$, such that for all $K_P \geq K_P^*(K_D)$, $K_D \leq K_D^*$, $K_d \leq K_d^*(K_D)$ and $\lambda_3 \leq \lambda_3^*(K_D)$,

1. *the trajectory of attitude dynamical system* (8.5) *given* (8.17) *and* (8.18) *with initial conditions $(q_0(0), q(0), \omega(0)) \in (0,1] \times \mathcal{Q} \times \Omega$ is bounded and $q_0(t) > \varepsilon$, $\forall t \geq 0$,*
2. *$\psi_c^z(q(t)) = 1$, $\forall t \geq T^*$.*

Proof. See [9]. □

Stabilization of Longitudinal and Lateral Dynamics

It will be shown now how q_1 and q_2 can be manipulated to produce horizontal stability. The control law (8.8) that has been designed for vertical stabilization also appears in the longitudinal (8.2) and lateral (8.3) dynamics. By expanding the numerator of (8.8) as

$$gM_0 + u \quad = \quad gM + d_z + y_\eta(\eta, w),$$

where $\tilde{\Psi} = [0 \ \tilde{\Psi}_2]$ and

$$\begin{aligned} y_\eta(\eta, w) \quad &= \quad \tilde{\Psi}\bar{\tau}_z(w, \mu, \varrho) + (\tilde{\Psi} + \Psi_\varrho)(\chi - GM\dot{z}) \\ &\quad +k_2(\dot{z} + k_1 z), \end{aligned}$$

(8.2) and (8.3) can be rewritten as

$$\begin{aligned} \ddot{x} \quad &= \quad \frac{-\tilde{d}(\mathbf{q}, t)q_2 + m(\mathbf{q}, t)q_1 q_3 + n_x(\mathbf{q})y_\eta(\eta, w)}{M} + \frac{d_x}{M}, \\ \ddot{y} \quad &= \quad \frac{\tilde{d}(\mathbf{q}, t)q_1 + m(\mathbf{q}, t)q_2 q_3 + n_y(\mathbf{q})y_\eta(\eta, w)}{M} + \frac{d_y}{M}, \end{aligned}$$

where

$$\begin{aligned}
\tilde{d}(\mathbf{q},t) &= \frac{2(gM+d_z)q_0}{1-\text{sat}_c(2q_1^2+2q_2^2)},\\
m(\mathbf{q},t) &= -\frac{2(gM+d_z)}{1-\text{sat}_c(2q_1^2+2q_2^2)},\\
n_x(\mathbf{q}) &= \frac{-(2q_1q_3+2q_0q_2)}{1-\text{sat}_c(2q_1^2+2q_2^2)},\\
n_y(\mathbf{q}) &= \frac{-(2q_2q_3-2q_0q_1)}{1-\text{sat}_c(2q_1^2+2q_2^2)}.
\end{aligned}$$

Recall that from the previous analysis on vertical stabilization, with an appropriate selection of the design parameters, $y_\eta(\eta, w)$ is an asymptotically diminishing signal.

Next by introducing a group of integrators $\dot{\eta}_x = x$, $\dot{\eta}_y = y$ and $\dot{\eta}_q = q_3$, the following new state variables are defined,

$$\begin{aligned}
\zeta_1 &:= [\eta_y\ \eta_x]^\top,\\
\zeta_2 &:= [y\ x]^\top + \lambda_1\sigma(\frac{K_1}{\lambda_1}\zeta_1),\\
\zeta_3 &:= [\dot{y}\ \dot{x}\ \eta_q\ 0\ \cdots\ 0]^\top + P_1\lambda_2\sigma(\frac{K_2}{\lambda_2}\zeta_2),
\end{aligned} \tag{8.21}$$

where

$$P_1 = \begin{bmatrix} 0 & 1 & 0 & \cdots & 0\\ 1 & 0 & 0 & \cdots & 0 \end{bmatrix}^\top_{(4N+2)\times 2}.$$

By adopting the following *nested saturated* control law

$$q^* = -P_2\lambda_3\sigma(\frac{K_3}{\lambda_3}\zeta_3), \tag{8.22}$$

where P_2 is a matrix, $\sigma(\cdot)$ is a vector-valued saturation function of suitable dimension (see [9]), K_i, λ_i, $i = 1, 2, 3$ are design parameters, the time derivatives can be written as

$$\begin{aligned}
\dot{\zeta}_1 &= -\lambda_1\sigma(\frac{K_1}{\lambda_1}\zeta_1) + \zeta_2,\\
\dot{\zeta}_2 &= -\lambda_2\sigma(\frac{K_2}{\lambda_2}\zeta_2) + P_0\zeta_3 + K_1\sigma'(\frac{K_1}{\lambda_1}\zeta_1)\dot{\zeta}_1,\\
M\dot{\zeta}_3 &= -\tilde{D}(t)P_2\lambda_3\sigma(\frac{K_3}{\lambda_3}\zeta_3) + \tilde{D}(t)q_d,\\
&\quad + MK_2P_1\sigma'(\frac{K_2}{\lambda_2}\zeta_2)\dot{\zeta}_2 - \tilde{D}(t)\tilde{\eta}_1 + p + d_h,
\end{aligned} \tag{8.23}$$

in which

$$
\begin{aligned}
D_1(t) &= \begin{bmatrix} \tilde{d}(\mathbf{q},t) & m(\mathbf{q},t)q_3 & 0 \\ m(\mathbf{q},t)q_3 & -\tilde{d}(\mathbf{q},t) & 0 \\ 0 & 0 & M \end{bmatrix}, \\
\tilde{D}(t) &= \underbrace{\begin{bmatrix} D_1(t) & 0 \\ 0 & 0 \end{bmatrix}}_{(4N+2)\times(4N+2)}, \\
p &= \begin{bmatrix} n_y(\mathbf{q})y_\eta(\eta,w) \\ n_x(\mathbf{q})y_\eta(\eta,w) \\ 0 \\ \vdots \\ 0 \end{bmatrix}, \; d_h = \begin{bmatrix} d_y \\ d_x \\ 0 \\ \vdots \\ 0 \end{bmatrix}, \; \tilde{\eta}_1 = \begin{bmatrix} \eta_1 \\ 0 \\ \vdots \\ 0 \end{bmatrix}, \\
P_0 &= \underbrace{\begin{bmatrix} 1 & 0 & 0 & \cdots & 0 \\ 0 & 1 & 0 & \cdots & 0 \end{bmatrix}}_{2\times(4N+2)}.
\end{aligned}
$$

In a generic notation, for $\sigma : \mathbb{R}^n \to \mathbb{R}^n$, $\sigma'(\upsilon) = d\sigma(\upsilon)/d(\upsilon)$, where $\upsilon \in \mathbb{R}^n$. Note that if one can set $q_d = -D_0(t)d_h$, where

$$
D_0(t) = \begin{bmatrix} D_1^{-1}(t) & 0 \\ 0 & 0 \end{bmatrix},
$$

the disturbance d_h can be completely eliminated from subsystem (8.23). In this case, (8.23) can be shown to be *input-to-state stable* (ISS) with restrictions on the inputs $(\tilde{\eta}_1, p)$ and linear asymptotic gains [6, Lemma 5.7.4].

Since q_d is a function of uncertain M and unknown d_h, it cannot be generated directly. Thus the following is proposed,

$$
q_d := -K_d \tilde{D}_0(t)\hat{d}, \tag{8.24}
$$

where $\hat{d} = [\hat{d}_y \; \hat{d}_x \; 0 \; \cdots \; 0]^\top$ is a disturbance estimate to be adapted and

$$
\begin{aligned}
\tilde{D}_1(t) &= \begin{bmatrix} \tilde{d}_0(\mathbf{q},t) & m_0(\mathbf{q},t)q_3 & 0 \\ m_0(\mathbf{q},t)q_3 & -\tilde{d}_0(\mathbf{q},t) & 0 \\ 0 & 0 & 1 \end{bmatrix}, \\
\tilde{D}_0(t) &= \underbrace{\begin{bmatrix} \tilde{D}_1(t) & 0 \\ 0 & 0 \end{bmatrix}}_{(4N+2)\times(4N+2)},
\end{aligned} \tag{8.25}
$$

where

$$
\begin{aligned}
\tilde{d}_0(\mathbf{q},t) &= \frac{\big(1 - \text{sat}_c(2q_1^2 + 2q_2^2)\big)q_0}{2(q_0^2+q_3^2)(gM_0+u)}, \\
m_0(\mathbf{q},t) &= \frac{-\big(1 - \text{sat}_c(2q_1^2 + 2q_2^2)\big)}{2(q_0^2+q_3^2)(gM_0+u)},
\end{aligned}
$$

with u given by (8.11) (see [9, Appendix C] for the expression of $\hat{d}$). It is important to notice at this point that a constraint on d_z should be imposed. Because $\lim_{t\to\infty}\big(gM_0 +$

$u(t)\big) = gM + d_z$, it is required that $d_z(t) \neq -gM$ for all $t \geq 0$ to avoid singularities in (8.25). In this paper we assume that $|d_z(t)| < gM$ for all $t \geq 0$. As a result, $T_M > 0$ for all $t \geq 0$. Next, the following state variable are defined,

$$\eta_2 := \tilde{\omega} - \omega_d - \frac{1}{K_D}\tilde{\eta}_1, \tag{8.26}$$

$$\eta_3 := \tilde{J}\eta_2 - K_d e_\xi, \tag{8.27}$$

where e_ξ is the internal model error, and $\tilde{\omega}$ and $\tilde{J}$ is a vector and a matrix respectively (see [9]). Note that in (8.26), η_2 is redefined to represent a different variable than that of in (8.13). From (8.24), we may write $q_d = [q_{d1}\ q_{d2}\ 0\ \cdots\ 0]^\top$ and the desired angular velocity is defined as

$$\omega_d = Q_d \dot{q}_d, \tag{8.28}$$

Taking the time derivatives,

$$\begin{aligned}
\dot{\tilde{\eta}}_1 &= -\frac{1}{2}\big(q_0 I + \tilde{S}(q)\big)(\eta_2 + \frac{1}{K_D}\tilde{\eta}_1 + \omega_d) + \dot{q}_r, \\
\tilde{J}\dot{\eta}_2 &= -\tilde{S}(\omega)\tilde{J}(\eta_2 + \frac{1}{K_D}\tilde{\eta}_1 + \omega_d) - K_P K_D \tilde{L}(T_M)\eta_2 \\
&\quad + \tilde{\Delta}(T_M) - \tilde{J}\dot{\omega}_d - \frac{1}{K_D}\tilde{J}\dot{\tilde{\eta}}_1, \\
\dot{\eta}_3 &= \tilde{J}\dot{\eta}_2 - K_d \dot{e}_\xi.
\end{aligned} \tag{8.29}$$

See [9, Appendix C] for a complete expression of (8.28) and (8.29).

We will now study the stability of feedback interconnection of subsystems (8.23) and (8.29). Subsystem (8.23) is a system with state $(\zeta_1, \zeta_2, \zeta_3)$ and input $(\tilde{\eta}_1, \eta_2, \eta_3, p_0)$, while subsystem (8.29) has $(\tilde{\eta}_1, \eta_2, \eta_3)$ and $(y_{\zeta 0}, y_{\zeta 1}, I_{\tilde{\eta}_1}, I_{\eta_2}, I_{\eta_3})$ as its state and input respectively (see [9, Appendix C]). Since the vertical stability analysis in first part of Section 8.3 guarantees that $q_0(t) > \varepsilon > 0$ for all $t \geq 0$ for an allowed range of the design parameters and initial conditions, it is assumed so in the next proposition. Morever, let M^L, M^U, d^L and d^U be such that $M^L \leq M \leq M^U$ and $0 < d^L \leq \tilde{d}(\mathbf{q}, t) \leq d^U$ for all $t \geq 0$. With that, the following proposition is presented.

Proposition 4. *Let K_D be fixed and let K_i^* and λ_i^*, $i = 1, 2, 3$, be such that the following inequalities are satisfied*

$$\begin{aligned}
&\frac{\lambda_2^*}{K_2^*} < \frac{\lambda_1^*}{4}, \quad \frac{\lambda_3^*}{K_3^*} < \frac{\lambda_2^*}{4}, \quad 4K_1^*\lambda_1^* < \frac{\lambda_2^*}{4}, \\
&4K_2^*\lambda_2^* < \frac{d^L}{M^U}\frac{\lambda_3^*}{8}, \quad 24\frac{K_1^*}{K_2^*} < \frac{1}{6} \\
&\textit{and} \quad 24\frac{K_2^*}{K_3^*} < \frac{1}{6}\frac{d^L}{d^U}\frac{M^L}{M^U}.
\end{aligned}$$

Then, there exist positive numbers K_P^*, K_d^*, ϵ_L^*, ϵ_U^*, $R_{\zeta 1}$, $\gamma_{\zeta 1}$, $\gamma_{\eta 1}$, $\gamma_{\eta 2}$ and $\gamma_{\eta 3}$ such that, taking $\lambda_i = \epsilon^{i-1}\lambda_i^*$ and $K_i = \epsilon K_i^*$, $i = 1, 2, 3$, for all $K_P \geq K_P^*$, $K_d \leq K_d^*$ and $\epsilon_L^* \leq \epsilon \leq \epsilon_U^*$, the feedback interconnection of subsystems (8.23) *and* (8.29) *is ISS*

1. *without restrictions on the initial state;*
2. *with restrictions* $(\epsilon^2 R_{\zeta 1}, R_{\eta 1}, R_{\eta 2}, R_{\eta 3})$ *on input* $(p_0, I_{\tilde{\eta}_1}, I_{\eta_2}, I_{\eta_3})$*, where* $R_{\eta 1}$*,* $R_{\eta 2}$ *and* $R_{\eta 3}$ *are arbitrary positive numbers;*
3. *with linear asymptotic gains.*

Therefore, if $\|p_0\|_\infty < \epsilon^2 R_{\zeta 1}$, $\|I_{\tilde{\eta}_1}\|_\infty < R_{\eta 1}$, $\|I_{\eta_2}\|_\infty < R_{\eta 2}$ and $\|I_{\eta_3}\|_\infty < R_{\eta 3}$, then $(\zeta_1(t), \zeta_2(t), \zeta_3(t), \tilde{\eta}_1(t), \eta_2(t), \eta_3(t))$ satisfies the asymptotic bound

$$\|(\zeta_1, \zeta_2, \zeta_3, \tilde{\eta}_1, \eta_2, \eta_3)\|_a \leq$$
$$\max\left\{\gamma_{\zeta 1}\|p_0\|_a, K_D\gamma_{\eta 1}\|I_{\tilde{\eta}_1}\|_a, \frac{\gamma_{\eta 2}}{K_P}\|I_{\eta_2}\|_a, \frac{\gamma_{\eta 3}}{K_P}\|I_{\eta_3}\|_a\right\},$$

where $\|\cdot\|_\infty$ and $\|\cdot\|_a$ denote the $\mathcal{L}_\infty$ norm and asymptotic $\mathcal{L}_\infty$ norm respectively [10].

Proof. The proof of Proposition 4 involves showing that subsystems (8.23) and (8.29) are ISS separately and that the composed system satisfies the *small gain theorem* (see [9]). □

Note that by choosing large enough K_P and sufficiently small λ_3 and K_d, requirements for vertical, longitudinal and lateral dynamics stabilization as dictated by Proposition 3 and 4 can be simultaneously satisfied. To conclude the control design, consider the controller given by (8.8), (8.11), (8.16), (8.18), (8.19), (8.20), (8.28), (8.22) and (8.24). Choose the design parameters according to Proposition 3 and 4. Then for any initial conditions $w(0) \in \mathcal{W}$, $\eta(0) \in \mathcal{Z}$, $(x(0), \dot{x}(0), y(0), \dot{y}(0)) \in \mathbb{R}^4$, $q_0(0) > 0$, $(q(0), \omega(0)) \in \mathcal{Q} \times \Omega$ where $\mathcal{Z}$ is an arbitrary compact set, $(x(t), \dot{x}(t), y(t), \dot{y}(t))$ converges to a neighborhood of the origin which can be rendered arbitrarily small by choosing K_P and K_D sufficiently large and small respectively. In addition,

$$\lim_{t\to\infty} \|(z(t), \dot{z}(t))\| = 0.$$

8.4 Simulation Results

Hover flight of an autonomous helicopter equipped with the proposed autopilot and influenced by a wind disturbance is simulated. The simulation results presented here are based on a model of a small autonomous helicopter from [11]. To test the robustness property of the controller, parameter uncertainties are taken up to 30% of the nominal values. Even though the controller is designed based on simplified force and torque equations as described by (8.1) and (8.6) respectively, the helicopter model assumes full torque, (8.5) and full force equations. The wind disturbance shown in Fig. 8.1 is presented to the helicopter as a persistently acting external force generated by a 8-dimensional neutrally stable exosystem with $\varrho = (1, 1.5, 0.1, 10)$, $w_x(0) = (20, 1, 4, 0, -1800, 0, -0.1, -0.02)$, $w_y(0) = (10, 2, 10, 2, 1500, 0, 0.1, 0)$ and $w_z(0) = (5, 0, 1, 0, 2000, 0, 0.01, 0.01)$. To further challenge the controller, only 5-dimensional internal models are used. Positions of the helicopter in the face of the wind disturbance without $(\gamma = 0)$ and with disturbance adaptation are given in Fig. 8.2 and 8.3 respectively.

Without disturbance adaptation, while the controller fails to stabilize the x and y positions, z does converge fairly close to zero as could be seen in Fig. 8.2. Apparently, T_M is

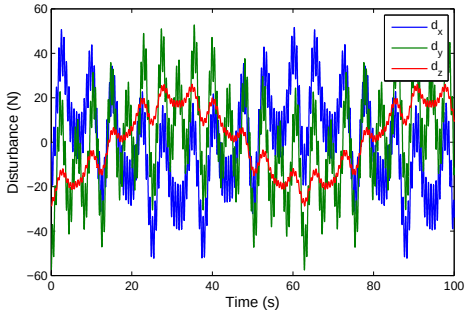

Figure 8.1: Wind disturbance

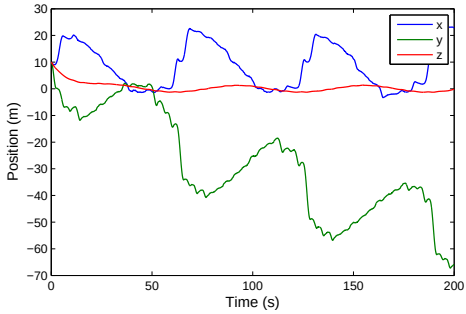

Figure 8.2: Position when disturbance adaptation is turned off.

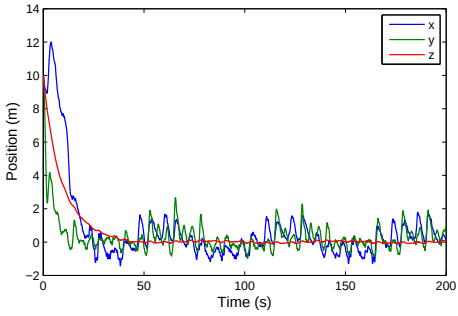

Figure 8.3: Position when disturbance adaptation is turned on.

still capable of acting as a vertical stabilizer to a certain degree although the disturbance adaptation is turned off due to the presence of other terms in (8.8). The importance of information on the disturbance to the longitudinal/lateral stabilizer is demonstrated in Fig. 8.3. Now that the disturbance adaptation is turned on, z converges to zero and, x and y converge to a small neighbourhood of the origin as guaranteed by Proposition 4.

8.5 Conclusion and Future Works

A robust controller for helicopter stabilization to reject wind disturbance is presented. The wind disturbance affecting the helicopter is assumed to be a function of time of a fixed structure with unknown parameters. By designing an internal model that estimates the disturbance, a control design is carried out for longitudinal, lateral and vertical dynamics stabilization. Despite the presence of helicopter parameter and model uncertainties, simulation results clearly demonstrates the effectiveness of the control technique. As future works, indoor and outdoor flights are to be carried out to test the feasibility of the proposed controller. That gives an immediate challenge caused by the presence of servo dynamics and limitations on wind disturbance that could be handled.

References

[1] X. Yang, H. Pota, and M. Garratt, "Design of a Gust-Attenuation Controller for Landing Operations of Unmanned Autonomous Helicopters," in *18th IEEE International Conference on Control Applications*, July 2009.

[2] F. N. Koumboulis, M. G. Skarpetis, and M. K. Griparis, "Rotary gust rejection for helicopters," in *In Proceedings of the IEEE International Conference on Control Applications*, 1998, pp. 103–107.

[3] H. Wang, A. A. Mian, D. Wang, and H. Duan, "Robust multi-mode flight control design for an unmanned helicopter based on multi-loop structure," *International Journal of Control, Automation, and Systems*, vol. 7, pp. 723–730, 2009.

[4] A. Isidori, *Nonlinear control systems*, 3rd ed., ser. Communications and Control Engineering Series. Berlin: Springer-Verlag, 1995.

[5] ——, *Nonlinear control systems. II*, ser. Communications and Control Engineering Series. London: Springer-Verlag London Ltd., 1999.

[6] A. Isidori, L. Marconi, and A. Serrani, *Robust Autonomous Guidance*. Secaucus, NJ, USA: Springer-Verlag New York, Inc., 2003.

[7] ——, "Robust nonlinear motion control of a helicopter," *IEEE Trans. Automat. Control*, vol. 48, no. 3, pp. 413–426, 2003. [Online]. Available: http://dx.doi.org/10.1109/TAC.2003.809147

[8] T. J. Koo and S. Sastry, "Output tracking control design of a helicopter model," in *In Proceedings of the 37th Conference on Decision and Control*, 1998, pp. 3635–3640.

[9] K. A. Danapalasingam, J. Leth, A. Cour-Harbo, and M. Bisgaard, "Robust helicopter stabilization with wind disturbance elimination," *Submitted to International Journal of Robust and Nonlinear Control*.

[10] A. R. Teel, "A nonlinear small gain theorem for the analysis of control systems with saturation," *IEEE Trans. Automat. Control*, vol. 41, no. 9, pp. 1256–1270, 1996. [Online]. Available: http://dx.doi.org/10.1109/9.536496

[11] O. Shakernia, Y. Ma, T. J. Koo, T. John, and S. Sastry, "Landing an unmanned air vehicle: Vision based motion estimation and nonlinear control," *Asian Journal of Control*, vol. 1, pp. 128–145, 1999.

Paper E

Nonlinear Feedforward Control for Wind Disturbance Rejection on Autonomous Helicopter

Morten Bisgaard, Anders la Cour-Harbo and Kumeresan A. Danapalasingam

This paper was published in:
In Proceedings of the 2010 IEEE/RSJ International Conference on Intelligent Robots and Systems
18-22 October 2010, Taipei, Taiwan

Abstract

This paper presents the design and verification of a model based nonlinear feedforward controller for vertical and horizontal wind disturbance rejection on autonomous helicopters. The feedforward control is based on a helicopter model that is derived using a number of carefully chosen simplifications to make it suitable for the purpose. The model is inverted for the calculation of rotor collective and cyclic pitch angles given the wind disturbance. The control strategy is then applied on a small helicopter in a controlled wind environment and the effectiveness and advantage of the feedforward controller is demonstrated through flight tests.

9.1 Introduction

Autonomous helicopters are small-scale helicopters, mostly equipped with on-board intelligence capable of performing various tasks like surveillance, search and rescue, law enforcement, aerial mapping, cinematography, inspection, etc. In this paper a feedforward control scheme capable of rejecting wind disturbances on the helicopter will be developed. The concept is to measure the wind disturbance at the helicopter and countering it before it can affect the position of the helicopter.

Sudden changes in wind can occur for instance when flying in an urban environment. An example of a system where wind disturbance rejection can be crucial is an emergency vehicle assistance system, where a small helicopter fly autonomously some distance in front of, say, an ambulance. The helicopter leapfrogs between intersections along the route of the ambulance, alerting nearby traffic to stay clear and report any possible problems ahead to the ambulance driver. An application like this requires, among other things, high performance control since the helicopter will operate in close proximity to obstacles like buildings, power lines, street lights, etc. Only very little error margin can be allowed in the trajectory tracking control and therefore the design of high performance controllers that could reject known and unknown disturbances to produce desired flight quality is crucial. When flying through a road intersection, sudden cross winds can be difficult to handle, even for a high performance feedback controller.

Another example where wind disturbance rejection is important is the use of an autonomous helicopter for inspection of offshore wind turbines and oil rig flare towers. The helicopter must operate very close to the turbine or tower and can easily experience very strong wind gusts which can lead to potentially dangerous situations.

This paper presents the design of a model based feedforward controller to counter wind disturbance effects on autonomous helicopters. This is achieved by deriving a simplified helicopter model in section 9.3. This model is then used for the design of the feedforward controller in section 9.4. In section 9.6 results are presented from flight tests of the feedforward controller in a controlled environment and finally a discussion and conclusion is given in section 9.7.

9.2 Previous Work

To date numerous feedback controller designs for autonomous helicopters have been accomplished with good results, but only little attention has been given to feedforward type control.

Nonlinear model predictive control (MPC) based on a neural network is used in conjunction with state dependent Riccati equation (SDRE) control in [1] for helicopter control. The SDRE controller provides robust stabilization of the helicopter using a simplified model while the neural MPC uses high fidelity nonlinear models for improved performance. The neural MPC was trained to include wind fields and simulations using a high fidelity wind model, including eddies and turbulence, and by accounting for the wind in a feedforward manner in the MPC, performance could be significantly improved. However, the use of nonlinear MPC – and also SDRE – as means of stabilizing the helicopter has the disadvantage that a highly intensive computational effort is needed for real time implementation of the control scheme. It can be difficult to achieve real time control of a small high-bandwidth helicopter with such methods. Therefore, a control system based only on SDRE, but with a nonlinear feedforward compensation to account for model simplifications has been proposed [2]. Good tracking performance is shown on two different helicopters. The nonlinear feedforward compensator is shown to be able to improve performance if provided with a static estimate of the wind conditions.

An adaptive trajectory tracking controller is presented in [3] where inverse dynamics together with a neural network is used for feedback linearization. The actual design is done using a cascading principle with a attitude controlling inner loop and a translational controlling outer loop. PD feedback from a reference model error is used to suppress disturbances and shape the two loops. The controller has been tested on a wide range of flying vehicles and has shown excellent tracking performance in a wide flight envelope, while being robust to changes in vehicle parameters. The approach with dynamic inversion resembles feedforward control and could most likely be extended to account for wind disturbances.

A feedforward control strategy augmented to an existing feedback controller is demonstrated for an autonomous helicopter in [4]. The purpose of the feedforward controller is to assist the feedback loop in rejecting wind disturbances based on wind velocity measurements made onboard the helicopter. The feedforward control actions are obtained through trimming of the helicopter model subjected to a simulated wind. These different trim points in state space are then used as training input for a neural network that is then used as the online feedforward controller. Simulations, using measured wind profiles, showed the feasibility of this approach for wind disturbance rejection. Stability for a nonlinear feedforward controller for wind disturbance rejection has been proven [5]. In a similar field, results on the use of feedforward on wind turbines to react to wind changes have been reported [6].

9.3 Helicopter Model

The helicopter model derived here is intended for use directly in the feedforward control and is a simplified version of the AAU Helisim model [7][1]. This simplified version neglects hinge offset and servo actuator dynamics. Inflow is assumed uniform and main rotor and stabilizer bar are considered steady state. The model is derived using blade element analysis and momentum theory.

While the model derived here is similar to models found in other literature, it is chosen to describe it thoroughly here as a number of specific assumptions are take to make it

[1] The AAU Helisim model can be downloaded for Matlab/Simulink at http://www.uavlab.org

feasible for inversion.

In the following the velocity of the helicopter with respect to a inertial reference frame is denoted $\boldsymbol{v} = [v_x, v_y, v_z]$ and the helicopter aerodynamic velocity, i.e. including external wind, is denoted $\boldsymbol{w} = [w_x, w_y, w_z]$. The blade advance ratio μ and rotor inflow ratio (λ) are defined as

$$\mu_x = \frac{w_x}{\Omega R}, \;\; \mu_y = \frac{w_y}{\Omega R}, \;\; \mu_z = \frac{w_z}{\Omega R}, \;\; \lambda = \frac{w_z - v_i}{\Omega R} \, . \tag{9.1}$$

where v_i is the rotor induced velocity, R is blade length, Ω is rotor angular velocity, and $\boldsymbol{\mu} = [\mu_x \;\; \mu_y \;\; \mu_z]^T$.

At any given azimuth station φ, the pitch of a point on a rotor blade (see figure 9.1) can be described by

$$\theta_r = \theta_{\text{col}} - \theta_{\text{lat}} \cos(\varphi) - \theta_{\text{lon}} \sin(\varphi) + \theta_t \frac{r}{R} \, , \tag{9.2}$$

where θ_{col} is the collective, θ_{lat} and θ_{lon} are cyclic pitch, θ_t is the blade twist, and r is the distance to the point of the blade. The flapping motion of the main rotor can be well approximated by the first terms of Fourier series

$$\beta = a_{\text{con}} - a_{\text{lon}} \cos(\varphi) + a_{\text{lat}} \sin(\varphi) \, , \tag{9.3}$$

which consists of the coning angle a_{con} as well as the longitudinal a_{lon} and lateral a_{lat} flapping angles. Figure 9.1 shows a blade cross section with the two forces affecting the infinitesimal blade element dr: The lift dL and the drag dD. The lift and drag are defined as force perpendicular and parallel, respectively, to the blade velocity. The lift on a small

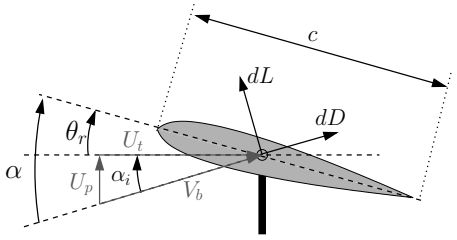

Figure 9.1: Cross section of the blade showing the blade element forces.

blade element can be described as

$$dL = \frac{1}{2} \rho V_b^2 C_l \alpha c \;\; dr \tag{9.4}$$

with air density ρ, blade velocity V_b, size of the blade (cord length) c, blade lift curve slope C_l, and blade angle of attack α. As is shown on figure 9.1 the angle of attack is equal to the sum of the pitch angle θ_r and the local inflow angle α_i. This means that the angle of attack can be described by

$$\alpha = \theta_r + \alpha_i = \theta_r + \frac{U_t}{U_p} \, , \tag{9.5}$$

where α_i is approximately equal to the ratio of the horizontal (U_t) to the vertical (U_p) elements of V_b when assuming that the induced velocity is much smaller that the rotational velocity of the blade. This assumption also gives

$$V_b = \sqrt{U_t^2 + U_p^2} \simeq U_t \,, \tag{9.6}$$

which leads to the final description of the lift as

$$dL = \frac{1}{2}\rho U_t^2 C_l c\Big(\theta_r + \frac{U_t}{U_p}\Big)\ dr \,. \tag{9.7}$$

The drag dD on the blade element can be described similar to the lift

$$dD = \frac{1}{2}\rho V_b^2 C_d c\ \ dr \,, \tag{9.8}$$

where C_d is the blade drag coefficient.

Two different contributions can be identified for the horizontal blade velocity. The rotation of the blade around the shaft and the helicopter motion. The contribution from the helicopter motion can be expressed as the translational velocities mapped to the blade by the blade azimuth station and together with element from the blade rotation it forms U_t as

$$U_t \simeq \Omega R\left(\frac{r}{R} + \mu_x sin(\varphi) - \mu_y cos(\varphi)\right) \,. \tag{9.9}$$

It is here assumed that the vertical blade velocity consists simply of the induced velocity from the rotor which result in

$$U_p \simeq \Omega R\big(\lambda - \mu_x\beta\cos(\varphi) - \mu_y\beta\sin(\varphi)\big) - \dot{\beta}r \,. \tag{9.10}$$

Flapping

The flapping of the main rotor and stabilizer bar is an integral part of the helicopter dynamics. However, both rotors have dynamics that are significantly faster than the rigid body dynamics and it is therefore in this case reasonable to consider them steady state.

In order to determine the dynamic flapping motion we use an equilibrium equation of the blade torques

$$\tau_a + \tau_{cf} + \tau_\beta = 0 \tag{9.11}$$

where the torques in order of appearance are aerodynamic, centrifugal, and inertial torque. Effects from helicopter motion are neglected and therefore Coriolis torque and torque from body angular and normal acceleration are zero. Furthermore, the torque due to the flexing of the blade is neglected as it is typically orders of magnitude smaller than the centrifugal torque.

The aerodynamic torque is the primary torque and it originates from the lift force acting on a blade. The torque around the flapping hinge is found by integrating the lift dL over the blade length to R and multiplying with the lever r. This yields

$$\tau_a = \int_0^R \frac{1}{2}\rho U_t^2 C_l c\Big(\theta_r + \frac{U_t}{U_p}\Big)r\ \ dr \,. \tag{9.12}$$

The centrifugal force acts perpendicular to the rotation axis and as the blade flaps this results in a torque around the flapping hinge. Assuming a small flapping angle, the centrifugal force can be found as

$$\tau_{cf} = -\Omega^2 I_b \beta \,, \tag{9.13}$$

where I_b is the blade moment of inertia. The torque due to flapping originates from the blade angular acceleration around the flapping hinge and can be expressed as

$$\tau_\beta = -I_b \ddot{\beta} \,. \tag{9.14}$$

The different torques are substituted into (9.11) and all higher harmonics are discarded. To find the tip-path plane dynamics, the elements containing $\sin(\varphi)$ form the equation for $\ddot{a_{\text{lat}}}$ and the elements containing $\cos(\varphi)$ form the equation for $\ddot{a_{\text{lon}}}$. Coning is neglected, effects from helicopter motion are discarded and all flapping derivatives are zeroed due to the steady state assumption. The resulting simplified equations are solved for the flapping angles and yields

$$a_{\text{lat}} = -2 \left(\frac{4}{3} \theta_{\text{col}} + \theta_t + \lambda \right) \mu_y - \theta_{\text{lat}} \tag{9.15}$$

$$a_{\text{lon}} = \quad 2 \left(\frac{4}{3} \theta_{\text{col}} + \theta_t + \lambda \right) \mu_x - \theta_{\text{lon}} \tag{9.16}$$

The flapping of the stabilizer bar is mixed with the pitch input from the swashplate through the Bell-Hiller gain and works as a rate-stabilizing feedback. It can be calculated in a similar fashion to the main rotor, but for most helicopters the deciding factor for the stabilizer bar flapping is the helicopter rotation and wind has little influence on it. Therefore, while the stabilizer bar is a very important part of the helicopter dynamics, it is resonable in this case to assume

$$a_{\text{lat},st} = -\theta_{\text{lat}}, \quad a_{\text{lon},st} = \theta_{\text{lon}} \,, \tag{9.17}$$

which effectively means that the control rotor has no influence on the feedforward.

Rotor Forces

Using these assumptions the infinitesimal force equations can be simplified to

$$\begin{aligned} dF_{x\,mr} &= -dD \sin(\varphi) + dL(\beta \cos(\varphi) \pm \alpha_i \sin(\varphi)) \,, \\ dF_{y\,mr} &= \quad dD \cos(\varphi) + dL(\beta \sin(\varphi) - \alpha_i \cos(\varphi)) \,, \\ dF_{z\,mr} &= -dL \,. \end{aligned}$$

The infinitesimal forces are then integrated over r along the blade from 0 to $R - e$. Averaging over one revolution is done by one more integration. Finally, the resulting

forces are found by multiplying with the number of blades b

$$F_x = \frac{bc}{2\pi}\frac{\rho}{2}\int_0^{2\pi}\int_0^R U_t^2\left(C_l\left(\theta_r + \frac{U_p}{U_t}\right)\frac{U_p}{U_t}\sin(\varphi) - C_d\sin(\varphi)\right)\ dr d\varphi\,, \tag{9.18}$$

$$F_y = \frac{bc}{2\pi}\frac{\rho}{2}\int_0^{2\pi}\int_0^R U_t^2\left(-C_l\left(\theta_r + \frac{U_p}{U_t}\right)\frac{U_p}{U_t}\cos(\varphi) + C_d\cos(\varphi)\right)\ dr d\varphi\,, \tag{9.19}$$

$$F_z = -\frac{bc}{2\pi}\frac{\rho}{2}C_l\int_0^{2\pi}\int_0^R U_t^2\left(\theta_r + \frac{U_t}{U_p}\right)\ dr d\varphi\,. \tag{9.20}$$

Solving the integrals yields

$$F_x = \frac{1}{2}\rho C_l bc\Omega^2 R^3\left(\left(\frac{1}{2}\mu_x\lambda - \frac{1}{3}a_{\text{lon}}\right)\theta_{\text{col}} - \frac{3}{4}\lambda a_{\text{lon}} + \frac{1}{4}\left(\mu_x\lambda - a_{\text{lon}}\right)\theta_t + \frac{1}{4}\left(\mu_x a_{\text{lon}} - \lambda\right)\theta_{\text{lon}} - \frac{Cd\,\mu_x}{2a}\right), \tag{9.21}$$

$$F_y = \frac{1}{2}\rho C_l bc\Omega^2 R^3\left(\left(\frac{1}{2}\mu_y\lambda + \frac{1}{3}a_{\text{lat}}\right)\theta_{\text{col}} + \frac{3}{4}\lambda a_{\text{lat}} + \frac{1}{4}\left(\mu_y\lambda + a_{\text{lon}}\right)\theta_t + \frac{1}{4}\left(\mu_y a_{\text{lat}} + \lambda\right)\theta_{\text{lat}} - \frac{Cd\,\mu_y}{2a}\right), \tag{9.22}$$

$$F_z = -\frac{1}{2}\rho C_l bc\Omega^2 R^3\left(\frac{1}{2}\lambda + \left(\frac{1}{2}{\mu_x}^2 + \frac{1}{3} + \frac{1}{2}{\mu_y}^2\right)\theta_{\text{col}} + \frac{1}{4}\left(1 + {\mu_x}^2 + {\mu_y}^2\right)\theta_t + \frac{1}{2}(\theta_{\text{lat}}\mu_y - \theta_{\text{lon}}\mu_x)\right). \tag{9.23}$$

Induced Inflow

Momentum theory assumes that the rotor behaves like a circular wing and thrust ($T = -F_z$) is generated when the rotor moves air downwards through what is assumed to be a virtual tube. The amount of thrust generated is determined by the change of momentum for the air when it is moved by the rotor from far above the helicopter (upstream) to far below the helicopter (downstream). As the steam tube is assumed a closed system, the mass flux is constant through it and therefore the change of momentum is generated by the air velocity change. This velocity change comes from the induced velocity v_i and relates to the thrust as

$$T = 2\rho A|\boldsymbol{v}|v_i \Leftrightarrow v_i = \frac{T}{2\rho A\sqrt{{w_x}^2 + {w_y}^2 + (w_z - v_i)^2}}\,.$$

A dimensionless thrust coefficient C_T is in introduced

$$C_T = \frac{T}{\rho A(\Omega R)^2}\,, \tag{9.24}$$

and substituted together with the expression for v_i into the inflow ratio λ

$$\lambda = \frac{w_z - v_i}{\Omega R} = \mu_z - \frac{C_T}{2\sqrt{(\mu_x^2 + \mu_y^2) + \lambda^2}}\,, \tag{9.25}$$

and λ is then found by analytically solving this fourth order equation.

9.4 Feedforward Control

Feedforward control is used to compensate for measured disturbances before they affect the system output. Ideally, given a perfect model of the system and an error free measurement of the disturbance, it is possible to entirely eliminate the effect of the disturbance. However, in reality with modeling approximations and measurement noise, feedforward control is seen as a tool to be used together with feedback control and thereby improve performance over systems with only feedback control.

In the helicopter case, a feedforward controller could be designed to counter wind disturbance if it is possible to invert the model such that the control signals can be calculated from the disturbance and helicopter states. Furthermore, it is necessary to use the feedforward in combination with a feedback controller that can stabilize the helicopter and do trajectory tracking. The full control architecture is shown in figure 9.2. A wind

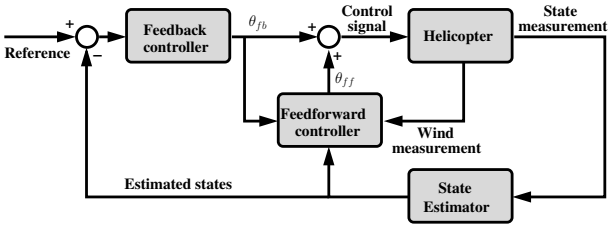

Figure 9.2: Combined feedback and feedforward control.

gust on a helicopter will cause a upward motion and a motion along with the wind where the upward motion is normally the stronger and the sideways motion the weaker effect. This means that both collective and cyclic control signals are needed to counter the disturbance.

The design of the feedforward controller includes a inversion of the helicopter model such that control signals can be calculated given wind and helicopter states. A step-wise approach is taken as an inversion of the full helicopter model mathematically cumbersome. A decoupling between the different axis is assumed such that the collective pitch couples mainly to the thrust and that the lateral and longitudinal pitch couples to the lateral and longitudinal force, respectively. Control of the tail will be neglected in this feedforward controller as the gyro system that controls the tail on most small scale helicopters has a very good disturbance rejection. However, the tail-yaw model equations could easily be included in the approach. Furthermore, it is observed that while changes in collective pitch have significant influence on the lateral and longitudinal forces, changes in cyclic pitch have little influence on the thrust. Therefore, the feedforward controller is synthesized by first calculating the collective pitch given the disturbance in x,y and z. This is then using that in the calculation of the lateral and longitudinal cyclic pitch.

The main idea behind the controller is to use the helicopter model to calculate the no-disturbance force, i.e. the force that would have resulted if there was no disturbance. This desired force, which can be considered as a reference for the controller, is then used in the inverted model with the disturbance present and the resulting control signal will result in the correct force for the given disturbance.

To calculate the no-disturbance model response (9.1) is calculated without wind dis-

turbance as

$$\mu_x^* = \frac{v_x}{\Omega R},\ \mu_y^* = \frac{v_y}{\Omega R},\ \mu_z^* = \frac{v_z}{\Omega R},\ \lambda^* = \frac{v_z - v_i}{\Omega R}\ , \tag{9.26}$$

where * indicates no-disturbance variable. The first step is to calculate the no-disturbance inflow ratio using the analytical solution to (9.25) as

$$\lambda^* = f_{(9.25)}(\boldsymbol{\mu}^*, \theta_{\text{col,fb}}, \theta_{\text{lat,fb}}, \theta_{\text{lon,fb}})\ , \tag{9.27}$$

which is then used in the calculation of the no-disturbance thrust

$$F_z^* = f_{(9.23)}(\lambda^*, \boldsymbol{\mu}^*, \theta_{\text{col,fb}}, \theta_{\text{lat,fb}}, \theta_{\text{lon,fb}})\ . \tag{9.28}$$

where $f_{(9.23)}$ is equation 9.23 as a function. We can then find the collective pitch that will result in a thrust force F_z^* given the disturbance. The corresponding λ given the disturbance is calculated

$$\lambda_{\text{ff}} = f_{(9.25)}(\boldsymbol{\mu}, F_z^*)\ , \tag{9.29}$$

and used in the final calculation of the feedforward collective pitch which is found trivially as (9.23) solved for θ_{col}

$$\theta_{\text{col,ff}} = f_{(9.23)}^{-1}(\boldsymbol{\mu}, F_z^*, \theta_{\text{lat,fb}}, \theta_{\text{lon,fb}})\ , \tag{9.30}$$

where $f_{(9.23)}^{-1}$ represent the model inversion of (9.23).

The procedure for the lateral and longitudinal axis is similar to the vertical axis. First the no-disturbance forces are calculated

$$a_{\text{lat}}^* = f_{(9.15)}(\boldsymbol{\mu}^*, \lambda_{\text{ff}}, \theta_{\text{col,ff}}, \theta_{\text{lat,fb}})\ , \tag{9.31}$$
$$a_{\text{lon}}^* = f_{(9.16)}(\boldsymbol{\mu}^*, \lambda_{\text{ff}}, \theta_{\text{col,ff}}, \theta_{\text{lon,fb}})\ , \tag{9.32}$$
$${F_y}^* = f_{(9.22)}(\boldsymbol{\mu}^*, \lambda_{\text{ff}}, a_{\text{lat}}^*, \theta_{\text{lat,ff}})\ , \tag{9.33}$$
$${F_x}^* = f_{(9.21)}(\boldsymbol{\mu}^*, \lambda_{\text{ff}}, a_{\text{lon}}^*, \theta_{\text{lon,ff}})\ . \tag{9.34}$$

For the next step, the flapping equations (9.15) and (9.16) are substituted into (9.21) and (9.22). The resulting (second order) equations are then solved for θ_{lat} and θ_{lon}, respectively

$$\theta_{\text{lat,ff}} = f_{(9.15),(9.22)}^{-1}(\boldsymbol{\mu}, \lambda_{\text{ff}}, \theta_{\text{col,ff}})\ , \tag{9.35}$$
$$\theta_{\text{lon,ff}} = f_{(9.16),(9.21)}^{-1}(\boldsymbol{\mu}, \lambda_{\text{ff}}, \theta_{\text{col,ff}})\ . \tag{9.36}$$

The final feedforward controller output is calculated as

$$\boldsymbol{\theta}_{\text{ff}} = \begin{bmatrix} \theta_{\text{col,ff}} \\ \theta_{\text{lat,ff}} \\ \theta_{\text{lon,ff}} \end{bmatrix} - \begin{bmatrix} \theta_{\text{col,fb}} \\ \theta_{\text{lat,fb}} \\ \theta_{\text{lon,fb}} \end{bmatrix}\ , \tag{9.37}$$

were the subtraction of $\boldsymbol{\theta}_{\text{fb}}$ is done to ensure that the feedforward controller generates perturbations from the feedback control trajectory. If no disturbance is present, the feedforward equations simply calculates back and forth and result in $\theta_{\text{col,fb}} = \theta_{\text{col,ff}}$ etc. which then in turn result in a zero $\boldsymbol{\theta}_{\text{ff}}$.

If the helicopter used is a fixed pitch type, which means that the thrust is controlled through main rotor speed Ω, it can be accommodated by solving (9.23) for Ω, considering $\boldsymbol{\theta}_{\text{col}}$ as a constant, and using the result instead of (9.30)

$$\Omega_{\text{ff}} = f_{(9.23)}(\boldsymbol{\mu}, F_z^*, \theta_{\text{lat,fb}}, \theta_{\text{lon,fb}}) \,. \tag{9.38}$$

9.5 Disturbance Measurement

In order to counter the disturbance on helicopter it is necessary to have a measurement or estimate of it. The disturbance in this case is wind which is difficult to predict and a wind measurement is therefore necessary. When measuring the wind at the helicopter, a number of challenges arise. The most obvious one is that the helicopter itself generates air flow, both from motion and from the rotors. The motion of the helicopter is known from the state estimator and the body velocities can be extracted from the wind measurements. The induced velocity from the rotor is more difficult to isolate and remove, but can be predicted using (9.25), and then subtracted. With the helicopter induced air flow subtracted, a measurement of the external wind is available. More theoretical and practical focus will be put on this in a near future publication.

9.6 Results

The control scheme will here be illustrated used on a small scale autonomous helicopter: The Aalborg University Corona Rapid Prototyping Platform which is a 1 kg fixed pitch electric helicopter. It performs fully autonomous flight with landings and takeoff using a set of gain-scheduled PID controllers. There is no computer onboard the helicopter and all control and estimation computation is done on ground in real time. It is powered from a power supply on the ground through wires that hangs from the nose of the helicopter and control signals to the servos are transmitted through a standard RC system. Helicopter state measurements are acquired using a Vicon motion tracking system at 100 Hz and with a sufficient accuracy for these to be considered as true values.

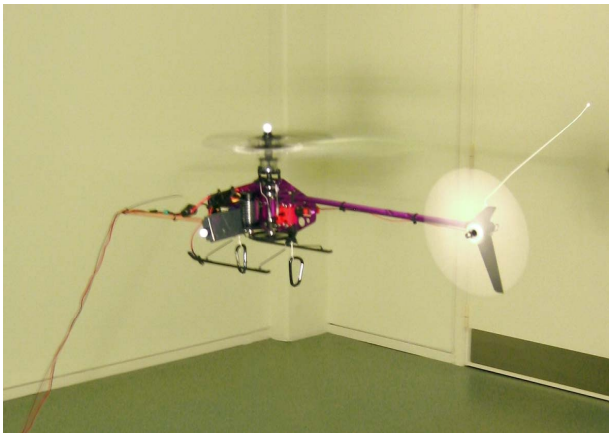

Figure 9.3: The Aalborg University Corona Rapid Prototyping Platform.

The laboratory is equipped with three Big Bear II fans with a diameter of 0.6 m, each capable of delivering wind of up to 16 m/s at 1 m distance. With these it is possible to deliver a controllable and known wind disturbance to the helicopter.

Two different flight tests have been carried out: In the first, the helicopter hovers in front of the fans which are then turned on, which is equivalent to a wind gust. In the second the helicopter flies through the wind stream of the running fans which is equivalent to the helicopter flying through cross winds in a road intersection.

The wind sensor used in these tests is a R.M. Young 81000 3D ultrasonic anemometer (32 Hz measurement with 1% accuracy). However, this sensor is both too big and too heavy to be mounted on the small helicopter and therefore different approaches are taken in the two tests to provide the feedforward controller with wind measurements without the sensor being mounted on the helicopter.

Flight Test: Gust disturbance

In the gust disturbance test, two fans are use. The fans are separate by some distance and does not influence each other. Two meters in front of the one fan the helicopter hovers with the nose pointing towards the fan. At the same distance, but in front of the other fan the wind sensor is placed. The two fans are controlled together and this means that the sensor will (ideally) see the same wind as the helicopter. A gust is emulated by turning the fans on and off in rapid succession and the helicopter response with and without feedforward is observed. The response of the helicopter to the gusts is shown in figure 9.4 and the actual wind gusts are shown in figure 9.5.

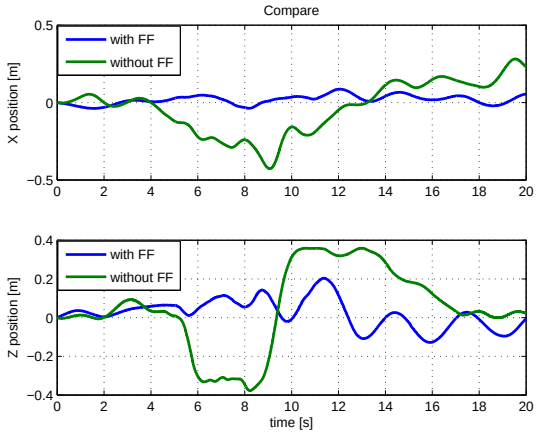

Figure 9.4: Helicopter gust response with and without feedforward.

It can be seen how the gust results in first an upward and backward motion and as the wind subsides a downward and forward motion. It is also evident how the use of the feedforward controller significantly reduces the deviations of helicopter due to the gust compared to the response without the feedforward controller.

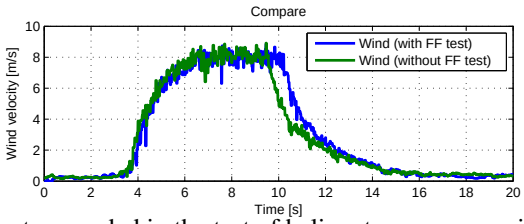

Figure 9.5: Wind gusts recorded in the test of helicopter response with and without feedforward.

Flight Test: Cross wind disturbance

In the cross wind disturbance test the helicopter flies sideways past the fan and thereby crossing in and out of the wind stream. The wind velocity estimation is done by measuring wind velocity as a function of position in front of the fan (using the anemometer) prior to flight and the during flight use interpolation on these measurements to predict the wind that the helicopter encounters at varying positions.

The response of the helicopter flying though the wind is shown in figure 9.6 and as before it can be seen how the feedforward is capable of reducing the helicopter response to the wind. The response can also be seen on figure 9.7 where the location of the wind

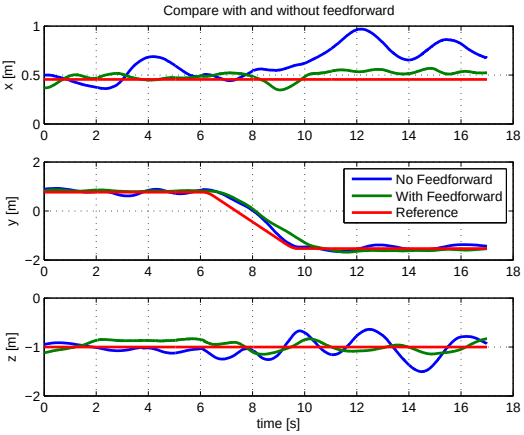

Figure 9.6: Helicopter cross wind response with and without feedforward.

corridor is also indicated.

9.7 Discussions and Future Works

Discussion

It has been demonstrated how a feedforward controller can be used, in augmentation with a feedback controller, to counter disturbances from external wind. The approach,

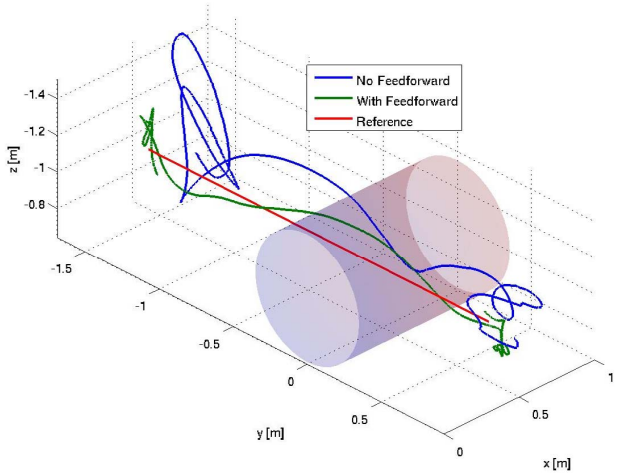

Figure 9.7: 3D plot of helicopter cross wind response with and without feedforward.

that involves calculating feedforward control signals to cancel the additional force from the wind, has been demonstrated to improve tracking performance in real flight. Even though the control scheme is based on model inversion, due to the reduced computation complexity that arises from the simplified model, the proposed method poses no problem for real time implementation. As the method is based on a feedforward approach, it is important that the model has a good correspondence with the actual behavior of the system to ensure an acceptable performance.

Future Works

Results on the theory and practice behind reliable wind measurements on a helicopter will be published in a near future. This includes detailed considerations on sensor types, more advanced helicopter inflow modeling, as well as measurement experiments. Furthermore, outdoor flight tests are to be carried out in uncontrolled wind settings.

References

[1] E. Wan, A. Bogdanov, R. Kieburtz, A. Baptista, M. Carlsson, Y. Zhang, and M. Zulauf, *Software Enabled Control: Information Technologies for Dynamical Systems*. John Wiley & Sons, 2003, ch. 10, Model predictive neural control for aggressive helicopter maneuvers.

[2] A. Bogdanov, E. Wan, and G. Harvey, "Sdre flight control for x-cell and r-max autonomous helicopters," in *The 43rd IEEE Conference on Decision and Control*, 2004.

[3] E. N. Johnson and S. K. Kannan, "Adaptive trajectory control for autonomous helicopters," *AIAA Journal of Guidance, Control, and Dynamics, Vol 28, No 3*, 2005.

[4] K. A. Danapalasingam, A. la Cour-Harbo, and M. Bisgaard, "Feedforward control of an autonomous helicopter using trim inputs," in *AIAA Infotech@Aerospace & AIAA Unmanned...Unlimited Conference and Exhibit*, 2009.

[5] ——, "Disturbance effects in nonlinear control systems and feedforward control strategy," in *7th International Conference on Control and Automation*, 2009.

[6] E. van der Hooft and T. van Engelen, "Estimated wind speed feed forward control for wind turbine operation optimisation," in *European wind energy conference*, 2004.

[7] M. Bisgaard, "Modeling, estimation, and control of helicopter slung load system," Ph.D. dissertation, Aalborg University, 2008.

Paper F

Robust Helicopter Stabilization with Wind Disturbance Elimination

Kumeresan A. Danapalasingam, John-Josef Leth, Anders la Cour-Harbo and Morten Bisgaard

This paper has been submitted to:
International Journal of Robust and Nonlinear Control

The layout has been revised

Abstract

When a helicopter is required to hover with minimum deviations from a desired position without measurements of a persistent wind disturbance, a robustly stabilizing control action is vital. In this paper, the stabilization of the position and translational velocity of a nonlinear helicopter model affected by a wind disturbance is addressed. The wind disturbance is assumed to be a sum of a fixed number of sinusoids with unknown amplitudes, frequencies and phases. An estimate of the disturbance is introduced to be adapted using state measurements for control purposes. A nonlinear controller is then designed based on nonlinear adaptive output regulation and robust stabilization of a chain of integrators by a saturated feedback. Simulation results show the effectiveness of the control design in the stabilization of helicopter motion and the built-in robustness of the controller in handling parameter and model uncertainties.

10.1 Introduction

Autonomous helicopters are highly agile and have six degree of freedom maneuverability making them a favourite candidate for a wide range of practical applications including agriculture, cinematography, inspection, surveillance, search and rescue, reconnaissance, etc. For certain tasks the ability of a helicopter to follow a given state reference is crucial for a successful outcome; for instance when hovering over a ship for rescue operations or when flying close to power lines or wind turbines for inspections. In windy conditions this becomes a significant challenge for any pilot and hence an autopilot capable of accounting effectively for the wind disturbance is a realistic alternative. In this work, the authors present a control design for longitudinal, lateral, and vertical helicopter stabilization in the presence of a wind disturbance, with intrinsic robustness property in handling parameter and model uncertainties.

Firstly, some previous works are reviewed. In [1], a feedback-feedforward proportional differential (PD) controller is developed for heave motion control. With the assistance of a gust estimator, the controller is reported to be able to handle the influence from horizontal gusts. The effects of rotary gusts in forward and downward velocity of a helicopter is addressed in [2]. It is shown that via a state feedback law, the rotary gust rejection problem is always solvable. In a work by Wang et al., a multi-mode linear control stategy is designed for unmanned helicopters in the presence of model uncertainties, atmospheric disturbances and handling qualities requirements [3].

In the present work, assuming that all the state variables (position, attitude and derivatives hereof) are available for measurements, a control strategy combining nonlinear adaptive output regulation and robust stabilization of a chain of integrators by a saturated feedback is carried out (see for instance, [4], [5] and [6]). Guided by a control solution for vertical trajectory tracking presented in [6] and [7], the design technique presented therein is extended here for helicopter stabilization in the presence of horizontal and vertical wind disturbance. This is done by means of a robust longitudinal, lateral and vertical stabilizer capable of compensating for parameter and model uncertainties.

In Section 10.2, a mathematical model governing a model helicopter and a problem statement are given. This is followed by Section 10.3 which covers the vertical, longitudinal and lateral stabilization. After the presentation of simulation results in Section 10.4, conclusion and future works are discussed in Section 10.5. Additionally, a number of appendices is included for relevant derivations and proofs.

10.2 Preliminaries

In this section, a mathematical model of a helicopter is described after which a problem statement is given.

Helicopter Model

The position and attitude of a helicopter in the three-dimensional Euclidean space $\mathbb{E}^3$ is described by the relative position and orientation respectively between a body-fixed coordinate frame $\mathcal{F}_b$ and an inertial coordinate frame $\mathcal{F}_i$. A coordinate frame $\mathcal{F}$ is denoted by the set

$$\mathcal{F} = \{O, i, j, k\},$$

where i, j and k are right-handed, mutually orthogonal unit vectors with a common origin O in $\mathbb{E}^3$.

The motion of the center of mass of a helicopter is expressed in an inertial coordinate frame $\mathcal{F}_i = \{O_i, i_i, j_i, k_i\}$ (whose axes are henceforth denoted as x, y and z axis) as

$$M\ddot{p}^i = \mathrm{R} f^b, \tag{10.1}$$

where M is the mass and $p^i = [x\ y\ z]^\top \in \mathbb{R}^3$ is the position of the center of mass of the helicopter with respect to O_i. The rotation matrix $\mathrm{R} := \mathrm{R}(\mathbf{q})$ is parametrized in terms of unit quaternions $\mathbf{q} = (q_0, q) \in S_4$ where q_0 and $q = [q_1\ q_2\ q_3]^\top$ denote the scalar and the vector parts of the quaternion respectively, as given by

$$\mathrm{R} = \begin{bmatrix} 1 - 2q_2^2 - 2q_3^2 & 2q_1q_2 - 2q_0q_3 & 2q_1q_3 + 2q_0q_2 \\ 2q_1q_2 + 2q_0q_3 & 1 - 2q_1^2 - 2q_3^2 & 2q_2q_3 - 2q_0q_1 \\ 2q_1q_3 - 2q_0q_2 & 2q_2q_3 + 2q_0q_1 & 1 - 2q_1^2 - 2q_2^2 \end{bmatrix}.$$

The overall force f^b that acts on the helicopter in a body-fixed coordinate frame $\mathcal{F}_b = \{O_b, i_b, j_b, k_b\}$ is given by

$$f^b = \begin{bmatrix} X_M \\ Y_M + Y_T \\ Z_M \end{bmatrix} + \mathrm{R}^\top \begin{bmatrix} 0 \\ 0 \\ Mg \end{bmatrix} + \mathrm{R}^\top \begin{bmatrix} d_x \\ d_y \\ d_z \end{bmatrix}, \tag{10.2}$$

where g is the gravitational acceleration and, d_x, d_y and d_z are wind disturbances that affect the helicopter motion in x, y and z axis respectively. Moreover,

$$\begin{aligned} X_M &= -T_M \sin a, \quad Y_M = T_M \sin b, \\ Z_M &= -T_M \cos a \cos b, \quad Y_T = -T_T, \end{aligned}$$

where T_M, T_T, a and b are main rotor thrust, tail rotor thrust, longitudinal main rotor tip path plane tilt angle and lateral main rotor tip path plane tilt angle respectively (see Fig. 10.1). For convenience of subsequent analysis, it is assumed that a and b are small such that

$$\sin a \approx a, \quad \sin b \approx b, \quad \cos a \approx 1 \quad \text{and} \quad \cos b \approx 1. \tag{10.3}$$

To simplify force equation (10.2), i_b component of T_M is neglected and it is assumed that j_b component of T_M is cancelled by T_T (i.e. $X_M = 0, Y_M + Y_T = 0$). Thus a simplified force equation is obtained,

$$f^b = \begin{bmatrix} 0 \\ 0 \\ -T_M \end{bmatrix} + \mathrm{R}^\top \begin{bmatrix} 0 \\ 0 \\ Mg \end{bmatrix} + \mathrm{R}^\top \begin{bmatrix} d_x \\ d_y \\ d_z \end{bmatrix}. \tag{10.4}$$

Subsequently the following equations of translational motion can be derived,

$$\ddot{x} = \frac{-(2q_1q_3 + 2q_0q_2)T_M}{M} + \frac{d_x}{M}, \tag{10.5}$$

$$\ddot{y} = \frac{-(2q_2q_3 - 2q_0q_1)T_M}{M} + \frac{d_y}{M}, \tag{10.6}$$

$$\ddot{z} = \frac{-(1 - 2q_1^2 - 2q_2^2)T_M}{M} + g + \frac{d_z}{M}. \tag{10.7}$$

Now for the angular dynamics,

$$J\dot{\omega}^b = -S(\omega^b)J\omega^b + \tau^b, \quad \dot{\mathbf{q}} = \frac{1}{2}\begin{bmatrix} -q^\top \\ q_0 I + S(q) \end{bmatrix}\omega^b, \tag{10.8}$$

where $\omega^b \in \mathbb{R}^3$ represents the angular velocity in $\mathcal{F}_b$ and J is the inertia matrix. In a generic notation, given any vector $\upsilon \in \mathbb{R}^3$,

$$S(\upsilon) = \begin{bmatrix} 0 & -\upsilon_3 & \upsilon_2 \\ \upsilon_3 & 0 & -\upsilon_1 \\ -\upsilon_2 & \upsilon_1 & 0 \end{bmatrix}.$$

The external torques τ^b expressed in $\mathcal{F}_b$ are given by the following equation,

$$\tau^b = \begin{bmatrix} \tau_{f_1} \\ \tau_{f_2} \\ \tau_{f_3} \end{bmatrix} + \begin{bmatrix} R_M \\ M_M + M_T \\ N_M \end{bmatrix}, \tag{10.9}$$

where τ_{f_1}, τ_{f_2} and τ_{f_3} are moments generated by the main and tail rotors. R_M, M_M, N_M and M_T are the torques of aerodynamic forces with the following relationships,

$$\begin{aligned} R_M &= c_b^M b - Q_M \sin a, \\ M_M &= c_a^M a - Q_M \sin b, \\ N_M &= -Q_M \cos a \cos b, \\ M_T &= -Q_T, \end{aligned}$$

where

$$\begin{aligned} Q_M &= c_M^Q T_M^{1.5} + D_M^Q, \\ Q_T &= c_T^Q T_T^{1.5} + D_T^Q \end{aligned}$$

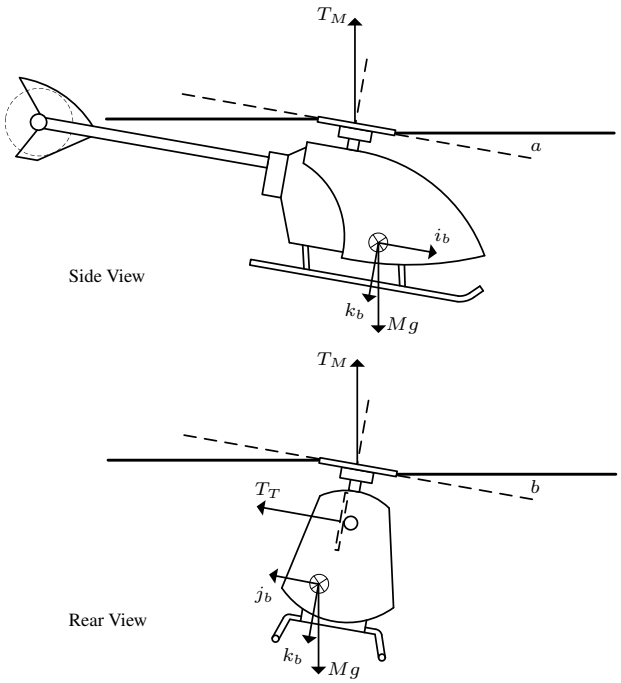

Figure 10.1: Side and rear view of the helicopter.

and, c_b^M, c_a^M, c_M^Q, c_T^Q, D_M^Q and D_T^Q are physical parameters [8]. With approximations $T_M^{1.5} \approx T_M$, $T_T^{1.5} \approx T_T$ and (10.3), a compact torque equation is obtained,

$$\tau^b \quad = \quad A(T_M)\mathbf{v} + B(T_M), \quad \mathbf{v} := [a\ b\ T_T]^\top, \tag{10.10}$$

where $A(T_M)$ and $B(T_M)$ are a matrix and a vector whose entries are functions of T_M with dependence on the helicopter parameters.

The mathematical model of the helicopter given by (10.5)-(10.8) is subject to parameter uncertainties. Taking μ as a vector of all uncertain parameters with a nominal value μ_0, the additive uncertainty is given by $\mu_\Delta = (\mu - \mu_0) \in \mathcal{P}$, where $\mathcal{P}$ is a given compact set. Correspondingly, $M = M_0 + M_\Delta$, $J = J_0 + J_\Delta$, $A(T_M) = A_0(T_M) + A_\Delta(T_M)$ and $B(T_M) = B_0(T_M) + B_\Delta(T_M)$. Now defining a state vector $\mathbf{x} = [p^i\ \dot{p}^i\ \omega^b\ \mathbf{q}]^\top$ and taking the vector $\mathbf{u} = [T_M\ \mathbf{v}]^\top$ as the control input, the helicopter model acted by the wind disturbance $\mathbf{d} = [d_x\ d_y\ d_z]^\top$ is summarized as

$$\dot{\mathbf{x}} = F(\mathbf{x}, \mathbf{u}, \mathbf{d}), \tag{10.11}$$

where F is a vector of functions (10.1) and (10.8) considering the full force and torque equations (10.2) and (10.9) respectively.

Problem Statement

The primary goal of Section 10.3 is to design a controller that is able to stabilize the helicopter affected by the disturbance $\mathbf{d}$. The disturbance that affects the acceleration

of the helicopter can be written as a linear combination of N (possibly ∞) sinusoidal functions of time modeled in the following form,

$$d_j = \sum_{i=1}^{N} A_{ji} \cos(\Omega_i t + \varphi_{ji}), \tag{10.12}$$

with unknown amplitudes A_{ji}, phases φ_{ji} and frequencies Ω_i, for $j = x, y, z$. In our setup however, it is assumed that $\mathbf{d}$ can be approximated with a small N. It can be shown that the disturbance is generated by the following linear time-invariant exosystem,

$$\begin{aligned} \dot{w}_j &= \mathrm{S}(\varrho) w_j, \\ d_j &= R\mathrm{S}^2(\varrho) w_j, \quad j = x, y, z, \end{aligned} \tag{10.13}$$

where $w_j \in \mathbb{R}^{2N}$, $\varrho = [\Omega_1 \ \Omega_2 \ \dots \ \Omega_N]^\top$, $\mathrm{S}(\varrho) = \mathrm{diag}\big(H(\Omega_1), \dots, H(\Omega_N)\big)$ with

$$H(\Omega_i) = \begin{bmatrix} 0 & \Omega_i \\ -\Omega_i & 0 \end{bmatrix}, \quad i = 1, \dots, N,$$

and $R = [1 \ 0 \ 1 \ 0 \ \dots \ 1 \ 0]$ a $1 \times 2N$ matrix (see [6, pp. 89-90]). We remark that the initial condition $w_j(0)$ of the exosystem represents the amplitudes A_{ji} and phases φ_{ji} of the disturbance. As the control design proceeds in the next section, it will be clear how the representation of the disturbance in such a form can be advantageous in the development of an internal model for stabilizing control input generation.

We will now concisely state the overall objective of the control design. Given the helicopter system (10.11), develop a robust controller of the form

$$\begin{aligned} \dot{\boldsymbol{\xi}} &= \phi(\boldsymbol{\xi}, p^i, \dot{p}^i), \\ \mathbf{u} &= \theta(\boldsymbol{\xi}, p^i, \dot{p}^i, q, \omega^b) \end{aligned} \tag{10.14}$$

such that the helicopter asymptotically tracks the reference position and quaternion (vector part)

$$\begin{aligned} [x^{\text{ref}}(t) \ y^{\text{ref}}(t) \ z^{\text{ref}}(t)]^\top = [0 \ 0 \ 0]^\top \quad \text{and} \\ q^{\text{ref}}(t) = [q_{d1}(t) \ q_{d2}(t) \ 0]^\top \end{aligned}$$

respectively, in the presence of parameter uncertainties involving the helicopter geometry, the aerodynamic forces and the disturbance. In the above formulation, $\boldsymbol{\xi}$ is the state of the controller and, $q_{d1}(t)$ and $q_{d2}(t)$ are functions of a disturbance estimate (see (10.31) in the second part of Section 10.3). Note that $q^{\text{ref}}(t)$ is the horizontal axis of rotation to be tracked to counter the horizontal disturbances d_x, d_y.

10.3 Controller Design

In this section, a controller of the form (10.14) is designed in two stages. In the first part of Section 10.3, a control law is constructed for $\mathbf{u}$ to achieve vertical (motion in z direction) stabilization. Next in the second part of Section 10.3, it is shown that the stabilizing $\mathbf{v}$ can be tuned separately (without jeopardizing the vertical stabilization) to render the horizontal (x and y direction) motion stable.

Stabilization of Vertical Dynamics

With reference to the vertical dynamics (10.7) given above, to counter the nominal effect of the gravity, the following preliminary control law is chosen,

$$T_M = \frac{gM_0 + u}{1 - \text{sat}_c(2q_1^2 + 2q_2^2)}, \tag{10.15}$$

where $\text{sat}_c(s) := \text{sign}(s)\min\{|s|, c\}$ with $0 < c < 1$ is a saturation function introduced to avoid singularities and u is an input to be designed. This yields

$$\ddot{z} \;=\; -\frac{\psi_c^z(q)u}{M} + g\big(1 - \frac{M_0}{M}\psi_c^z(q)\big) + \frac{d_z}{M},$$

where

$$\psi_c^z(q) = \frac{1 - 2q_1^2 - 2q_2^2}{1 - \text{sat}_c(2q_1^2 + 2q_2^2)}.$$

If q is small enough such that $\psi_c^z(q) = 1$, then a feedforward u needed for vertical stabilization is

$$c_u(w_z, \mu, \varrho) = gM_\Delta + d_z, \tag{10.16}$$

provided that the initial conditions are set to zero. The term *feedforward* is used to indicate that $c_u(w_z, \mu, \varrho)$ is a control applied to achieve a desired performance [9]. Since the steady-state control $c_u(w_z, \mu, \varrho)$ depends on unknown $M_\Delta \in \mu$ and d_z which is in turn influenced by unknown ϱ and the unmeasurable state w_z, it cannot be produced directly. However, it can be asymptotically generated by the use of an internal model. As a first step in designing a controller with an internal model, the desired control (10.16) is rewritten as an output of a linear system (recall that d_z is given by (10.13))

$$\begin{aligned} \frac{\partial \tau_z}{\partial w_z}\mathrm{S}(\varrho)w_z &= \Phi(\varrho)\tau_z(w_z, \mu), \\ c_u(w_z, \mu, \varrho) &= \Gamma(\varrho)\tau_z(w_z, \mu), \end{aligned}$$

where

$$\tau_z(w_z, \mu) = \begin{bmatrix} gM_\Delta \\ w_z \end{bmatrix}, \; \Phi(\varrho) = \begin{bmatrix} 0 & 0 \\ 0 & \mathrm{S}(\varrho) \end{bmatrix},$$

$$\Gamma(\varrho) = \begin{bmatrix} 1 & \Gamma_2(\varrho) \end{bmatrix},$$

and

$$\Gamma_2(\varrho) = \begin{bmatrix} -\Omega_1^2 & 0 & -\Omega_2^2 & 0 & \dots & -\Omega_N^2 & 0 \end{bmatrix}.$$

It is shown in [6, Lemma 3.3.1] that, by constructing a $(2N + 1) \times (2N + 1)$ Hurwitz matrix F and a $(2N + 1) \times 1$ vector G such that the pair (F, G) is controllable, there

exists a $(2N+1)\times(2N+1)$ nonsingular matrix T_ϱ such that $\Phi(\varrho) = T_\varrho^{-1}(F+G\Psi_\varrho)T_\varrho$ and $\Gamma(\varrho) = \Psi_\varrho T_\varrho$ where $\Psi_\varrho = [1\ \Psi_{2,\varrho}]$ is a $1\times(2N+1)$ vector. Hence,

$$\begin{aligned}\frac{\partial \bar{\tau}_z}{\partial w_z}\mathrm{S}(\varrho)w_z &= (F+G\Psi_\varrho)\bar{\tau}_z(w_z,\mu,\varrho),\\ c_u(w_z,\mu,\varrho) &= \Psi_\varrho\bar{\tau}_z(w_z,\mu,\varrho),\end{aligned}$$

where $\bar{\tau}_z(w_z,\mu,\varrho) = T_\varrho\tau_z(w_z,\mu)$. Consequently for any initial condition of exosystem (10.13) $w_z(0)$, the control $c_u(w_z,\mu,\varrho)$ can be viewed as an output of the linear system

$$\begin{aligned}\dot{\xi}_z &= (F+G\Psi_\varrho)\xi_z,\\ c_u(w_z,\mu,\varrho) &= \Psi_\varrho\xi_z\end{aligned} \tag{10.17}$$

if it is initialized as $\xi_z(0) = \bar{\tau}(w_z(0),\mu,\varrho)$, where

$$\xi_z = \begin{bmatrix}\xi_{z1}\\ \xi_{z2}\end{bmatrix} \in \mathbb{R}\times\mathbb{R}^{2N}.$$

Note that even if Ψ_ϱ and $\bar{\tau}(w_z(0),\mu,\varrho)$ are known and hence enabling the generation of the control $c_u(w_z,\mu,\varrho)$ by (10.17), vertical stabilization can only be achieved if the initial conditions of (10.7) are set correctly (i.e. $z=\dot{z}=0$). To deal with the unknowns in (10.17) and to obtain vertical stabilization given nonzero initial conditions, choose u in (10.15) as an output of the system

$$\begin{aligned}\dot{\xi}_z &= (F+G\hat{\Psi})\xi_z + g_{\text{stz}}\\ u &= \hat{\Psi}\xi_z + u_{\text{st}},\end{aligned} \tag{10.18}$$

where $u_{\text{st}} = k_2(\dot{z}+k_1 z)$ and $g_{\text{stz}} = Gu_{\text{st}} + FGM_0\dot{z}$ for $k_1,k_2>0$. The vector $\hat{\Psi} = [1\ \hat{\Psi}_2]$ with a $1\times 2N$ row vector $\hat{\Psi}_2$ is an estimate of Ψ_ϱ and is to be tuned by the adaptation law

$$\dot{\hat{\Psi}}_2 = \gamma\xi_{z2}^\top(\dot{z}+k_1 z) - \mathrm{tas}_d(\hat{\Psi}_2), \tag{10.19}$$

where $\gamma>0$ is a design parameter and $\mathrm{tas}_d(\hat{\psi}_i) := \hat{\psi}_i - \mathrm{sat}_d(\hat{\psi}_i)$ is a *dead zone* function in which $\hat{\psi}_i$ is the ith component of $\hat{\Psi}_2$ and $d > \max_{i=1}^{2N}\left\{|(\Psi_{2,\varrho})_i|\right\}$. Note that the term $\mathrm{tas}_d(\hat{\psi}_i)$ is zero as long as $|\hat{\psi}_i|\le d$ and has a stabilizing effect on $\hat{\psi}_i$ if the fixed bound is exceeded, thus making the adaptation law robust to the drift phenomena [10]. As demonstrated next, the inclusion of the stabilizing terms g_{stz} and u_{st} in (10.18) enables the convergence of ξ_z to the desired function $\bar{\tau}_z(w_z,\mu,\varrho)$ and renders $(z,\dot{z})$ globally asymptotically and locally exponentially stable under appropriate conditions.

To prove that the control defined by (10.15) and (10.18) stabilizes (10.7), let

$$\eta = \begin{bmatrix}\eta_1\\ \eta_2\end{bmatrix} = \begin{bmatrix}\eta_1\\ \tilde{\Psi}_2^\top\end{bmatrix}, \text{ with} \tag{10.20}$$

$$\eta_1 = \begin{bmatrix}\chi\\ z\\ \zeta\end{bmatrix}, \tag{10.21}$$

where

$$\begin{aligned}\chi &:= \xi_z - \bar{\tau}_z(w_z, \mu, \varrho) + GM\dot{z}\\ \tilde{\Psi}_2 &:= \hat{\Psi}_2 - \Psi_{2,\varrho}\\ \zeta &:= \dot{z} + k_1 z.\end{aligned}$$

The time derivative of η (see Appendix A for the derivation) is given by,

$$\begin{aligned}\dot{\eta}_1 &= \Big(A + A_1\big(\psi_c^z(q) - 1\big)\Big)\eta_1\\ &\quad - \Big(\frac{1}{M}b + B\big(\psi_c^z(q) - 1\big)\Big)\xi_{z2}^\top \eta_2 - B\rho\\ \dot{\eta}_2 &= \gamma\xi_{z2} b_0^\top \eta_1 - \text{tas}_d(\eta_2 + \Psi_{2,\varrho}^\top),\end{aligned} \tag{10.22}$$

where $\rho = \big(\psi_c^z(q) - 1\big)\big(gM_0 + \Psi_\varrho \bar{\tau}_z(w, \mu, \varrho)\big)$,

$$\begin{aligned}A &= \begin{bmatrix} F & k_1 FGM_\triangle & -FGM_\Delta \\ 0 & -k_1 & 1 \\ -\frac{1}{M}\Psi_\varrho & -k_1(\Psi_\varrho G + k_1) & (\Psi_\varrho G + k_1 - \frac{1}{M}k_2)\end{bmatrix},\\ A_1 &= \begin{bmatrix} -G\Psi_\varrho & -G\Psi_\varrho GMk_1 & G\Psi_\varrho GM - Gk_2 \\ 0 & 0 & 0 \\ -\frac{1}{M}\Psi_\varrho & -k_1\Psi_\varrho G & (\Psi_\varrho G - \frac{1}{M}k_2)\end{bmatrix},\\ b_0 &= \begin{bmatrix}0\\0\\1\end{bmatrix} \text{ and } B = \begin{bmatrix}G\\0\\\frac{1}{M}\end{bmatrix}.\end{aligned}$$

Using the same arguments as in [6, Proposition 3.3.2], it can be shown that there exists $k_2^* > 0$ such that if $k_2 > k_2^*$, then A is a Hurwitz matrix (see Appendix A for the proof). Let $\mathcal{W} \subset \mathbb{R}^{2N}$ be the set

$$\mathcal{W} = \mathcal{I}_{[\alpha,\beta]} \times \mathcal{I}_{[\alpha,\beta]} \times \ldots \times \mathcal{I}_{[\alpha,\beta]},$$

where

$$\mathcal{I}_{[\alpha,\beta]} = \{x_\mathcal{I} \in \mathbb{R}^2 : \alpha \leq \|x_\mathcal{I}\| \leq \beta\},$$

with $\alpha > 0$. Subsequently when q is small enough such that $\psi_c^z(q) = 1$, [6, Proposition 5.4.1] guarantees that if the initial state $w_z(0)$ of the exosystem belongs to the compact set $\mathcal{W}$, then system (10.22) is globally asymptotically and locally exponentially stable. Hence, η is bounded and $\lim_{t\to\infty}\eta(t) = 0$. Note that even though system equation (10.22) is different than that of in [6, Eq. (5.26)] due to the addition of a disturbance and therefore a different vertical control, the two propositions still apply.

It is only natural now to ensure that the condition $\psi_c^z(q) = 1$ can be achieved in finite time. Setting

$$\mathbf{v} = A_0(T_M)^{-1}\big(\tilde{\mathbf{v}} - B_0(T_M)\big) \tag{10.23}$$

with the assumption that $A_0(T_M(t))$ is nonsingular for all $t \geq 0$ and substituting in (10.10), yields the torque equation

$$\tau^b(\tilde{\mathbf{v}}) = L(T_M)\tilde{\mathbf{v}} + \Delta(T_M), \tag{10.24}$$

where $\tilde{\mathbf{v}}$ is an additional control input to be determined,

$$\begin{aligned} L(T_M) &= I + A_\Delta(T_M)A_0^{-1}(T_M) \text{ and} \\ \Delta(T_M) &= B_\Delta(T_M) - A_\Delta(T_M)A_0^{-1}(T_M)B_0(T_M). \end{aligned}$$

Dropping the superscript b in ω^b, choose

$$\tilde{\mathbf{v}} = K_P\big(\eta_1 - K_D(\omega - \omega_d)\big), \tag{10.25}$$

where $K_P, K_D > 0$ are design parameters,

$$\eta_1 := q_r - q \quad \text{and} \tag{10.26}$$

$$q_r = q^* + q_d. \tag{10.27}$$

To follow the notations in [6] closely, η_1 is redefined in (10.26) to represent a different quantity than (10.21). While the expressions for the reference angular velocity ω_d and reference quaternion q_r are given in the next subsection (see (10.35), (10.29), (10.31)), it is important to mention here that $\|q^*(t)\| \leq \sqrt{3}\lambda_3$ and it is assumed that $\|q_d(t)\| \leq K_d m_{q_d}$, $\|\omega_d(t)\| \leq K_d m_{\omega_d}$, $\|\dot{\omega}_d(t)\| \leq m_{\dot{\omega}_d}$ for all $t \geq 0$, where $K_d > 0$, $\lambda_3 > 0$ are design parameters and $m_{q_d}, m_{\omega_d}, m_{\dot{\omega}_d}$ are fixed positive numbers. Next, for the problem in hand the following proposition is stated.

Proposition 5. *Suppose there exists $l_1^* > 0$ such that*

$$0 < 2l_1^* \leq L(T_M) + L^\top(T_M)$$

and let l_2^*, $\delta^* > 0$ satisfy

$$\|L(T_M)\| \leq l_2^*, \quad \|\Delta(T_M)\| \leq \delta^*.$$

Choose $0 < \varepsilon < 1$ arbitrarily and fix compact sets $\mathcal{Q}$, Ω of initial conditions for $q(t)$ and $\omega(t)$ respectively, with $\mathcal{Q}$ contained in the set

$$\{q \in \mathbb{R}^3 : \|q\| < \sqrt{1-\varepsilon^2}\}.$$

Then for any $T^* > 0$, there exist $K_P^*(K_D) > 0$, $K_D^* > 0$, $K_d^*(K_D) > 0$ and $\lambda_3^*(K_D) > 0$, such that for all $K_P \geq K_P^*(K_D)$, $K_D \leq K_D^*$, $K_d \leq K_d^*(K_D)$ and $\lambda_3 \leq \lambda_3^*(K_D)$,

1. *the trajectory of attitude dynamical system* (10.8) *given* (10.24) *and* (10.25) *with initial conditions $(q_0(0), q(0), \omega(0)) \in (0,1] \times \mathcal{Q} \times \Omega$ is bounded and $q_0(t) > \varepsilon$, $\forall t \geq 0$,*
2. *$\psi_c^z(q(t)) = 1$, $\forall t \geq T^*$.*

Proof. In Appendix B, the existence of a Lyapunov function for attitude dynamical system (10.8) is shown. This condition is a key element in the proof of Proposition 5. For the rest of the proof, see [6, Proof of Proposition 5.7.1]. □

It is worth pointing out the fact that $q_0(t)$ is always positive prevents the helicopter from overturning during the initial transient.

In this first part of the control design, we have shown that the design parameters k_2, K_P, K_D, K_d and λ_3 of the controllers (10.15), (10.18) and (10.23), (10.25) with the adaptation law (10.19) can be tuned to steer $\dot{z}$ and z asymptotically to zero despite the influence of the vertical disturbance d_z.

Stabilization of Longitudinal and Lateral Dynamics

It will be shown now how q_1 and q_2 can be manipulated as *virtual controls* to produce horizontal stability. The control law (10.15) that has been designed for vertical stabilization also appears in the longitudinal (10.5) and lateral (10.6) dynamics. By expanding the numerator of (10.15) as

$$\begin{aligned} gM_0 + u &= gM_0 + \hat{\Psi}\xi_z + k_2(\dot{z} + k_1 z) \\ &= gM_0 + (\tilde{\Psi} + \Psi_\varrho)(\chi + \bar{\tau}_z(w, \mu, \varrho) - GM\dot{z}) \\ &\quad + k_2(\dot{z} + k_1 z) \\ &= gM_0 + c_u(w_z, \mu, \varrho) + y_\eta(\eta, w) \\ &= gM + d_z + y_\eta(\eta, w), \end{aligned}$$

where $\tilde{\Psi} = [0 \ \tilde{\Psi}_2]$ and

$$\begin{aligned} y_\eta(\eta, w) &= \tilde{\Psi}\bar{\tau}_z(w, \mu, \varrho) + (\tilde{\Psi} + \Psi_\varrho)(\chi - GM\dot{z}) \\ &\quad + k_2(\dot{z} + k_1 z), \end{aligned}$$

(10.5) and (10.6) can be rewritten as

$$\begin{aligned} \ddot{x} &= \frac{-\tilde{d}(\mathbf{q}, t)q_2 + m(\mathbf{q}, t)q_1 q_3 + n_x(\mathbf{q})y_\eta(\eta, w)}{M} + \frac{d_x}{M}, \\ \ddot{y} &= \frac{\tilde{d}(\mathbf{q}, t)q_1 + m(\mathbf{q}, t)q_2 q_3 + n_y(\mathbf{q})y_\eta(\eta, w)}{M} + \frac{d_y}{M}, \end{aligned}$$

where

$$\begin{aligned} \tilde{d}(\mathbf{q}, t) &= \frac{2(gM + d_z)q_0}{1 - \text{sat}_c(2q_1^2 + 2q_2^2)}, \\ m(\mathbf{q}, t) &= -\frac{2(gM + d_z)}{1 - \text{sat}_c(2q_1^2 + 2q_2^2)}, \\ n_x(\mathbf{q}) &= \frac{-(2q_1 q_3 + 2q_0 q_2)}{1 - \text{sat}_c(2q_1^2 + 2q_2^2)}, \\ n_y(\mathbf{q}) &= \frac{-(2q_2 q_3 - 2q_0 q_1)}{1 - \text{sat}_c(2q_1^2 + 2q_2^2)}. \end{aligned}$$

Recall that from the previous analysis on vertical stabilization, with an appropriate selection of the design parameters, $y_\eta(\eta, w)$ is an asymptotically diminishing signal.

Next by introducing a group of integrators $\dot{\eta}_x = x$, $\dot{\eta}_y = y$ and $\dot{\eta}_q = q_3$, the following

new state variables are defined,

$$\begin{aligned}
\zeta_1 &:= \begin{bmatrix} \eta_y \\ \eta_x \end{bmatrix}, \\
\zeta_2 &:= \begin{bmatrix} y \\ x \end{bmatrix} + \lambda_1 \sigma(\frac{K_1}{\lambda_1}\zeta_1), \\
\zeta_3 &:= \begin{bmatrix} \dot{y} \\ \dot{x} \\ \eta_q \\ 0 \\ \vdots \\ 0 \end{bmatrix} + P_1 \lambda_2 \sigma(\frac{K_2}{\lambda_2}\zeta_2),
\end{aligned} \tag{10.28}$$

where

$$P_1 = \begin{bmatrix} 1 & 0 \\ 0 & 1 \\ 0 & 0 \\ \vdots & \vdots \\ 0 & 0 \end{bmatrix}_{(4N+2)\times 2}.$$

By adopting the following *nested saturated* control law

$$q^* = -P_2 \lambda_3 \sigma(\frac{K_3}{\lambda_3}\zeta_3), \tag{10.29}$$

where $\sigma(\cdot)$ is a vector-valued saturation function of suitable dimension (see [6, Appendix C.1]), K_i, λ_i, $i = 1, 2, 3$ are design parameters and

$$P_2 = \begin{bmatrix} 1 & 0 & 0 & 0 & & 0 \\ 0 & -1 & 0 & 0 & & 0 \\ 0 & 0 & 1 & 0 & \dots & 0 \\ 0 & 0 & 0 & 0 & & 0 \\ & & \vdots & & \ddots & \\ 0 & 0 & 0 & 0 & & 0 \end{bmatrix}_{(4N+2)\times(4N+2)},$$

the time derivatives can be written as

$$\begin{aligned}
\dot{\zeta}_1 &= -\lambda_1 \sigma(\frac{K_1}{\lambda_1}\zeta_1) + \zeta_2, \\
\dot{\zeta}_2 &= -\lambda_2 \sigma(\frac{K_2}{\lambda_2}\zeta_2) + P_0\zeta_3 + K_1 \sigma'(\frac{K_1}{\lambda_1}\zeta_1)\dot{\zeta}_1, \\
M\dot{\zeta}_3 &= -\tilde{D}(t) P_2 \lambda_3 \sigma(\frac{K_3}{\lambda_3}\zeta_3) + \tilde{D}(t) q_d, \\
&\quad + M K_2 P_1 \sigma'(\frac{K_2}{\lambda_2}\zeta_2)\dot{\zeta}_2 - \tilde{D}(t)\tilde{\eta}_1 + p + d_h,
\end{aligned} \tag{10.30}$$

in which

$$
\begin{aligned}
D_1(t) &= \begin{bmatrix} \tilde{d}(\mathbf{q},t) & m(\mathbf{q},t)q_3 & 0 \\ m(\mathbf{q},t)q_3 & -\tilde{d}(\mathbf{q},t) & 0 \\ 0 & 0 & M \end{bmatrix}, \\
\tilde{D}(t) &= \underset{(4N+2)\times(4N+2)}{\begin{bmatrix} D_1(t) & 0 \\ 0 & 0 \end{bmatrix}}, \\
p &= \begin{bmatrix} n_y(\mathbf{q})y_\eta(\eta,w) \\ n_x(\mathbf{q})y_\eta(\eta,w) \\ 0 \\ \vdots \\ 0 \end{bmatrix}, \; d_h = \begin{bmatrix} d_y \\ d_x \\ 0 \\ \vdots \\ 0 \end{bmatrix}, \; \tilde{\eta}_1 = \begin{bmatrix} \eta_1 \\ 0 \\ \vdots \\ 0 \end{bmatrix}, \\
P_0 &= \underset{2\times(4N+2)}{\begin{bmatrix} 1 & 0 & 0 & \cdots & 0 \\ 0 & 1 & 0 & \cdots & 0 \end{bmatrix}}.
\end{aligned}
$$

In a generic notation, for $\sigma : \mathbb{R}^n \to \mathbb{R}^n$, $\sigma'(\upsilon) = d\sigma(\upsilon)/d(\upsilon)$, where $\upsilon \in \mathbb{R}^n$. Note that if one can set $q_d = -D_0(t)d_h$, where

$$
D_0(t) = \begin{bmatrix} D_1^{-1}(t) & 0 \\ 0 & 0 \end{bmatrix},
$$

the disturbance d_h can be completely eliminated from subsystem (10.30). In this case, (10.30) can be shown to be *input-to-state stable* (ISS) with restrictions on the inputs $(\tilde{\eta}_1, p)$ and linear asymptotic gains [6, Lemma 5.7.4].

Since q_d is a function of uncertain M and unknown d_h, it cannot be generated directly. However, by defining q_d in terms of the nominal value of M and an estimate of d_h, the horizontal disturbance can be removed asymptotically from subsystem (10.30) (see (10.53) in Appendix C). Thus the following is proposed,

$$
q_d = -K_d \tilde{D}_0(t)\hat{d}, \tag{10.31}
$$

where $\hat{d} = [\hat{d}_y \; \hat{d}_x \; 0 \; \cdots \; 0]^\top$ is a disturbance estimate to be adapted and

$$
\begin{aligned}
\tilde{D}_1(t) &= \begin{bmatrix} \tilde{d}_0(\mathbf{q},t) & m_0(\mathbf{q},t)q_3 & 0 \\ m_0(\mathbf{q},t)q_3 & -\tilde{d}_0(\mathbf{q},t) & 0 \\ 0 & 0 & 1 \end{bmatrix}, \\
\tilde{D}_0(t) &= \underset{(4N+2)\times(4N+2)}{\begin{bmatrix} \tilde{D}_1(t) & 0 \\ 0 & 0 \end{bmatrix}},
\end{aligned} \tag{10.32}
$$

where

$$
\begin{aligned}
\tilde{d}_0(\mathbf{q},t) &= \frac{\big(1 - \text{sat}_c(2q_1^2 + 2q_2^2)\big)q_0}{2(q_0^2 + q_3^2)(gM_0 + u)}, \\
m_0(\mathbf{q},t) &= \frac{-\big(1 - \text{sat}_c(2q_1^2 + 2q_2^2)\big)}{2(q_0^2 + q_3^2)(gM_0 + u)},
\end{aligned}
$$

with u given by (10.18). It is important to notice at this point that a constraint on d_z should be imposed. Because $\lim_{t\to\infty}\big(gM_0 + u(t)\big) = gM + d_z$, it is required that $d_z(t) \neq -gM$ for all $t \geq 0$ to avoid singularities in (10.32). Since d_z is given by (10.12), in this paper we assume that $|d_z(t)| < gM$ for all $t \geq 0$. As a result, $T_M > 0$ for all $t \geq 0$. Next, the following state variable are defined,

$$\eta_2 := \tilde{\omega} - \omega_d - \frac{1}{K_D}\tilde{\eta}_1, \tag{10.33}$$

$$\eta_3 := \tilde{J}\eta_2 - K_d e_\xi, \tag{10.34}$$

where e_ξ is the internal model error (10.48),

$$\tilde{\omega} = \begin{bmatrix}\omega \\ 0 \\ \vdots \\ 0\end{bmatrix} \text{ and } \tilde{J} = \begin{bmatrix}J & 0 \\ 0 & I\end{bmatrix}.$$

Note that in (10.33), η_2 is redefined to represent a different variable than that of in (10.20). From (10.31), we may write $q_d = [q_{d1}\ q_{d2}\ 0\ \cdots\ 0]^\top$ and the desired angular velocity is defined as

$$\omega_d = Q_d \dot{q}_d, \tag{10.35}$$

where

$$\begin{aligned} Q_{d0} &= \frac{2}{\tilde{\varepsilon}}\begin{bmatrix}\tilde{\varepsilon}^2 + q_{d1}^2 & q_{d1}q_{d2} & -\tilde{\varepsilon}q_{d2} \\ q_{d1}q_{d2} & \tilde{\varepsilon}^2 + q_{d2}^2 & \tilde{\varepsilon}q_{d1} \\ \tilde{\varepsilon}q_{d2} & -\tilde{\varepsilon}q_{d1} & \tilde{\varepsilon}^2\end{bmatrix}, \\ Q_d &= \begin{bmatrix}Q_{d0} & 0 \\ 0 & 0\end{bmatrix}, \end{aligned}$$

for arbitrary $\varepsilon < \tilde{\varepsilon} < 1$. Taking the time derivatives,

$$\begin{aligned} \dot{\tilde{\eta}}_1 &= -\frac{1}{2}\big(q_0 I + \tilde{S}(q)\big)(\eta_2 + \frac{1}{K_D}\tilde{\eta}_1 + \omega_d) + \dot{q}_r, \\ \tilde{J}\dot{\eta}_2 &= -\tilde{S}(\omega)\tilde{J}(\eta_2 + \frac{1}{K_D}\tilde{\eta}_1 + \omega_d) - K_P K_D \tilde{L}(T_M)\eta_2 \\ &\quad + \tilde{\Delta}(T_M) - \tilde{J}\dot{\omega}_d - \frac{1}{K_D}\tilde{J}\dot{\tilde{\eta}}_1, \\ \dot{\eta}_3 &= \tilde{J}\dot{\eta}_2 - K_d\dot{e}_\xi, \end{aligned} \tag{10.36}$$

where

$$\begin{aligned}
\tilde{S}(q) &= \underset{(4N+2)\times(4N+2)}{\begin{bmatrix} S(q) & 0 \\ 0 & 0 \end{bmatrix}}, \\
\tilde{S}(\omega) &= \underset{(4N+2)\times(4N+2)}{\begin{bmatrix} S(\omega) & 0 \\ 0 & 0 \end{bmatrix}}, \\
\tilde{L}(T_M) &= \underset{(4N+2)\times(4N+2)}{\begin{bmatrix} L(T_M) & 0 \\ 0 & I \end{bmatrix}}, \\
\tilde{\Delta}(T_M) &= \underset{(4N+2)\times 1}{\begin{bmatrix} \Delta(T_M) \\ 0 \end{bmatrix}}.
\end{aligned}$$

See Appendix C for a complete expression of (10.36).

We will now study the stability of feedback interconnection of subsystems (10.30) and (10.36). Note that subsystem (10.30) is a system with state $(\zeta_1, \zeta_2, \zeta_3)$ and input $(\tilde{\eta}_1, \eta_2, \eta_3, p_0)$ (see (10.53)), while subsystem (10.36) has $(\tilde{\eta}_1, \eta_2, \eta_3)$ and $(y_{\zeta 0}, y_{\zeta 1}, I_{\tilde{\eta}_1}, I_{\eta_2}, I_{\eta_3})$ as its state and input respectively (see (10.57), (10.60) and (10.62)). Since the vertical stability analysis in the first part of Section 10.3 guarantees that $q_0(t) > \varepsilon > 0$ for all $t \geq 0$ for an allowed range of the design parameters and initial conditions, it is assumed so in the next proposition. Morever, let M^L, M^U, d^L and d^U be such that $M^L \leq M \leq M^U$ and $0 < d^L \leq \tilde{d}(\mathbf{q}, t) \leq d^U$ for all $t \geq 0$. With that, the following proposition is presented.

Proposition 6. *Let K_D be fixed and let K_i^* and λ_i^*, $i = 1, 2, 3$, be such that the following inequalities are satisfied*

$$\begin{aligned}
&\frac{\lambda_2^*}{K_2^*} < \frac{\lambda_1^*}{4}, \quad \frac{\lambda_3^*}{K_3^*} < \frac{\lambda_2^*}{4}, \quad 4K_1^*\lambda_1^* < \frac{\lambda_2^*}{4}, \\
&4K_2^*\lambda_2^* < \frac{d^L}{M^U}\frac{\lambda_3^*}{8}, \quad 24\frac{K_1^*}{K_2^*} < \frac{1}{6} \\
&\textit{and} \quad 24\frac{K_2^*}{K_3^*} < \frac{1}{6}\frac{d^L}{d^U}\frac{M^L}{M^U}.
\end{aligned}$$

Then, there exist positive numbers K_P^*, K_d^*, ϵ_L^*, ϵ_U^*, $R_{\zeta 1}$, $\gamma_{\zeta 1}$, $\gamma_{\eta 1}$, $\gamma_{\eta 2}$ and $\gamma_{\eta 3}$ such that, taking $\lambda_i = \epsilon^{i-1}\lambda_i^*$ and $K_i = \epsilon K_i^*$, $i = 1, 2, 3$, for all $K_P \geq K_P^*$, $K_d \leq K_d^*$ and $\epsilon_L^* \leq \epsilon \leq \epsilon_U^*$, the feedback interconnection of subsystems (10.30) *and* (10.36) *is ISS*

1. *without restrictions on the initial state;*
2. *with restrictions $(\epsilon^2 R_{\zeta 1}, R_{\eta 1}, R_{\eta 2}, R_{\eta 3})$ on input $(p_0, I_{\tilde{\eta}_1}, I_{\eta_2}, I_{\eta_3})$, where $R_{\eta 1}$, $R_{\eta 2}$ and $R_{\eta 3}$ are arbitrary positive numbers;*
3. *with linear asymptotic gains.*

Therefore, if $\|p_0\|_\infty < \epsilon^2 R_{\zeta 1}$, $\|I_{\tilde{\eta}_1}\|_\infty < R_{\eta 1}$, $\|I_{\eta_2}\|_\infty < R_{\eta 2}$ and $\|I_{\eta_3}\|_\infty < R_{\eta 3}$, then $(\zeta_1(t), \zeta_2(t), \zeta_3(t), \tilde{\eta}_1(t), \eta_2(t), \eta_3(t))$ satisfies the asymptotic bound

$$\begin{aligned}
&\|(\zeta_1, \zeta_2, \zeta_3, \tilde{\eta}_1, \eta_2, \eta_3)\|_a \leq \\
&\max\left\{\gamma_{\zeta 1}\|p_0\|_a, K_D\gamma_{\eta 1}\|I_{\tilde{\eta}_1}\|_a, \frac{\gamma_{\eta 2}}{K_P}\|I_{\eta_2}\|_a, \frac{\gamma_{\eta 3}}{K_P}\|I_{\eta_3}\|_a\right\},
\end{aligned}$$

where $\|\cdot\|_\infty$ and $\|\cdot\|_a$ denote the $\mathcal{L}_\infty$ norm and asymptotic $\mathcal{L}_\infty$ norm respectively [11]. The proof of Proposition 6 involves showing that subsystems (10.30) and (10.36) are ISS separately and that the composed system satisfies the *small gain theorem* (see for instance, [5]). Examining subsystem (10.36) first, the following result is presented.

Lemma 3. *Let K_D be fixed and assume that $q_0(t) > \varepsilon > 0$, $\tilde{L}(T_M(t)) \geq l_3$, $\tilde{L}(T_M(t))\tilde{J}^{-1} \geq l_4$, for all $t \geq 0$ and some positive l_3, l_4. There exist positive numbers $\bar{K}_P^*(K_D)$, $\bar{K}_d^*$, $\bar{K}_3^*(K_D)$, $\bar{\lambda}_3^*$ and $r_{\zeta 0}$, $r_{\zeta 1}$, r_{I1}, r_{I2}, r_{I3} such that, for all $K_P \geq \bar{K}_P^*(K_D)$, $K_d \leq \bar{K}_d^*$, $K_3 \leq \bar{K}_3^*(K_D)$ and $\lambda_3 \leq \bar{\lambda}_3^*$, system* (10.36) *is ISS*

1. *without restrictions on the initial state;*
2. *without restrictions on input $(y_{\zeta 0}, y_{\zeta 1}, I_{\tilde{\eta}_1}, I_{\eta_2}, I_{\eta_3})$;*
3. *with linear asymptotic gains.*

Therefore, for all bounded inputs $y_{\zeta 0}$, $y_{\zeta 1}$, $I_{\tilde{\eta}_1}$, I_{η_2} and I_{η_3}, the state $(\tilde{\eta}_1, \eta_2, \eta_3)$ satisfies the asymptotic bound

$$\begin{aligned}\|(\tilde{\eta}_1, \eta_2, \eta_3)\|_a \quad \leq \quad & \max\big\{r_{\zeta 0}\|y_{\zeta 0}\|_a, r_{\zeta 1}\|y_{\zeta 1}\|_a, \\ & K_D r_{I1}\|I_{\tilde{\eta}_1}\|_a, \frac{r_{I2}}{K_P}\|I_{\eta_2}\|_a, \frac{r_{I3}}{K_P}\|I_{\eta_3}\|_a\big\}.\end{aligned}$$

Proof. See Appendix C. □

Completion of Proof of Proposition 6. Next concerning system (10.30), the state ζ_3 can be decomposed as

$$\zeta_3 = \begin{bmatrix}\zeta_3' \\ \zeta_3''\end{bmatrix}, \text{ where } \zeta_3' = \begin{bmatrix}\zeta_{31}' \\ \zeta_{32}'\end{bmatrix} \in \mathbb{R}^2 \text{ and } \zeta_3'' \in \mathbb{R}^{4N}.$$

As a result, system (10.30) can be viewed as a cascade connection between

$$\dot{\zeta}_3'' \quad = \quad -\lambda_3\sigma(\frac{K_3}{\lambda_3}\zeta_3'') - P_3\tilde{\eta}_1 \tag{10.37}$$

and

$$\dot{\zeta}_3' \quad = \quad -L(t)\lambda_3\sigma(\frac{K_3}{\lambda_3}\zeta_3') + K_2\sigma'(\frac{K_2}{\lambda_2}\zeta_2)\dot{\zeta}_2 + W, \tag{10.38}$$

where

$$P_3 = \begin{bmatrix}0 & 0 & 1 & & 0 \\ 0 & 0 & 0 & \cdots & 0 \\ & & \vdots & \ddots & \\ 0 & 0 & 0 & & 0\end{bmatrix}.$$

Expressions for $L(t)$ and W are given in the derivation of (10.38) in Appendix D. Based on the same arguments as in [6] and [7], subsystem (10.30) can be shown to be ISS without restrictions on the initial state, restrictions on the inputs and with linear asymptotic gains. Subsequently, also based on discussion therein, since the feedback interconnection of subsystems (10.30) and (10.36) can be proven to satisfy all the conditions of the small gain theorem, the proof of Proposition 6 is completed. □

In this second part of the control design, we have shown that having K_D fixed as imposed by Proposition 5, there exists design parameters K_i, λ_i, $i = 1, 2, 3$ and K_P, K_d such that the feedback interconnection of subsystems (10.30) and (10.36) is ISS without restriction on the initial state, with restrictions on inputs p_0, $I_{\tilde{\eta}_1}$, I_{η_2}, I_{η_3} and with asymptotic gains on the inputs which can be made arbitrarily small by choosing an arbitrarily small K_D and an arbitrarily large K_P. Note that from (10.58), (10.61) and (10.63), inputs $I_{\tilde{\eta}_1}$, I_{η_2} and I_{η_3} are bounded. Therefore, the arbitrary numbers $R_{\eta 1}$, $R_{\eta 2}$ and $R_{\eta 3}$ in Proposition 6 can be chosen such that

$$\|I_{\tilde{\eta}_1}\|_\infty < R_{\eta 1},\ \|I_{\eta_2}\|_\infty < R_{\eta 2} \text{ and } \|I_{\eta_3}\|_\infty < R_{\eta 3},$$

so that the restrictions on inputs $I_{\tilde{\eta}_1}$, I_{η_2} and I_{η_3} are always fulfilled. Moreover, due to the fact that $\lim_{t\to\infty} p_0(t) = 0$ (see (10.54)), the restriction on input p_0 is fulfilled in finite time since there always exists a finite $T > 0$ such that

$$\|p_0\|_{\infty,T} < \epsilon^2 R_{\zeta 1},$$

where $\|p_0\|_{\infty,T} = \sup_{t\in[T,\infty)} \|p_0(t)\|$. Thus,

$$\begin{aligned}&\|(\zeta_1, \zeta_2, \zeta_3, \tilde{\eta}_1, \eta_2, \eta_3)\|_a \leq \\ &\max\left\{K_D\gamma_{\eta 1}\|I_{\tilde{\eta}_1}\|_a, \frac{\gamma_{\eta 2}}{K_P}\|I_{\eta_2}\|_a, \frac{\gamma_{\eta 3}}{K_P}\|I_{\eta_3}\|_a\right\}.\end{aligned}$$

Summary of the Control Design

Note that by choosing large enough K_P and sufficiently small λ_3 and K_d, requirements for vertical, longitudinal and lateral dynamics stabilization as dictated by Proposition 5 and 6 can be simultaneously satisfied. The designed controller that makes a stable hover possible can now be summarized as follows,

1. *Vertical dynamics stabilizer*

$$\begin{aligned}\dot{\xi}_z &= (F + G\hat{\Psi})\xi_z + k_2 G(\dot{z} + k_1 z) + FGM_0\dot{z}, \\ \dot{\hat{\Psi}}_2 &= \gamma\xi_{z2}^\top(\dot{z} + k_1 z) - \text{tas}_d(\hat{\Psi}_2),\end{aligned} \tag{10.39}$$

$$T_M = \frac{gM_0 + \hat{\Psi}\xi_z + k_2(\dot{z} + k_1 z)}{1 - \text{sat}_c(2q_1^2 + 2q_2^2)}. \tag{10.40}$$

2. *Longitudinal and lateral dynamics stabilizer*

$$\begin{aligned}\dot{\xi} &= \hat{F}\xi + g_{\text{st}}, \\ \hat{d} &= \hat{P}\xi, \\ q_d &= -K_d\tilde{D}_0(t)\hat{d}, \\ \omega_d &= Q_d\dot{q}_d, \\ q_r &= q^* + q_d, \\ \mathbf{v} &= A_0(T_M)^{-1}\big(K_P(q_r - q) - K_P K_D(\omega^b - \omega_d) \\ &\quad -B_0(T_M)\big),\end{aligned} \tag{10.41}$$

where

$$\xi = \begin{bmatrix} \xi_y \\ \xi_x \end{bmatrix}, \text{ with } \xi_i = \begin{bmatrix} \xi_{i1} \\ \xi_{i2} \end{bmatrix} \in \mathbb{R} \times \mathbb{R}^{2N}, \ i = x, y,$$

$$\hat{F} = \begin{bmatrix} F + G\hat{\Psi} & 0 \\ 0 & F + G\hat{\Psi} \end{bmatrix}, \ \hat{P} = \begin{bmatrix} \hat{\Psi} & 0 \\ 0 & \hat{\Psi} \\ 0 & 0 \end{bmatrix} \text{ and}$$

$$g_{\text{st}} = \begin{bmatrix} k_4(\dot{y} + k_3 y)G \\ k_4(\dot{x} + k_3 x)G \end{bmatrix}, \ k_3, k_4 > 0.$$

Thus, a controller of the from (10.14) is developed where

$$\boldsymbol{\xi} = \begin{bmatrix} \xi \\ \xi_z \\ \hat{\Psi}_2^\top \end{bmatrix}.$$

To conclude the control design, consider the controller above and choose the design parameters according to Proposition 5 and 6. Then for any initial conditions $w(0) \in \mathcal{W}$, $\eta(0) \in \mathcal{Z}$, $(x(0), \dot{x}(0), y(0), \dot{y}(0)) \in \mathbb{R}^4$, $q_0(0) > 0$, $(q(0), \omega(0)) \in \mathcal{Q} \times \Omega$ where $\mathcal{Z}$ is an arbitrary compact set, $(x(t), \dot{x}(t), y(t), \dot{y}(t))$ converges to a neighborhood of the origin which can be rendered arbitrarily small by choosing K_P and K_D sufficiently large and small respectively. In addition,

$$\lim_{t \to \infty} \|(z(t), \dot{z}(t))\| = 0.$$

10.4 Simulation Results

Hover flight of an autonomous helicopter equipped with the proposed autopilot and influenced by a wind disturbance is simulated.

The simulation results presented here are based on a model of a small autonomous helicopter from [12]. To test the robustness property of the controller, parameter uncertainties are taken up to 30% of the nominal values. Even though the controller is designed based on simplified force and torque equations as described by (10.4) and (10.10) respectively, the helicopter model assumes full torque, (10.9) and full force equations. The wind disturbance shown in Fig. 10.2 is presented to the helicopter as a persistently acting external force generated by a 8-dimensional neutrally stable exosystem with $\varrho = (1, 1.5, 0.1, 10)$, $w_x(0) = (20, 1, 4, 0, -1800, 0, -0.1, -0.02)$, $w_y(0) = (10, 2, 10, 2, 1500, 0, 0.1, 0)$ and $w_z(0) = (5, 0, 1, 0, 2000, 0, 0.01, 0.01)$. To further challenge the controller, only 5-dimensional internal models (10.39) and (10.41) are used for each axis. Position of the helicopter in the face of the wind disturbance when disturbance measurements are available without parameter uncertainties are shown in Fig. 10.3. When wind disturbance measurements are not available, helicopter position without ($\gamma = 0$) and with disturbance adaptation are given in Fig. 10.4 and 10.5 respectively.

Without disturbance adaptation, while the controller fails to stabilize the x and y positions, z does converge fairly close to zero as could be seen in Fig. 10.4. Apparently, T_M is still capable of acting as a vertical stabilizer to a certain degree although the disturbance adaptation is turned off due to the presence of other terms in (10.40). The importance of

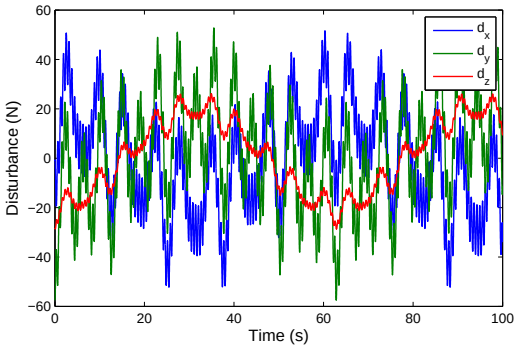

Figure 10.2: Wind disturbance

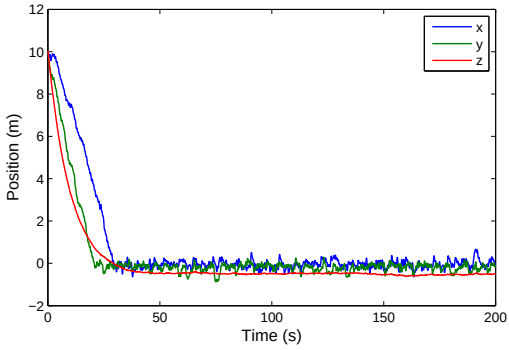

Figure 10.3: Position when disturbance measurements are available without parameter uncertainties.

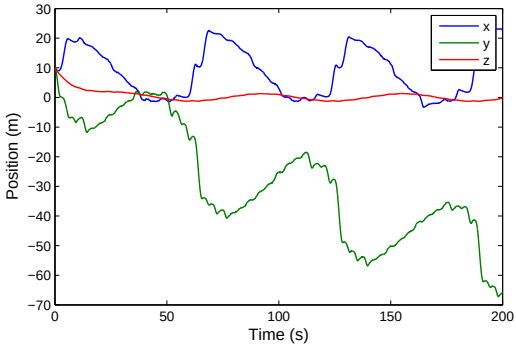

Figure 10.4: Position when disturbance adaptation is turned off.

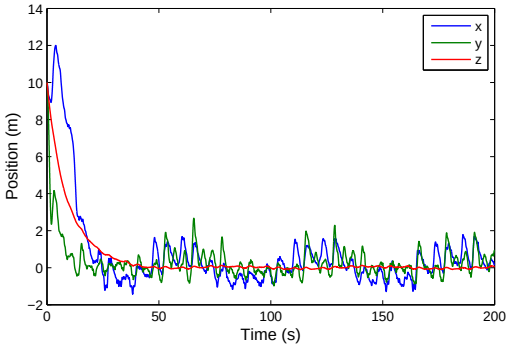

Figure 10.5: Position when disturbance adaptation is turned on.

information on the disturbance to the longitudinal/lateral stabilizer is demonstrated in Fig. 10.5. Now that the disturbance adaptation is turned on, z converges to zero and, x and y converge to a small neighbourhood of the origin as guaranteed by Proposition 6. In Fig. 10.3, even with disturbance measurements and perfect knowledge of helicopter parameters, a poor z position control is obtained. The slight offset in z position is a consequence of the absence of integral action in the vertical control.

10.5 Conclusion and Future Works

A robust controller for helicopter stabilization to reject wind disturbance is presented. The wind disturbance affecting the helicopter is assumed to be a function of time of a fixed structure with unknown parameters. By designing an internal model that estimates the disturbance, a control design is carried out for longitudinal, lateral and vertical dynamics stabilization. Despite the presence of helicopter parameter and model uncertainties, simulation results clearly demonstrates the effectiveness of the control technique. As future works, indoor and outdoor flights are to be carried out to test the feasibility of the proposed controller. That gives an immediate challenge caused by the presence of servo dynamics and limitations on wind disturbance that could be handled.

Appendix A

The derivation of (10.22) is first given. Let $e_{\xi z} := \xi_z - \bar{\tau}_z(w, \mu, \varrho)$. Given $\chi := e_{\xi z} + GM\dot{z}$, then $\dot{\chi} = \dot{e}_{\xi z} + GM\ddot{z}$. Solving for $\dot{e}_{\xi z}$,

$$\begin{aligned}
\dot{e}_{\xi z} &= \dot{\xi}_z - \dot{\bar{\tau}}_z \\
&= (F + G\hat{\Psi})\xi_z + g_{\text{stz}} - (F + G\Psi_\varrho)\bar{\tau}_z \\
&= F\xi_z + G\hat{\Psi}\xi_z + g_{\text{stz}} - (F + G\Psi_\varrho)\bar{\tau}_z \\
&= F\xi_z + G(\Psi_\varrho e_{\xi z} + \Psi_\varrho \bar{\tau}_z + \tilde{\Psi}_2 \xi_{z2}) + g_{\text{stz}} - (F + G\Psi_\varrho)\bar{\tau}_z \\
&= F(\xi_z - \bar{\tau}_z) + G\Psi_\varrho e_{\xi z} + G(\Psi_\varrho \bar{\tau}_z + \tilde{\Psi}_2 \xi_{z2} - \Psi_\varrho \bar{\tau}_z) + g_{\text{stz}} \\
&= (F + G\Psi_\varrho)e_{\xi z} + G\tilde{\Psi}_2 \xi_{z2} + g_{\text{stz}}.
\end{aligned}$$

Since $g_{\text{stz}} = Gu_{\text{st}} + FGM_0\dot{z}$,

$$\begin{aligned}
\dot{e}_{\xi z} &= (F + G\Psi_\varrho)e_{\xi z} + G\tilde{\Psi}_2 \xi_{z2} + Gu_{\text{st}} + FGM_0\dot{z} \\
&= (F + G\Psi_\varrho)e_{\xi z} + G(\tilde{\Psi}_2 \xi_{z2} + u_{\text{st}}) + FGM_0\dot{z}.
\end{aligned}$$

Now for the derivation of $\ddot{z}$, use

$$\begin{aligned}
\ddot{z} &= -\frac{\psi_c^z(q)u}{M} + g\big(1 - \frac{M_0}{M}\psi_c^z(q)\big) + \frac{\Psi_\varrho \bar{\tau}_z - gM_\Delta}{M} \\
&= \frac{-\psi_c^z(q)u + gM_0\big(1 - \psi_c^z(q)\big) + \Psi_\varrho \bar{\tau}_z}{M}
\end{aligned}$$

and

$$\begin{aligned}
u &= \hat{\Psi}\xi_z + u_{\text{st}} \\
&= \Psi_\varrho e_{\xi z} + \Psi_\varrho \bar{\tau}_z + \tilde{\Psi}_2 \xi_{z2} + u_{\text{st}}
\end{aligned}$$

thus making

$$\begin{aligned}
\ddot{z} &= \frac{1}{M}\Big(- \psi_c^z(q)(\Psi_\varrho e_{\xi z} + \Psi_\varrho \bar{\tau}_z + \tilde{\Psi}_2 \xi_{z2} + u_{\text{st}}) + gM_0\big(1 - \psi_c^z(q)\big) + \Psi_\varrho \bar{\tau}_z\Big) \\
&= \frac{1}{M}\Big(- (\Psi_\varrho e_{\xi z} + \tilde{\Psi}_2 \xi_{z2} + u_{\text{st}})\psi_c^z(q) - \Psi_\varrho \bar{\tau}_z \psi_c^z(q) + gM_0\big(1 - \psi_c^z(q)\big) \\
&\quad + \Psi_\varrho \bar{\tau}_z\Big) \\
&= \frac{1}{M}\Big(- (\Psi_\varrho e_{\xi z} + \tilde{\Psi}_2 \xi_{z2} + u_{\text{st}})\psi_c^z(q) + \big(1 - \psi_c^z(q)\big)\Psi_\varrho \bar{\tau}_z + gM_0\big(1 - \psi_c^z(q)\big)\Big) \\
&= \frac{1}{M}\Big(- (\Psi_\varrho e_{\xi z} + \tilde{\Psi}_2 \xi_{z2} + u_{\text{st}})\psi_c^z(q) + (gM_0 + \Psi_\varrho \bar{\tau}_z)\big(1 - \psi_c^z(q)\big)\Big).
\end{aligned}$$

Now,

$$\begin{aligned}
\dot{\chi} &= \dot{e}_{\xi z} + GM\ddot{z} \\
&= (F + G\Psi_\varrho)e_{\xi z} + G(\tilde{\Psi}_2\xi_{z2} + u_{\text{st}}) + FGM_0\dot{z} + G\Big(- (\Psi_\varrho e_{\xi z} + \tilde{\Psi}_2\xi_{z2} + u_{\text{st}}) \\
&\quad \psi_c^z(q) + (gM_0 + \Psi_\varrho\bar{\tau}_z)\big(1 - \psi_c^z(q)\big)\Big) \\
&= Fe_{\xi z} + FGM_0\dot{z} + G(\Psi_\varrho e_{\xi z} + \tilde{\Psi}_2\xi_{z2} + u_{\text{st}}) - G(\Psi_\varrho e_{\xi z} + \tilde{\Psi}_2\xi_{z2} + u_{\text{st}})\psi_c^z(q) \\
&\quad + G(gM_0 + \Psi_\varrho\bar{\tau}_z)\big(1 - \psi_c^z(q)\big) \\
&= Fe_{\xi z} + FGM_0\dot{z} + G(\Psi_\varrho e_{\xi z} + \tilde{\Psi}_2\xi_{z2} + u_{\text{st}})\big(1 - \psi_c^z(q)\big) + G(gM_0 + \Psi_\varrho\bar{\tau}_z) \\
&\quad \big(1 - \psi_c^z(q)\big) \\
&= Fe_{\xi z} + FGM_0\dot{z} + G(\Psi_\varrho e_{\xi z} + \tilde{\Psi}_2\xi_{z2} + u_{\text{st}} + gM_0 + \Psi_\varrho\bar{\tau}_z)\big(1 - \psi_c^z(q)\big) \\
&= Fe_{\xi z} + FG(M - M_\Delta)\dot{z} + G(\Psi_\varrho e_{\xi z} + \tilde{\Psi}_2\xi_{z2} + u_{\text{st}} + gM_0 + \Psi_\varrho\bar{\tau}_z) \\
&\quad \big(1 - \psi_c^z(q)\big) \\
&= F(e_{\xi z} + GM\dot{z}) - FGM_\Delta\dot{z} + G(\Psi_\varrho e_{\xi z} + \tilde{\Psi}_2\xi_{z2} + u_{\text{st}} + gM_0 + \Psi_\varrho\bar{\tau}_z) \\
&\quad \big(1 - \psi_c^z(q)\big) \\
&= F\chi - FGM_\Delta(\dot{z} + k_1 z - k_1 z) + G(\Psi_\varrho e_{\xi z} + \tilde{\Psi}_2\xi_{z2} + u_{\text{st}} + gM_0 + \Psi_\varrho\bar{\tau}_z) \\
&\quad \big(1 - \psi_c^z(q)\big) \\
&= F\chi - FGM_\Delta(\zeta - k_1 z) - G(\Psi_\varrho e_{\xi z} + \tilde{\Psi}_2\xi_{z2} + u_{\text{st}} + gM_0 + \Psi_\varrho\bar{\tau}_z) \\
&\quad \big(\psi_c^z(q) - 1\big).
\end{aligned}$$

Continuing with $u_{\text{st}} = k_2(\dot{z} + k_1 z) = k_2\zeta$,

$$\begin{aligned}
\dot{\chi} &= F\chi - FGM_\Delta(\zeta - k_1 z) - G(\Psi_\varrho e_{\xi z} + \tilde{\Psi}_2\xi_{z2} + k_2\zeta + gM_0 + \Psi_\varrho\bar{\tau}_z) \\
&\quad \big(\psi_c^z(q) - 1\big) \\
&= \Big(\begin{bmatrix} F & k_1 FGM_\Delta & -FGM_\Delta \end{bmatrix} + \begin{bmatrix} -G\Psi_\varrho & -G\Psi_\varrho GMk_1 & G\Psi_\varrho GM - Gk_2 \end{bmatrix} \\
&\quad \big(\psi_c^z(q) - 1\big)\Big) \begin{bmatrix} \chi \\ z \\ \zeta \end{bmatrix} - G\big(\psi_c^z(q) - 1\big)\xi_{z2}^\top\eta_2 - G\big(\psi_c^z(q) - 1\big)(gM_0 + \Psi_\varrho\bar{\tau}_z).
\end{aligned}$$

Moreover since $\zeta := \dot{z} + k_1 z$,

$$\begin{aligned}
\dot{\zeta} &= \ddot{z} + k_1\dot{z} \\
&= \frac{1}{M}\Big(- (\Psi_\varrho e_{\xi z} + \tilde{\Psi}_2\xi_{z2} + k_2\zeta)\psi_c^z(q) + (gM_0 + \Psi_\varrho\bar{\tau}_z)\big(1 - \psi_c^z(q)\big)\Big) + k_1\dot{z} \\
&= \Big(\big[-\tfrac{1}{M}\Psi_\varrho \quad -k_1(\Psi_\varrho G + k_1) \quad (\Psi_\varrho G + k_1 - \tfrac{1}{M}k_2)\big] + \\
&\quad \big[-\tfrac{1}{M}\Psi_\varrho \quad -k_1\Psi_\varrho G \quad (\Psi_\varrho G - \tfrac{1}{M}k_2)\big] \big(\psi_c^z(q) - 1\big)\Big) \begin{bmatrix} \chi \\ z \\ \zeta \end{bmatrix} - \big[\frac{1}{M} + \frac{1}{M} \\
&\quad \big(\psi_c^z(q) - 1\big)\big]\xi_{z2}^\top\eta_2 - \frac{1}{M}\big(\psi_c^z(q) - 1\big)(gM_0 + \Psi_\varrho\bar{\tau}_z).
\end{aligned}$$

Collecting the derived equations above,

$$\begin{bmatrix}\dot{\chi}\\ \dot{z}\\ \dot{\zeta}\end{bmatrix} = \Bigg(\begin{bmatrix} F & k_1 FGM_\triangle & -FGM_\Delta \\ 0 & -k_1 & 1 \\ -\frac{1}{M}\Psi_\varrho & -k_1(\Psi_\varrho G + k_1) & (\Psi_\varrho G + k_1 - \frac{1}{M}k_2)\end{bmatrix} + \begin{bmatrix} -G\Psi_\varrho & -G\Psi_\varrho GMk_1 & G\Psi_\varrho GM - Gk_2 \\ 0 & 0 & 0 \\ -\frac{1}{M}\Psi_\varrho & -k_1\Psi_\varrho G & (\Psi_\varrho G - \frac{1}{M}k_2)\end{bmatrix}\big(\psi_c^z(q)-1\big)\Bigg)\begin{bmatrix}\chi\\ z\\ \zeta\end{bmatrix} - \Bigg(\frac{1}{M}\begin{bmatrix}0\\0\\1\end{bmatrix} + \begin{bmatrix}G\\0\\\frac{1}{M}\end{bmatrix}\big(\psi_c^z(q)-1\big)\Bigg)\xi_{z2}^\top\eta_2 - \begin{bmatrix}G\\0\\\frac{1}{M}\end{bmatrix}\big(\psi_c^z(q)-1\big)(gM_0 + \Psi_\varrho\bar{\tau}_z).$$

Now guided by the steps taken in [6, Proof of Proposition 3.3.2], it is shown that with an appropriate selection of k_2, A can be made Hurwitz. Recall that F is Hurwitz and thus there exists a symmetric positive definite matrix Q such that

$$QF + F^\top Q = -I.$$

As a result, a positive definite matrix

$$P = \begin{bmatrix} Q & 0 & 0 \\ 0 & a & 0 \\ 0 & 0 & 1\end{bmatrix}$$

can be constructed where $a > 0$. Next the following matrix equation is solved,

$$PA + A^\top P = \begin{bmatrix} -I & m_1 & m_2 \\ m_1^\top & -2ak_1 & m_3 \\ m_2^\top & m_3 & m_4\end{bmatrix},$$

where

$$\begin{aligned} m_1 &= k_1 QFGM_\Delta \\ m_2 &= -QFGM_\Delta - \frac{1}{M}\Psi_\varrho^\top \\ m_3 &= a - k_1(\Psi_\varrho G + k_1) \\ m_4 &= 2(\Psi_\varrho G + k_1 - \frac{1}{M}k_2). \end{aligned}$$

Consider the block

$$\begin{bmatrix} -I & m_1 \\ m_1^\top & -2ak_1\end{bmatrix}.$$

It is shown now that given any number $0 < a_0 < 1$, there exists a^* such that if $a \geq a^*$,

$$\begin{bmatrix} -I & m_1 \\ m_1^\top & -2ak_1\end{bmatrix} \leq -a_0 I.$$

Recall that the above inequality is by definition

$$x_0^\top \left(\begin{bmatrix} -I & m_1 \\ m_1^\top & -2ak_1 \end{bmatrix} + a_0 I \right) x_0 \leq 0,$$

for all non-zero vectors $x_0 = [x_1 \; x_2]^\top \in \mathbb{R}^{2N+1} \times \mathbb{R}$. Expanding,

$$(a_0 - 1)x_1^\top x_1 + (a_0 - 2ak_1)x_2^2 + 2x_2 x_1^\top m_1 \leq 0.$$

It is easy to see that there exists a number a^*, such that if $a \geq a^*$ then the above inequality holds. Fixing such an a, let us compute $x_4^\top (PA + A^\top P) x_4$,

$$x_4^\top \begin{bmatrix} -I & m_1 & m_2 \\ m_1^\top & -2ak_1 & m_3 \\ m_2^\top & m_3 & m_4 \end{bmatrix} x_4 = x_0^\top \begin{bmatrix} -I & m_1 \\ m_1^\top & -2ak_1 \end{bmatrix} x_0 + m_4 x_3^2 + 2x_3 x_0^\top [m_2^\top \; m_3]^\top,$$

where $x_4 = [x_0 \; x_3]^\top \in \mathbb{R}^{2N+2} \times \mathbb{R}$ is a non-zero vector. Thus there exists a number k_2^* such that for all $k_2 \geq k_2^*$,

$$PA + A^\top P \leq -a_0 I.$$

Appendix B

In this appendix, a candidate Lyapunov function for attitude dynamical system (10.8) is chosen and shown that it can be made strictly negative with an appropriate selection of the design parameters. Defining $\tilde{\omega} := \omega + \bar{K}_D q$ where $\bar{K}_D := \frac{1}{K_D}$, the chosen control law becomes

$$\tilde{\mathbf{v}} = K_P q_r - \frac{K_P}{\bar{K}_D}\tilde{\omega} + \frac{K_P}{\bar{K}_D}\omega_d.$$

Consider a Lyapunov function candidate

$$V(q_0, \tilde{\omega}) = \frac{1-q_0}{q_0-\varepsilon} + \frac{1}{2}\tilde{\omega}^\top J\tilde{\omega}$$

defined on $(\varepsilon, 1] \times \mathbb{R}^3$. Thus,

$$\begin{aligned}\dot{V} = &-\frac{(1-\varepsilon)}{2(q_0-\varepsilon)^2}\bar{K}_D\|q\|^2 + \tilde{\omega}^\top\Big(\frac{(1-\varepsilon)}{2(q_0-\varepsilon)^2}I - \bar{K}_D^2 S(q)J - \frac{\bar{K}_D^2}{2}q_0 J\Big)q \\ &+\tilde{\omega}^\top\Big(\bar{K}_D S(q)J - \frac{K_P}{\bar{K}_D}L(T_M) + \frac{\bar{K}_D}{2}q_0 J + \frac{\bar{K}_D}{2}JS(q)\Big)\tilde{\omega} + K_P\tilde{\omega}^\top L(T_M)q_r \\ &+\frac{K_P}{\bar{K}_D}\tilde{\omega}^\top L(T_M)\omega_d + \tilde{\omega}^\top\Delta(T_M).\end{aligned}$$

Using [6, Lemma 5.9.1], a $T^* > 0$ can be chosen such that if $\psi_c^z(q(t)) = 1$ for all $t \geq T^*$, then $2l_1 I \leq L(T_M(t)) + L^T(T_M(t))$, $\|L(T_M(t))\| \leq l_2$ and $\|\Delta(T_M(t))\| \leq \delta$ for all $t > 0$. Since $\|q^*\| \leq \sqrt{3}\lambda_3$, $\|q_d\| \leq K_d m_{q_d}$ and $\|\omega_d\| \leq K_d m_{\omega_d}$,

$$\begin{aligned}\dot{V} \leq &-\bar{K}_D\frac{(1-\varepsilon)}{2(q_0-\varepsilon)^2}\|q\|^2 + (2\bar{K}_D c_2 - \frac{K_P}{\bar{K}_D}l_1)\|\tilde{\omega}\|^2 + \Big(a_3 + \frac{3}{2}\bar{K}_D^2 c_2 + K_P l_2(\sqrt{3}\lambda_3 \\ &+K_d m_{q_d}) + \delta + \frac{K_P}{\bar{K}_D}K_d l_2 m_{\omega_d}\Big)\|\tilde{\omega}\|,\end{aligned}$$

where $0 < c_1 \leq \|J\| \leq c_2$ and

$$a_3 = \max_{q_0 \in \mathcal{S}} \frac{1-\varepsilon}{2(q_0-\varepsilon)^2},$$

with the compact set $\mathcal{S}$ and the open set $\mathcal{M}$ as defined in [6, Proof of Proposition 5.7.1]. To show that $\dot{V}$ can be made negative definite, it is desired to have

$$\begin{aligned}&(2\bar{K}_D c_2 - \frac{K_P}{\bar{K}_D}l_1)\|\tilde{\omega}\|^2 + \Big(a_3 + \frac{3}{2}\bar{K}_D^2 c_2 + K_P l_2(\sqrt{3}\lambda_3 + K_d m_{q_d}) + \delta + \\ &\frac{K_P}{\bar{K}_D}K_d l_2 m_{\omega_d}\Big)\|\tilde{\omega}\| \leq -\bar{K}_D\frac{1-\varepsilon}{4}c_2\|\tilde{w}\|^2.\end{aligned}$$

Rearranging and letting

$$a_1 = \min_{\tilde{\omega} \in \mathcal{S}/\mathcal{M}} \|\tilde{\omega}\|, \quad a_2 = \max_{\tilde{\omega} \in \mathcal{S}/\mathcal{M}} \|\tilde{\omega}\|,$$

we obtain

$$\begin{aligned}&\frac{K_P}{\bar{K}_D}\big(l_1a_1-\sqrt{3}\lambda_3\bar{K}_Dl_2-K_d(\bar{K}_Dm_{q_d}+m_{\omega_d})l_2\big)\\&\geq\Big(a_3+\frac{3}{2}\bar{K}_D^2c_2+\delta\Big)+\bar{K}_Dc_2\Big(\frac{9-\varepsilon}{4}\Big)a_2.\end{aligned}$$

If $\lambda_3\leq\lambda_3^*(K_D)$, $K_d\leq K_d^*(K_D)$ and $K_P\geq K_P^*(K_D)$, where

$$\begin{aligned}\lambda_3^*(K_D)&=\frac{l_1a_1}{4\sqrt{3}\bar{K}_Dl_2},\quad K_d^*(K_D)=\frac{l_1a_1}{4(\bar{K}_Dm_{q_d}+m_{\omega_d})l_2},\\K_P^*(K_D)&=\frac{3c_2}{a_1l_1}\bar{K}_D^3+\frac{(9-\varepsilon)a_2c_2}{2a_1l_1}\bar{K}_D^2+\frac{2(a_3+\delta)}{a_1l_1}\bar{K}_D,\end{aligned}$$

then

$$\dot{V}(q_0,\tilde{\omega})\leq-\bar{K}_D\frac{1-\varepsilon}{2}\Big(\frac{\|q\|^2}{(q_0-\varepsilon)^2}+\frac{c_2}{2}\|\tilde{\omega}\|^2\Big)$$

for a fixed $\bar{K}_D\geq\bar{K}_D^*$ and all $(q_0,\tilde{\omega})\in\mathcal{S}$, where $\bar{K}_D^*$ is a positive number as defined in [6, Proof of Proposition 5.7.1].

Appendix C

In this part, we expand the equations of subsystem (10.36) and show that it is ISS. But first, expressions for some relevant variables are derived.

The disturbance $d_y(w_y)$ that affects the helicopter translational motion in y-axis is generated by an autonomous exosystem given by

$$\begin{aligned} \dot{w}_y &= \mathrm{S}(\varrho) w_y \\ d_y(w_y) &= R\mathrm{S}^2(\varrho) w_y, \end{aligned} \tag{10.42}$$

where $w_y \in \mathbb{R}^{2N}$. Note that N is the number of sinusoids with unknown constant frequencies Ω_i, amplitudes A_i and phases φ_i for $i = 1, \ldots, N$, that compose $d_y(w_y)$. Similar to the approach taken in the stabilization of vertical dynamics, d_y can be regarded as an output of a linear system. Defining

$$\tau_y(w_y) = \begin{bmatrix} 0 \\ w_y \end{bmatrix},$$

exosystem (10.42) can be rewritten as,

$$\begin{aligned} \frac{\partial \tau_y}{\partial w_y} \mathrm{S}(\varrho) w_y &= \Phi(\varrho) \tau_y(w_y) \\ d_y(w_y) &= \Gamma(\varrho) \tau_y(w_y). \end{aligned}$$

Please refer to Section 10.3 for quantities that are not defined here. Consequently, referring to [6, Lemma 3.3.1], $d_y(w_y)$ can be thought of as generated by

$$\begin{aligned} \frac{\partial \bar{\tau}_y}{\partial w_y} \mathrm{S}(\varrho) w_y &= (F + G\Psi_\varrho) \bar{\tau}_y(w_y) \\ d_y(w_y) &= \Psi_\varrho \bar{\tau}_y(w_y), \end{aligned}$$

where $\bar{\tau}_y(w_y) = T_\varrho \tau_y(w_y)$. Accordingly, the disturbance that affects the helicopter translational motion in x-axis can be taken as

$$\begin{aligned} \frac{\partial \bar{\tau}_x}{\partial w_x} \mathrm{S}(\varrho) w_x &= (F + G\Psi_\varrho) \bar{\tau}_x(w_x) \\ d_x(w_x) &= \Psi_\varrho \bar{\tau}_x(w_x). \end{aligned}$$

Therefore, the horizontal disturbance vector $d_h(w_x, w_y) = [d_y(w_y)\ d_x(w_x)\ 0\ \cdots\ 0]^\top$ can be given by

$$\dot{\bar{\tau}}(w_x, w_y) = \tilde{F} \bar{\tau}(w_x, w_y) \tag{10.43}$$

$$d_h(w_x, w_y) = P \bar{\tau}(w_x, w_y), \tag{10.44}$$

where

$$\bar{\tau}(w_x, w_y) = \begin{bmatrix} \bar{\tau}_y(w_y) \\ \bar{\tau}_x(w_x) \end{bmatrix},\ \tilde{F} = \begin{bmatrix} F + G\Psi_\varrho & 0 \\ 0 & F + G\Psi_\varrho \end{bmatrix} \text{ and}$$

$$P = \underset{(4N+2)\times(4N+2)}{\begin{bmatrix} \Psi_\varrho & 0 \\ 0 & \Psi_\varrho \\ 0 & 0 \end{bmatrix}}.$$

Since $d_h(w_x, w_y)$ is a function of unmeasurable states w_x and w_y, and depends on unknown ϱ, it has to be estimated by means of an internal model of the form

$$\dot{\xi} = \hat{F}\xi + g_{\text{st}} \tag{10.45}$$
$$\hat{d} = \hat{P}\xi, \tag{10.46}$$

where $\hat{d}$ is an estimate of $d_h(w_x, w_y)$ and

$$\begin{aligned} g_{\text{st}} = \begin{bmatrix} g_{\text{sty}} \\ g_{\text{stx}} \end{bmatrix} &= \begin{bmatrix} k_4(\dot{y} + k_3 y)G \\ k_4(\dot{x} + k_3 x)G \end{bmatrix} \\ &= k_4\hat{G}(\dot{\zeta}_2 - K_1\sigma'(\frac{K_1}{\lambda_1}\zeta_1)\dot{\zeta}_1 + k_3\dot{\zeta}_1) \end{aligned}$$

for arbitrary $k_3, k_4 > 0$. Also,

$$\xi = \begin{bmatrix} \xi_y \\ \xi_x \end{bmatrix}, \text{ where } \xi_i = \begin{bmatrix} \xi_{i1} \\ \xi_{i2} \end{bmatrix} \in \mathbb{R} \times \mathbb{R}^{2N} \text{ for } i = x, y,$$

$$\hat{F} = \begin{bmatrix} F + G\hat{\Psi} & 0 \\ 0 & F + G\hat{\Psi} \end{bmatrix}, \ \hat{P} = \underset{(4N+2)\times(4N+2)}{\begin{bmatrix} \hat{\Psi} & 0 \\ 0 & \hat{\Psi} \\ 0 & 0 \end{bmatrix}}, \qquad \hat{G} = \begin{bmatrix} G & 0 \\ 0 & G \end{bmatrix}.$$

Note that the earlier assumption in the first part of Section 10.3 that q_d is bounded implies that ξ is bounded too. Recall that since $\tilde{\Psi}_2 = \hat{\Psi}_2 - \Psi_{2,\varrho}$,

$$\begin{aligned} \hat{\Psi}\xi_i &= \begin{bmatrix} 1 & \tilde{\Psi}_2 + \Psi_{2,\varrho} \end{bmatrix} \xi_i \\ &= \left(\begin{bmatrix} 1 & \Psi_{2,\varrho} \end{bmatrix} + \begin{bmatrix} 0 & \tilde{\Psi}_2 \end{bmatrix} \right) \xi_i \\ &= \Psi_\varrho \xi_i + \tilde{\Psi}_2 \xi_{i2}, \quad i = x, y. \end{aligned}$$

Hence,

$$\hat{d} = P\xi + \tilde{P}_2\xi_2, \tag{10.47}$$

where

$$\xi_2 = \begin{bmatrix} \xi_{y2} \\ \xi_{x2} \end{bmatrix} \quad \text{and} \quad \tilde{P}_2 = \underset{(4N+2)\times 4N}{\begin{bmatrix} \tilde{\Psi}_2 & 0 \\ 0 & \tilde{\Psi}_2 \\ 0 & 0 \end{bmatrix}}.$$

Recall from the first part of Section 10.3 that the internal model in (10.18) can be designed to generate $\hat{\Psi}_2$ that converges to $\Psi_{2,\varrho}$ in steady state. Therefore, the objective of internal model (10.45) is set to produce ξ that converges to $\bar{\tau}(w_x, w_y)/K_d$ which in turn multiplied by $\hat{P}$, yields $d_h(w_x, w_y)/K_d$ in steady state. The following internal model error is then defined,

$$e_\xi = \frac{\xi - \bar{\tau}(w_x, w_y)/K_d}{K_d}, \tag{10.48}$$

where

$$e_\xi = \begin{bmatrix} e_{\xi y} \\ e_{\xi x} \end{bmatrix}.$$

Further steps are taken now to obtain a practical expression of $\hat{d}$. Continuing from (10.47) by substituting ξ with an expression derived from (10.48) where $\bar{\tau} := \bar{\tau}(w_x, w_y)$,

$$\hat{d} = P(K_d e_\xi + \frac{1}{K_d}\bar{\tau}) + \tilde{P}_2\xi_2. \tag{10.49}$$

Next solving for e_ξ from (10.34),

$$\begin{aligned}\hat{d} &= K_d P(\frac{\tilde{J}\eta_2 - \eta_3}{K_d}) + \frac{1}{K_d}P\bar{\tau} + \tilde{P}_2\xi_2 \\ &= P\tilde{J}\eta_2 - P\eta_3 + \frac{1}{K_d}P\bar{\tau} + \tilde{P}_2\xi_2.\end{aligned}$$

Before proceeding further, an equation for ξ_2 is developed. Note that

$$\xi_{y2} = P_4\xi_y,$$

where

$$P_4 = \begin{bmatrix} 0\,1\,0\cdots & 0 \\ 0\,0\,1 & 0 \\ \vdots \quad \ddots & \vdots \\ & 0 \\ 0\,0\,0\cdots 0 & 1 \end{bmatrix}_{2N\times(2N+1)}.$$

So,

$$\begin{aligned}\xi_2 &= P_5\xi \\ &= P_5(K_d e_\xi + \bar{\tau}/K_d) \\ &= K_d P_5(\frac{\tilde{J}\eta_2 - \eta_3}{K_d}) + \frac{1}{K_d}P_5\bar{\tau} \\ &= P_5\tilde{J}\eta_2 - P_5\eta_3 + \frac{1}{K_d}P_5\bar{\tau},\end{aligned}$$

where

$$P_5 = \begin{bmatrix} P_4 & 0 \\ 0 & P_4 \end{bmatrix}.$$

Back to $\hat{d}$,

$$\begin{aligned}\hat{d} = P\tilde{J}\eta_2 - P\eta_3 + \frac{1}{K_d}P\bar{\tau} + \tilde{P}_2(P_5\tilde{J}\eta_2 - P_5\eta_3 + \\ \frac{1}{K_d}P_5\bar{\tau}) = G_0\tilde{J}\eta_2 - G_0\eta_3 + \frac{1}{K_d}G_0\bar{\tau},\end{aligned}$$

where $G_0 = P + \tilde{P}_2P_5$.

Before the time derivatives of (10.26), (10.33) and (10.34) are computed, $\dot{\hat{d}}$, q_d, $\dot{q}_d$, $\dot{q}^*$ and $\dot{e}_\xi$ have to be expressed in a suitable form. Starting with $\dot{\hat{d}}$, from (10.49),

$$\dot{\hat{d}} = K_d P \dot{e}_\xi + \frac{1}{K_d} P \dot{\bar{\tau}} + \dot{\tilde{P}}_2 \xi_2 + \tilde{P}_2 \dot{\xi}_2.$$

An expression for $\dot{e}_\xi$ is first developed. From (10.45),

$$\begin{aligned}
\dot{\xi}_y &= (F + G\hat{\Psi})\xi_y + g_{\text{sty}} \\
&= F(K_d e_{\xi y} + \frac{1}{K_d}\bar{\tau}_y) + G(\Psi_\varrho \xi_y + \tilde{\Psi}_2 \xi_{y2}) + g_{\text{sty}} \\
&= K_d F e_{\xi y} + \frac{1}{K_d} F \bar{\tau}_y + G\Psi_\varrho (K_d e_{\xi y} + \frac{1}{K_d}\bar{\tau}_y) + G\tilde{\Psi}_2 \xi_{y2} + g_{\text{sty}} \\
&= K_d (F + G\Psi_\varrho) e_{\xi y} + \frac{1}{K_d}(F + G\Psi_\varrho)\bar{\tau}_y + G\tilde{\Psi}_2 \xi_{y2} + g_{\text{sty}}
\end{aligned}$$

and similarly,

$$\dot{\xi}_x = K_d (F + G\Psi_\varrho) e_{\xi x} + \frac{1}{K_d}(F + G\Psi_\varrho)\bar{\tau}_x + G\tilde{\Psi}_2 \xi_{x2} + g_{\text{stx}}.$$

Thus,

$$\begin{aligned}
\dot{\xi} &= K_d \tilde{F} e_\xi + \frac{1}{K_d}\tilde{F}\bar{\tau} + \tilde{G}\tilde{P}_2 \xi_2 + g_{\text{st}} \\
&= K_d \tilde{F}(\frac{\tilde{J}\eta_2 - \eta_3}{K_d}) + \frac{1}{K_d}\tilde{F}\bar{\tau} + \\
&\quad \tilde{G}\tilde{P}_2(P_5 \tilde{J}\eta_2 - P_5\eta_3 + \frac{1}{K_d}P_5\bar{\tau}) + g_{\text{st}} \\
&= G_1 \tilde{J}\eta_2 - G_1\eta_3 + \frac{1}{K_d} G_1 \bar{\tau} + g_{\text{st}},
\end{aligned}$$

where $G_1 = \tilde{F} + \tilde{G}\tilde{P}_2 P_5$ and

$$\tilde{G} = \underset{(4N+2)\times(4N+2)}{\begin{bmatrix} G & 0 & 0 \\ 0 & G & 0 \end{bmatrix}}.$$

Rearranging and dividing by K_d,

$$\frac{\dot{\xi} - \frac{1}{K_d}\tilde{F}\bar{\tau}}{K_d} = \frac{1}{K_d}\big(G_1 \tilde{J}\eta_2 - G_1\eta_3 + \frac{1}{K_d}\tilde{G}\tilde{P}_2 P_5 \bar{\tau} + g_{\text{st}}\big).$$

Referring to (10.43) and (10.48),

$$\dot{e}_\xi = \frac{1}{K_d}\big(G_1 \tilde{J}\eta_2 - G_1\eta_3 + \frac{1}{K_d}\tilde{G}\tilde{P}_2 P_5 \bar{\tau} + g_{\text{st}}\big). \tag{10.50}$$

Now back to $\dot{\hat{d}}$,

$$\begin{aligned}\dot{\hat{d}} &= P(G_1\tilde{J}\eta_2 - G_1\eta_3 + \frac{1}{K_d}\tilde{G}\tilde{P}_2P_5\bar{\tau} + g_{\text{st}}) + \frac{1}{K_d}P\tilde{F}\bar{\tau} + \dot{\tilde{P}}_2(P_5\tilde{J}\eta_2 - P_5\eta_3 + \\ &\quad \frac{1}{K_d}P_5\bar{\tau}) + \tilde{P}_2P_5(G_1\tilde{J}\eta_2 - G_1\eta_3 + \frac{1}{K_d}G_1\bar{\tau} + g_{\text{st}}) \\ &= G_2\tilde{J}\eta_2 - G_2\eta_3 + \frac{1}{K_d}G_2\bar{\tau} + G_0g_{\text{st}},\end{aligned}$$

where $G_2 = PG_1 + \dot{\tilde{P}}_2P_5 + \tilde{P}_2P_5G_1$.

Recall that $q_d = -K_d\tilde{D}_0(t)\hat{d}$. Hence,

$$q_d = -K_d\tilde{D}_0(t)(G_0\tilde{J}\eta_2 - G_0\eta_3 + \frac{1}{K_d}P\bar{\tau} + \frac{1}{K_d}\tilde{P}_2P_5\bar{\tau}).$$

From (10.44),

$$q_d = -K_d\tilde{D}_0(t)(G_0\tilde{J}\eta_2 - G_0\eta_3) - \tilde{D}_0(t)d_h - \tilde{D}_0(t)\tilde{P}_2P_5\bar{\tau}, \tag{10.51}$$

where $d_h := d_h(w_x, w_y)$.

With $\tilde{D}_0 := \tilde{D}_0(t)$, an expression for $\dot{q}_d$ is developed.

$$\begin{aligned}\dot{q}_d &= -K_d(\dot{\tilde{D}}_0\hat{d} + \tilde{D}_0\dot{\hat{d}}) \\ &= -K_d\dot{\tilde{D}}_0(G_0\tilde{J}\eta_2 - G_0\eta_3 + \frac{1}{K_d}G_0\bar{\tau}) - K_d\tilde{D}_0(G_2\tilde{J}\eta_2 - G_2\eta_3 + \frac{1}{K_d}G_2\bar{\tau} + \\ &\quad G_0g_{\text{st}}) \\ &= -K_dG_3\tilde{J}\eta_2 + K_dG_3\eta_3 - G_3\bar{\tau} - K_d\tilde{D}_0G_0g_{\text{st}},\end{aligned} \tag{10.52}$$

where $G_3 = \dot{\tilde{D}}_0G_0 + \tilde{D}_0G_2$.

Before an equation for $\dot{q}^*$ could be developed, an expression for $\dot{\zeta}_3$ is needed. From (10.30),

$$\dot{\zeta}_3 = -\frac{1}{M}\tilde{D}P_2\lambda_3\sigma(\frac{K_3}{\lambda_3}\zeta_3) + \frac{1}{M}\tilde{D}q_d + K_2P_1\sigma'(\frac{K_2}{\lambda_2}\zeta_2)\dot{\zeta}_2 - \frac{1}{M}\tilde{D}\tilde{\eta}_1 + \frac{p}{M} + \frac{d_h}{M},$$

where $\tilde{D} := \tilde{D}(t)$. Substituting (10.51),

$$\begin{aligned}\dot{\zeta}_3 = &-\frac{1}{M}\tilde{D}P_2\lambda_3\sigma(\frac{K_3}{\lambda_3}\zeta_3) + K_2P_1\sigma'(\frac{K_2}{\lambda_2}\zeta_2)\dot{\zeta}_2 + \frac{p}{M} + \frac{d_h}{M} - \frac{1}{M}L_dd_h - \frac{1}{M}\tilde{D}\eta_1 - \\ &\frac{K_d}{M}L_dG_0\tilde{J}\eta_2 + \frac{K_d}{M}L_dG_0\eta_3 - \frac{1}{M}L_d\tilde{P}_2P_5\bar{\tau},\end{aligned}$$

where $L_d = \tilde{D}\tilde{D}_0$. Note that

$$L_{d0} = \begin{bmatrix} l_d & 0 & 0 \\ 0 & l_d & 0 \\ 0 & 0 & M \end{bmatrix},\ L_d = \begin{bmatrix} L_{d0} & 0 \\ 0 & 0 \end{bmatrix},$$

where

$$l_d = \frac{gM + d_z}{gM + d_z + y_\eta(\eta, w)}$$

and thus $d_h/M - L_d d_h/M = (I - L_d)d_h/M$ is asymptotically vanishing since

$$\lim_{t\to\infty} L_d(t) = \begin{bmatrix} L_{d1} & 0 \\ 0 & 0 \end{bmatrix},\ L_{d1} = \begin{bmatrix} 1 & 0 & 0 \\ 0 & 1 & 0 \\ 0 & 0 & M \end{bmatrix}.$$

Collecting all asymptotically vanishing terms in p_0 (recall that by [6, Proposition 5.4.1], $\lim_{t\to\infty} p(t) = 0$ and $\lim_{t\to\infty} \tilde{P}_2(t) = 0$),

$$\dot{\zeta}_3 = -\frac{1}{M}\tilde{D}P_2\lambda_3\sigma(\frac{K_3}{\lambda_3}\zeta_3) + K_2P_1\sigma'(\frac{K_2}{\lambda_2}\zeta_2)\dot{\zeta}_2 + \frac{p_0}{M} - \frac{1}{M}\tilde{D}\tilde{\eta}_1 - \frac{K_d}{M}L_dG_0\tilde{J}\eta_2 + \frac{K_d}{M}L_dG_0\eta_3, \tag{10.53}$$

where

$$p_0 = p + (d_h - L_d d_h) - L_d\tilde{P}_2P_5\bar{\tau}. \tag{10.54}$$

It is known that

$$\dot{q}^* = -K_3P_2\sigma'(\frac{K_3}{\lambda_3}\zeta_3)\dot{\zeta}_3.$$

Hence,

$$\begin{aligned}\dot{q}^* &= -K_3P_2\sigma'(\frac{K_3}{\lambda_3}\zeta_3)\big(-\frac{1}{M}\tilde{D}P_2\lambda_3\sigma(\frac{K_3}{\lambda_3}\zeta_3) + K_2P_1\sigma'(\frac{K_2}{\lambda_2}\zeta_2)\dot{\zeta}_2 + \frac{p_0}{M}\big) \\ &\quad + \frac{K_3}{M}P_2\sigma'(\frac{K_3}{\lambda_3}\zeta_3)\tilde{D}\tilde{\eta}_1 + \frac{K_dK_3}{M}P_2\sigma'(\frac{K_3}{\lambda_3}\zeta_3)L_dG_0\tilde{J}\eta_2 \\ &\quad - \frac{K_dK_3}{M}P_2\sigma'(\frac{K_3}{\lambda_3}\zeta_3)L_dG_0\eta_3 \\ &= y_{\zeta 0} + K_3G_4\tilde{\eta}_1 + K_dK_3G_5\tilde{J}\eta_2 - K_dK_3G_5\eta_3,\end{aligned} \tag{10.55}$$

where

$$\begin{aligned} y_{\zeta 0} &= -K_3P_2\sigma'(\frac{K_3}{\lambda_3}\zeta_3)\big(-\frac{1}{M}\tilde{D}P_2\lambda_3\sigma(\frac{K_3}{\lambda_3}\zeta_3) + K_2P_1\sigma'(\frac{K_2}{\lambda_2}\zeta_2)\dot{\zeta}_2 + \frac{p_0}{M}\big) \\ G_4 &= \frac{1}{M}P_2\sigma'(\frac{K_3}{\lambda_3}\zeta_3)\tilde{D}, \\ G_5 &= \frac{1}{M}P_2\sigma'(\frac{K_3}{\lambda_3}\zeta_3)L_dG_0. \end{aligned} \tag{10.56}$$

Now with all the required equations in hand, $\dot{\eta}_1$ is computed. From (10.26) and (10.27), it is known that

$$\dot{\eta}_1 = \dot{q}^* + \dot{q}_d - \dot{q}.$$

Based on (10.8), (10.33), (10.35), (10.52) and (10.55),

$$\begin{aligned}\dot{\tilde{\eta}}_1 &= -\frac{1}{2}\big(q_0 I + \tilde{S}(q)\big)(\eta_2 + \frac{1}{K_d}\tilde{\eta}_1) + \Big(I - \frac{1}{2}\big(q_0 I + \tilde{S}(q)\big)Q_d\Big)(-K_d G_3 \tilde{J}\eta_2 + \\ &\quad K_d G_3 \eta_3 - G_3\bar{\tau} - K_d \tilde{D}_0 G_0 g_{\text{st}}) + y_{\zeta 0} + K_3 G_4 \tilde{\eta}_1 + K_d K_3 G_5 \tilde{J}\eta_2 - K_d K_3 G_5 \eta_3 \\ &= \Big(-\frac{1}{2K_D} q_0 I - \frac{1}{2K_D}\tilde{S}(q) + K_3 G_4\Big)\tilde{\eta}_1 - \Bigg(\frac{1}{2}\big(q_0 I + \tilde{S}(q)\big) + K_d\Big(\Big(I - \frac{1}{2}\big(q_0 I \\ &\quad + \tilde{S}(q)\big)Q_d\Big)G_3 - K_3 G_5\Big)\tilde{J}\Bigg)\eta_2 + K_d\Big(\Big(I - \frac{1}{2}\big(q_0 I + \tilde{S}(q)\big)Q_d\Big)G_3 \\ &\quad - K_3 G_5\Big)\eta_3 - K_d k_4\Big(I - \frac{1}{2}\big(q_0 I + \tilde{S}(q)\big)Q_d\Big)\tilde{D}_0 G_0 y_{\zeta 1} + y_{\zeta 0} + I_{\tilde{\eta}_1}, \end{aligned} \tag{10.57}$$

where

$$I_{\tilde{\eta}_1} = -\Big(I - \frac{1}{2}\big(q_0 I + \tilde{S}(q)\big)Q_d\Big)G_3\bar{\tau}, \tag{10.58}$$

$$y_{\zeta 1} = \hat{G}(\dot{\zeta}_2 - K_1\sigma'(\frac{K_1}{\lambda_1}\zeta_1)\dot{\zeta}_1 + k_3\dot{\zeta}_1). \tag{10.59}$$

Next from (10.33),

$$\tilde{J}\dot{\eta}_2 = \tilde{J}\dot{\tilde{\omega}} - \tilde{J}\dot{\omega}_d - \frac{1}{K_D}\tilde{J}\dot{\tilde{\eta}}_1.$$

Solving $\tilde{J}\dot{\tilde{\omega}}$ first, from (10.8), (10.24), (10.25) and (10.33),

$$\begin{aligned}\tilde{J}\dot{\tilde{\omega}} &= -\tilde{S}(\omega)\tilde{J}\tilde{\omega} + \tilde{L}(-K_P K_D \eta_2) + \tilde{\Delta} \\ &= -\frac{1}{K_D}\tilde{S}(\omega)\tilde{J}\tilde{\eta}_1 - \big(\tilde{S}(\omega)\tilde{J}(I - K_d Q_d G_3 \tilde{J}) + K_P K_D \tilde{L}\big)\eta_2 - K_d\tilde{S}(\omega)\tilde{J}Q_d G_3\eta_3 \\ &\quad + \tilde{S}(\omega)\tilde{J}Q_d G_3\bar{\tau} + K_d\tilde{S}(\omega)\tilde{J}Q_d\tilde{D}_0 G_0 g_{\text{st}} + \tilde{\Delta},\end{aligned}$$

where $\tilde{L} := \tilde{L}(T_M)$ and $\tilde{\Delta} := \tilde{\Delta}(T_M)$. Thus,

$$\begin{aligned}\tilde{J}\dot{\eta}_2 &= \Big(-\frac{1}{K_D}\tilde{S}(\omega)\tilde{J} + \frac{1}{2K_D^2}\tilde{J}\big(q_0 I + \tilde{S}(q)\big) - \frac{K_3}{K_D}\tilde{J}G_4\Big)\tilde{\eta}_1 + \Bigg(-K_P K_D\tilde{L} \\ &\quad - \tilde{S}(\omega)\tilde{J}(I - K_d Q_d G_3\tilde{J}) + \frac{1}{2K_D}\tilde{J}\big(q_0 I + \tilde{S}(q)\big) + \frac{K_d}{K_D}\tilde{J}\Big(\Big(I - \frac{1}{2}\big(q_0 I + \\ &\quad \tilde{S}(q)\big)Q_d\Big)G_3 - K_3 G_5\Big)\tilde{J}\Bigg)\eta_2 - K_d\Bigg(\Big(\tilde{S}(\omega)\tilde{J}Q_d + \frac{1}{K_D}\tilde{J}\Big(I - \frac{1}{2}\big(q_0 I \\ &\quad + \tilde{S}(q)\big)Q_d\Big)\Big)G_3 - \frac{K_3}{K_D}\tilde{J}G_5\Bigg)\eta_3 + K_d k_4\Big(\tilde{S}(\omega)\tilde{J}Q_d + \frac{1}{K_D}\tilde{J}\Big(I - \frac{1}{2}\big(q_0 I + \\ &\quad \tilde{S}(q)\big)Q_d\Big)\Big)\tilde{D}_0 G_0 y_{\zeta 1} - \frac{1}{K_D}\tilde{J}y_{\zeta 0} + I_{\eta_2},\end{aligned} \tag{10.60}$$

where

$$I_{\eta_2} = \Big(\tilde{S}(\omega)\tilde{J}Q_d + \frac{1}{K_D}\tilde{J}\Big(I - \frac{1}{2}\big(q_0 I + \tilde{S}(q)\big)Q_d\Big)\Big)G_3\bar{\tau} + \tilde{\Delta} - \tilde{J}\dot{\omega}_d. \tag{10.61}$$

Finally for $\dot{\eta}_3$, from (10.34) and (10.50),

$$\begin{aligned}
\dot{\eta}_3 &= \tilde{J}\dot{\eta}_2 - K_d\dot{e}_\xi \\
&= \Big(-\frac{1}{K_D}\tilde{S}(\omega)\tilde{J} + \frac{1}{2K_D^2}\tilde{J}\big(q_0 I + \tilde{S}(q)\big) - \frac{K_3}{K_D}\tilde{J}G_4\Big)\tilde{\eta}_1 + \Big(-K_P K_D\tilde{L} \\
&\quad -\tilde{S}(\omega)\tilde{J}(I - K_d Q_d G_3\tilde{J}) + \frac{1}{2K_D}\tilde{J}\big(q_0 I + \tilde{S}(q)\big) + \frac{K_d}{K_D}\tilde{J}\Big(\Big(I - \frac{1}{2}\big(q_0 I + \\
&\quad \tilde{S}(q)\big)Q_d\Big)G_3 - K_3 G_5\Big)\tilde{J}\Big)\tilde{J}^{-1}(\eta_3 + K_d e_\xi) - K_d\Big(\Big(\tilde{S}(\omega)\tilde{J}Q_d + \frac{1}{K_D}\tilde{J}\Big(I - \\
&\quad \frac{1}{2}\big(q_0 I + \tilde{S}(q)\big)Q_d\Big)\Big)G_3 - \frac{K_3}{K_D}\tilde{J}G_5\Big)\eta_3 + K_d k_4\Big(\tilde{S}(\omega)\tilde{J}Q_d + \frac{1}{K_D}\tilde{J}\Big(I - \\
&\quad \frac{1}{2}\big(q_0 I + \tilde{S}(q)\big)Q_d\Big)\Big)\tilde{D}_0 G_0 y_{\zeta 1} - \frac{1}{K_D}\tilde{J}y_{\zeta 0} + \Big(\tilde{S}(\omega)\tilde{J}Q_d + \frac{1}{K_D}\tilde{J}\Big(I - \frac{1}{2}\big(q_0 I \\
&\quad +\tilde{S}(q)\big)Q_d\Big)\Big)G_3\bar{\tau} + \tilde{\Delta} - \tilde{J}\dot{\omega}_d - \big(G_1\tilde{J}\tilde{J}^{-1}(\eta_3 + K_d e_\xi) - G_1\eta_3 + \frac{1}{K_d}\tilde{G}\tilde{P}_2 P_5\bar{\tau} \\
&\quad +g_{\text{st}}\big) \\
&= \Big(-\frac{1}{K_D}\tilde{S}(\omega)\tilde{J} + \frac{1}{2K_D^2}\tilde{J}(q_0 I + \tilde{S}(q)) - \frac{K_3}{K_D}\tilde{J}G_4\Big)\tilde{\eta}_1 + \Big(-K_P K_D\tilde{L}\tilde{J}^{-1} - \\
&\quad \tilde{S}(\omega)\tilde{J}(I - K_d Q_d G_3\tilde{J})\tilde{J}^{-1} + \frac{1}{2K_D}\tilde{J}(q_0 I + \tilde{S}(q))\tilde{J}^{-1} + \frac{K_d}{K_D}\tilde{J}\big(I - \frac{1}{2}(q_0 I + \\
&\quad \tilde{S}(q))Q_d\big)G_3 - K_d\Big(\tilde{S}(\omega)\tilde{J}Q_d + \frac{1}{K_D}\tilde{J}\big(I - \frac{1}{2}(q_0 I + \tilde{S}(q))Q_d\big)\Big)G_3\Big)\eta_3 + \\
&\quad k_4\Big(K_d\Big(\tilde{S}(\omega)\tilde{J}Q_d + \frac{1}{K_D}\tilde{J}\Big(I - \frac{1}{2}\big(q_0 I + \tilde{S}(q)\big)Q_d\Big)\Big)\tilde{D}_0 G_0 - I\Big)y_{\zeta 1} - \\
&\quad \frac{1}{K_D}\tilde{J}y_{\zeta 0} + I_{\eta_3},
\end{aligned} \tag{10.62}$$

where

$$\begin{aligned}
I_{\eta_3} &= \Big(\Big(\tilde{S}(\omega)\tilde{J}Q_d + \frac{1}{K_D}\tilde{J}\Big(I - \frac{1}{2}\big(q_0 I + \tilde{S}(q)\big)Q_d\Big)\Big)G_3 - \frac{1}{K_d}\tilde{G}\tilde{P}_2 P_5\Big)\bar{\tau} + \tilde{\Delta} - \\
&\quad \tilde{J}\dot{\omega}_d + K_d\Big(\Big(-K_P K_D\tilde{L} - \tilde{S}(\omega)\tilde{J}(I - K_d Q_d G_3\tilde{J}) + \frac{1}{2K_D}\tilde{J}\big(q_0 I + \tilde{S}(q)\big) \\
&\quad + \frac{K_d}{K_D}\tilde{J}\Big(I - \frac{1}{2}\big(q_0 I + \tilde{S}(q)\big)Q_d\Big)G_3\tilde{J}\Big) - G_1\tilde{J} - \frac{K_d K_3}{K_D}\tilde{J}G_5\tilde{J}\Big)\tilde{J}^{-1}e_\xi
\end{aligned} \tag{10.63}$$

Now we are ready for the proof of Lemma 3. Define a candidate ISS-Lyapunov function for (10.36)

$$\begin{aligned} V(\tilde{\eta}_1, \eta_2, \eta_3) &= V_1(\tilde{\eta}_1) + V_2(\eta_2) + V_3(\eta_3) \\ &= \tilde{\eta}_1^\top \tilde{\eta}_1 + \frac{1}{2}\eta_2^\top \tilde{J}\eta_2 + \frac{1}{2}\eta_3^\top \eta_3. \end{aligned} \tag{10.64}$$

Taking the derivatives along the solutions of subsystem (10.36),

$$\begin{aligned} \dot{V}_1 &= 2\tilde{\eta}_1^\top \dot{\tilde{\eta}}_1 \\ &< \big(-\frac{1}{K_D}\varepsilon + \frac{1}{K_D}(\sqrt{3}\lambda_3 + K_d m_{q_d}) + 2K_3 m_4\big)\|\tilde{\eta}_1\|^2 + 2\Big(1 + K_d c_3\big(m_3(1 + \\ &\quad m_{Q_d}) + K_3 m_5\big)\Big)\|\tilde{\eta}_1\|\,\|\eta_2\| + 2K_d\big(m_3(1+m_{Q_d}) + K_3 m_5\big)\|\tilde{\eta}_1\|\,\|\eta_3\| \\ &\quad + 2K_d k_4 m_{\tilde{D}_0} m_0(1+m_{Q_d})\|\tilde{\eta}_1\|\,\|y_{\zeta 1}\| + 2\|\tilde{\eta}_1\|\,\|y_{\zeta 0}\| + 2\|\tilde{\eta}_1\|\,\|I_{\tilde{\eta}_1}\|, \\ \dot{V}_2 &= \eta_2^\top \tilde{J}\dot{\eta}_2 \\ &\leq \frac{1}{K_D}c_3\big(m_\omega + \frac{1}{K_D} + K_3 m_4\big)\|\tilde{\eta}_1\|\,\|\eta_2\| + \Big(-K_P K_D l_3 + m_\omega c_3(1 + \\ &\quad K_d m_{Q_d} m_3 c_3) + \frac{1}{K_D}c_3 + \frac{K_d}{K_D}c_3^2\big(m_3(1+m_{Q_d}) + K_3 m_5\big)\Big)\|\eta_2\|^2 + K_d \\ &\quad \Big(m_3\big(m_\omega c_3 m_{Q_d} + \frac{1}{K_D}c_3(1+m_{Q_d})\big) + \frac{K_3}{K_D}c_3 m_5\Big)\|\eta_2\|\,\|\eta_3\| + \\ &\quad K_d k_4 m_{\tilde{D}_0} m_0\big(m_\omega c_3 m_{Q_d} + \frac{1}{K_D}c_3(1+m_{Q_d})\big)\|\eta_2\|\,\|y_{\zeta 1}\| + \frac{1}{K_D}c_3\|\eta_2\|\,\|y_{\zeta 0}\| \\ &\quad + \|\eta_2\|\,\|I_{\eta_2}\| \\ \dot{V}_3 &= \eta_3^\top \dot{\eta}_3 \\ &\leq \frac{1}{K_D}c_3\big(m_\omega + \frac{1}{K_D} + K_3 m_4\big)\|\tilde{\eta}_1\|\,\|\eta_3\| + \Big(-K_P K_D l_4 + c_3 m_6\big(m_\omega + \frac{1}{K_D}\big) + \\ &\quad 2\frac{K_d}{K_D}c_3 m_3(1+m_{Q_d}) + K_d c_3 m_3 m_\omega m_{Q_d}(1 + c_3 m_6)\Big)\|\eta_3\|^2 + \\ &\quad k_4\Big(K_d m_{\tilde{D}_0} m_0\Big(m_\omega c_3 m_{Q_d} + \frac{1}{K_D}c_3(1+m_{Q_d})\Big) + 1\Big)\|\eta_3\|\,\|y_{\zeta 1}\| + \\ &\quad \frac{1}{K_D}c_3\|\eta_3\|\,\|y_{\zeta 0}\| + \|\eta_3\|\,\|I_{\eta_3}\|, \end{aligned}$$

where $\|\tilde{J}\| \leq c_3$, $\|q_0 I + \tilde{S}(q)\| \leq 2$, $\|\tilde{S}(q)\| = \|S(q^* + q_d - \eta_1)\| \leq \|S(q^*)\| + \|S(q_d)\| + \|S(\eta_1)\|$ and $\eta_1^\top S(\eta_1) = 0$. Besides, $\|G_0\| \leq m_0$, $\|G_1\| \leq m_1$, $\|G_3\| \leq m_3$, $\|G_4\| \leq m_4$, $\|G_5\| \leq m_5$, $\|Q_d\| \leq m_{Q_d}$, $\|\tilde{D}_0\| \leq m_{\tilde{D}_0}$, $\|\omega\| \leq m_\omega$, $\|\tilde{J}^{-1}\| \leq m_6$, $\tilde{L} \geq l_3$ and $\tilde{L}\tilde{J}^{-1} \geq l_4$ and for fixed positive numbers c_3, m_0, m_1, m_3, m_4, m_5, m_6, m_{Q_d}, $m_{\tilde{D}_0}$ and m_ω. Therefore,

$$\begin{aligned} \dot{V} &< \ell_1\|\tilde{\eta}_1\|^2 + \ell_2\|\eta_2\|^2 + \ell_3\|\eta_3\|^2 + \ell_4\|\tilde{\eta}_1\|\,\|\eta_2\| + \ell_5\|\tilde{\eta}_1\|\,\|\eta_3\| + \ell_6\|\eta_2\|\,\|\eta_3\| + \\ &\quad \ell_7\|\tilde{\eta}_1\|\,\|y_{\zeta 1}\| + \ell_8\|\eta_2\|\,\|y_{\zeta 1}\| + \ell_9\|\eta_3\|\,\|y_{\zeta 1}\| + 2\|\tilde{\eta}_1\|\,\|y_{\zeta 0}\| + \frac{1}{K_D}c_3\|\eta_2\|\,\|y_{\zeta 0}\| \\ &\quad + \frac{1}{K_D}c_3\|\eta_3\|\,\|y_{\zeta 0}\| + 2\|\tilde{\eta}_1\|\,\|I_{\tilde{\eta}_1}\| + \|\eta_2\|\,\|I_{\eta_2}\| + \|\eta_3\|\,\|I_{\eta_3}\|, \end{aligned}$$

where

$$\ell_1 = -\frac{1}{K_D}\varepsilon + \frac{1}{K_D}(\sqrt{3}\lambda_3 + K_d m_{q_d}) + 2K_3 m_4$$

$$\ell_2 = -K_P K_D l_3 + m_\omega c_3(1 + K_d m_{Q_d} m_3 c_3) + \frac{1}{K_D}c_3 + \frac{K_d}{K_D}c_3^2\big(m_3(1 + m_{Q_d}) + K_3 m_5\big)$$

$$\ell_3 = -K_P K_D l_4 + c_3 m_6\big(m_\omega + \frac{1}{K_D}\big) + 2\frac{K_d}{K_D}c_3 m_3(1 + m_{Q_d}) + K_d c_3 m_3 m_\omega m_{Q_d}(1 + c_3 m_6)$$

$$\ell_4 = 2\Big(1 + K_d c_3\big(m_3(1 + m_{Q_d}) + K_3 m_5\big)\Big) + \frac{1}{K_D}c_3\big(m_\omega + \frac{1}{K_D} + K_3 m_4\big)$$

$$\ell_5 = 2K_d\big(m_3(1 + m_{Q_d}) + K_3 m_5\big) + \frac{1}{K_D}c_3\big(m_\omega + \frac{1}{K_D} + K_3 m_4\big)$$

$$\ell_6 = K_d\Big(m_3\big(m_\omega c_3 m_{Q_d} + \frac{1}{K_D}c_3(1 + m_{Q_d})\big) + \frac{K_3}{K_D}c_3 m_5\Big)$$

$$\ell_7 = 2K_d k_4 m_{\tilde{D}_0} m_0(1 + m_{Q_d})$$

$$\ell_8 = K_d k_4 m_{\tilde{D}_0} m_0\big(m_\omega c_3 m_{Q_d} + \frac{1}{K_D}c_3(1 + m_{Q_d})\big)$$

$$\ell_9 = k_4\Big(K_d m_{\tilde{D}_0} m_0\Big(m_\omega c_3 m_{Q_d} + \frac{1}{K_D}c_3(1 + m_{Q_d})\Big) + 1\Big).$$

From Young's inequalities,

$$\begin{aligned}
\|\tilde{\eta}_1\|\,\|\eta_2\| &\leq \frac{\delta_0}{2}\|\tilde{\eta}_1\|^2 + \frac{1}{2\delta_0}\|\eta_2\|^2\\
\|\tilde{\eta}_1\|\,\|\eta_3\| &\leq \frac{\delta_0}{2}\|\tilde{\eta}_1\|^2 + \frac{1}{2\delta_0}\|\eta_3\|^2\\
\|\tilde{\eta}_1\|\,\|y_{\zeta 0}\| &\leq \frac{\delta_0}{2}\|\tilde{\eta}_1\|^2 + \frac{1}{2\delta_0}\|y_{\zeta 0}\|^2\\
\|\tilde{\eta}_1\|\,\|y_{\zeta 1}\| &\leq \frac{\delta_0}{2}\|\tilde{\eta}_1\|^2 + \frac{1}{2\delta_0}\|y_{\zeta 1}\|^2\\
\|\tilde{\eta}_1\|\,\|I_{\tilde{\eta}_1}\| &\leq \frac{\delta_0}{2}\|\tilde{\eta}_1\|^2 + \frac{1}{2\delta_0}\|I_{\tilde{\eta}_1}\|^2\\
\|\eta_2\|\,\|\eta_3\| &\leq \frac{\delta_1}{2}\|\eta_2\|^2 + \frac{1}{2\delta_1}\|\eta_3\|^2\\
\|\eta_2\|\,\|y_{\zeta 0}\| &\leq \frac{\delta_1}{2}\|\eta_2\|^2 + \frac{1}{2\delta_1}\|y_{\zeta 0}\|^2\\
\|\eta_2\|\,\|y_{\zeta 1}\| &\leq \frac{\delta_1}{2}\|\eta_2\|^2 + \frac{1}{2\delta_1}\|y_{\zeta 1}\|^2\\
\|\eta_2\|\,\|I_{\eta_2}\| &\leq \frac{\delta_1}{2}\|\eta_2\|^2 + \frac{1}{2\delta_1}\|I_{\eta_2}\|^2\\
\|\eta_3\|\,\|y_{\zeta 0}\| &\leq \frac{\delta_2}{2}\|\eta_3\|^2 + \frac{1}{2\delta_2}\|y_{\zeta 0}\|^2\\
\|\eta_3\|\,\|y_{\zeta 1}\| &\leq \frac{\delta_2}{2}\|\eta_3\|^2 + \frac{1}{2\delta_2}\|y_{\zeta 1}\|^2\\
\|\eta_3\|\,\|I_{\eta_3}\| &\leq \frac{\delta_2}{2}\|\eta_3\|^2 + \frac{1}{2\delta_2}\|I_{\eta_3}\|^2,
\end{aligned}$$

for arbitrary $\delta_0 > 0$, $\delta_1 > 0$ and $\delta_2 > 0$. Consequently,

$$\begin{aligned}
\dot{V} < &\Big(\ell_1 + \frac{\delta_0}{2}\big(\ell_4+\ell_5+\ell_7+4\big)\Big)\|\tilde{\eta}_1\|^2 + \Big(\ell_2 + \frac{\ell_4}{2\delta_0} + \frac{\delta_1}{2}\big(\ell_6+\ell_8+\frac{1}{K_D}c_3 +\\
&1\big)\Big)\|\eta_2\|^2 + \Big(\ell_3 + \frac{1}{2}\big(\frac{\ell_5}{\delta_0}+\frac{\ell_6}{\delta_1}\big) + \frac{\delta_2}{2}\big(\ell_9+\frac{1}{K_D}c_3+1\big)\Big)\|\eta_3\|^2\\
&+\Big(\frac{1}{\delta_0}+\frac{1}{2K_D}c_3\big(\frac{1}{\delta_1}+\frac{1}{\delta_2}\big)\Big)\|y_{\zeta 0}\|^2 + \frac{1}{2}\Big(\frac{\ell_7}{\delta_0}+\frac{\ell_8}{\delta_1}+\frac{\ell_9}{\delta_2}\Big)\|y_{\zeta 1}\|^2 + \frac{1}{\delta_0}\|I_{\tilde{\eta}_1}\|^2\\
&+\frac{1}{2\delta_1}\|I_{\eta_2}\|^2 + \frac{1}{2\delta_2}\|I_{\eta_3}\|^2.
\end{aligned}$$

Firstly set

$$\begin{aligned}
\bar{\lambda}_3^* &= \frac{\varepsilon}{5\sqrt{3}},\\
\bar{K}_d^* &= \frac{\varepsilon}{5m_{q_d}},\\
\bar{K}_3^*(K_D) &= \frac{\varepsilon}{10K_D m_4},\\
\delta_0 &= \frac{2\varepsilon}{5K_D(\ell_4+\ell_5+\ell_7+4)},
\end{aligned}$$

and thus for all $K_d \leq \bar{K}_d^*$, $K_3 \leq \bar{K}_3^*(K_D)$ and all $\lambda_3 \leq \bar{\lambda}_3^*$,

$$\ell_1 + \frac{\delta_0}{2}\big(\ell_4 + \ell_5 + \ell_7 + 4\big) \leq -\frac{\varepsilon}{5K_D}.$$

Next define

$$\begin{aligned}
\ell_2^*(K_P, K_D) &= -K_P K_D l_3 + m_\omega c_3(1 + \bar{K}_d^* m_{Q_d} m_3 c_3) + \frac{1}{K_D} c_3 + \frac{\bar{K}_d^*}{K_D} c_3^2 \big(m_3(1 + \\
&\quad m_{Q_d}) + \bar{K}_3^*(K_D) m_5\big), \\
\ell_4^*(K_D) &= 2\Big(1 + \bar{K}_d^* c_3\big(m_3(1 + m_{Q_d}) + \bar{K}_3^* m_5\big)\Big) + \frac{1}{K_D} c_3\big(m_\omega + \frac{1}{K_D} + \\
&\quad \bar{K}_3^* m_4\big), \\
\ell_5^*(K_D) &= 2\bar{K}_d^*\big(m_3(1 + m_{Q_d}) + \bar{K}_3^* m_5\big) + \frac{1}{K_D} c_3\big(m_\omega + \frac{1}{K_D} + \bar{K}_3^* m_4\big), \\
\ell_7^* &= 2\bar{K}_d^* k_4 m_{\tilde{D}_0} m_0(1 + m_{Q_d}), \\
\delta_0^*(K_D) &= \frac{2\varepsilon}{5K_D\big(\ell_4^*(K_D) + \ell_5^*(K_D) + \ell_7^* + 4\big)},
\end{aligned}$$

and hence for all $K_d \leq \bar{K}_{d1}^*$ and all $K_3 \leq \bar{K}_3^*(K_D)$,

$$\ell_2 + \frac{\ell_4}{2\delta_0} \leq \ell_2^*(K_P, K_D) + \frac{\ell_4^*(K_D)}{2\delta_0^*(K_D)}.$$

By fixing

$$\delta_1 = \frac{K_P K_D l_3}{\ell_6 + \ell_8 + \frac{1}{K_D} c_3 + 1},$$

it is easy to see that there exists a number $\bar{K}_{P1}^* > 0$ such that for all $K_P \geq \frac{\bar{K}_{P1}^*}{K_D}$,

$$\ell_2^*(K_P, K_D) + \frac{\ell_4^*(K_D)}{2\delta_0^*(K_D)} + \frac{1}{2} K_P K_D l_3 \leq -\frac{\varepsilon}{5K_D}.$$

Hence for all $K_d \leq \bar{K}_d^*$ and all $K_3 \leq \bar{K}_3^*(K_D)$ and $K_P \geq \frac{\bar{K}_{P1}^*}{K_D}$,

$$\ell_2 + \frac{\ell_4}{2\delta_0} + \frac{\delta_1}{2}\big(\ell_6 + \ell_8 + \frac{c_2}{K_D} + 1\big) \leq -\frac{\varepsilon}{5K_D}.$$

Now let

$$\begin{aligned}
\ell_3^*(K_P, K_D) &= -K_P K_D l_4 + c_3 m_6\big(m_\omega + \frac{1}{K_D}\big) + 2\frac{\bar{K}_d^*}{K_D} c_3 m_3(1 + m_{Q_d}) + \\
&\quad \bar{K}_d^* c_3 m_3 m_\omega m_{Q_d}(1 + c_3 m_6), \\
\ell_6^*(K_D) &= \bar{K}_d^*\Big(m_3\big(m_\omega c_3 m_{Q_d} + \frac{1}{K_D} c_3(1 + m_{Q_d})\big) + \frac{\bar{K}_3^*}{K_D} c_3 m_5\Big), \\
\ell_8^*(K_D) &= \bar{K}_d^* k_4 m_{\tilde{D}_0} m_0\big(m_\omega c_3 m_{Q_d} + \frac{1}{K_D} c_3(1 + m_{Q_d})\big), \\
\delta_1^*(K_P, K_D) &= \frac{K_P K_D l_3}{\ell_6^*(K_D) + \ell_8^*(K_D) + \frac{1}{K_D} c_3 + 1}.
\end{aligned}$$

Note that for all $K_d \leq \bar{K}_d^*$ and all $K_3 \leq \bar{K}_3^*(K_D)$,

$$\ell_3 + \frac{1}{2}\big(\frac{\ell_5}{\delta_0} + \frac{\ell_6}{\delta_1}\big) \leq \ell_3^*(K_P, K_D) + \frac{1}{2}\big(\frac{\ell_5^*(K_D)}{\delta_0^*(K_D)} + \frac{\ell_6^*(K_D)}{\delta_1^*(K_P, K_D)}\big),$$

and by choosing

$$\delta_2 = \frac{K_P K_D l_4}{\ell_9 + \frac{1}{K_D}c_3 + 1},$$

there exists a number $\bar{K}_{P2}^* > 0$ such that for all $K_P \geq \frac{\bar{K}_{P2}^*}{K_D}$, $K_d \leq \bar{K}_d^*$ and all $K_3 \leq \bar{K}_3^*(K_D)$,

$$\ell_3 + \frac{1}{2}\big(\frac{\ell_5}{\delta_0} + \frac{\ell_6}{\delta_1}\big) + \frac{\delta_2}{2}\big(\ell_9 + \frac{1}{K_D}c_3 + 1\big) \leq -\frac{\varepsilon}{5K_D}.$$

As a result, for any given K_D, for all $K_d \leq \bar{K}_d^*$, $K_3 \leq \bar{K}_3^*(K_D)$, $\lambda_3 \leq \bar{\lambda}_3^*$ and all $K_P \geq \bar{K}_P^* \frac{1}{K_D}$,

$$\begin{aligned}\dot{V} < -\frac{\varepsilon}{5K_D}(\|\tilde{\eta}_1\|^2 + \|\eta_2\|^2 + \|\eta_3\|^2) + \Big(\frac{1}{\delta_0^*(K_D)} + \frac{1}{2K_D}c_3\big(\frac{1}{\delta_1^*(K_D)} + \\ \frac{1}{\delta_2^*(K_P, K_D)}\big)\Big)\|y_{\zeta 0}\|^2 + \frac{1}{2}\Big(\frac{\ell_7^*}{\delta_0^*(K_D)} + \frac{\ell_8^*(K_D)}{\delta_1^*(K_D)} + \frac{\ell_9^*(K_D)}{\delta_2^*(K_P, K_D)}\Big)\|y_{\zeta 1}\|^2 + \\ \frac{1}{\delta_0^*(K_D)}\|I_{\tilde{\eta}_1}\|^2 + \frac{1}{2\delta_1^*(K_P, K_D)}\|I_{\eta_2}\|^2 + \frac{1}{2\delta_2^*(K_P, K_D)}\|I_{\eta_3}\|^2,\end{aligned}$$

where $\bar{K}_P^*(K_D) = \frac{1}{K_D}\max\{\bar{K}_{P1}^*, \bar{K}_{P2}^*\}$,

$$\begin{aligned}\ell_9^*(K_D) &= k_4\bigg(\bar{K}_d^* m_{\tilde{D}_0} m_0\Big(m_\omega c_3 m_{Q_d} + \frac{1}{K_D}c_3(1 + m_{Q_d})\Big) + 1\bigg), \\ \delta_2^*(K_P, K_D) &= \frac{K_P K_D l_4}{\ell_9^*(K_D) + \frac{1}{K_D}c_3 + 1}.\end{aligned}$$

The above inequality confirms that (10.64) is an ISS-Lyapunov function (see [5, Lemma 10.4.2]) for subsystem (10.36). Accordingly, subsystem (10.36) is ISS and conforms with Lemma 3 [5, Theorem 10.4.1].

Appendix D

Here, given

$$\zeta_3' = \begin{bmatrix} \dot{y} \\ \dot{x} \end{bmatrix} + \begin{bmatrix} 1 & 0 \\ 0 & 1 \end{bmatrix} \lambda_2 \sigma(\frac{K_2}{\lambda_2}\zeta_2)$$

and

$$M \begin{bmatrix} \ddot{y} \\ \ddot{x} \end{bmatrix} = \begin{bmatrix} \tilde{d} & mq_3 \\ mq_3 & -\tilde{d} \end{bmatrix} \begin{bmatrix} q_1 \\ q_2 \end{bmatrix} + p' + d_h',$$

where $\tilde{d} := \tilde{d}(\mathbf{q}, t)$, $m := m(\mathbf{q}, t)$, $p' = [p_y \ p_x]^\top$ and $d_h' = [d_y \ d_x]^\top$, $\dot{\zeta}_3'$ is derived. Taking the time derivative,

$$\begin{aligned} \dot{\zeta}_3' &= \begin{bmatrix} \ddot{y} \\ \ddot{x} \end{bmatrix} + \begin{bmatrix} 1 & 0 \\ 0 & 1 \end{bmatrix} K_2 \sigma'(\frac{K_2}{\lambda_2}\zeta_2)\dot{\zeta}_2 \\ &= T_1 + \frac{1}{M}p' + \frac{1}{M}d_h' + K_2\sigma'(\frac{K_2}{\lambda_2}\zeta_2)\dot{\zeta}_2, \end{aligned}$$

where

$$T_1 = \frac{1}{M} \begin{bmatrix} \tilde{d} & mq_3 \\ mq_3 & -\tilde{d} \end{bmatrix} \begin{bmatrix} q_1 \\ q_2 \end{bmatrix}.$$

Next,

$$\begin{aligned} T_1 &= -\frac{1}{M} \begin{bmatrix} \tilde{d} & mq_3 \\ mq_3 & -\tilde{d} \end{bmatrix} (q_r' - q' - q_r') \\ &= T_2 + T_3, \end{aligned}$$

where $q' = [q_1 \ q_2]^\top$, $q_r' = [q_{r1} \ q_{r2}]^\top$,

$$\begin{aligned} T_2 &= -\frac{1}{M} \begin{bmatrix} \tilde{d} & mq_3 \\ mq_3 & -\tilde{d} \end{bmatrix} (q_r' - q') \quad \text{and} \\ T_3 &= \frac{1}{M} \begin{bmatrix} \tilde{d} & mq_3 \\ mq_3 & -\tilde{d} \end{bmatrix} q_r'. \end{aligned}$$

Recall that from (10.27) and (10.29),

$$q_r = \begin{bmatrix} q_{r1} \\ q_{r2} \\ q_{r3} \end{bmatrix} = \begin{bmatrix} -\lambda_3\sigma(\frac{K_3}{\lambda_3}\zeta_{31}') + q_{d1} \\ \lambda_3\sigma(\frac{K_3}{\lambda_3}\zeta_{32}') + q_{d2} \\ -\lambda_3\sigma(\frac{K_3}{\lambda_3}\zeta_3''), \end{bmatrix}$$

since $q_d = [q_{d1}\ q_{d2}\ 0]^\top$. Expanding T_3,

$$\begin{aligned}
T_3 &= \frac{1}{M}\begin{bmatrix}\tilde{d} & mq_3\\ mq_3 & -\tilde{d}\end{bmatrix}\begin{bmatrix}-\lambda_3\sigma(\frac{K_3}{\lambda_3}\zeta_{31}') + q_{d1}\\ \lambda_3\sigma(\frac{K_3}{\lambda_3}\zeta_{32}') + q_{d2}\end{bmatrix}\\
&= -L(t)\begin{bmatrix}\lambda_3\sigma(\frac{K_3}{\lambda_3}\zeta_{31}')\\ \lambda_3\sigma(\frac{K_3}{\lambda_3}\zeta_{32}')\end{bmatrix} + \frac{1}{M}\begin{bmatrix}mq_3\lambda_3\sigma(\frac{K_3}{\lambda_3}\zeta_{32}')\\ -mq_3\lambda_3\sigma(\frac{K_3}{\lambda_3}\zeta_{31}')\end{bmatrix}\\
&\quad -\frac{1}{M}K_d\begin{bmatrix}\tilde{d} & mq_3\\ mq_3 & -\tilde{d}\end{bmatrix}\begin{bmatrix}\tilde{d}_0 & m_0q_3\\ m_0q_3 & -\tilde{d}_0\end{bmatrix}\hat{d}'\\
&= -L(t)\begin{bmatrix}\lambda_3\sigma(\frac{K_3}{\lambda_3}\zeta_{31}')\\ \lambda_3\sigma(\frac{K_3}{\lambda_3}\zeta_{32}')\end{bmatrix} + \frac{1}{M}\begin{bmatrix}mq_3\lambda_3\sigma(\frac{K_3}{\lambda_3}\zeta_{32}')\\ -mq_3\lambda_3\sigma(\frac{K_3}{\lambda_3}\zeta_{31}')\end{bmatrix} - \frac{1}{M}K_dL_d'\hat{d}',
\end{aligned}$$

where $\hat{d}' = [\hat{d}_y\ \hat{d}_x]^\top$,

$$L(t) = \frac{1}{M}\begin{bmatrix}\tilde{d} & 0\\ 0 & \tilde{d}\end{bmatrix} \quad \text{and} \quad L_d' = \begin{bmatrix}l_d & 0\\ 0 & l_d\end{bmatrix}.$$

Continuing with T_2,

$$\begin{aligned}
T_2 &= -\frac{1}{M}\begin{bmatrix}\tilde{d} & mq_3\\ mq_3 & -\tilde{d}\end{bmatrix}\begin{bmatrix}-\lambda_3\sigma(\frac{K_3}{\lambda_3}\zeta_{31}') + q_{d1} - q_1\\ \lambda_3\sigma(\frac{K_3}{\lambda_3}\zeta_{32}') + q_{d2} - q_2\end{bmatrix}\\
&= -\frac{1}{M}\begin{bmatrix}\tilde{d} & mq_3\\ mq_3 & -\tilde{d}\end{bmatrix}\begin{bmatrix}-\lambda_3\sigma(\frac{K_3}{\lambda_3}\zeta_{31}') + q_{d1} - q_1\\ \lambda_3\sigma(\frac{K_3}{\lambda_3}\zeta_{32}') + q_{d2} - q_2\end{bmatrix}\\
&\quad -\frac{1}{M}\begin{bmatrix}\big(m\lambda_3\sigma(\frac{K_3}{\lambda_3}\zeta_{32}')\big)\big(-\lambda_3\sigma(\frac{K_3}{\lambda_3}\zeta_3'') - q_3\big)\\ \big(-m\lambda_3\sigma(\frac{K_3}{\lambda_3}\zeta_{31}')\big)\big(-\lambda_3\sigma(\frac{K_3}{\lambda_3}\zeta_3'') - q_3\big)\end{bmatrix}\\
&\quad +\frac{1}{M}\begin{bmatrix}\big(m\lambda_3\sigma(\frac{K_3}{\lambda_3}\zeta_{32}')\big)\big(-\lambda_3\sigma(\frac{K_3}{\lambda_3}\zeta_3'') - q_3\big)\\ \big(-m\lambda_3\sigma(\frac{K_3}{\lambda_3}\zeta_{31}')\big)\big(-\lambda_3\sigma(\frac{K_3}{\lambda_3}\zeta_3'') - q_3\big)\end{bmatrix}\\
&= -\frac{1}{M}R(t)\begin{bmatrix}-\lambda_3\sigma(\frac{K_3}{\lambda_3}\zeta_{31}') + q_{d1} - q_1\\ \lambda_3\sigma(\frac{K_3}{\lambda_3}\zeta_{32}') + q_{d2} - q_2\\ -\lambda_3\sigma(\frac{K_3}{\lambda_3}\zeta_3'') - q_3\end{bmatrix}\\
&\quad +\frac{1}{M}\begin{bmatrix}\big(m\lambda_3\sigma(\frac{K_3}{\lambda_3}\zeta_{32}')\big)\big(-\lambda_3\sigma(\frac{K_3}{\lambda_3}\zeta_3'') - q_3\big)\\ \big(-m\lambda_3\sigma(\frac{K_3}{\lambda_3}\zeta_{31}')\big)\big(-\lambda_3\sigma(\frac{K_3}{\lambda_3}\zeta_3'') - q_3\big)\end{bmatrix}\\
&= -\frac{1}{M}R(t)(q_r - q) + \frac{1}{M}\begin{bmatrix}\big(m\lambda_3\sigma(\frac{K_3}{\lambda_3}\zeta_{32}')\big)\big(-\lambda_3\sigma(\frac{K_3}{\lambda_3}\zeta_3'')\big)\\ \big(-m\lambda_3\sigma(\frac{K_3}{\lambda_3}\zeta_{31}')\big)\big(-\lambda_3\sigma(\frac{K_3}{\lambda_3}\zeta_3'')\big)\end{bmatrix}\\
&\quad +\frac{1}{M}\begin{bmatrix}-mq_3\lambda_3\sigma(\frac{K_3}{\lambda_3}\zeta_{32}')\\ mq_3\lambda_3\sigma(\frac{K_3}{\lambda_3}\zeta_{31}')\end{bmatrix}\\
&= -\frac{1}{M}R(t)(q_r - q) + \frac{1}{M}E(t)\lambda_3\sigma(\frac{K_3}{\lambda_3}\zeta_3'') + \frac{1}{M}\begin{bmatrix}-mq_3\lambda_3\sigma(\frac{K_3}{\lambda_3}\zeta_{32}')\\ mq_3\lambda_3\sigma(\frac{K_3}{\lambda_3}\zeta_{31}')\end{bmatrix},
\end{aligned}$$

where

$$R(t) = \begin{bmatrix} \tilde{d} & mq_3 & m\lambda_3\sigma(\frac{K_3}{\lambda_3}\zeta'_{32}) \\ mq_3 & -\tilde{d} & -m\lambda_3\sigma(\frac{K_3}{\lambda_3}\zeta'_{31}) \end{bmatrix} \quad \text{and}$$

$$E(t) = \lambda_3 \begin{bmatrix} -\sigma(\frac{K_3}{\lambda_3}\zeta'_{32}) \\ \sigma(\frac{K_3}{\lambda_3}\zeta'_{31}) \end{bmatrix} m.$$

Now back to T_1,

$$\begin{aligned} T_1 &= T_2 + T_3 \\ &= -\frac{1}{M}R(t)(q_r - q) + \frac{1}{M}E(t)\lambda_3\sigma(\frac{K_3}{\lambda_3}\zeta''_3) - L(t)\lambda_3\sigma(\frac{K_3}{\lambda_3}\zeta'_3) - \frac{1}{M}K_dL'_d\hat{d}', \end{aligned}$$

and hence

$$\begin{aligned} \dot{\zeta}'_3 = &-L(t)\lambda_3\sigma(\frac{K_3}{\lambda_3}\zeta'_3) + K_2\sigma'(\frac{K_2}{\lambda_2}\zeta_2)\dot{\zeta}_2 + \frac{1}{M}p' - \frac{1}{M}R(t)\eta_1 + \frac{1}{M}E(t)\lambda_3\sigma(\frac{K_3}{\lambda_3}\zeta''_3) \\ &-\frac{1}{M}K_dL'_d\hat{d}' + \frac{1}{M}d'_h. \end{aligned}$$

From (10.44) and (10.50),

$$\begin{aligned} \hat{d}' &= G'_0P_3J\eta_2 - G'_0\eta_3 + \frac{1}{K_d}G'_0\bar{\tau} \\ &= G'_0P_3J\eta_2 - G'_0\eta_3 + \frac{1}{K_d}d'_h + \frac{1}{K_d}\tilde{P}'_2P_5\bar{\tau}, \end{aligned}$$

where $G'_0 = P' + \tilde{P}'_2P_5$,

$$P' = \begin{bmatrix} \Psi_\varrho & 0 \\ 0 & \Psi_\varrho \end{bmatrix} \quad \text{and} \quad \tilde{P}'_2 = \begin{bmatrix} \tilde{\Psi}_2 & 0 \\ 0 & \tilde{\Psi}_2 \end{bmatrix}.$$

Thus,

$$\begin{aligned} \dot{\zeta}'_3 = &-L(t)\lambda_3\sigma(\frac{K_3}{\lambda_3}\zeta'_3) + K_2\sigma'(\frac{K_2}{\lambda_2}\zeta_2)\dot{\zeta}_2 + \frac{1}{M}p' - \frac{1}{M}R(t)\eta_1 + \frac{1}{M}E(t)\lambda_3\sigma(\frac{K_3}{\lambda_3}\zeta''_3) \\ &-\frac{1}{M}K_dL'_d\big(G'_0P_3J\eta_2 - G'_0\eta_3 + \frac{1}{K_d}d'_h + \frac{1}{K_d}\tilde{P}'_2P_5\bar{\tau}\big) + \frac{1}{M}d'_h \\ = &-L(t)\lambda_3\sigma(\frac{K_3}{\lambda_3}\zeta'_3) + K_2\sigma'(\frac{K_2}{\lambda_2}\zeta_2)\dot{\zeta}_2 + W, \end{aligned}$$

where

$$\begin{aligned} W = &\frac{1}{M}p' - \frac{1}{M}R(t)\eta_1 - \frac{1}{M}K_dL'_d\big(G'_0P_3J\eta_2 - G'_0\eta_3\big) \\ &+\frac{1}{M}E(t)\lambda_3\sigma(\frac{K_3}{\lambda_3}\zeta''_3) + \frac{1}{M}(I - L'_d)d'_h - \frac{1}{M}L'_d\tilde{P}'_2P_5\bar{\tau}. \end{aligned} \tag{10.65}$$

References

[1] X. Yang, H. Pota, and M. Garratt, "Design of a Gust-Attenuation Controller for Landing Operations of Unmanned Autonomous Helicopters," in *18th IEEE International Conference on Control Applications*, July 2009.

[2] F. N. Koumboulis, M. G. Skarpetis, and M. K. Griparis, "Rotary gust rejection for helicopters," in *In Proceedings of the IEEE International Conference on Control Applications*, 1998, pp. 103–107.

[3] H. Wang, A. A. Mian, D. Wang, and H. Duan, "Robust multi-mode flight control design for an unmanned helicopter based on multi-loop structure," *International Journal of Control, Automation, and Systems*, vol. 7, pp. 723–730, 2009.

[4] A. Isidori, *Nonlinear control systems*, 3rd ed., ser. Communications and Control Engineering Series. Berlin: Springer-Verlag, 1995.

[5] ——, *Nonlinear control systems. II*, ser. Communications and Control Engineering Series. London: Springer-Verlag London Ltd., 1999.

[6] A. Isidori, L. Marconi, and A. Serrani, *Robust autonomous guidance: An internal model approach*, ser. Advances in Industrial Control. Secaucus, NJ, USA: Springer-Verlag New York, Inc., 2003.

[7] ——, "Robust nonlinear motion control of a helicopter," *IEEE Trans. Automat. Control*, vol. 48, no. 3, pp. 413–426, 2003. [Online]. Available: http://dx.doi.org/10.1109/TAC.2003.809147

[8] T. J. Koo and S. Sastry, "Output tracking control design of a helicopter model," in *In Proceedings of the 37th Conference on Decision and Control*, 1998, pp. 3635–3640.

[9] T. Meurer, K. Graichen, and E.-D. Gilles, *Control and observer design for nonlinear finite and infinite dimensional systems*. Birkhäuser, 2005.

[10] P. Ioannou, "Robust direct adaptive control," in *Decision and Control, 1984. The 23rd IEEE Conference on*, vol. 23, dec. 1984, pp. 1015 –1020.

[11] A. R. Teel, "A nonlinear small gain theorem for the analysis of control systems with saturation," *IEEE Trans. Automat. Control*, vol. 41, no. 9, pp. 1256–1270, 1996. [Online]. Available: http://dx.doi.org/10.1109/9.536496

[12] O. Shakernia, Y. Ma, T. J. Koo, T. John, and S. Sastry, "Landing an unmanned air vehicle: Vision based motion estimation and nonlinear control," *Asian Journal of Control*, vol. 1, pp. 128–145, 1999.